OSTEOLOGY, PHYLOGENY, TAPHONOMY, AND ONTOGENETIC HISTOLOGY OF *ORYCTODROMEUS CUBICULARIS*, FROM THE MIDDLE CRETACEOUS (ALBIAN-CENOMANIAN) OF MONTANA AND IDAHO

by

L.J. Krumenacker

A dissertation submitted in partial fulfillment
of the requirements for the degree

of

Doctor of Philosophy

in

Earth Sciences

MONTANA STATE UNIVERSITY
Bozeman, Montana

May 2017

DEDICATION

This dissertation is dedicated to my children, Elise and Shawn. You are everything to me and I will ALWAYS be here for you. The universe is full of wonderful unknowns. Find your own questions and seek the answers. Leave the world and the people you meet better than you found them. I love you.

ACKNOWLEDGEMENTS

Remember in “Jurassic Park” where the *Tyrannosaurus* eats a poorly dressed lawyer with thinning hair- that is the best scene… Despite all the opposition, I finished this PhD (and am working on cloning a *T. rex*). I am forever grateful to the people who walked me through these dark times: Cass Powell, you walked with me through the worst part of my life, being a true friend, helping me to find strength and worth in myself and reminding me how important it is to be active; thank you. Chancey Ringer, Liz Greenfield, Shardai Urdahl, Amanda Tebay, and all of FGHO, I genuinely wouldn’t have finished this degree without your patience, help, and friendship. Ash “Queen of Pine Bar” Ferguson, thanks for the encouragement and support.

Thanks to my chair, Dr. Dave Varricchio, who helped me carve out a niche to work in the Cretaceous of Idaho, helped me learn to be a better scientist and writer, and who tirelessly helped me improve this work. Dr. Chris Organ and Dr. David Bowen provided valuable input and opportunities for improvement. Dr. Ted Dyman provided enjoyable learning in the field and input in all aspects of this project. Takuya Imai, Kelli Taddy, Eric Metz, and the crew of the Paleontology Field Course, thank you. Michael Holland, Bob Harmon, and Ellen Lamme, thank you for helping me in lab. Thanks to Haley Dunkel for friendship and employment for a large portion of my doctoral work. Steve Robison, Ali Abusaid, and Diane Wheeler provided permitting assistance while Leif Tapanila, Mary Thompson, and John Scannella allowed access to specimens. Josh Cotton provided awesome artwork for this dissertation and future publication. Thanks to Megan Maier for formatting help and Dan Lawver for computer help.

FUNDING ACKNOWLEDGEMENT

Funding for this research from the Jurassic Foundation and the Montana State University Graduate School were instrumental in aspects of this research and are gratefully acknowledged. Many thanks to Bob Simon for his generous personal donation that facilitated numerous aspects of this research as well.

TABLE OF CONTENTS

TABLE OF CONTENTS CONTINUED

TABLE OF CONTENTS CONTINUED

TABLE OF CONTENTS CONTINUED

TABLE OF CONTENTS CONTINUED

LIST OF TABLES

LIST OF FIGURES

Figure Page

LIST OF FIGURES CONTINUED

Figure Page

LIST OF FIGURES CONTINUED

Figure Page

ABSTRACT

Oryctodromeus is a small bipedal dinosaur known from middle Cretaceous (95-100 My) Wayan Formation of Idaho and the Vaughn Member of the Blackleaf Formation of Montana. This taxon is hypothesized to be a burrowing dinosaur, which cared for its young within these burrows. This dissertation is a broad three-part treatment of this taxon, and excepting the introductory and concluding chapters this dissertation consists of three main chapters. Chapter two describes the osteology and phylogenetic relationships of this animal. Notable features of the *Oryctodromeus* skeleton described include a network of ossified tendons along the vertebral column that completely ensheath the tail, a long tail that forms more than half the length of the animal, and unusual femoral heads whose morphology may be related to burrowing behavior. The first full skeletal and skull reconstructions of this animal are presented. Chapter three investigates patterns of preservation of *Oryctodromeus*. Data suggests that preservation of single to multiple individuals of this taxon typically occurred in burrows that may be difficult to impossible to recognize in the fossil record. New examples of burrows from *Oryctodromeus* from the Vaughn and Wayan, as well as additional evidence for social behavior, are also described. A third chapter details the ontogenetic histology, growth rates and patterns of skeletal fusion based on seven limb elements (femora and tibiae) from different individuals. Based on the data in this dissertation, three growth stages can be recognized in *Oryctodromeus* based on bone histology. Juveniles are defined by more rapidly growing fibrolamellar tissue, sub-adults are defined by a cortex of inner fibrolamellar tissue and outer zonal parallel fibered tissue, and near-adult individuals have tissue similar to sub adults with dense avascular bone in the outermost cortex that signals a decrease in growth rate. LAG's suggest a minimum age of six to seven years for more mature individuals. Patterns of neurocentral fusion in *Oryctodromeus* appear similar to those of crocodylians and some other small ornithischians, while the growth rates of *Oryctodromeus* appear slower than those of some dinosaurs, but similar to taxa such as *Orodromeus* and *Tenontosaurus*.

CHAPTER ONE

INTRODUCTION TO DISSERTATION

Orodromines were small neornithischian dinosaurs that formed distinct components of Cretaceous paleocommunities in North American and Asia. Members of this clade consist of *Zephryosaurus* from the Aptian-Albian Cloverly Formation of Montana and Wyoming, *Oryctodromeus* from the Albian-Cenomanian Wayan Formation of Idaho and the coeval Vaughn Member of the Blackleaf Formation of Montana, *Orodromeus* from the Campanian Two Medicine Formation of Montana, an unnamed taxon from the Campanian Kaparowits Formation of Utah, *Albertadromeus* from the Campanian Oldman Formation of Alberta, and *Koreanosaurus* from the Campanian Seonso Conglomerate (Sues, 1980; Scheetz, 1999; Varricchio *et al*., 2007: Krumenacker, 2010; Huh, 2011; Brown *et al*., 2013; Gates *et al*., 2013). Due to the established burrowing habit of *Oryctodromeus*, skeletal features inferred as related to digging, and similar taphonomic patterns of preservation among some of these taxa, it has been postulated that orodromines were a clade specialized for digging (Varricchio *et al*., 2007; Huh, 2011). *Oryctodromeus* is the dominant vertebrate taxon in the fossil assemblages of the Wayan Formation and the Vaughn Member, and is well represented skeletally, with over a dozen partial to near complete skeletons being known, as well as numerous less complete remains. In this dissertation I provide a tripartite treatment of *Oryctodromeus*, with three chapters that focus on different aspects of this taxon.

Oryctodromeus is one of the best represented orodromines, and in chapter one an in depth description of the osteology of this taxon is given. Most orodromine taxa are much less completely known than *Oryctodromeus*, and this treatment provides a much better understanding of the osteological features of this clade and provide a basis for comparison with other specimens in the future. Specimens exhibiting key osteological features are figured in multiple angles, with specimens from the Wayan and Vaughn both being utilized. Additionally this chapter examines the phylogenetic relationships of *Oryctodromeus*. Previously this taxon has placed solidly within the orodromines clade in numerous analyses using parsimony analysis (Varricchio *et al*., 2007; Boyd, 2015). Here Bayesian analysis is used as an alternative method to compare the results with those of previous analyses.

The apparent extreme dominance of *Oryctodromeus* in the Vaughn and Wayan assemblages raises questions regarding the original paleoecology of these paleocommunities and suggests the possibility of biases favoring the preservation of this taxon (Krumenacker, 2010; Krumenacker *et al*., 2016). Questions raised include whether or not *Oryctodromeus* really is the dominant taxon in these assemblages, and if so why is it the dominant taxon? Also, the initial description of *Oryctodromeus* included evidence for parental care and burrowing behavior in this taxon, and this raises the question if there is additional evidence for these behaviors in this taxon? The second chapter of this dissertation described additional burrows attributable to *Oryctodromeus* and addresses questions of social behavior and possible taphonomic biases through the analysis of the taphonomic setting and attributes of *Oryctodromeus* specimens found up to this date.

Understanding of the histology of orodromines dinosaurs has previously been limited to the description of histological features of *Orodromeus* from the Campanian Two Medicine Formation of Montana (Horner *et al*., 2009). The moderately large sample size of *Oryctodromeus* specimens facilitates histological studies to assess general histological features, growth rates, and degree of maturity of the individual specimens examined. These data, which are discussed in the third chapter, serve as a basis of comparison for the previous work with *Orodromeus* and provide more data on the histological variation and skeletochronology of this clade.

Literature Cited

Boyd, C. A. 2015. The systematic relationships and biogeographic history of ornithischian dinosaurs. *PeerJ* 3:e1523.

Brown, C. M., D. C. Evans, M. J. Ryan, and A. P. Russell. 2013. New data on the diversity and abundance of small-bodied ornithopods (Dinosauria, Ornithischia) from the Belly River Group (Campanian) of Alberta. Journal of Vertebrate Paleontology 33(3): 495-520.

Gates, T. A., E. K. Lund, C. A. Boyd, D. D. DeBlieux, A. L. Titus, D. C. Evans, M. A. Getty, J. I. Kirkland, and J. G. Eaton, J. G. 2013. Ornithopod dinosaurs from the Grand Staircase-Escalante National Monument Region, Utah, and their role in paleobiogeographic and macroevolutionary studies, in At the Top of the Grand Staircase: The Late Cretaceous in Southern Utah, Titus, A. L., and Loewen, M. A. (eds). 463-481. Indiana University Press.

Horner, J. R., Ricqles A. R., K. Padian, R. D. Scheetz. 2009 Comparative Long Bone Histology and Growth of the 'Hypsilophodontid' Dinosaurs *Orodromeus makelai*, *Dryosaurus altus*, and *Tenontosaurus tillettii* (Ornithischia: Euornithopoda). Journal of Vertebrate Paleontology 29: 734–747.

Huh, M., D. G. Lee, J. K. Kim, J. D. Lim, and P. Godefroit. 2011. A new basal ornithopod dinosaur from the Upper Cretaceous of South Korea. Neues Jahrbuch fur Geologie und Palaontologie Abhandlungen 259: 1-24.

Krumenacker, L. J. 2010, Chronostratigraphy and paleontology of the mid-Cretaceous Wayan Formation of eastern Idaho, with a description of the first *Oryctodromeus* specimens from Idaho: Brigham Young University, MS thesis.

Krumenacker, L.J., Simon, D. J., Scofield, G., and Varricchio, D. J., 2016. Theropod dinosaurs from the Albian–Cenomanian Wayan Formation of eastern Idaho. Historical Biology 29(2)170-186.

Scheetz, R.D., 1999, Osteology of *Orodromeus makelai* and the phylogeny of basal ornithopod dinosaurs. PhD. Thesis in Biology, Montana State University, Bozeman, 189 pp.

Sues, H. D. 1980. Anatomy and relationships of a new hypsilophodontid dinosaur from the Lower Cretaceous of North America. Palaeontographica Abteilung a Palaeozoologie-Stratigraphie 169(1–3): 51–72.

Varricchio, D. J., A. J. Martin, and Y. Katsura. 2007. First trace and body fossil evidence of a burrowing, denning dinosaur: Proceedings of the Royal Society B: Biological Sciences 274:1361–1368.

CHAPTER TWO

OSTEOLOGY AND PHYLOGENY OF THE NEORNITHISCHIAN DINOSAUR *ORYCTODROMEUS CUBICULARIS* FROM THE MIDDLE CRETACEOUS (ALBIAN-CENOMANIAN) OF MONTANA AND IDAHO

Contribution of Authors and Co-Authors

Manuscript in Chapter 2

Author: L.J. Krumenacker

Contributions: Conceived the study, performed the analyses, interpreted results, and wrote the manuscript.

Co-Author: David J. Varricchio

Contributions: Conceived the study, discussed results and implications, and edited earlier manuscripts.

Co-Author: Chris Organ.

Contributions: Performed analyses, discussed implications, edited earlier manuscripts.

Co-Author: Clint Boyd.

Contributions: Provided data set for analyses, assisted with data matrix revisions.

Co-Author: Brooks Britt

Contributions: Assisted with figures.

Manuscript Information Page

L.J. Krumenacker, David J. Varricchio, Chris Organ, Clint Boyd, Brooks Britt

Journal of Vertebrate Paleontology

Status of Manuscript:
__X_ Prepared for submission to a peer-reviewed journal
____ Officially submitted to a peer-review journal
____ Accepted by a peer-reviewed journal
____ Published in a peer-reviewed journal

Abstract

ABSTRACT-The Albian to Cenomanian Wayan Formation of eastern Idaho and the coeval Vaughn Member of the Blackleaf Formation of southwestern Montana contain vertebrate assemblages dominated by the small burrowing orodromine dinosaur *Oryctodromeus cubicularis*. The holotype and paratype specimens of *Oryctodromeus* have undergone only preliminary description. Here we describe in detail the osteology of *Oryctodromeus* as represented by additional specimens. These specimens provide a suite of additional characters useful for the diagnosis of *Oryctodromeus*: an elongate preacetabular process of the ilium, elongate cervical centra 1.6 times as long as high, elongate dorsal centra 1.4 times as long as high, over 55 elongate caudal vertebrae often enveloped in hypaxial and epaxial tendons, and a femoral head, similar to that of *Koreanosaurus*, projecting from the greater trochanter at roughly 35° on an elongate neck. A phylogenetic analysis conducted using new characters supports the monophyly of Orodrominae, a neornithischian clade known from the middle to Late Cretaceous of Asia and western North America that may have been specialized for burrowing. Unfortunately this new analysis provides no additional data on the placement of *Oryctodromeus* within this clade. The tail, comprising two-thirds of the animals total length of roughly three meters, and associated tendon sheaths in the axial column suggest greater flexibility than has been previously supposed for ossified tendons; or alternatively suggest the possibility of *Oryctodromeus* burrows having separate or multiple entrances and exits. The elongate

and angled femoral head probably played a role in the animal bracing itself with a splayed-leg posture while digging.

INTRODUCTION

The terrestrial vertebrate fossil record for the earliest Late Cretaceous of North America has grown dramatically over the past two decades mainly due to discoveries in the Mussentuchit Member of the Cedar Mountain Formation of eastern Utah (eg. Kirkland and Madsen, 2007; McDonald *et al*., 2012; Zanno and Makovicky, 2013). However, discoveries outside of this area are much less common and are poorly understood. The Wayan Formation of eastern Idaho and the Vaughn Member of the Blackleaf Formation of southwestern Montana are two coeval geological units that occur north of the Colorado Plateau. *Oryctodromeus cubicularis*, from the Wayan and Vaughn, represents the most completely known Cenomanian dinosaur taxon north of the Mussentuchit assemblage (Krumenacker 2010; Krumenacker *et al*., 2016; Varricchio *et al*., 2007). Orodromines, defined by Brown (2013), share characters that include a sacropubal articulation, a sharp scapular spine, and a D-shaped cross-section of the fibula. Excluding *Oryctodromeus* other orodromine taxa include *Zephyrosaurus schaffi* from the Aptian-Albian Cloverly Formation of Montana (Sues, 1980), *Orodromeus makelai* from the Campanian Two Medicine Formation of Montana (Horner and Weishampel, 1988; Scheetz, 1999), *Albertadromeus syntarsus* from the Campanian Belly River Group of Alberta (Brown *et al*., 2013), *Koreanosaurus boseongensis* from the Santonian to Campanian Seonso Conglomerate of South Korea, and an unnamed taxon,

the “Kaiparowits Orodromine” from the Campanian Kaiparowits Formation of southern Utah (Gates *et al*., 2013; Boyd 2015).

Oryctodromeus was originally described from associated adult (MOR 1636a) and juvenile (MOR 1636b) materials found in the Cenomanian Vaughn Member of the Blackleaf Formation in southwestern Montana (Varricchio *et al*., 2007). These previously described materials consist of cranial and postcranial materials of one presumably mature and two juvenile individuals that were found in association in the expanded distal chamber of an infilled burrow (Varricchio *et al*., 2007). This discovery provided the first evidence of burrowing and denning behavior in the Dinosauria, and additionally provided evidence of parental care for this taxon. Further published work on *Oryctodromeus* has been limited to an analysis of the forelimb and pectoral girdle by Fearon and Varricchio (2015), which supported specialization of the forelimbs for scratch digging. Since the initial description, additional materials, comprising numerous more individuals, have since been recognized and prepared from other localities in the Vaughn Member and in the Wayan Formation of southeastern Idaho (Krumenacker, 2010; Krumenacker *et al*., 2016). These new specimens, together with the holotype (MOR 1636a) and paratype (MOR 1636b) specimens, include nearly all skeletal elements with the exception of the sternals, and some cranial and manual elements. This relative abundance of specimens makes *Oryctodromeus* among the most well-represented orodromines and basal neornithischians. Here a detailed description of *Oryctodromeus* osteology is given with comparisons to other orodromines as well as other ornithischian taxa. The phylogenetic

placement and taphonomic setting for *Oryctodromeus* and the functional implications of its morphology are also discussed.

GEOLOGICAL SETTING

In the Caribou Range of southeastern Idaho (Fig. 1), Cretaceous strata (Fig. 2) consist of a thick non-marine alluvial plain sequence. The Wayan Formation occurs in the upper portion of this packet where it is underlain by the Smiths Formation and overlain by the Sage Junction Formation (Durkee, 1980; Dorr, 1985; Oriel and Platt, 1980; Rubey, 1973). The Wayan Formation consists of pedogenically altered siltstones and mudstones with subordinate sandstones and rare tuffs (Schmitt and Moran, 1982; Krumenacker, 2010). Deposition occurred in a seasonal inland meandering floodplain environment (Schmitt and Moran, 1982; Dorr, 1985; Krumenacker, 2010). A thickness of 1,344 meters has been documented in the Tincup Canyon area of Caribou County (Krumenacker, 2010). Recent detrital zircon U-Pb dating indicates an age near the Albian/Cenomanian stage boundary for the base of the formation with an early to middle Cenomanian age for the middle to upper part of the formation (Krumenacker, 2010). *Oryctodromeus* specimens are known from at least the lower and middle portions of the Wayan Formation (Krumenacker, 2010).

The Blackleaf Formation (Figs. 1, 2) crops out in southwestern and west-central Montana (Fig. 1; Cobban *et al*., 1959). It is underlain by the Aptian-Albian Kootenai Formation and overlain by the Cenomanian-Santonian Frontier Formation in the Lima Peaks area of southwestern Montana and the Cenomanian-Santonian Marias River Shale in more northern areas (Cobban *et al*., 1959; Cobban *et al*., 1976; Dyman *et al*., 1997).

Cobban *et al*. (1959) divided the Blackleaf into four members near Great Falls, including in ascending order the Flood, Taft Hill, Vaughn, and Bootlegger members. Dyman and Nichols (1988) only recognized the Vaughn and Flood members in the Lima Peaks area. *Oryctodromeus* specimens are known from the Vaughn Member in the Lima Peaks area of Beaverhead County. In this area the Vaughn Member has been measured at 270 meters thick, while it is over 1000 meters thick in west-central Montana (Dyman and Nichols, 1988). Palynomorphs and radiometric dates indicate a Cenomanian age for the Vaughn Member in this area (Dyman *et al*., 1997; Dyman and Nichols, 1988; Zartman *et al*., 1995). The stratigraphic placement of *Oryctodromeus* within the Vaughn Member is uncertain due to the placement of fossil localities within an isolated and incomplete section.

OCCURRENCE

Multiple individual associations of *Oryctodromeus*, similar to that reported for the holotype and paratype specimens have been noted. MOR 1642 consists of a minimum of two similar sized and presumably mature individuals, based on the presence of two left femora and two supraoccipitals. IMNH 44939 consists of the remains of three different individuals based on the proportions of larger tibiae and pes from two presumably mature individuals and a much smaller partial pes. IMNH 50846 consists of the associated remains of a larger, presumably mature individual as well as centra of a juvenile comparable in size to the paratype (juvenile) MOR 1636b. The common occurrence of multiple-individuals strengthens the evidence for parental care and social groups with this taxon.

Oryctodromeus occurs only in the Wayan Formation of Idaho and the Vaughn Member of the Blackleaf Formation of southwestern Montana. The Wayan and Vaughn represent the same depositional packet, which has been disrupted since deposition by tectonic events and volcanism (Krumenacker *et al*., 2016). *Oryctodromeus* is the most common vertebrate known in the Wayan and Vaughn fossil assemblages (Krumenacker, 2010; Krumenacker *et al*., 2016); fossil evidence from floodplain deposits for other vertebrates, excluding eggshell, is extremely rare in these geological units (Krumenacker, 2010; Krumenacker *et al*., 2016). The marked dominance of these fossorial organisms in the Wayan and Vaughn, suggests a possible bias favoring their preservation.

INSTITUTIONAL ABBREVIATIONS

BYU, Brigham Young University, Provo, Utah; **IMNH**, Idaho Museum of Natural History, Pocatello, Idaho; **MOR**, Museum of the Rockies, Bozeman, Montana

ANATOMICAL ABBREVIATIONS

ac, acetabulum; *af*, articulation facet; *al*, alveoli; *an*, angular; *ao*, antorbital fenestra; *ap*, anterior process; *as*, articular socket; *asp*, ascending process; *boc*, basioccipital; *bpt*, basipterygoid process; *bs*, brevis shelf; *bsp*, basisphenoid; *bt*, basal tuber; *cc*, cnemial crest; *cf*, coracoid foramen; *chf*, chevron facet; *cp*, capitulum; *d*, dentary; *dc*, deltapectoral crest; *dia*, diapophysis; *doc*, dorsal condyle; *ec*, erupting crown; *ecf*, ectopterygoid facet; *ecs*, ectopterygoid shelf; *eg*, extensor intercondylar groove; *en*, external naris; *f*, frontal; *fg*, flexor intercondylar groove; *fh*, femoral head; *fo*, fossa; *fs*, fossa subarcuata; *ftr*, fourth trochanter; *gb*, globular boss; *gf*, glenoid fossa; *gl*, glenoid; *gt*, greater trochanter;

hh, humeral head; *icl*, insertion pit for *M. caudifemoralis longus*; *ip*, iliac peduncle; *isp*; ischiac peduncle; *j*, jugal; *jp*, jugal process; *jw*, jugal wing; *l*, lachrymal; *lc*, lateral condyle; *ldt*, lateral distal tarsal; *lf*, lateral fossa; *lm*, lateral malleolus; *ls*, lateral sulcus; *lt*, lateral tuberosity; *ltf*, lateral temporal fenestra; *ltr*, lesser trochanter; *mc*, medial condyle; *mr*, median ridge; *mri*, medial ridge on ilium; *mt*, medial tuberosity; *mx*, maxilla; *mxs*, slot for jugal process of the maxilla; *na*, nasal; *obf*, obturator foramen; *mm*, medial malleolus; *mtc*, metacarpal; *obp*, obturator process; *oc*, occipital condyle; *op*, olecranon process; *op-exo*, opisthotics-exoccipital; *opi*, opisthotic; *or*, orbit; *pa*, parietal; *par*, parapophysis; *pcp*, paroccipital process; *pd*, predentary; *pep*, preacetabular process; *pf*, prefrontal; *pmx*, premaxilla; *po*, postorbital; *pop*, postacetabular process; *por*, postorbital process; *poz*, postzygapophysis; *pp*, posterior process; *ppp*, postpubic process; *pr*, primary ridge; *pro*, prootic; *prp*, prepubic process; *prz*, prezygapophysis; *ps*, parasphenoid; *pup*, pubic peduncle; *pw*, pterygoid wing; *q*, quadrate, *qj*, quadratojugal *rc*, radial condyle; *rs*, rugose surface; *sa*, surangular; *so*, supraorbital; soc, supraoccipital; *sp*, sacropubal articulation; *spr*, sternal process; *sq*, squamosal; *sqp*, squamosal process; *ss*, scapular spine; *sys*, synovial socket; *tb*, tuberculum; *uc*, ulnar condyle; *vc*, ventral condyle; *vf*, ventral fossa; *vp*, ventral process.

TERMINOLOGY AND METHODS

Preparation of specimens was conducted using standard preparation techniques. IMNH specimens were prepared by the lead author in the Vertebrate Paleontology lab at BYU and at the Varricchio Paleontology Lab in Gaines Hall at Montana State University.

MOR specimens were beautifully prepared by Carrie Ancell in the fossil preparation lab at the Museum of the Rockies.

We follow the assessment of Boyd (2015) and refer to *Oryctodromeus* as a basal neornithischian in the clade Parksosauridae, placing outside of a more restricted Ornithopoda. In the description, the terminologies and descriptive methodologies of Scheetz (1999) are used. Comparisons with *Orodromeus*, *Zephyrosaurus*, and the unnamed Kaiparowits Formation orodromine were based on direct specimen comparisons and published osteological descriptions (Scheetz, 1999; Sues, 1980; Varricchio *et al*. 2007). Comparisons to other genera were conducted through the available literature.

Descriptions are based primarily on the best preserved and prepared specimens, MOR 1636a and b, as well as MOR 1642. More specific references in the text cite specific specimens best demonstrating the described features, or in describing features specific to individual specimens. Multiple individuals may be represented by the same specimen number, as IMNH and MOR catalogue multiple individuals associated from the same locality under one specimen number (eg. IMNH 44939 and MOR 1642).

For the phylogenetic analysis MrBayes v3.2.6 (Ronquist *et al*., 2012) was used to infer the phylogenetic relationships within Orodrominae and an updated version of the morphological dataset from Boyd (2015). Four MCMC replicates were run for 10,000,000 generations, each with four chains and a sampling frequency of 2,000. The average standard deviation of split frequencies between the MrBayes runs was less than 0.0056, which indicates that the runs adequately converged as shown in a time series plot

(supplementary data-Figure 22) using the program Tracer 1.6 (Rambaut, Suchard, Xie, & Drummond, 2014). ESS estimates (with values of 7323 and 7395) indicate an adequate approximation of true posterior distributions.

SYSTEMATIC PALEONTOLOGY

DINOSAURIA Owen, 1842

ORNITHISCHIA Seeley, 1887

NEORNITHISCHIA Cooper, 1985 (sensu Butler at al., 2008)

PARKSOSAURIDAE Buchholz, 2002 (sensu Boyd, 2015)

ORODROMINAE Brown *et al*., 2013

ORYCTODROMEUS Varricchio *et al*., 2007

(Figs. 3-20)

Etymology—The species name, '*cubicularis'*, translates to 'of the lair', and refers to the denning habit of this taxon.

Holotype—MOR 1636a, partial skeleton of one individual, consisting of a fused premaxilla, posterior/occipital region of the braincase, three cervical, six dorsal, sacrum, and 23 caudal vertebrae, three dorsal ribs, scapulocoracoid, scapula, coracoid, humerus, ulna, radius, tibiae, distal fibula, and metatarsal IV.

Paratype—MOR 1636b, associated cranial and postcranial materials of two juvenile individuals measuring 55% to 65% of the adult holotype and found in association with the holotype.

Referred Material—Numerous additional partial skeletons have been recovered since the initial description of *Oryctodromeus*. The more complete and better preserved of the currently prepared materials are used for description here. Referred specimens consist of: IMNH 44920, partial skeleton consisting of partial axial column, partial forelimbs, pelvic girdle fragments, partial hindlimbs; IMNH 44939, portions of three associated individuals preserving partial axial column, partial hindlimbs, pelvic fragments, partial hindlimbs; IMNH 44946, skull fragments, partial axial column, forelimb fragments, hindlimb fragments; IMNH 44951, partial articulated skeleton with partial axial column, partial forelimbs, partial pelvic girdle, partial hindlimbs; IMNH 45081, partial pelvis; IMNH 45596, partially prepared specimen consisting of partial axial and hindlimb elements; IMNH 46169: partial skeleton with skull fragments, partial axial column, partial forelimb, partial hindlimbs; IMNH 49842, partially prepared specimen consisting of axial, forelimb, and hindlimb elements; IMNH 50846, associated elements from juvenile and presumed adult individual consisting of axial and hindlimb fragments; and IMNH 50847, partially prepared specimen from a burrow fill with axial and hindlimb elements. MOR 1634, axial fragments and fragments from the forelimbs and hindlimbs; MOR 1635, fragments from the axial column and hindlimb; MOR 1638, skull fragments, axial fragments, hindlimb fragments; MOR 1639, hindlimb fragments; MOR 1640, axial fragments, forelimb and hindlimb fragments; MOR 1642, portions of

two associated individuals consisting of disarticulated skull elements, partial axial columns, partial forelimbs, partial pelvic girdles, partial hind limbs; MOR 8660, axial and hindlimb fragments; MOR 8683, axial and hindlimb fragments; and MOR 8684, hindlimb and pelvic fragments.

Locality and Horizon—MOR specimens are from the latest Albian to Cenomanian Vaughn Member of the Blackleaf Formation (Figs.1 and 2), near Lima Peaks, Beaverhead County, Montana. IMNH specimens are from the latest Albian to Cenomanian Wayan Formation (Fig. 1 and 2) of Bonneville and Caribou counties, Idaho. Specific locality information is on file at the respective institutions.

Diagnosis—Varricchio *et al*. (2007) defined the autapomorphic features of *Oryctodromeus* as: long paraoccipital processes; basioccipital with a steeply sided ventral 'box' just rostral to the occipital condyle, seven sacral vertebrae, including two sacralized posterior dorsals and their ribs; large scapula with a sharply angled and narrow acromion process bearing a thin-edged laterally projecting scapular spine and a distinct posterior bend to the scapular blade; ilium with very short pre-acetabular and long post-acetabular portions; brevis shelf slopes mediolaterally and is visible laterally throughout its length; and long prepubic process with a transversely broad proximal portion possessing an elongate ventral fossa.

The referred specimens from the Wayan and Vaughn provide the following additional characters, that while variably distributed among other taxa, are additionally useful for diagnosis: elongate cervical centra about 1.6 times as long as high; posterior dorsal centra 1.4 times as long as high; squat sacral centra with transversely expanded

articular faces with W or U- shaped cross sections; elongate tail containing over fifty-five vertebrae, caudal vertebrae sometimes encased in a sheath of hypaxial and epaxial tendons; distal two-thirds of caudal vertebrae elongate with centrum length more than twice centrum height; coracoid with elongate ovoid fossa below the glenoid cavity; robust olecranon process; well-defined femoral head set on elongate neck projecting from the femoral shaft at 38°; laterally flattened greater trochanter; modest to weak anterior intercondylar groove on the femur; and bifid ascending process of the astragalus.

DESCRIPTION

Skull

A complete skull for *Oryctodromeus* is unknown. Skull elements for the holotype (MOR 1636a) are limited to the partial posterior portion of an articulated braincase and a premaxilla. Articulated skull elements are limited to the partial braincases of MOR 1636a and MOR 1642. The braincase of MOR 1636a consists of the basioccipital, exoccipitals and opisthotics, the supraoccipital, the basisphenoid, and prootics. For the juvenile paratype specimens (MOR 1636b) a left dentary, a postorbital, and a maxilla are known. MOR 1642, representing a minimum of two individuals, includes a partial articulated and associated braincase consisting of the basioccipital, basisphenoid, parasphenoid, and portions of the prootic. Additionally the cranial elements for MOR 1642 include the paroccipitals, the opisthotics and exoccipitals, predentaries, partial dentaries, a premaxilla, maxillae, frontals, a jugal, a paraoccipital, a postorbital, two supraoccipitals, and two quadrates.

As best as can be determined from the available elements, the overall shape of the skull (Fig. 3) is similar to other orodromines such as *Orodromeus* (Scheetz, 1999) and *Zephyrosaurus* (Sues, 1980). The skull has a large orbit and is triangular in lateral view. The premaxillae have gently rounded distal portions and the predentary comes to a sharp point, giving the rostrum a sharp beak and suggesting a selective dietary habit. Unlike *Orodromeus* (Scheetz, 1999) and *Zephyrosaurus* (Sues, 1980) the jugal does not exhibit a distinct horn-like boss, though the posterior portion is rugose and suggests the presence of a cartilaginous feature.

The teeth are large, triangular, and pointed; and not packed densely into the dentary or maxilla. There are five premaxillary teeth in each side of the premaxilla indicated by the alveoli.

Supraoccipital—Supraoccipitals are known in articulation with the braincase (Fig. 4A, C) from the adult holotype, MOR 1636a; as well as two loose examples from MOR 1642 (Fig. 5A-D). Those specimens from MOR 1642 are smaller than the supraoccipital in the presumably adult holotype (MOR 1636a) and either represent juvenile individuals or indicate negative allometry (the elements reducing size near adulthood) for this element in *Oryctodromeus*.

The supraoccipital is somewhat hexagonally-shaped in posterior view. The posterior surface bears a median ridge (nuchal crest), more pronounced than that in *Orodromeus*, extending from the anterior edge to just posterior of the central portion of the element, where the ridge transitions into a gently concave surface. This ridge is best

defined on MOR 1636a. On either side of this ridge the surface is gently concave, with the lateral edges flaring outward and forming ridges along the dorso-lateral edge. The postero-lateral portions of this ridge forms distinct points at the contact with the opisthotics. The ventral surfaces are anteroposteriorly concave. The sutural junction with the prootic bear medial excavations of the fossa subarcuata that are less deep than those seen in *Orodromeus* (Scheetz, 1999).

Opisthotics and Exoccipitals—The exocccipital and opisthotics are known from the fused braincase of MOR 1636a and MOR 1642 where they are fused with the paroccipitals. As in *Orodromeus* (Scheetz, 1999) the exoccipitals appear to be indistinctly fused with the opisthotics.

The opisthotics expand into long robust paroccipital processes (Fig. 4) similar to those of *Hypsilophodon* (Galton, 1974) and other orodromines such as *Zephyrosaurus* (Sues, 1980). These extend postero-laterally. A moderately deep ventrolateral fossa extends anteroposteriorly along the base of each paroccipital process and is roofed by the prootic. The distal ends of the processes extend dorso-ventrally and end in semi-rounded ventral points giving the processes a hatchet shape similar to *Orodromeus* (Scheetz, 1999) and *Thescelosaurus* (Boyd, 2014). The sutural contacts with the supraoccipital occurs dorsomedially while sloping ventrally to the foramen magnum.

Basioccipital—MOR 1636a contains the basioccipital in articulation with the braincase (Fig. 4A-B); MOR 1642 includes a partial basioccipital in articulation with the basisphenoid (Fig. 5E-G). This description is based on both specimens.

Posteriorly, the basioccipital forms the occipital condyle which is well-developed with a smooth and robust articulation. The occipital condyle is broad and u-shaped, with these features being most prominent in MOR 1642. The foramina for cranial nerve XII (best exhibited on MOR 1642) occur on the lateral portion of the basioccipital near the suture for the opisthotics. Ventrally the basioccipital consists of a steeply sided ventral 'box' (Varricchio *et al*., 2007), rostral to the occipital condyle. The venter of this box is less rounded than the venter of the same element in *Zephyrosaurus*. The ventral profile of the element is dumbbell shaped with the posterior portion of the element being wider than the rostral portion (Fig. 5E).

Prootic— A partial prootic is represented in articulation with the braincase of MOR 1636a (Fig. 4). As in *Hypsilophodon* (Galton, 1974), this is an irregularly shaped bone, and being fused with the surrounding elements makes discernment of details difficult. As in *Orodromeus* and *Zephyrosaurus,* the ventral portion of the prootics contain the foramina for cranial nerve V.

Basisphenoid and Parasphenoid—MOR 1636a includes a partial basisphenoid fused with the basioccipital (Fig. 4A-B). MOR 1642 includes a partial fused parasphenoid and basisphenoid fused with a basioccipital (Fig 5E-G).

The partial basisphenoid of MOR 1642 is fully fused to the rostral portion of the basioccipital. Ventrally, a distinct deep sulcus extends anteroposteriorly, as in *Zephyrosaurus* (Sues, 1980). The basipterygoid processes (Fig. 5E-G) are distinct and flare ventrolaterally with a wedge-shaped distal end. In lateral view there is a deep

excavation on both sides of the element, with a broken central portion suggesting originally that a thin central sheet of bone occupied this area as in *Hypsilophodon* (Galton, 1974).

The parasphenoid (Fig. 5E-F) is fused to the basisphenoid and emerges from the basisphenoid just dorsal to the basipterygoid processes. The parasphenoid is incomplete but appears similar to other orodromines such as *Orodromeus* (Scheetz, 1999) and *Zephyrosaurus* (Sues, 1980) in being blade-like and laterally compressed.

Laterosphenoid—One partial right laterosphenoid (Fig. 5H-I) is known from MOR 1642. The dorsal portion of the laterosphenoid has a prominent and robust head. As in *Hypsilophodon* (Galton, 1974), the lateral surface is convex ventrodorsally and concave anteroposteriorly. A small ridge runs anteroposteriorly on the preserved portion of the latero-dorsal portion of the element.

Premaxilla—Two nearly complete and fused pairs of premaxillae are known, one from MOR 1636a (Fig. 6A-D) and one from MOR 1642. The specimen for MOR 1642 is somewhat crushed with the holotype specimen being the best preserved. Both are used for description here.

As in *Zephyrosaurus* (Sues, 1980), the premaxillae are fused. Each premaxilla is roughened and rugose in the main body of the snout, as in *Zephyrosaurus* and *Thescelosaurus* (Boyd, 2014; Sues, 1980), indicating a keratinous beak that extended from the posteriormost alveoli to the tip of the snout. Anteriorly the fused premaxillae come to a moderately rounded point in dorsal and ventral view. In lateral view the

articulated premaxillae have numerous foramina or fossa placed anteriorly as well as one pair placed ventrally (one on each premaxilla) near the anterior tip of the snout and anterior of the first alveolus. In ventral view the element is gently concave laterally, with the premaxilla being more mediolaterally narrow than in *Zephyrosaurus* and similar to that of *Thescelosaurus* (Boyd, 2014). Ventrally each premaxilla has five alveoli (Fig. 6C) that are slightly anteroposteriorly elongate, indicating the presence of five premaxillary teeth as in *Orodromeus* (Scheetz, 1999), *Hypsilophodon* (Galton, 1974), but dissimilar to the six premaxillary teeth present in *Thescelosaurus* (Boyd, 2014). The anterior-most alveolus occurs slightly posterior of the tip. Medial of the alveoli the palatal roof is placed dorsally of the lateral margin and consists of a very thin sheet of bone. The anterior and posterior processes of the premaxillae are missing their distal ends. The distal posterior processes are flat and thin in cross section. As in *Hypsilophodon* (Galton, 1974) the posterior processes are rounded anteriorly and sharper posteriorly.

Maxilla—Maxillae consist of partial left maxilla known from MOR 1642 (Fig. 6E-F), a mostly complete right maxilla from MOR 1636b, as well as a few possible fragments from IMNH 46169. MOR 1642 is the best preserved and is used for the description here.

The preserved body of the maxilla consists of a poorly preserved elongate rod preserving tooth roots and the ectopterygoid shelf. Little other detail is discernible. It is difficult to determine the exact number of alveoli in MOR 1642. However, there is a minimum of thirteen alveoli, many with preserved tooth roots, in the most complete specimen. Scheetz (1999) also reports thirteen maxillary alveoli in a larger specimen of

Orodromeus (MOR 473). The tips of some partially erupted replacement maxillary teeth are visible in MOR 1642 and IMNH 46169.

Jugal—Two jugals are known. One poorly preserved right jugal from MOR 1636b, and one partial right jugal from MOR 1642 (Fig. 7A-C). This second specimen is missing the ends of the postorbital and maxillary processes. Both are used for the description.

The jugal is a mediolaterally narrow element that forms the lower and posterior portions of the orbit. The dorsal portion of the jugal that forms the border of the orbit exhibits a dorso-lateral ridge that runs anteroposteriorly. This ridge is sharp anteriorly and moderately rounded posteriorly, ascending with the postorbital process. Ventrally the surface of the jugal forms a moderately rounded keel posteriorly that flares medially into the ectopterygoid shelf. The ectopterygoid shelf is pronounced and robust, and occurs in the anterior two-thirds of the element, with the ectopterygoid facet occurring centrally on in the medial portion of the jugal. This postero-ventral corner of the orbit forms a distinct gently medially concave surface. The postorbital process is moderately robust and triangular in cross section.

Oryctodromeus lacks a pronounced jugal boss, such as those found in *Orodromeus* (Scheetz, 1999) and *Zephyrosaurus* (Sues, 1980), having instead a rugose ornamentation similar to the nodular jugal ornamentation of *Jeholosaurus* (Fig. 7A; Barrett and Han, 2009). This feature on the large *Oryctodromeus* individual (MOR 1642) suggests a more subtle keritinaceous feature than the pronounced jugal boss of

Orodromeus (Scheetz, 1999) and *Zephyrosaurus* (Sues, 1980). The jugal of MOR 1636b (the juvenile paratype) is smooth surfaced.

Supraorbital—One right supraorbital is preserved with MOR 1642. This element is complete. The supraorbital (Fig. 7D-F) is a distinctly curved, somewhat J-shaped element. The anterior articular surface has a moderately robust projection as in *Orodromeus* (Scheetz, 1999). The shaft has an ovoid cross-section and a moderate medial ridge. The shaft is curved and tapers slightly more distal of the well-developed articulation with the prefrontal, before slightly expanding again at the distal end.

Postorbital—One nearly complete left postorbital (Fig. 7G-I) occurs with MOR 1642. As in other orodromines, this element is triradiate and robust, with a ventrally tapering jugal process and a moderately robust posterior squamosal process. A pronounced synovial socket occurs above and posterior to the orbit, as in *Orodromeus* (Scheetz, 1999). The posterior wall of the orbit formed by this element is concave and most robust at the junction of the processes. The dorso-lateral edge of the orbit forms a rounded process that projects slightly anteriorly into the orbit. The portion of the jugal process forming the orbit is gently concave proximally and nearly flat distally, with a ridge forming the lateral and medial portions. The dorsal surface of the jugal is slightly convex. The jugal process tapers distally and has a triangular cross section.

Frontal—A partial left and right frontal (Fig. 8A-B) are known from MOR 1642, but they offer little information. What is preserved indicates an elongate platy pair of

elements that are concave ventrally, similar to *Orodromeus* (Scheetz, 1999) and *Zephyrosaurus* (Sues, 1980).

Quadrate—MOR 1642 preserves a left and a right quadrate. The right is nearly complete, while the left is missing portions of the pterygoid wing and the jugal wing.

The quadrate (Fig. 8C-H) consists of a columnar main body, bowed, anteriorly, with a robust, ventral condylar region that ascends into a more delicate main body with two thin bony plates, the pterygoid wing and the jugal wing, which project anteriorly from the mid-region of the quadrate. The jugal wing is laterally placed and is less pronounced than the medial pterygoid wing. A dorsoventrally elongate and pronounced fossa, like that in *Thescelosaurus* (Boyd, 2014), occurs centrally on the medial surface of the pterygoid wing. The dorsal condyle is gracile and less pronounced in comparison to the lateromedially expanded ventral condyle.

Predentary—MOR 1642 includes two nearly complete predentaries. The predentary (Fig. 9A-E) is generally similar in form to those of other basal ornithischians in being sharply pointed and triangular in dorsal and ventral view, but is distinct in being markedly more elongate in contrast to forms such as *Hypsilophodon* (Galton, 1974) and *Thescelosaurus* (Boyd, 2014), but similar to that of *Jeholosaurus* (Barrett and Han, 2009). Predentaries from other orodromines are unreported. The palatal surface is very slightly concave in lateral view while in dorsal and ventral views the lateral surfaces are moderately concave. A lateral sulcus originates between the lateral processes and the ventral process, runs anteroposteriorly, and extends to very near the anterior tip. The

ventral process extends significantly more posteriorly than the lateral processes. The posterior end of the ventral process is bifurcated in one example from MOR 1642 (Fig. 9E), as in *Thescelosaurus* (Boyd, 2014), while a second example from MOR 1642 is not (Fig. 9A-D).

Dentary—Partial dentaries are known from MOR 1636b, MOR 1642, IMNH 44946 and IMNH 46169. MOR 1642 contains partial left and right dentaries, MOR 1636b consists of a nearly complete left dentary with some poorly preserved teeth, MOR 1642 consists of two partial dentaries represented by the mid and posterior portions with poorly preserved teeth in place, IMNH 46169 consists of a fragment with a partial tooth, while IMNH 44946 consists of the more anterior portion of the element. It contains six partial to complete tooth crowns. This description is based on MOR1636b and 1642, and IMNH 44946.

The dentary (Fig. 9F-K) is similar in form to other orodromines and basal neornithischians in consisting of a narrow and laterally compressed bone with an anteriorly pointed end that would have fit between the ventral and dorsal processes of the predentary. The meckelian groove extends ventrally and mesially through the posterior and mid-portion of the dentary. The tooth row is more inset from the lateral surface of the element posteriorly, while the teeth are more laterally placed anteriorly. Alveoli are smaller anteriorly and increase in size posteriorly. Though hard to distinguish, MOR 1642 contains the alveoli of at least twelve teeth, some with partially erupted replacement crowns. One of the incomplete dentaries of MOR 1642 exhibits twelve alveoli and is missing at least one-fifth (the more anterior portion) of the element, suggesting more than

thirteen dentary teeth in more mature individuals. Nutrient foramina occur more anteriorly in MOR 1636b about mid-height on the lateral surface of the dentary; in MOR 1642 (which is missing the more anterior portion) they occur more posteriorly and are also mid-height on the lateral surface.

Dentary Teeth—Tooth crowns described here (Fig. 9G-K) are from the best-preserved example, the dentary of IMNH 44946 (Fig. 9I-J), which contains anterior dentary teeth, with the lateral portion of the specimen being reinforced by cyanoacrylate. The single tooth in IMNH 46169 and the few partial crowns in MOR 1642 (Fig. 9F-H) are identical to those in IMNH 44946. Teeth in MOR 1636b are poorly-preserved and offer no details.

As in *Orodromeus* (Scheetz, 1999) the crowns are triangular in medial and lateral view, distinctly constricted just above the root, slightly asymmetrical, and laterally compressed. Unlike *Orodromeus* however, *Oryctodromeus* teeth are nearly half again larger relative to the size of the dentary. In teeth positioned more posterior in the dentary, crown height exceeds the breadth, while in teeth more anteriorly placed in the dentary crowns breadth exceeds height. The moderately developed cingulum is supported by a centrally placed bulbous primary vertical ridge that flares ventrally into the cingulum. The tooth apex is formed by the primary ridge. The mesial and caudal ridges of each tooth are comprised of prominent, dorsoventrally elongate denticles which number up to nine on each side of the crown. Denticles located mid-series on each side of the primary ridge descend farthest forming the longest secondary ridges which nearly reach the cingulum. Though no crown is perfectly preserved and none preserve a full set of

denticles, the number of denticles on the mesial and caudal side of the crowns is similar. Secondary denticles are preserved on some primary denticles. Tooth roots exposed in MOR 1642 are hollow and round to triangular.

Axial Skeleton

The axial skeleton is well represented, excluding cervical vertebrae, which probably numbered nine as in *Orodromeus* (Scheetz, 1999). Dorsal vertebrae number fourteen, and sacral vertebrae number seven. Caudal vertebrae are extensive and number at least fifty-five in the most complete caudal sections.

Cervical Vertebrae—Cervicals are the most poorly represented vertebrae. Assuming the typical cervical formula for orodromines such as *Orodromeus,* there would have been nine cervical vertebrae in the column. The atlas/axis is unknown, with three cervical vertebrae (possibly IV, V, and VI) being known from MOR 1636a, MOR 1642 preserves one posterior cervical vertebra (probably VIII or IX), IMNH 46169 preserves two cervical centra, and IMNH 44951 preserves one cervical.

As in other orodromines (Boyd, 2015) each centrum (Fig. 10C-G) is strongly ventrolaterally concave with a pronounced ventral keel, a similar ventral keel is present in some iguanodontians such as *Dryosaurus* as well (Galton, 1981). Cervical vertebrae are weakly opisthocoelous. The anterior articular faces are wider than high with a heart-shaped outline. Parapophyses are situated just posterior of the anterior edge of the centra and just below the neurocentral suture. The diapophyses occur on the edges of the transverse processes just posterior of and dorsal to the parapophyses. The neural canal is

large and D-shaped in cross-section with a flat to excavated ventral aspect. The neural arches contact the centra on a horizontal plane.

The posterior articular faces are wider than high in the vertebrae referred to cervicals V and VI, while in the referred cervical IV the face is higher than wide. These posterior articular faces are D-shaped. In the more posterior cervical from MOR 1642 the neural canal is markedly taller and less wide than the specimens from MOR 1636a. Small and thin neural spines originate on the neural arch near the head of the diverging postzygapophyses in the middle vertebrae, and extend anteriorly roughly half way to the edge of the neural arch. In these vertebrae the prezygapophyses and postzygapophyses are roughly of equal length; while in the more posterior vertebra from MOR1642 the postzygapophyses were probably more elongate than the incomplete prezygapophyses.

In comparison to most related forms, such as *Zephyrosaurus* and *Orodromeus*, which have shorter middle cervical centra, the middle cervical centra of *Oryctodromeus* are somewhat more elongate with broader articular faces. Centra in *Oryctodromeus* measure about 1.6 times as long as high. *Koreanosaurus* (Huh *et al*., 2010), *Dryosaurus* (Galton, 1981) and *Hypsilophodon* (Galton, 1974) also have similarly elongate cervical centra; while *Zephyrosaurus* has slightly shorter cervical centra.

Cervical Ribs—MOR 1642 preserves one more posteriorly placed cervical rib. The morphology of the cervical rib (Fig. 10A-B) is identical to those of other orodromines and ornithischians in general. In this specimen the tuberculum extends anterodorsally and is shorter than the anteroventrally projecting capitulum. The articular

heads of the capitulum and tuberculum are subequal in size. At the junction of the capitulum and tuberculum there is a short ridge that runs anteroposteriorly along the more proximal portion of the lateral surface of the rib shaft.

Dorsal Vertebrae—The dorsal column (Fig. 11) is completely represented in *Oryctodromeus*, with fourteen dorsals being present in a complete column (with the two posterior-most, not counted as dorsals here, being incorporated into the seven vertebrae sacrum). Six dorsal vertebrae are preserved in MOR 1636a, with some anterior and more posterior vertebrae being preserved. MOR 1642 has a consecutive series of five anterior vertebrae, and at least ten fragmentary more posterior dorsal vertebrae. IMNH 44951 contains an articulated series of vertebrae here referred to two of the posterior-most cervicals as well as fourteen dorsal vertebrae and two sacral vertebrae. Because some matrix was left on the specimen for stability, and the anterior-most vertebrae (tentatively recognized as the two posterior-most cervicals) of the specimen is heavily crushed, details are less discernible, and assignment of specific positions of the vertebrae are tentative. IMNH 44920 contains two loose dorsal centra and three articulated posterior-most dorsals. The descriptions of dorsals one through twelve are based on IMNH 44951, MOR 1636a, and MOR 1642; with dorsals thirteen and fourteen being based on IMNH 44920 and MOR 1636a.

Like the cervical centra, all dorsal centra are elongate. *Oryctodromeus* dorsal centra are slightly amphicoelous more anteriorly to platycoelus more posteriorly, with spool-shaped centra in ventral view. Outlines of anterior and posterior articular faces are U-shaped with a flat dorsal portion forming the base of the neural canal. The

prezygapophyses are larger and more widely separated than the postzygapophyses throughout the dorsal column.

Anterior dorsal vertebrae are strongly keeled and more laterally constricted, while posterior dorsal centra are more robust with no ventral keel. The keel is less pronounced by dorsal five and is absent by dorsal nine. Dorsal centra are 1.5 times as long as high more anteriorly and 1.4 times as long as high more posteriorly. This elongation is similar to the elongate middle dorsal centra from an undescribed iguanodontian (Blane Quarry Iguanodont reposited at BYU-Provo) from the Yellow Cat Member of the Cedar Mountain Formation (pers. obs.), as well as *Zephyrosaurus*, *Koreanosaurus*, *Albertadromeus* and *Dryosaurus* but dissimilar to *Orodromeus* (Brown *et al*., 2013; Galton, 1981; Huh *et al*., 2010; Scheetz, 1999). In some specimens the posterior dorsal centra bear a weakly developed ventral sulcus. Posteriorly in the series the centra become more robust (less ventrolaterally compressed) and exhibit roughened and rugose intervertebral muscle scars on the lateral articular edges, these are typical of some ornithopod dorsal centra, being found in forms such as *Dryosaurus* (Galton, 1981), *Thescelosaurus* (Gilmore, 1915) and other orodromines. Ossified epaxial tendons occur throughout the dorsal column of IMNH 44951 and also form a thick epaxial sheath in the more posterior dorsal vertebrae of MOR 1642.

In the anterior dorsal vertebrae (Fig. 11A-E) the parapophyses are high on the neural arch and somewhat centrally placed under the transverse processes, with the diapophyses occurring at the ends of the transverse processes. In the most posterior portion of the dorsal column, the parapophyses and diapophyses merge into one articular

facet. Transverse processes originate just above the neurocentral suture, have a wide base, are longest in the anterior-most dorsals and decrease in length moving posteriorly in the column. In comparison to those of the posterior dorsals the transverse processes of the anterior dorsals are more steeply inclined. In the more posterior dorsals the inclination of the transverse processes is nearly on a horizontal plane and they angle anteriorly. The prezygapophyses and postzygapophyses of the posterior dorsals in MOR 1642 (representing the largest *Oryctodromeus* specimen) are slightly more elongate, more robust and pronounced than in smaller specimens. Neural spines on the anterior dorsal vertebrae are narrower in lateral view and increase in anteroposterior width more posteriorly in the series. Neural spines (which are partially missing in MOR 1642) of the mid and posterior dorsals flare slightly anteroposteriorly distally, as in *Orodromeus* (Scheetz, 1999), are nearly equal in height to the centra, originate slightly behind the anterior edge of the centra, and extend just beyond the posterior edge of the centra.

Dorsal Ribs— MOR 1642 includes eight near complete dorsal ribs (Fig. 12) and numerous rib fragments, including some proximal ribs still in articulation on loose posterior dorsal vertebrae; MOR 1636a preserves three dorsal ribs. Most dorsal ribs are represented in articulation in IMNH 44951 and details are less discernible. Ribs in this specimen are longest on dorsal seven or eight. The dorsal ribs of MOR 1636a all are recurved and belong in the middle portion of the dorsal column. In posterior view a broad sulcus is present proximally on the ribs that narrows and moves laterally more distally. All except the posterior-most of the dorsal ribs are double-headed, with the capitulum and tuberculum becoming progressively closer more posteriorly in the column.

Sacral Vertebrae— MOR 1636a and MOR 1642 both preserve a complete sacrum. IMNH 44920, 44930, 44951, and 46169 preserve partial sacra and separate sacral centra. IMNH 45081 includes a partial sacrum with five vertebrae (the anterior most and posterior most vertebrae being missing possibly due to weathering and possibly breakage. This specimen may be part of the same individual catalogued as IMNH 44951 due to the proximity of the specimens in the field, similar preservation, identical matrix lithology, and non-overlapping elements. If so this would give IMNH 44951 a complete seven centra sacrum. Here, the sacrals from MOR 1636a, IMNH 44920 and IMNH 45081 are used for description.

Oryctodromeus has seven sacral vertebrae (Fig. 13), having incorporated the two posterior-most dorsal vertebrae into the sacrum (Varricchio *et al*., 2007). The anterior-most three vertebrae are the most robust, with sacrals four through six being distinctly less robust. Sacral one has a broad and moderately deep ventral sulcus. This feature is present on all sacral vertebrae, but is less distinct in sacrals two and three, regaining prominence in the more posterior vertebrae. Sacrals two, three, and four display a moderately flat venter in comparison to the other vertebrae. Distinct in IMNH 44951, the first two sacrals appear to be preserved in one massive, and somewhat indistinct, fused unit that is flanked by ossified tendons more robust than in other portions of the vertebral column. In IMNH 44920 the first sacral has a squat u-shaped cross section. Three more loose sacral centra associated with this specimen have centra that are wider than tall and have a W or U-shape in cross section, as in the “Kaiparowits orodromine” (pers. obs.).

The two anterior-most sacrals retain ribs similar to the preceding dorsals, with the ribs angling anteriorly and originating above the neurocentral suture. The ribs of the first are most elongate with those of the second being about half the length of the preceding. The remaining sacral ribs are dorsoventrally thicker, angled lower, and originate on the anterior portion of the centra flanking the neurocentral suture as robust processes. The sacral ribs are moderately inclined and form a long iliac attachment (Varricchio *et al*., 2007). As in *Orodromeus* (Scheetz, 1999), the second and third centra are noticeably wider where they meet and share a sacropubal articulation (Fig. 13C) extending ventrolaterally from the articulation of the centra. This articulation faces ventrally, is reinforced by the sacral ribs of the second and third vertebrae, and consists of an anteroposteriorly elongate articulation. The neural spines are very thin transversely, with the first sacrodorsals spine being unfused to the adjacent spine, while the remaining sacral neural spines are fused in MOR 1636a. The neural spines are not visible in MOR 1642 due to a sheath of epaxial tendons.

Caudal Vertebrae—While caudal vertebrae (Fig. 14) are the most commonly found remains of *Oryctodromeus*, no complete articulated tail has been found. MOR 1642 (representing a minimum of two individuals) preserves at least fifty-seven caudal vertebrae with roughly half of these occurring as articulated or associated bundles within or associated with tendon sheaths. IMNH 44920 (representing one individual) preserves fifty-five articulated and associated caudal centra, many also within a tendon sheath. IMNH 44920 likely represents a nearly complete series. The following description is based primarily on the nearly complete series of IMNH 44920 and MOR 1642.

The lateral and ventral surfaces of all caudal centra are concave, with the centra having a spool-shaped profile in ventral view. Depending on individual specimens, the ventral surfaces of most to all caudal vertebrae have a sulcus extending anteroposteriorly and connecting the chevron facets. On MOR 1642 the proximal-most caudal vertebrae have a very deep and distinct sulcus, with this being less developed in MOR 1636a. As in *Hypsilophodon* (Galton, 1974), the first caudal vertebra is opisthocoelous, with a flat proximal articulation and a gently concave posterior articulation. The box shaped and less elongate proximal and middle caudal vertebrae (Fig. 14A-E) are amphicoelous, with the more elongate distal caudals (Fig. 14F-K) transitioning to a procoelous condition, with flat distal articulations and gently concave anterior articular ends. Centra quickly become elongate (with a general length two times the centrum height) in the caudal column, with only the first two caudal centra being approximately equidimensionsal in height and length, and the succeeding centra being longer than tall. More than half of the tail is comprised of distinct very elongate vertebrae (with a general length of at least four times the centrum height; Fig. 14F-K), with this distinct elongation occurring in the middle of the tail. The distal caudal vertebrae are very similar to those of *Zephyrosaurus* (pers. obs.) due to their elongate body and hexagonal cross-section. Close to caudal twenty the centra are at least twice as long as high. Near this point the articular ends of the centra change from being taller than wide to more equal in width and height, gaining a hexagonal cross-section due to a dorsolaterally placed ridge that extends anteroposteriorly along the centra. This ridge gains prominence on centra lacking transverse processes.

Chevron facets are either absent or poorly developed on the first caudal, with well-developed facets occurring on the distal portion of the second caudal. Chevron facets remain throughout the observed column, occurring on the anterior and posterior ventral faces of the centra, with those on the more distal and elongate vertebrae being less distinct. Transverse processes originate just above the neurocentral suture and project slightly dorsally and posteriorly. More anteriorly, the transverse processes are roughly equal in length to the neural spines, with the transverse processes gently tapering into a rounded terminus. Based on MOR 1642, the initially long transverse processes steadily diminish in length and end near caudal fifteen, near this point the transverse processes are short stubs and originate on or just below the neurocentral suture. In successive caudal vertebrae that lack transverse processes, a distinct anteroposterior ridge flanks the entire lateral sides of the centra. In the more anterior caudal vertebrae the neural spines are elongate and originate near the midsection of the centra, extending over the more anterior portion of the succeeding centrum. The tips of these anterior neural spines flare anteroposteriorly being greater in length than at their base. Based on a tall neural spine on what is approximately caudal twenty, elongate neural spines persisted through at least this position before becoming reduced to spines about equal to the centra in height. In the more distal caudals neural spines originate much farther back on the centra, and are anteroposteriorly longer than they are dorsoventrally tall. In the anterior caudals pre- and post-zygopophyses extend just beyond the centra and are of moderate size, being angled sub-horizontally. In the middle and posterior caudal vertebrae the pre-zygopophyses become more prominent, while the post-zygopophyses become much reduced.

Chevrons—Despite the abundance of caudal vertebrae, chevrons (Fig. 15) are less common. IMNH 44920 has one chevron in a matrix block, and IMNH 44930 has two chevrons associated with a proximal caudal centrum, and one chevron articulated with two mid-caudals. MOR 1642 preserves at least fourteen chevrons, most of these are loose, but a few are still in matrix blocks. The description is based on chevrons from MOR 1642 and IMNH 44930.

The paucity of chevrons makes interpretation of their changing morphology as they proceed distally untenable. The chevrons bear anterior and posterior articular facets, with the posterior facets being more steeply inclined. The hemal canal is oval shaped and much taller dorsoventrally than wide. Chevrons are longer than corresponding neural spines in contrast to the condition in ornithopods such as *Tenontosaurus* (Forster, 1990) where chevrons are equal in length to corresponding neural spines; and more similar to *Hypsilophodon* (Galton, 1974), where the mid-caudal chevrons are longer than the corresponding neural spines. In lateral view the proximal and distal ends of the chevrons are slightly expanded anteroposteriorly.

Ossified Tendons—Though the initial description of *Oryctodromeus* discusses a lack of ossified tendons (Varricchio *et al.*, 2007), some specimens recovered and prepared subsequently (IMNH 44920, IMNH 44939, IMNH 44951, IMNH 44956, IMNH 45081, and MOR 1642) have discrete bundles of hypaxial and epaxial tendons (Fig. 15A, D). These tendons run parallel to the long axis of the centra, as in *Hypsilophodon* (Galton, 1974) and *Tenontosaurus* (Ostrom, 1970). *Oryctodromeus* specimens exhibit either very few ossified tendons as float in the matrix near the specimens, or conspicuous

bundles of tendons. IMNH 44951 and MOR 1624 have epaxial tendons in the preserved portions of the dorsal (Fig. 20A and D) and sacral columns; epaxial and hypaxial tendons are also present throughout the caudal column and form distinct bundles around the vertebrae. IMNH 44920 and 44930 have identical tendon bundles encompassing the caudal vertebrae. IMNH 44946 and 46169 have only a few traces of ossified tendons, mostly in the matrix associated with the specimens. The disarticulated holotype specimen (MOR 1636a), which includes a few loose caudal vertebrae, included only a few fragments of loose ossified tendons in the matrix.

As in other basal ornithopods such as *Tenontosaurus* (Foster, 1990) *Jeholosaurus* (Han *et al*., 2012) and *Hypsilophodon* (Galton, 1974), the tendons are long, slender, and circular in outline; extending across at least five vertebrae in MOR 1642. On MOR 1642 and IMNH 44951 epaxial tendons on the dorsal vertebrae occur above the prezygapophyses and postzygapophyses and angle anteroventral and anterodorsal at roughly ten degrees. Those tendons near the neural spines are arcuate and follow the convex curve of the top of the neural spine. Along the dorsal vertebrae the tendons occur in a layer that is one to two deep, with at least seven individual tendons occurring along the neural arch (Fig. 15A).

Along the sacrum in MOR 1642 and IMNH 45081 tendons occur as dorsoventrally smaller individuals and as more dorsoventrally tall examples. Again these follow the long axis of the sacrum and gently undulate parallel to the sacrum. One of the more anterior broad tendons above sacral vertebra two in MOR 1642 splits into three of

the thinner tendons as it progresses anteriorly. Here the tendon bundle appears to be at least two tendons deep and seven high.

Along the caudal column in MOR 1642 (Fig. 15A, D), IMNH 44920, and IMNH 44939, some tendons have been removed during preparation. Here the remaining tendons, which are mostly retained along the middle and distal caudals, occur as multiple linear bundles that are either sub-parallel to the long axis of and occur on the caudal vertebrae and chevrons, or as bundles that gently undulate on and along the neural spines. Discrete bundles can be recognized along the centra, at the base of the neural spines, near the top of the neural spines, and along the mid-bodies of the chevrons. These bundles generally consist of at least four tendons or more vertically stacked and one or two tendons deep. Individual tendons occur for at least the length of three vertebrae, possibly five (preparation makes this uncertain) in some of the matrix blocks containing multiple caudal vertebrae. At least twenty-four tendons can occur on the outermost portion of the caudals and surrounding areas from the base of the chevrons on the tail to the tip of the neural spines.

APPENDICULAR SKELETON

Scapula—Scapulae (Fig. 16A) are known for IMNH 44939 (left), IMNH 44951 (left and right), IMNH 46169 (left), MOR 1636a (left and right), MOR 1636b (right), and MOR 1642 (left and right). The scapulae of *Oryctodromeus* specimens are often but not always fused with the coracoid in most adult specimens. The thescelosaurine *Haya griva* also exhibits fused scapulocoracoids (Makovicky *et al*., 2011). Both the left and right

scapulocoracoids of MOR 1642 and the left scapulocoracoid of MOR 1636a are fused. However, the right scapula of MOR 1636a is not fused with the coracoid. For clarity of description, the scapula will be described with the blade oriented horizontally, in the same manner as *Orodromeus* (Scheetz 1999). MOR 1636a and MOR 1642 are used for the description below.

The scapular blade is thin when viewed ventrally or dorsally, and the expanded anterior end curves medially. The glenoid faces ventrally and is bisected by the fusion of the scapula and coracoid. Above the glenoid the coracoid articulation forms an excavated and rugose surface that includes the prominent scapular spine, which is borne on the acromion process. The scapular spine is similar in angle and form to other orodromines such as *Orodromeus* (Scheetz, 1999) and *Zephyrosaurus*. A complete scapula is unknown in *Koreanosaurus* so the presence of a scapular spine in this taxon is undetermined (Huh *et al*., 2010). The ventral region of the anterior scapula is thickened near the glenoid. The tall scapular spine extends from the robust region of the glenoid projecting anterodorsally and ends in a blunt projection. The lateral side of the scapular spine has a anteroposteriorly extending ridge that ends dorsal to the glenoid.

The blade of the scapula exhibits a distinct posterior bend (Varricchio *et al*., 2007) that is distinct from the straight-bodied scapulae of *Orodromeus* (Scheetz, 1999) and *Koreanosaurus* (Huh *et al*., 2010). The ventral edge of the scapular blade is highly concave, ending anteriorly at the scapular side of the glenoid. In the mid and posterior portions the blade is expanded dorsoventrally, similar to the expansion of the distal scapula of *Orodromeus* (Scheetz 1999). The straight dorsal edge of the scapular blade is

relatively short, extending roughly perpendicular to the scapular spine projecting from the acromion process. The lateral and medial surfaces of the posterior blade have a roughened surface, indicative of muscle scarring (Fearon and Varricchio, 2016).

Coracoid—Coracoids (Fig. 16A-C) are well represented. IMNH 44939 preserves one left coracoid, IMNH 44920 preserves coracoid fragments, and IMNH 44951 has a crushed and fragmented left coracoid still in place that appears to be fused with the scapula. MOR 1636a preserves one fused left scapulocoracoid, and one unfused right coracoid. MOR 1636b preserves one unfused left coracoid. MOR 1642 includes fused left and right scapulocoracoids.

The coracoid has an ovoid outline, as in *Orodromeus* (Scheetz, 1999) but dissimilar to the more square coracoid of *Koreanosaurus* (Huh, 2010). This element is robust near the glenoid, with a hatchet-shaped sternal process located anteroventrally. The coracoid rapidly thins anterodorsally. The anterior-most margin of the coracoid curves medially, but otherwise the coracoid is nearly flat. The scapular articulation is bordered ventrally by the robust glenoid cavity. The coracoid contribution to the glenoid extends ventrally and forms the anterior portion of the articulation for the humerus. Anterior to the glenoid the ventral margin of the coracoid curves ventrally again forming the sternal process. The ovoid coracoid foramen is placed well anterior of the scapula and fully enclosed within the coracoid, unlike *Hypsilophodon* (Galton, 1974) but similar to that of *Orodromeus* (Scheetz, 1999) and *Koreanosaurus* (Huh *et al*., 2010). In larger specimens, a medially placed shallow linear depression extends from the coracoid foramen towards the scapular articulation. In some specimens, a shallow, elongate, ovoid

fossa (Fig. 16C, referred to here as the ventral fossa) is located on the ventral aspect and faces ventrally, between the sternal process and the glenoid fossa. In IMNH 44930, another shallow, circular fossa (Fig. 16B, referred to here as the lateral fossa) is present on the lateral surface of the coracoid, located just dorsal to the ventral fossa.

Humerus—MOR 1636a preserves a right humerus ; MOR 1636b preserves a left humerus; and MOR 1642 included two right humeri, one left humerus, and the distal condyles from another left humerus. Humeri are also known from IMNH 44946 and IMNH 44951, while a proximal portion is known from IMNH 44920 and fragments from IMNH 46169. Here descriptions are based on IMNH 44939, MOR 1636a, MOR 1636b, and MOR 1642.

While similar in robustness to that of *Orodromeus* (Scheetz, 1999)and other small basal ornithischians, the humerus (Fig. 16D-G) of *Oryctodromeus* is not as robust as in *Koreanosaurus* (Huh *et al*., 2010). In lateral view the humerus is sigmoidal with a prominent deltopectoral crest. Proximally the humerus is expanded into the humeral head, with the head being slightly raised above the lateral and medial tuberosities. In the juvenile assemblage MOR 1636b the humeral head is less prominent than in the more mature individuals. The deltopectoral crest extends about one third the length of the humerus from the proximal end, with the apex of the deltopectoral crest having a rugose texture. The deltopectoral crest thins and shortens distally beyond the apex. Distal to the deltopectoral crest, the shaft of the humerus, which has an ovoid cross section, narrows and then expands again into the transversely expanded bicondylar distal end. The two condyles, which are sub-equal in morphology, are separated by an intercondylar groove

which is more evident on the strongly concave anterior surface. In distal view, the humerus is dumbbell shaped.

Ulna—Ulnae are represented with MOR 1642 (partial right), MOR 1636a (right); IMNH 46169 (proximal and possible distal end), and IMNH 44951 (partial left). This description is based on MOR 1636a, MOR 1642, and IMNH 46169.

The ulna (Fig. 16H-K) is slightly bowed in shape and is longer than the radius. The proximal end of the ulna is expanded and triangular in dorsal view. The olecranon process is prominent and extends proximally, posterior to the humeral articular surface of the ulna. The olecranon process is robust like that of *Koreanosaurus* (Huh *et al*., 2010). The proximal surface anterior to the olecranon is slightly concave for articulation with the ulnar condyle. The ulna is widest at its proximal end and narrows rapidly in the proximal fourth of its length. The medial surface of the proximal shaft is slightly concave, with a slightly rough articular surface for the radius distal to the olecranon. The central shaft is roughly triangular to oval in cross-section. The distal ends of the ulnae are triangular in cross section and transversely expanded.

Radius—Radii occur with MOR 1642 (possible left and right, one of which is partial and one that is crushed), MOR 1636a (possible left missing distal end), IMNH 44951, and IMNH 44946 (possible right missing proximal portion).

The radii (Fig. 16L-M), similar in form to other orodromines, have a straight to somewhat bowed shaft and slightly expanded proximal and distal ends. The proximal portion is reniform, with the convex edge facing laterally and the concave edge facing

medially. The proximal articular surface is overall slightly convex, but with a slight central concavity. The shaft of the radius is roughly oval to triangular in cross section with a smooth surface. The distal ends of available specimens are either missing or crushed, but appear similar to other basal ornithischians with a sub-circular shape. In IMNH 44951, the radius is slightly over 90% the length of the humerus.

Manus—An incomplete manus (Fig. 16N-P) is represented in MOR 1642 by what are interpreted as intermedia as well as multiple examples of other carpal elements, a complete (possibly III) and two partial metacarpals (possibly II and IV), and five partial to complete manual phalanges. In MOR 1642 the metacarpals (Fig. 16P) are loose, better preserved, and much more useful for description. A partial articulated right manus is preserved in IMNH 44951 (Fig. 20C) which includes metacarpals tentatively assigned as II, III, IV, and V. Unfortunately, II was only an imprint that was inadvertently removed during preparation.

The element interpreted as the intermedium (Fig. 16N) is sub-cubical in shape. It has two opposing surfaces, possibly articular surfaces, with a smooth finish resembling a polish. The remaining four surfaces are not polished. Another possible carpal, a cuboidal element (Fig. 16O) with one polished convex surface, likely represents the radiale or ulnare based on the *Hypsilophodon* manus description (Galton 1974).

The incomplete element interpreted as metacarpal II consists of the proximal and distal portions, with the proximal and distal portions being expanded similarly to metacarpal III. The element interpreted as metacarpal III is the longest metacarpal; this

element is elongate and slender, with, as in metacarpal II, the proximal end being transversely wider than the less expanded distal ends. The proximal end of metacarpal III is slightly wider transversely than it is tall. What is tentatively identified as the palmar surface of the proximal half of metacarpal III is concave. The distal end is weakly bicondylar, with a roughly flat dorsal surface, and a slight concavity ventrally. The lateral and medial faces of the condyles are slightly concave.

Metacarpal IV is shorter with a convex, wider-than-tall proximal end, and a squarer convex distal end. All of the metacarpals are more elongate and slender than those in the unnamed Kaiparowits Formation orodromine (Gates *et al*., 2014), but similar to those of *Orodromeus* (Scheetz, 1999).

Four squat manual phalanges are preserved in MOR 1642, but no ungual phalanges are known. These phalanges (Fig. 16P) are proximally and distally expanded; they exhibit very slightly concave proximal ends and bicondylar distal ends with lateral and medial ligament pits. The distal phalanges are proximodistally shorter than the proximal phalanges, but otherwise similar in form. The ungual phalanges may have been similar to the anteroposteriorly short but proximally transversely expanded ungual phalanges of the Kaiparowits orodromine (Gates *et al*., 2013).

Ilium—A complete juvenile right ilium (Fig. 17B-C) is preserved in MOR 1636b and an adult right ilium (Fig. 16A) in MOR 1642, where it is articulated with the sacrum. Fragments of ilia are known from most Wayan specimens, but are of little diagnostic value. The ilia of MOR 1636b and MOR 1642 are used for description here. Variation

between the juvenile (MOR 1636b) and adult (MOR 1642) ilia, such as the orientation of the ischiac peduncle and the form of the postacetabular process reflect taphonomic distortion and/or ontogenetic change.

The ilium (Fig. 17A-C) is an elongate blade-like element. Originally, based on MOR 1636b, the ilium of *Oryctodromeus* was described as having a short preacetabular process (Varricchio *et al*., 2007), but it is now recognized that the anterior-most portion of the paratype ilium represents a broken surface. Based on MOR 1642, the preacetabular process is more elongate as in other basal neornithischians. In MOR 1636b, the dorsal margin is slightly concave in lateral view, while in MOR 1642 the dorsal margin is slightly convex. The acetabulum is placed more anteriorly in MOR 1642 in comparison to that of MOR 1636b. As in *Orodromeus* (Scheetz, 1999), the top of the acetabulum is transversely expanded forming a roof. The pubic peduncle is anteroventrally directed and moderately mediolaterally expanded with a flat ventral termination. The ischial peduncle is robust and ventrolaterally directed and features a prominent globular boss. The brevis shelf consists of a mediolaterally sloping shelf that expands medially and begins at the ischial peduncle and extends to the end of the postacetabular process. A prominent ridge runs along the medial side of the preacetabular process, centrally placed on the ilium of MOR 1636b (the medial surface is not visible on MOR 1642), and extends to above the acetabulum.

Pubis—MOR 1636b and MOR 1642 both preserve complete pubes. Fragmentary pubes are known from IMNH 44930 and IMNH 44920. Description here is based on MOR 1642, a complete left pubis.

The pubis (Fig. 17D-E) is elongate and very delicate with long prepubic and a very long and slender postpubic processes. The laterally compressed prepubis extends and tapers anteriorly. The post-pubic process is straight and laterally compressed proximally, becoming more rod-like distally. The robust main body of the pubis forms the anteroventral portion of the acetabulum and contains a medially projecting boss that articulates with the sacropubal articulation of the second and third sacral centra. In MOR 1642 and MOR 1636b the obturator foramen are both open, retaining a small posterior gap.

Ischium—Nearly complete left and right ischiae are preserved in MOR 1642, and fragments of ischiae are known from Wayan specimens. Description here is based on ischiae from MOR 1642.

The ischium (Fig. 17F-G) consists of an elongate rod-shaped bone which expands in the proximal portions to form the obturator process, pubic and iliac peduncles as well as the acetabular border. The pubic peduncle is smaller than the iliac peduncle and the acetabular border is slightly concave. The hook-like obturator process occurs approximately at one-third of the length of the element coming from the proximal portion. The posterior portion of the element becomes thinner and more blade-like. The distal third portion of the ischial blade, bearing a sulcus and dorsoventrally flanking ridges, slightly flares dorsoventrally and then tapers again. The distal-most portion terminates in a small expanded boss.

Femur—Most specimens preserve at least partial femora. A well preserved, but smaller, near complete left femur is known from IMNH 44920 and a larger but slightly crushed complete right femur is known from MOR 1642. Both of these femora are utilized for this description.

The femur (Fig. 18A-F) is moderately robust in larger individuals such as MOR 1642 and slightly more gracile in smaller individuals such IMNH 44920. The shaft is bowed anteriorly in undeformed specimens such as IMNH 44920. At midshaft near the fourth trochanter the shafts are triangular in cross section. The femoral head in all specimens is born on a distinct elongate neck, with a deep sulcus for the ligamentum capitis femoris angles obliquely on the caudal portion of the head, as in *Orodromeus* (Scheetz, 1999) and *Hypsilophodon* (Galton, 1974). With the shaft vertical, IMNH 44920, the prominent globular femoral head projects from the greater trochanter at an angle of about 35° from the horizontal, similar to the condition in *Koreanosaurus* (Huh *et al*., 2011) but different from that of other orodromines such as *Orodromeus* (Scheetz, 1999), which have a less prominent and straighter head. The angulation of the femoral head in MOR 1642 is slightly less, with juvenile specimen MOR 1636b displaying a nearly horizontal femoral head. The greater trochanter is laterally flattened as in the "Kaiparowits orodromine" and *Orodromeus* (Scheetz, 1999). The lesser trochanter is anterior of the greater trochanter and is separated from the greater trochanter by a small lateral cleft in the dorsal-most portion, with the rest of the lesser trochanter being fused to the greater. A pendant triangular fourth trochanter projects posteromedially on the proximal portion of the shaft, as in other taxa, e.g. *Orodromeus* (Scheetz, 1999). A

shallow pit for the insertion of the caudifemoralis muscle occurs medially on the shaft adjacent to the upper portion of the fourth trochanter, this pit is most prominent in larger individuals such as MOR 1642. Distally, the lateral condyle is smaller than, and projects slightly farther posteriorly, than the medial condyle. When femora are viewed anteriorly or posteriorly in a straight vertical plane, the medial condyle sits more proximally relative to the lateral condyle, suggesting the femur bowed out slightly laterally from the axis of the body when in articulation. The flexor intercondylar groove is deep while the extensor intercondylar groove is undeveloped in smaller individuals and modest in larger individuals such as MOR 1642.

Tibia— Portions of tibiae are known for all specimens included in this study. A smaller left tibia and a larger right tibia (from two different individuals) are associated with IMNH 44930, one complete tibia is known for MOR 1636a and three tibiae (two right and one left) occur with MOR 1642. All are the basis for this description.

Tibiae (Fig. 18G-M) are gracile in comparison to and longer than the femora, and bear a modest and rounded cnemial crest and a bifurcated lateral condyle, similar to *Orodromeus* but dissimilar to the "Kaiparowits orodromine". The lateral condyle is subequal in size to the medial condyle and the anterior cnemial crest. In lateral view tibiae are slightly bowed posteriorly, with the midshaft being triangular in cross section. In anterior view, the medial and lateral malleoli are separated by a ligament groove, widest at the base, which ascends the shaft up to one-quarter of its length. The anterior surface of the outer malleolus is flat while the posterior surface is markedly concave. In

contrast the posterior face of the inner malleolus is slightly convex while the anterior face is slightly concave.

Fibula—Fibulae are rare among remains so far recovered, two incomplete fibulae are known from IMNH 44930, and both are incomplete and lack distal ends. Proximal and distal portions of fibulae are also associated with MOR 1642, with one proximal fibula still in articulation with a right tibia. IMNH 44930 forms the basis for the description here.

The fibula (Fig. 18N-O) is a long, slender, simple element. The proximal head is anteroposteriorly expanded, with a significant medial concavity. The midshaft has a D-shaped cross section with the flat side medial, and changes to ovoid more distally, similar to *O. makelai* (Scheetz, 1999).

Tarsus—Astragali and calcanea are known for IMNH 46169, IMNH 44920, and IMNH 44939, and MOR 1642. In most of these specimens the astragali and calcanea are still in articulation, and in the loose specimens bone quality is poor, making discernment of details difficult. In IMNH 44939, the specimen described below, an astragalus is articulated on a left tibia (Fig. 18M) and a calcaneum and astragalus are articulated on a larger right tibia. A free left, loose astragalus also occurs with IMNH 44930 and two partial astragali with MOR 1642. What it tentatively identified as the lateral distal tarsal is preserved with MOR 1642, and a medial distal tarsal element is still in articulation with the proximal portion of metatarsal II.

The astragalus (Fig. 18M, 19A-C) is very similar in form to *Orodromeus*, having a transversely elongate and low profile in anterior view, with a forked ascending process, similar to that of *Orodromeus* and *Jeholosaurus* (Han *et al*., 2012; Scheetz, 1999). The astragalus is roughly twice the mediolateral length of the calcaneum. Few details are discernible on the calcaneum due to them still being articulated with the astragali. In distal view the calcaneum is diamond shaped, while in lateral view it is ovoid The calcaneum fits firmly against the astragalus in IMNH 44939.

The lateral distal tarsal (Fig. 19D-F) is an irregularly and rectangular shaped bone overall similar in form to that of *Orodromeus* (Scheetz, 1999). As in *Hypsilophodon* (Galton, 1974) and *Orodromeus*, the proximal and distal surfaces are concave. Few details are discernible on the medial distal tarsal (Fig. 19G-I) since it is still in articulation, but overall its form is similar to that of other small neornithischians such as *Hypsilophodon* (Galton, 1974). This element is transversely elongate, with a mediolaterally extending ridge that occurs proximally on the more medial two-thirds of this element. There is a prominent groove exposed ventrally on the more lateral portion exposed in MOR 1642.

Pes—Pes elements are known from most *Oryctodromeus* specimens. Fully articulated left and right pes elements (from two differently sized individuals) occur in IMNH 44939 In addition this specimen has a third smaller partial articulated pes. MOR 1642 includes a beautifully preserved mostly complete right pes (Fig. 19G-K) and fragmentary additional pes elements. IMNH 44930 and MOR 1642 are used for this description.

The pes is similar in form to basal ornithopods such as *Hypsilophodon* (Galton, 1974), *Orodomeus* (Scheetz, 1999) and *Zephyrosaurus*. As in most ornithopods, the foot consists of five metatarsals, three of which are functionally weight bearing. The phalangeal formula is 2-3-4-5-0.

Proximally, metatarsal I, which is slightly less than half the length of metatarsal III, is thin and laterally flattened. Just distal of the midsection, the shaft of metatarsal I expands into a shaft with an ovoid cross section, as in *Orodromeus* (Scheetz, 1999), that ends in an articular condyle. The mediolaterally compressed metatarsal II, which ends in two well-developed articular condyles, diverges medially from metatarsal III near the distal third of metatarsal III. Metatarsal III is the stoutest and largest metatarsal, with the head being rectangular while the head of metatarsal IV is triangular. Metatarsal III has the most well-developed distal condyles. Distally, metatarsal IV, which ends in weakly-developed condyles, diverges from metatarsal III as in *Orodromeus* (Scheetz, 1999). Metatarsal IV and II are roughly equal in length, and shorter than metatarsal III. Metatarsal V is a thin blade-like bone with a rounded proximal articulation and rounded point at the distal end. Metatarsal V is two-thirds the length of metatarsal I.

Non-terminal phalanges are of the typical basal ornithopod form, with well-developed collateral ligament pits. Phalange II-1 is distinctly elongate in comparison to the rest of the non-terminal phalanges, as in other forms such as *Orodromeus* (Scheetz, 1999) and *Jeholosaurus* (Han *et al*., 2012). The proximal-most phalanges have single proximal concavities for articulation with the distal ends of the metatarsals, while the more distal phalanges have bi-lobed proximal articular surfaces that articulate with the

condyles of the preceding phalanges. Pedal unguals (Fig. 19K) are slightly wider than high, distinctly elongate, triangular in cross-section, and slightly concave to entirely flat ventrally. A groove flanks both sides of the unguals and extends to the distal tips, which end in sharp points.

DISCUSSION

Phylogenetic Analysis and Review— Orodromines, first defined by Brown *et al*. (2013), are defined as all neornithischians more closely related to *Orodromeus makelai* than to *Thescelosaurus neglectus* (Brown *et al*., 2013; Boyd, 2015). The placement of *Oryctodromeus* within the clade Orodrominae is well supported from numerous analyses (Varrichhio *et al*., 2007; Brown *et al*., 2013; Boyd, 2015). In the original description, Varricchio *et al.* (2007) used the character matrix of Scheetz (1999) to place *Oryctodromeus* phylogenetically using parsimony. They found that *Oryctodromeus* was a sister taxon to a clade composed of *Orodromeus* and *Zephyrosaurus*. In this same analysis it was found that *Oryctodromeus*, *Orodromeus*, and *Zephyrosaurus* formed a more inclusive clade of basal ornithopods that were united through the presence of the sharp scapular spine and the sacropubal articulation. The analysis of Brown *et al*. (2013), recovered the same results for the clade Orodrominae, with an *Orodromeus-Albertadromeus-Zephyrosaurus* subclade that was sister to a subclade containing *Oryctodromeus* and a partial orodromine skeleton (TMP 2008.045.0002). Most recently, the Orodrominae have been recovered as a subclade of the Parksosauridae, and sister taxon to the Thescelosaurinae (Fig. 22A). Parksosauridae includes the majority of ’hypsilophodont-grade’ ornithopods (Boyd, 2015). Two unambiguous synapomorphies

unite the Orodrominae, a sharp scapular spine (character 158) and a fibular shaft that is "D-shaped" in cross section throughout its length (character 233). In the analysis of Boyd (2015), the Orodrominae is composed of two subclades, one containing *Oryctodromeus* and *Koreanosaurus*, and one consisting of *Zephyrosaurus*, *Orodromeus*, and the Kaiparowits orodromine.

Results and Discussion— To elucidate the phylogenetic position of *Oryctodromeus* within orodrominae and among basal neornithischians, we modified the matrix of Boyd (2015). We corrected and added new data for *Oryctodromeus* from additional specimens, primarily MOR 1642 (see Appendix 1 for the character scores). The revised matrix consists of 255 characters and consists of the original 65 taxa from Boyd (2015). We updated 33 characters for *Oryctodromeus* (not available previously) from the original matrix of Boyd (2015). *Albertadromeus* was not included in this analysis due to the lack of a dataset for the matrix.

Our analysis placed *Oryctodromeus* in an unresolved polytomy consisting of *Oryctodromeus*, *Zephyrosaurus*, *Orodromeus*, *Koreanosaurus*, and the 'Kaiparowits orodromine'. The successive outgroup to this polytomy consists of a larger polytomy of basal cerapodan taxa. Due to the recovery of the initial polytomy, the analysis was run twice more removing successively more fragmentary taxa (those missing eighty percent or more and fifty percent or more data). Results of the second analysis (where taxa with eighty percent or more of the characters were unknown) are indicated in figure 22B. Unfortunately with each subsequent analysis the same polytomy was recovered. The removal of the two most fragmentary orodromine taxa in the final analysis,

Koreanosaurus and the Kaiparowits taxon, offered no further resolution as well. The persistence of this polytomy suggests caution in overconfidence of parsimony analyses. It has been demonstrated that parsimony analysis has the potential to produce false phylogenies that do not converge on the true phylogeny, even as more data is added to the data set (Felsenstein, 1978). The use of Bayesian anaylsis as utilized here provides an alternate method to test the results that have been recovered from the previous parsimony analyses discussed. This testing allows the potential for alternate phylogenies that could be further investigated when recovered. Though our results add nothing new on the placement of *Oryctodromeus* within the Orodrominae, our analysis confirms previous analyses supporting the monophyly of the Orodrominae, as well as shows the need for more research and more complete specimens of orodromines and other neornithischian taxa.

Numerous additional problems remain to be addressed within this and closely grouped clades. In his analysis, Boyd (2015) notes that the longest ghost lineage of any ornithischian taxa is the ghost lineage for Parksosauridae, with a time span of at least 40 myr between the Late Jurassic (Bathonian) and the Early Cretaceous (Aptian). This strongly demonstrates the need for more data to show the earlier evolution of this Parksosauridae.

Anatomical Summary—As one of the most well-represented members of the Orodrominae, *Oryctodromeus* specimens allows a substantial understanding of the basic anatomy of this organism (Fig. 20-21). The tentative skull reconstruction (Fig. 3), based on the available elements, indicates a broad posterior portion of the skull, with a laterally

compressed and pointed and beaked muzzle. The narrowness of the beak suggests a more selective dietary habit. Additionally, large orbits and eyes are suggested by the available elements. In summary these features of the skull are similar to those of other orodromines.

Based on a skeletal mount at the Museum of the Rockies incorporated from cast elements of MOR 1642 and MOR 1636a, and on the number of caudals indicated by IMNH 44920, a total length of 3.3 meters is indicated for larger individuals. More than half of this animal's total length consists of the tail (Fig. 21). A weight of twenty-eight kilograms is suggested for the largest individual (MOR 1642) through the equation of Anderson *et al*. (1995). The elongate dorsal and cervical centra indicate a longer neck and somewhat longer torso (Fig. 20A-B) in comparison to other related taxa such as *Orodromeus*. The significance of this slight elongation of the vertebrae is currently unknown.

A hip height of roughly one meter is indicated by the skeletal mount and recovered specimens. As discussed by Varricchio *et al*. (2007), a relatively narrow trunk breadth of roughly 30 cm is indicated by the dorsal ribs and scapulocoracoid of MOR 1636a, with MOR 1642 representing a slightly larger individual. Varricchio *et al*. (2007) noted that the width of the holotype burrow was virtually identical to the estimated width of the holotype burrow tunnel.

The forelimb and hindlimbs of *Oryctodromeus* are similar in proportions to those of most closely related taxa, excluding *Koreanosaurus*. The forelimbs are less than half

the length of the hindlimbs, indicating a bipedal habit as in most other orodromines; and the tibia is slightly longer than the femur, indicating at the least a moderate running capability.

Osteological Implications—Unique features observed in the skeleton of *Oryctodromeus* have been attributed to its fossorial habit. These features include the fused premaxilla, often fused and robust scapulocoracoids, scapular spine, slightly more robust humerus (in comparison to other basal neornithischians), and additional sacral vertebrae in the sacrum (Varricchio *et al*., 2007; Fearon, 2015). Newly observed features described above appear to be related to a fossorial habit as well as complicate the fossorial interpretation. These features occur in the axial column as well as the appendicular skeleton.

As described above there is an extreme length of the tail with the high count (55+) of caudal vertebrae. The tail accounts for roughly two-thirds the length of *Oryctodromeus*. Though originally described as lacking ossified tendons (Varricchio *et al*., 2007), newly prepared specimens of *Oryctodromeus* demonstrate that at least some of the specimens (Fig. 15A, D; IMNH 44920, IMNH 44939, IMNH 44951, IMNH 45081, MOR 1642) have prominent tendon bundles. In the most complete specimen (Fig. 20A-B; IMNH 44951) prominent tendon bundles begin at the base of the neck and extends throughout the rest of the axial column. Presumably, the presence of ossified tendons and a tail representing roughly two-thirds of the body length would make maneuvering in a confined space, such as a burrow, a more difficult task. However, perhaps the mediolateral flexibility of a caudal column flanked by longitudinally arranged epaxial

and hypaxial tendons, as discussed by Organ (2006), would have allowed sufficient mediolateral flexibility while maintaining dorsoventral rigidity. Additionally, a specimen of *Tenontosaurus* in the MOR collections (MOR 682; Maxwell and Ostrom, 1995), has a nearly complete tail, encased in ossified tendons, curled dorsally back above itself suggesting significant flexibility in the ossified tendons.

A second problem involving the tail is its extreme length in *Oryctodromeus*, comprising roughly two-thirds of the animals length (roughly two of three meters). The holotype specimen was found in a burrow fill with a diameter of the tunnel leading to the terminal chamber being on average about 30 cm (Varricchio *et al*., 2007). The extreme length of the entire animal would suggest a fairly long complete burrow or burrow system substantially longer than the holotype burrow (Varricchio *et al*., 2007). Unfortunately the entire dimensions of the terminal chamber found with the holotype are unknown due to modern weathering of the trace fossil before it was discovered. The possibility exists that *Oryctodromeus* burrows had separate or multiple entrances and exits. This can only be tested with the discovery of additional burrow specimens.

The angle and length of the femoral head, which is more pronounced than in most other basal ornithopods (see above), is nearly identical to that of *Koreanosaurus* (Min *et al*., 2010). Interestingly, *Koreanosaurus* and *Oryctodromeus* form their own subclade within the Orodrominae in the analysis of Boyd (2015). As Min *et al*. (2010) postulates for *Koreanosaurus*, it is suggested here that this femoral morphology in *Oryctodromeus* allowed a more splayed posture of the hindlimbs for bracing of the body while the forelimbs and beak were engaged in scratch digging. In contrast to *Koreanosaurus*,

Oryctodromeus lacks the more extreme forelimb modifications, such as the robust humerus, that have been suggested to indicate a quadrapedal posture in *Koreanosaurus* (Min *et al*., 2010).

CONCLUSIONS

Oryctodromeus, known cumulatively from the majority of the skeleton, is among the most completely represented orodromine neornithischians, with only *Orodromeus* being known more completely. Only portions of the skull, cervical column, sternals, and some manual elements are presently unknown in *Oryctodromeus*. The skeleton exhibits numerous features consistent with a fossorial habit. These include previously described characters such as the fused premaxillae, useful for manipulation of soil; the fused scapulocoracoid with the scapular spine, providing an increased surface for muscle attachment; and the expanded sacrum and proximal caudals, also serving as areas for increased muscle attachment (Varricchio *et al*., 2007). The recovery of additional specimens since the original description has demonstrated an additional feature likely related to a fossorial habit, the elongate and angular head of the femora. As noted by Hildebrand (1985), extant fossorial mammals that dig with their forelimbs brace themselves with their hindlimbs. The morphology of *Oryctodromeus* femora likely allowed the animal to splay-out its hindlimbs for bracing while digging. An identical morphology and habit has been inferred for the orodromine *Koreanosaurus* (Huh *et al*., 2011).

These newly described *Oryctodromeus* specimens exhibit new characters distinct from other orodromines, and that are useful for diagnosis in conjunction with the previously described autapomorphies (Varricchio *et al*., 2007). These characters include elongate cervical centra, longer than those of *Orodromeus* and *Zephyrosaurus*, 1.6 times as long as high; elongate dorsal centra, similar to those of *Zephyrosaurus* but dissimilar to *Orodromeus*, 1.4 times as long as high; over 55 mostly elongate caudal vertebrae, similar to those of *Zephyrosaurus*, often enveloped in hypaxial and epaxial tendons; and a femoral head on an elongate neck, similar to that of *Koreanosaurus* but dissimilar to other orodromines, projecting from the greater trochanter at roughly 35° from the horizontal. The extremely long tail, often with a thick lattice of ossified tendons, composes roughly two-thirds the length of the animal. The occurrence of the tendon lattice in the tail as well as tendons in the sacral and dorsal column of this burrowing taxon suggest a greater degree of flexibility for ossified tendons than has often been supposed.

The orodromine clade is rapidly increasing in diversity with the recent reports of *Koreanosaurus*, *Albertadromeus*, and the unnamed "Kaiparowits orodromine" (Huh, 2010; Brown *et al*., 2013: Gates). Recent analyses have strongly supported the monophyly of this clade (Brown *et al*., 2013; Boyd 2015). However, the less complete nature of some taxa such as *Zephyrosaurus* and *Koreanosaurus* demonstrate how much more there is to learn about the osteology of some orodromines. This additional data would further refine future phylogenetic analyses. This data and the discovery of more

basal taxa would assist with resolving the ghost-lineage for the Parksosauridae, which is currently the longest known ghost lineage for the Ornithischia (Boyd, 2015).

ACKNOWLEDGEMENTS

We thank the Jurassic Foundation, the Graduate School of Montana State University, and Robert Simon for funding that assisted with aspects of this research. L.K. thanks committee members T. Dyman, D. Bowen, and J. Horner for their assistance and revisions which improved the quality of this manuscript. Appreciation is expressed to M. Thompson and J. Scannella who allowed access to specimens under their care. A. Abusaidi and S. Robison assisted in the permitting process for collection of specimens from Caribou-Targhee National Forest and Barbara Beasley for permitting through Beaverhead-Deerlodge National Forest. A. Ferguson, K. Sutherland, and J. Wilson provided assistance in the field and with collection of *Oryctodromeus* specimens.

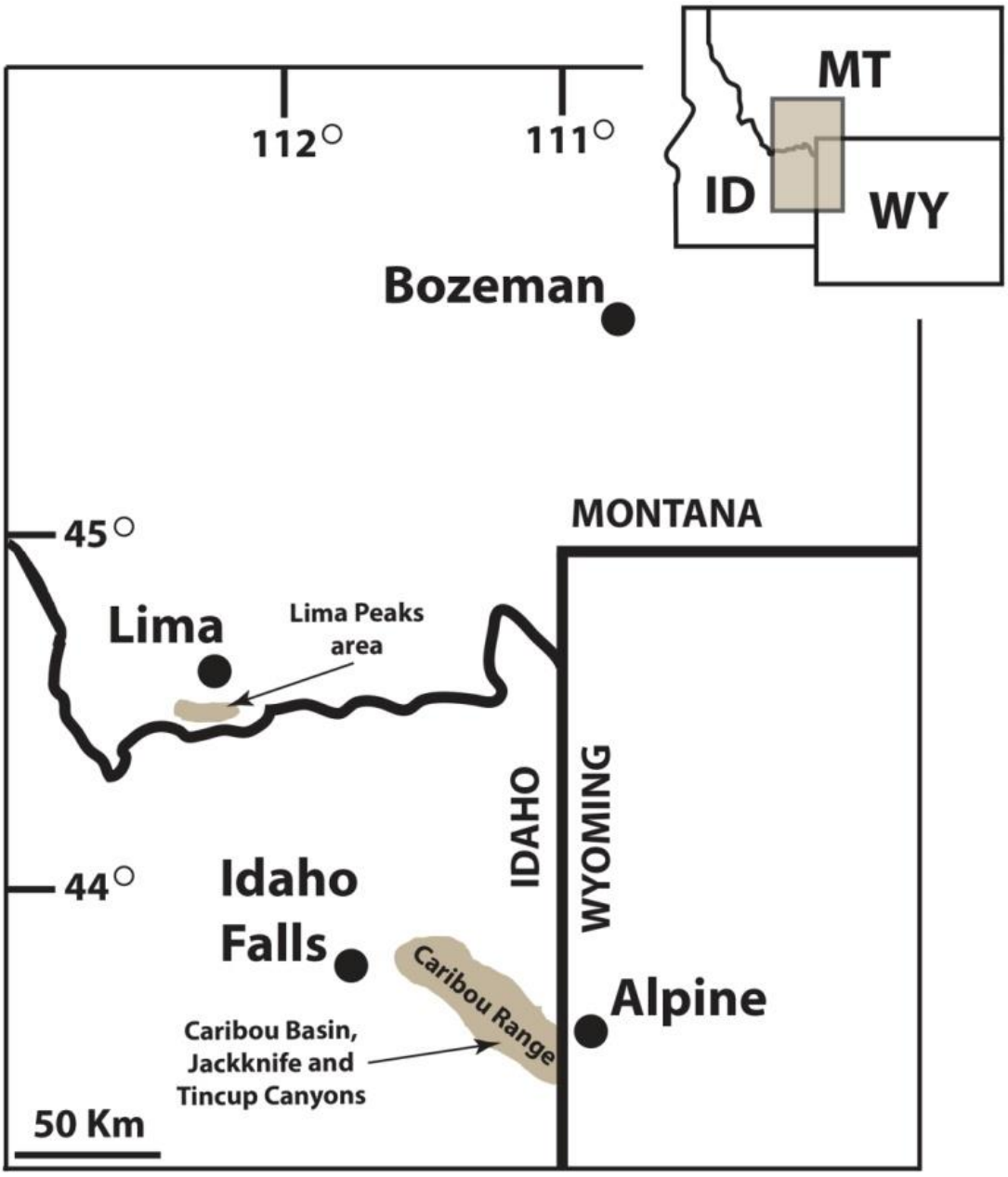

FIGURE 2.1. Outcrop areas of Wayan Formation (Idaho) and Vaughn Member of the Blackleaf Formation (Montana) where Oryctodromeus specimens have been recovered.

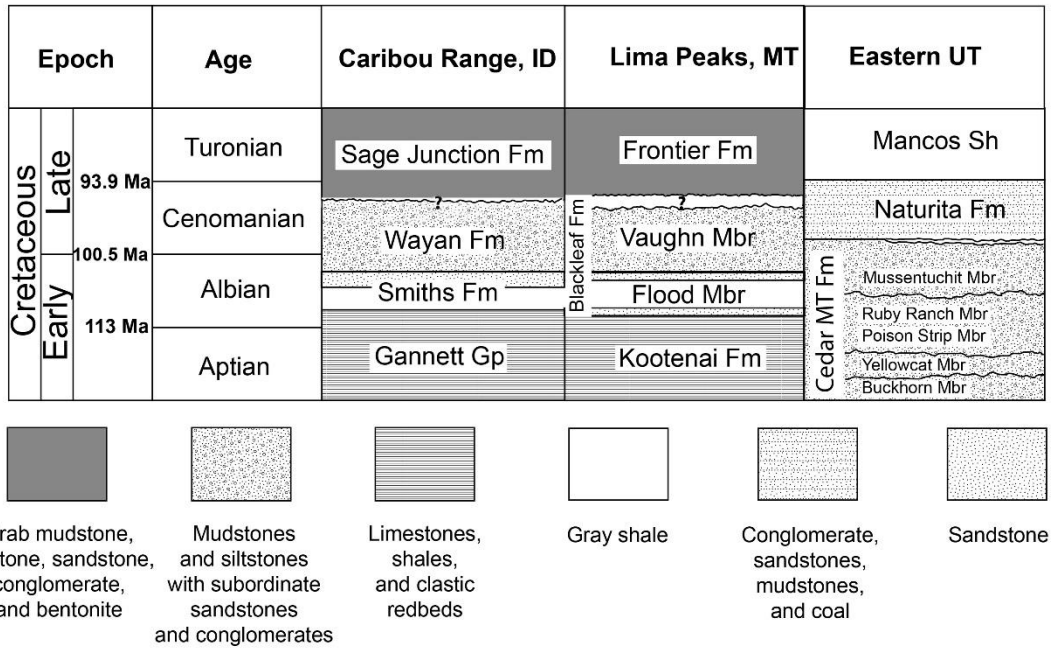

FIGURE 2.2. Stratigraphic setting and ages of the Wayan Formation (Idaho) and Vaughn Member of the Blackleaf Formation (Montana). Coeval geological units of eastern Utah are included as a basis for comparison with other Early to early Late Cretaceous vertebrate assemblages. Modified from Dorr (1985).

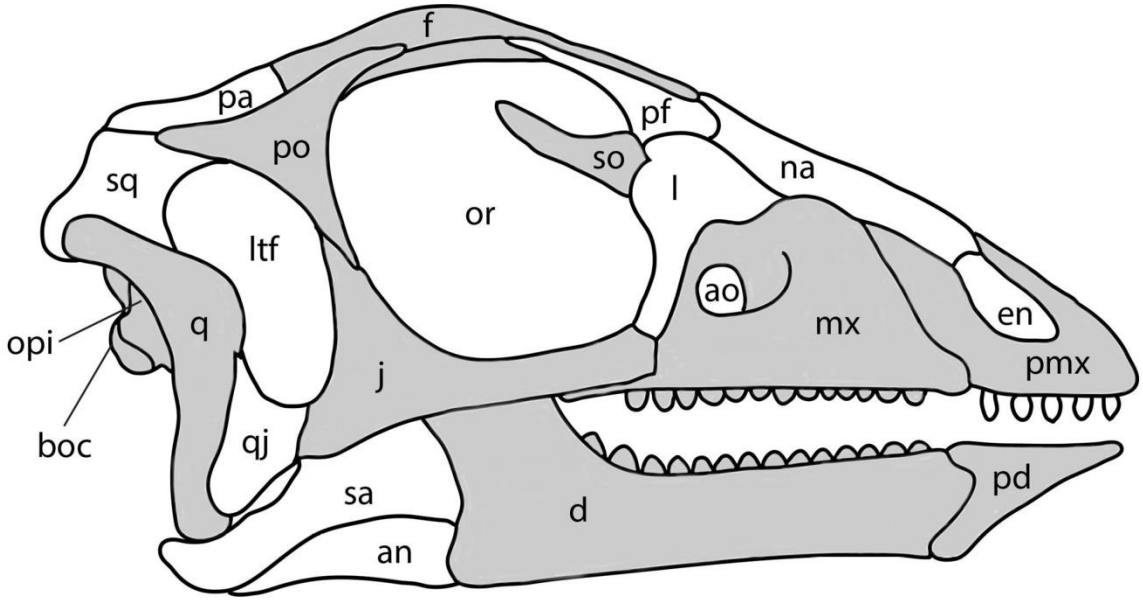

FIGURE 2.3. Reconstructed skull of *Oryctodromeus* in right lateral view. The reconstruction is based on elements from MOR 1636a and MOR 1642; as well as Scheetz (1999) restoration of the skull of *Orodromeus*. Elements not known are indicated in white, while elements known are indicated in gray. Not all elements known are complete bones (see text). A quadratojugal foramen is not shown since the quadrate is unknown and the foramen is variably present in *Orodromeus*. *Abbreviations*: *an*, angular; ao, antorbital fenestra; *boc*, basioccipital; *d*, dentary; *en*, external naris; *f*, frontal; *j*, jugal; *l*, lachrymal; *ltf*, lateral temporal fenestra; *mx*, maxilla; *na*, nasal; *opi*, opisthotic; *or*, orbit; *pa*, parietal; *pd*, predentary; *pf*, prefrontal; *pmx*, premaxilla; *po*, postorbital; *q*, quadrate; *qj*, quadratojugal; *sa*, surangular; *so*, supraorbital; *sq*, squamosal. Art by lead author. Scale bar equals 7 cm.

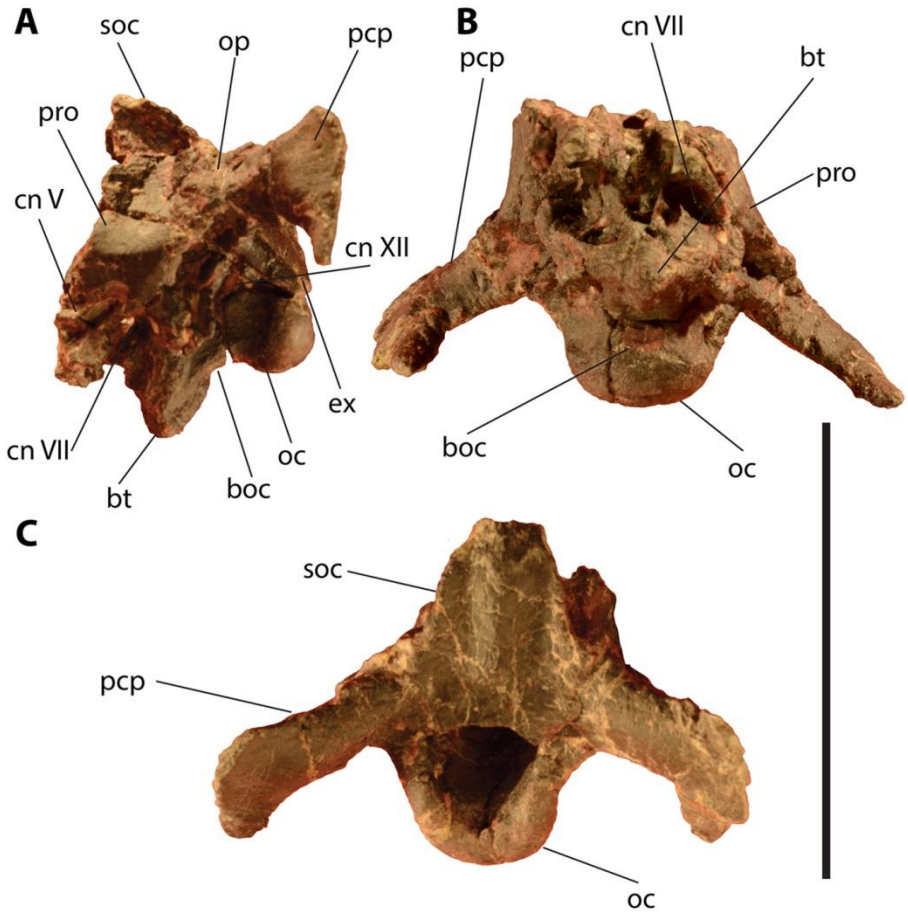

FIGURE 2.4. Braincase of *Oryctodromeus*. **A**, left lateral; **B**, ventral; **C**, caudal views. **Abbreviations**: **boc**, basioccipital; **bt**, basal tuber; **oc**, occipital condyle; **op-exo,** opisthotic-exoccipital; **pcp**, paraoccipital process; **soc**, supraoccipital. Scale bar equals 5 cm.

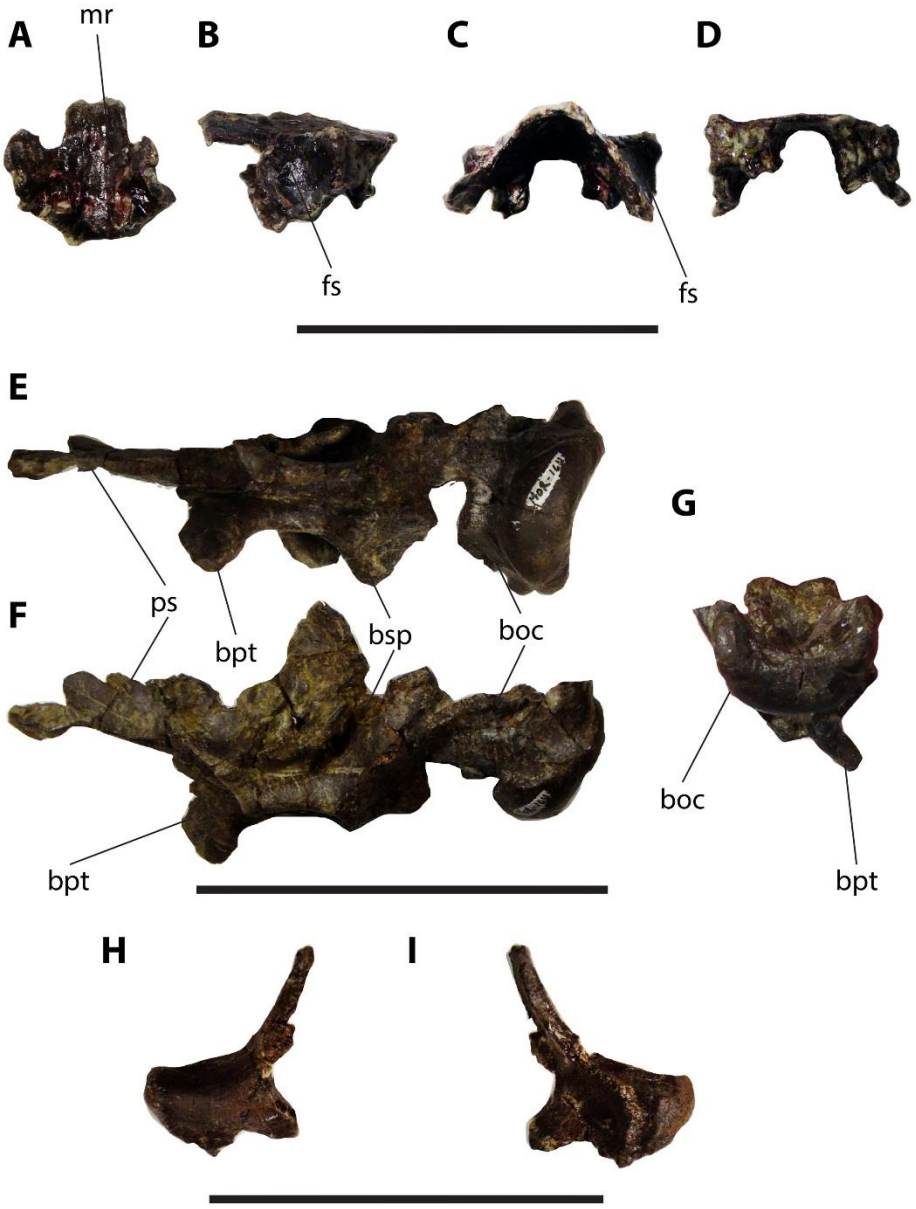

FIGURE 2.5. Supraoccipital, basioccipital, basisphenoid-parasphenoid, and laterosphenoid of *Oryctodromeus*. **A**, dorsal; **B**, left lateral; **C**, anterior; D**,** posterior views of supraoccipital from MOR 1642. **E**, ventral; **F**, left lateral; **G**, posterior views of basioccipital-basisphenoid-parasphenoid from MOR 1642. **H,** lateral; **I** medial views of aterosphenoid from MOR 1642. **Abbreviations**: **boc**, basioccipital; **bpt**, basipterygoid process; **bsp**, basisphenoid; **fs**, fossa subarcuata; **mr**, median ridge; **ps**, parasphenoid. Scale bars are 5 cm.

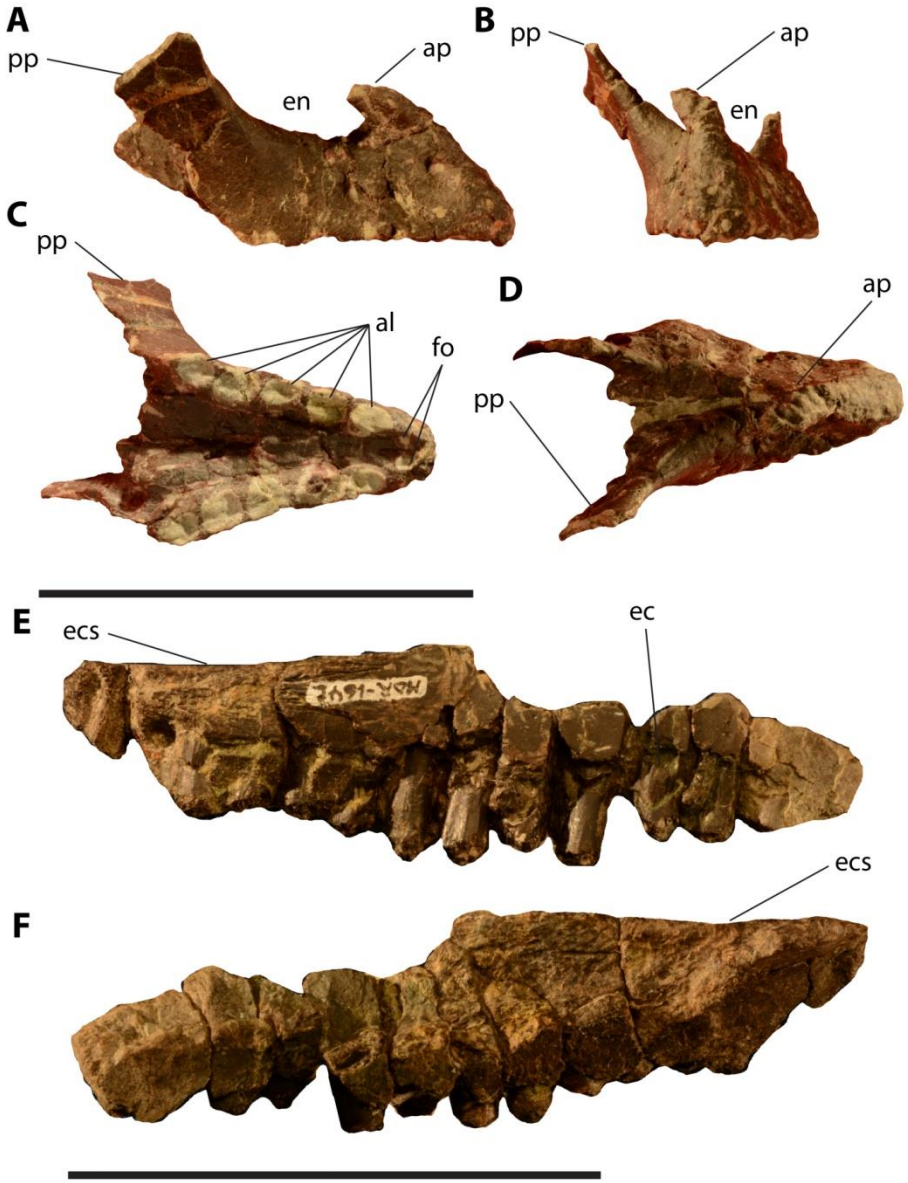

FIGURE 2.6. Premaxilla and maxilla of *Oryctodromeus*. **A**, right lateral; **B**, rostral; **C**, ventral; **D**, dorsal views of fused premaxilla of MOR 1636a. **E**, lateral; **F**, medial views of partial left maxilla of MOR 1642. **Abbreviations**: **al**, alveoli; **ap**, anterior process; **ec**, erupting maxillary tooth crown; **ecs**; ectopterygoid shelf; **en**, external naris; **fo**, foramina; **pp**, posterior process. Both scale bars equal 5 cm.

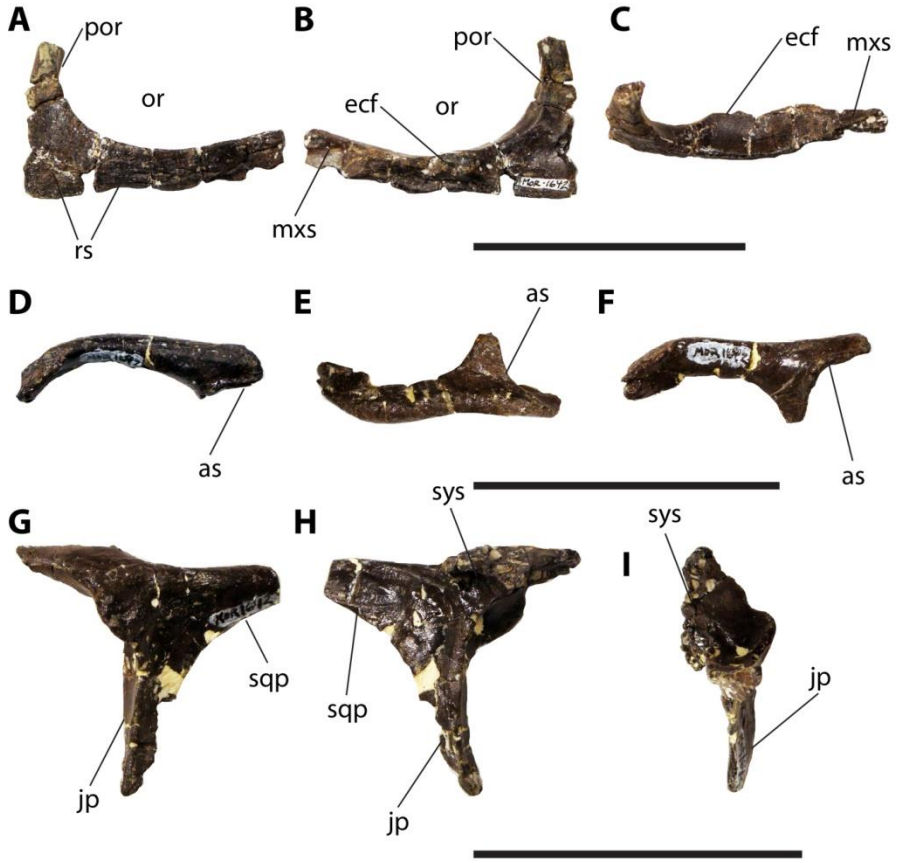

FIGURE 2.7. Jugal, supraorbital, and postorbital of *Oryctodromeus*. **A**, left lateral; **B**, medial; **C**, dorsal views of left jugal from MOR 1642. **D**, lateral; **E**, dorsal; **F**, ventral views of right supraorbital of MOR 1642. **G**, lateral; **H**, medial; **I**, ventral views of left postorbital from MOR 1642. **Abbreviations**: **as**; articular socket; **ecf**, ectopterygoid facet; **jp**, jugal process; **mxs**, slot for the jugal process of the maxilla; **or**, orbit; **por**, postorbital process; **rs**, rugose surface; **sqp**, squamosal process; **sys**, synovial socket. Scale bars equal 5 cm.

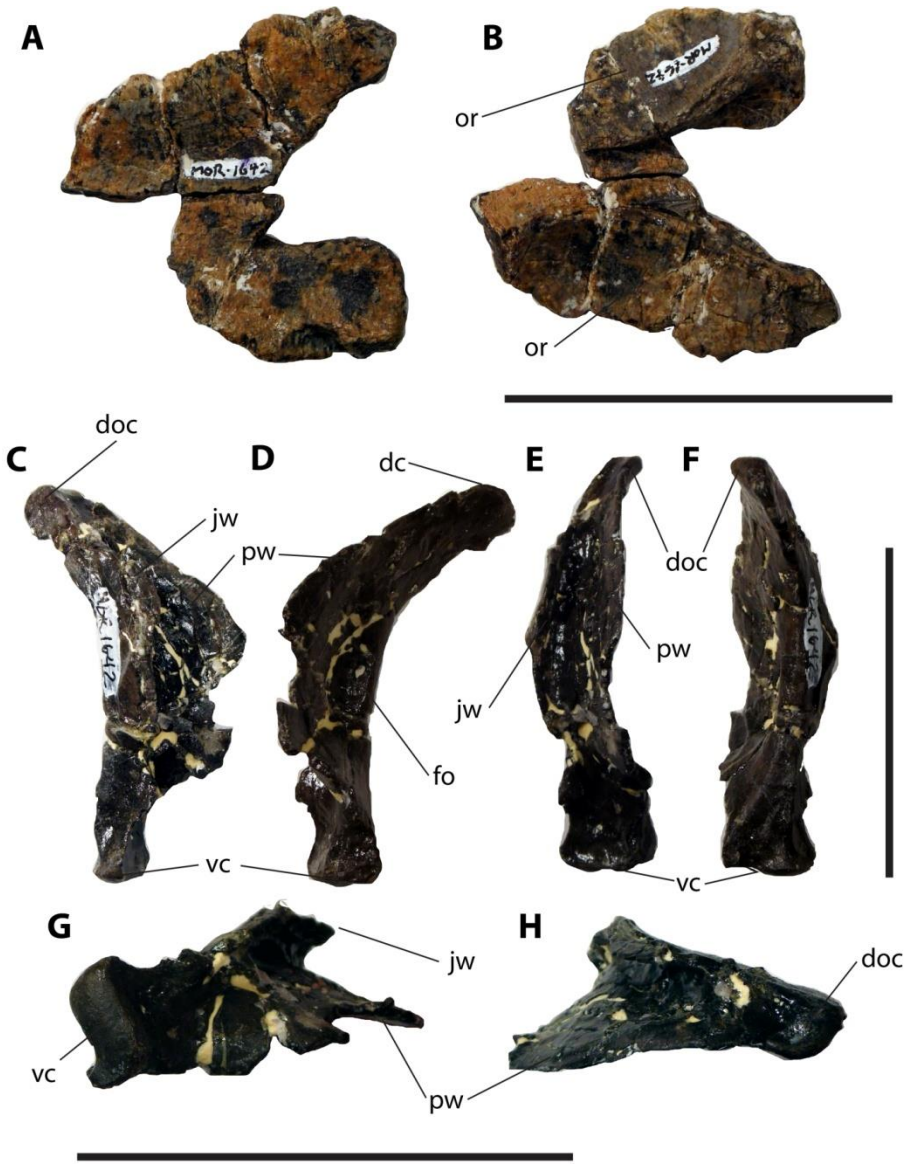

FIGURE 2.8. Frontals and quadrate of *Oryctodromeus*. **A**, dorsal; **B**, ventral views of partial left and right frontals from MOR 1642. **C**, lateral; **D**, medial; **E**, anterior; **F**, posterior; **G**, ventral; **H**, dorsal views of right quadrate from MOR 1642. **Abbreviations**: **doc**, dorsal condyle; **fo**, fossa; **jw**, jugal wing; **or**, orbit; **pw**, pterygoid wing; **vc**, ventral condyle. Scale bars are 5 cm.

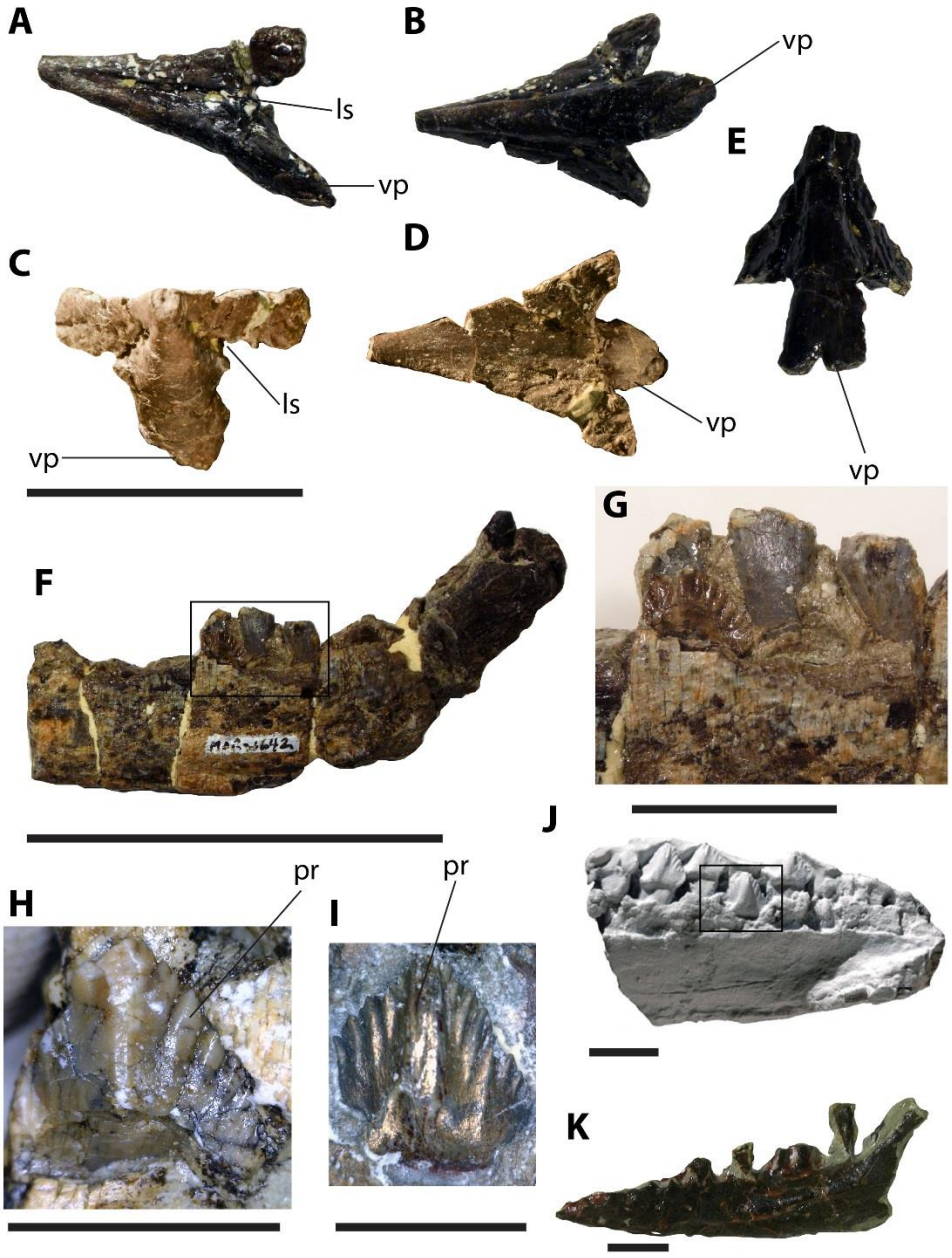

FIGURE 2.9. Predentary, dentary, and dentary teeth of *Oryctodromeus***. A**, left lateral; **B**, ventral; **C**, anterior; **D**, dorsal views of one predentary from MOR 1642. **E**, ventral view of second predentary from MOR 1642 showing the bifurcated ventral process. **F**, medial view of partial right dentary from MOR 1642. **G** and **H**, lingual views of dentary teeth of MOR 1642. The box in **F** highlights the area shown in **G**. **I**, view of dentary tooth highlighted by box in **J**. **J**, lingual view of partial left dentary with teeth of IMNH 44946. **K**, lateral view of left dentary of MOR 1636b. Scale bars A-E equal 3 cm; F equals 5 cm; G equals 1 cm; H equals 5 mm, I equals .5 cm, J and K equals 1 cm.

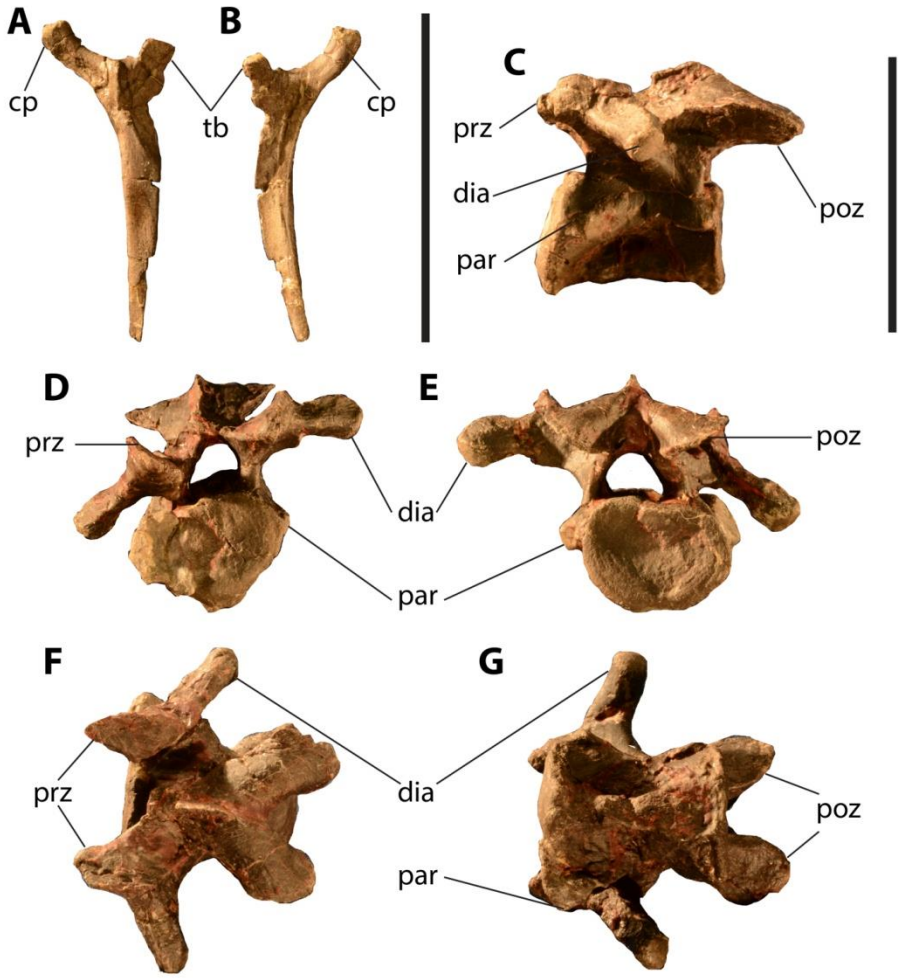

FIGURE 2.10. Cervical rib and cervical vertebra of *Oryctodromeus***. A**, cranial; **B** caudal views of cervical rib of MOR 1642. **C**, left lateral; **D**,cranial; **E**, caudal; **F**, dorsal; **G**, ventral views of middle cervical vertebra of MOR 1636a. **Abbreviations**: **cp**, capitulum, **dia**, diapophysis; **par**, parapophysis; **poz**, postzygapophysis; **prz**, prezygapophysis; **tb**, tuberculum. Scale bar for cervical rib is 5 cm, scale bar for cervical vertebra is 4 cm.

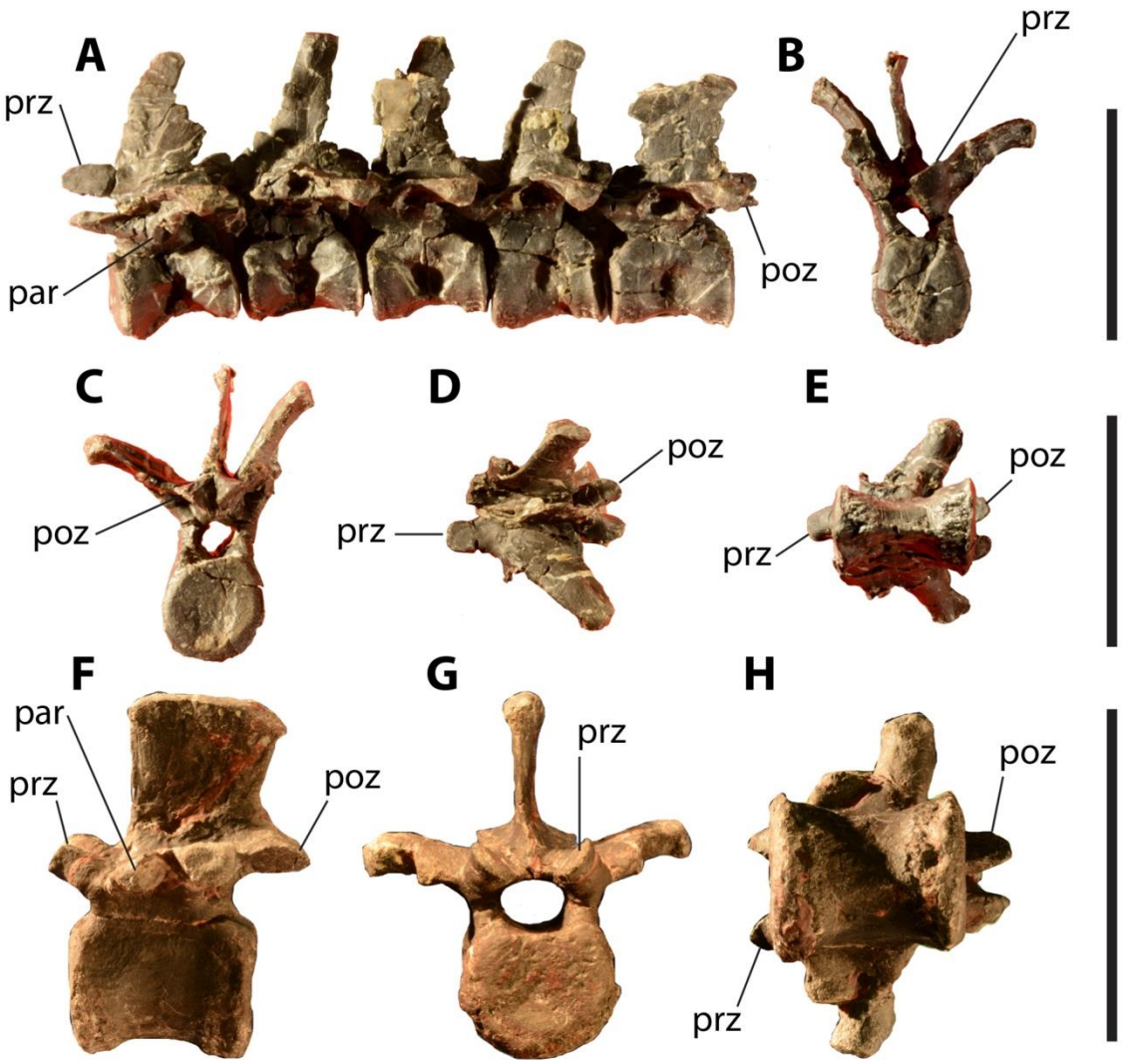

FIGURE 2.11. Dorsal vertebrae of *Oryctodromeus*. **A**, left lateral view of articulating series of five anterior dorsal vertebrae from MOR 1642. **B**, anterior; **C**, posterior; **D**, dorsal; **E**, ventral views of posterior-most vertebra of same articulating series from MOR 1642. **F**, lateral; **G**, anterior; **H**, ventral views of posterior dorsal vertebra from MOR 1636a. **Abbreviations**: **par**, parapophysis; **poz**, postzygapophysis; **prz**, prezygapophysis. Scale bars equal 5 cm.

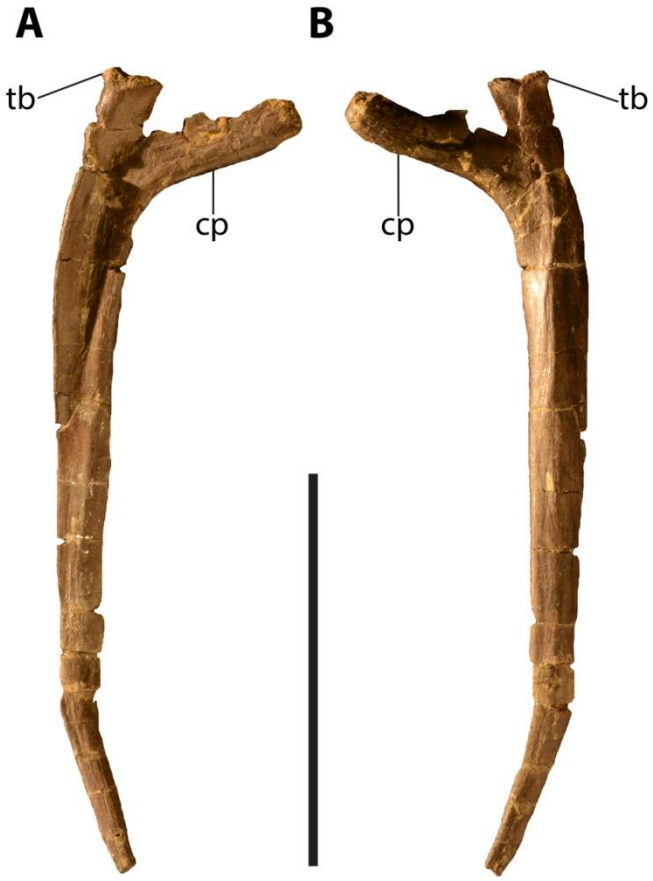

FIGURE 2.12. Dorsal rib of *Oryctodromeus*. **A**, caudal; **B**, cranial views of left dorsal rib of MOR 1642. **Abbreviations**: **cp**, capitulum; **tb**, tuberculum. Scale bar equals 5 cm.

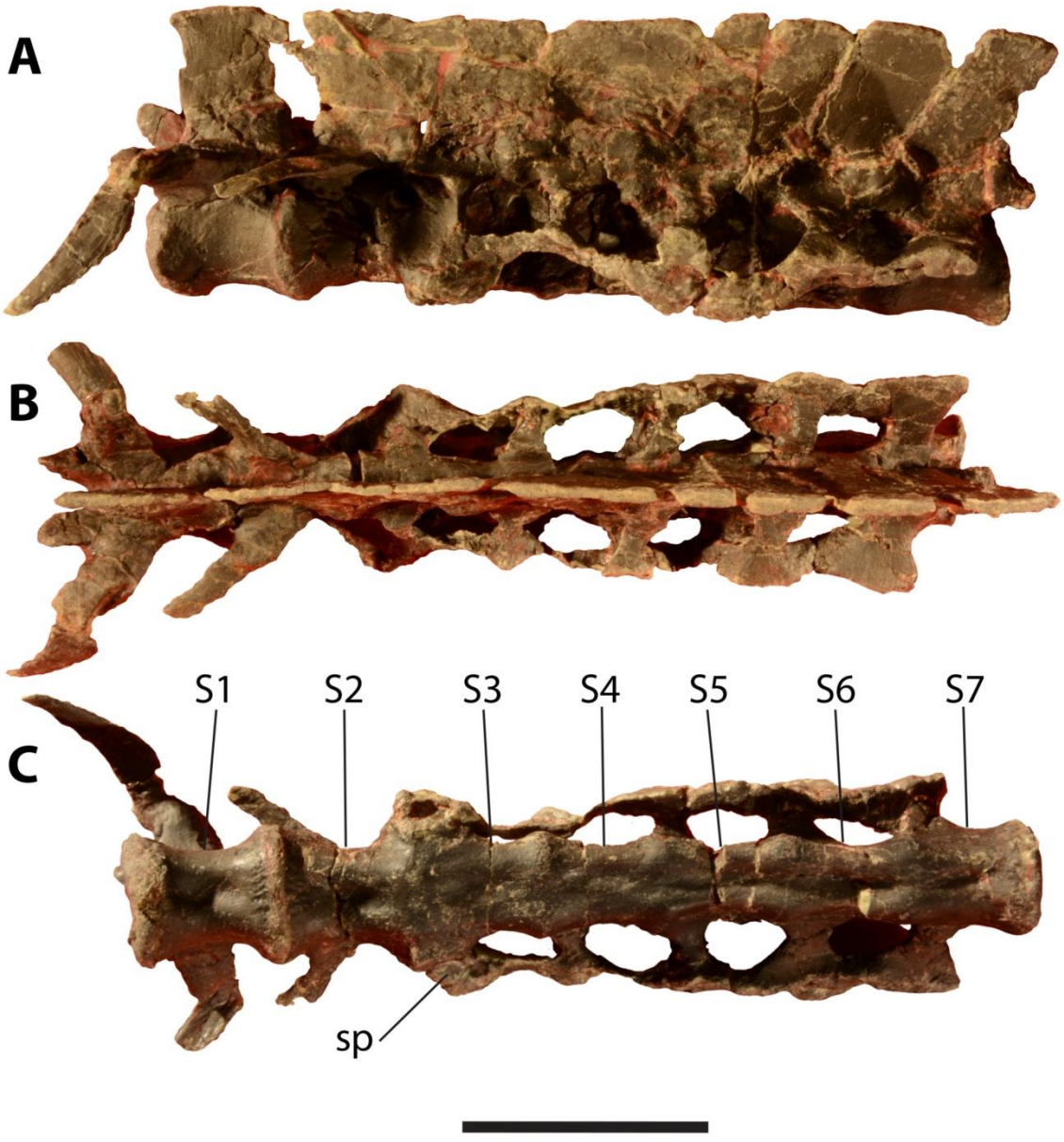

FIGURE 2.13. Sacrum of *Oryctodromeus* with individual sacral vertebrae (S1-S7) indicated. **A**, left lateral; **B**, dorsal, **C**, ventral views of sacrum of MOR 1636a. **Abbreviation**: **sp**, sacropubal articulation. Scale bar equals 5 cm.

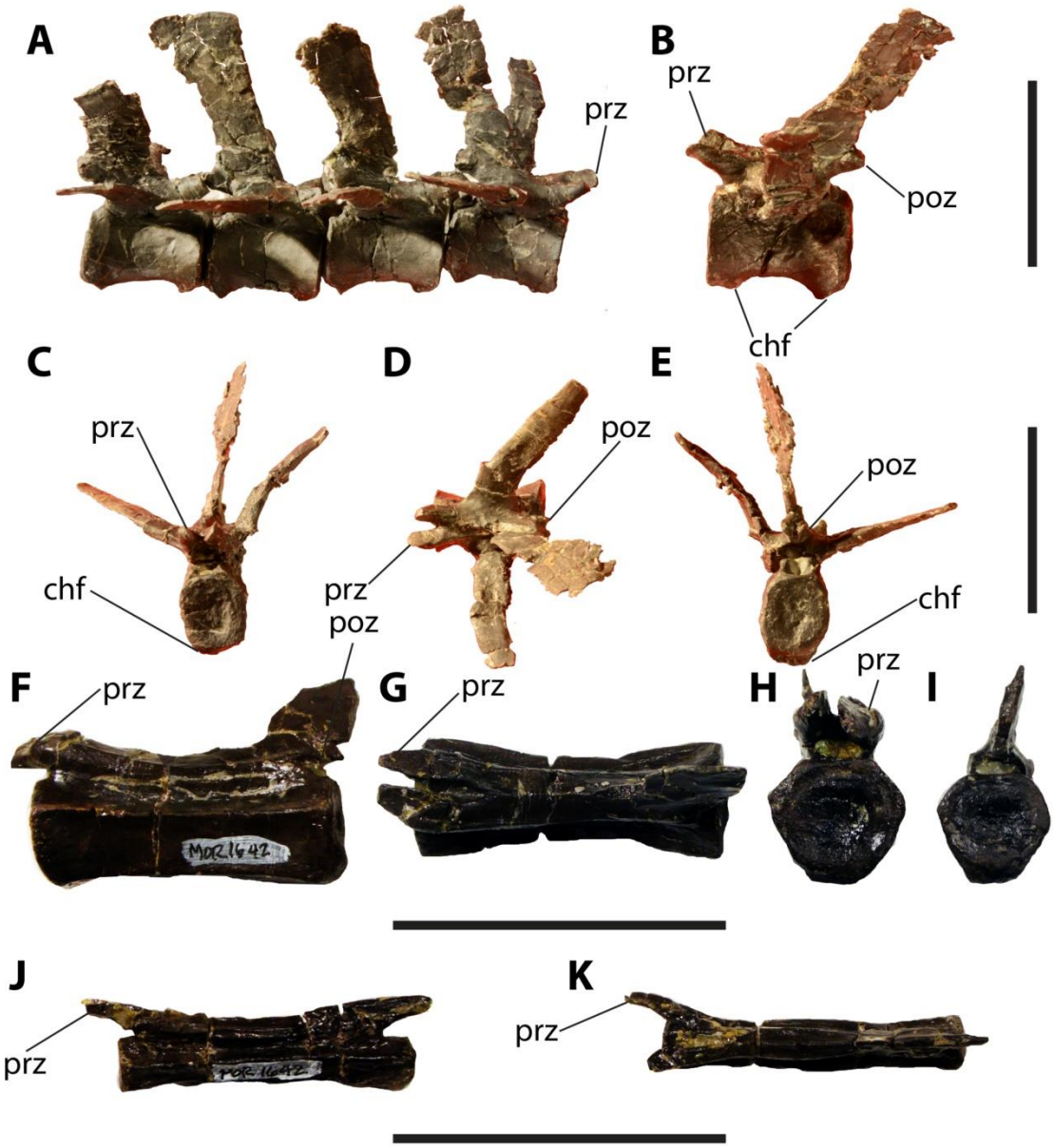

FIGURE 2.14. Caudal vertebrae of *Oryctodromeus*. **A**, right lateral view of articulating series of four proximal caudal vertebrae from MOR 1642. **B**, left lateral; **C**,anterior; **D**, dorsal; **E**, posterior views of anterior-most caudal vertebra from same series. **F**, left lateral; **G**, dorsal; **H**, anterior; **I**, posterior views of mid-caudal vertebra from MOR 1642. **J**, left lateral; **K**, dorsal views of distal caudal vertebra from MOR 1642. **Abbreviations**: **chf**, chevron facet; **poz**, postzygapophysis; **prz**, prezygapophysis. Scale bars equal 5 cm.

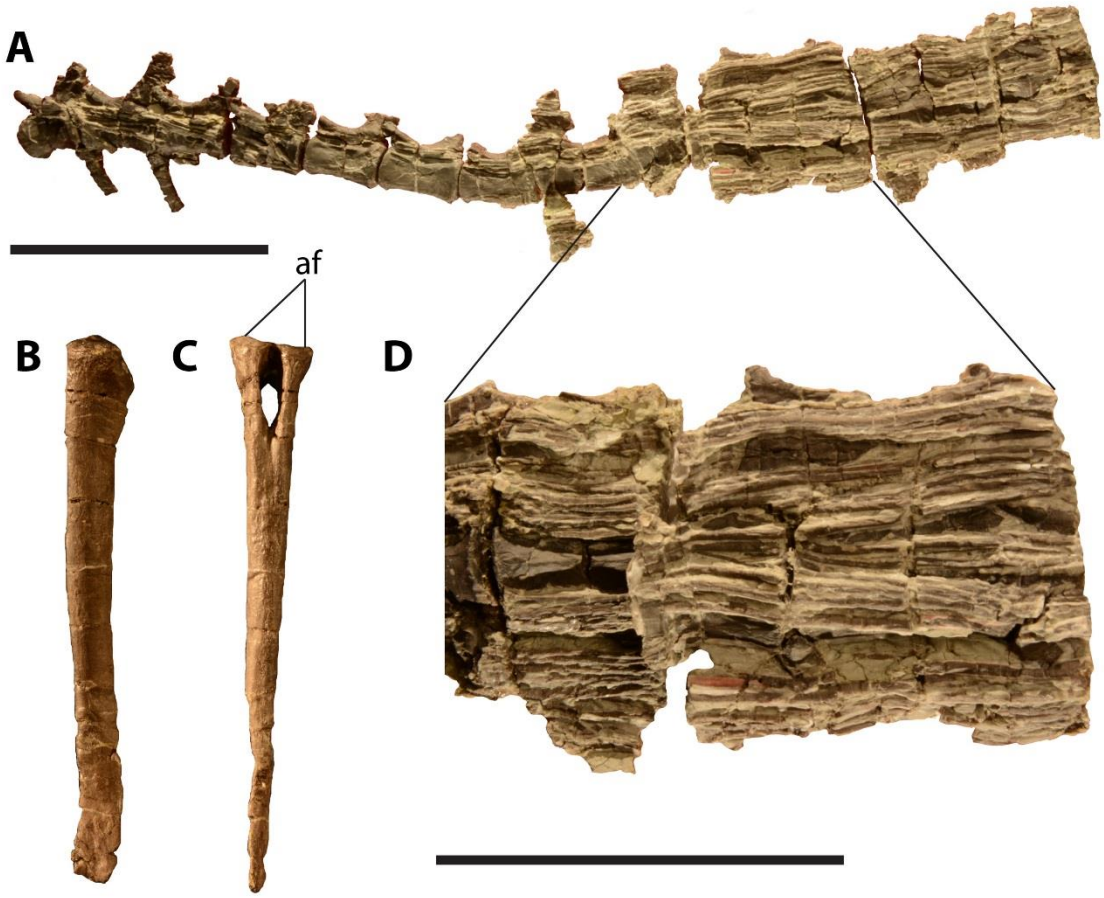

FIGURE 2.15. Ossified tendons and chevron of *Oryctodromeus*. **A**, left lateral view of articulated mid-caudal series of MOR 1642 with ossified tendons. Some tendons were removed on the more anterior portion during preparation of the specimen. **B**, left lateral view; **C**, anterior views of proximal or mid-chevron. **D**, closer view of tendon lattice in left lateral view. **Abbreviations**: **af**, articulation facet. Scale bars equal 5 cm.

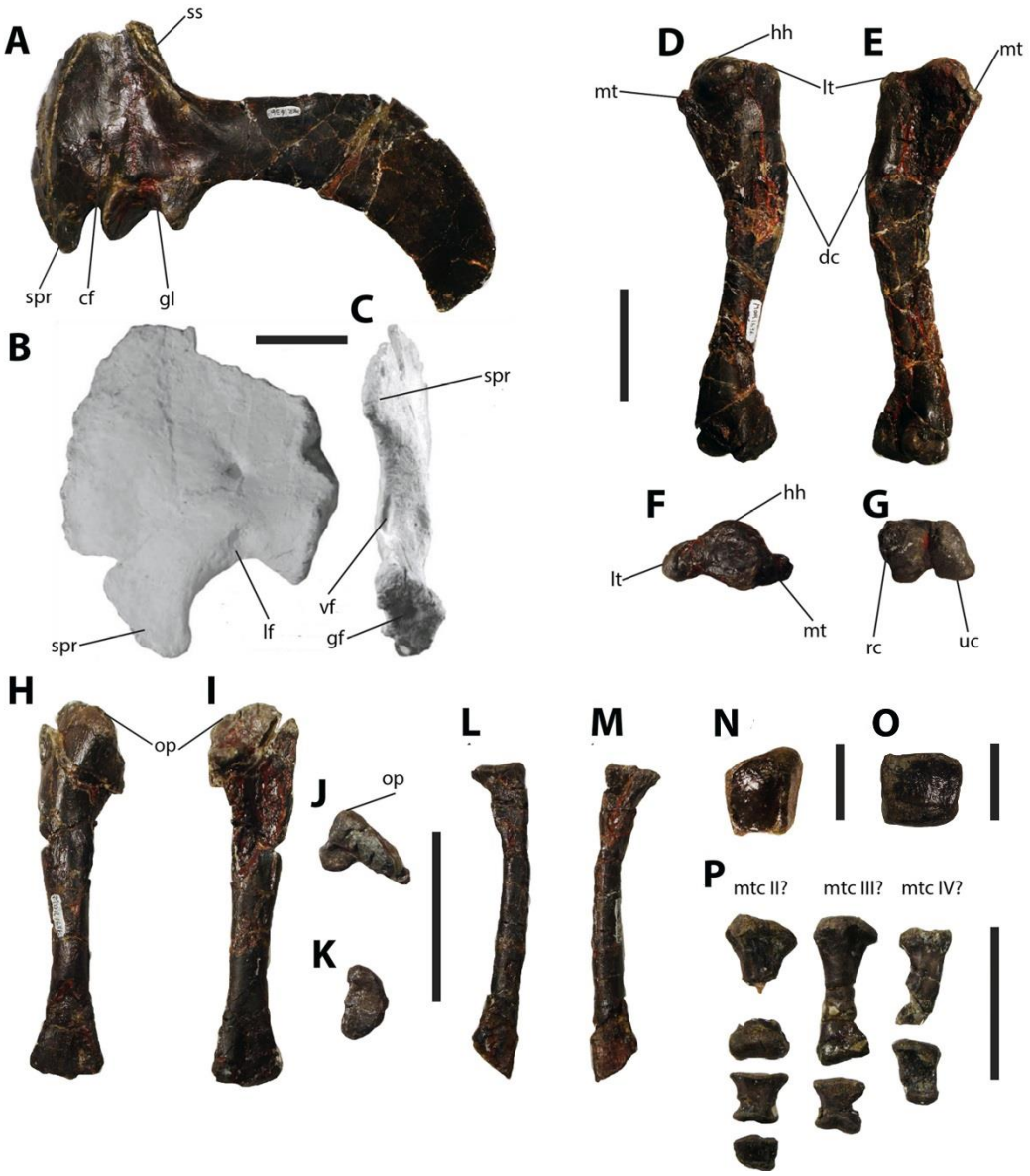

FIGURE 2.16. Pectoral girdle, forelimb, and manus of *Oryctodromeus*. **A**, lateral view of fused left scapulocoracoid from MOR 1636a. **B**, lateral; **C**, ventral views of left coracoid of IMNH 44939. **D**, lateral; **E**, medial; **F**, proximal; **G** distal views of right humerus of MOR 1636a. **H**, lateral; **I**, medial; **J**, proximal; **K**, distal views right ulna of MOR 1636a. **L**, lateral; **M**, medial views of radius from MOR 1636a. **N**, dorsal view of intermedium from MOR 1642; **O**, possible dorsal view of tentative radiale or ulnare from MOR 1642. **P**, dorsal view of partial manus. **Abbreviations**: **cf**, coracoid foramen; **dc**, deltapectoral crest; **hh**, humeral head; **lt**, lateral tuberosity; **mt**, medial tuberosity; **mtc**, metacarpal; **op**, olecranon process; **rc**, radial condyle; **ss**, scapular spine; **uc**, ulnar condyle. Scale bar (A, C-L) equal 5 cm. Scale bar (B) equals 2 cm. Scale bar (M-N) equals 1 cm. Scale bar (N-O) equals 2 cm.

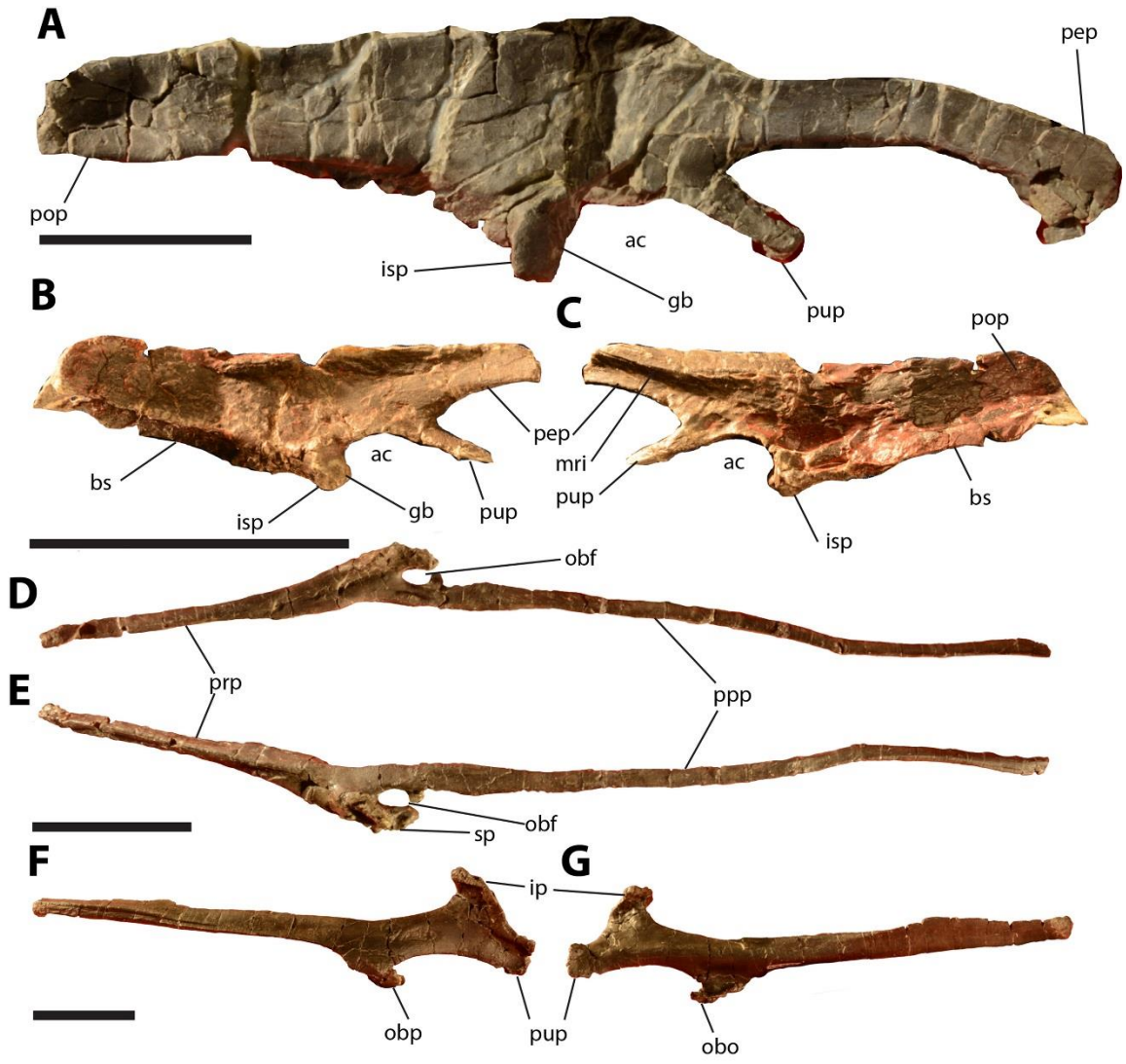

FIGURE 2.17. Pelvic girdle of *Oryctodromeus*. **A**, right lateral view of right ilium of MOR 1642. This specimen has been digitally cut away from the sacral and caudal section it is articulated with. **B**, lateral; **C**, medial views of right ilium of MOR 1636b. **D**, lateral, **E**, medial views of left pubis of MOR 1642. **F**, lateral, **G**, medial views of right ischium of MOR 1642. **Abbreviations**: **ac**, acetabulum; **bs**, brevis shelf; **ip**, iliac peduncle; **isp**; ischiac peduncle; **mri**, medial ridge on ilium; **obf**, obturator foramen; **obp**, obturator process; **pep**, preacetabular process; **pop**, postacetabular process; **ppp**, postpubic process; **prp**, prepubic process; **pup**, pubic peduncle; **sp**, sacropubal articulation. Scale bars equal 5 cm.

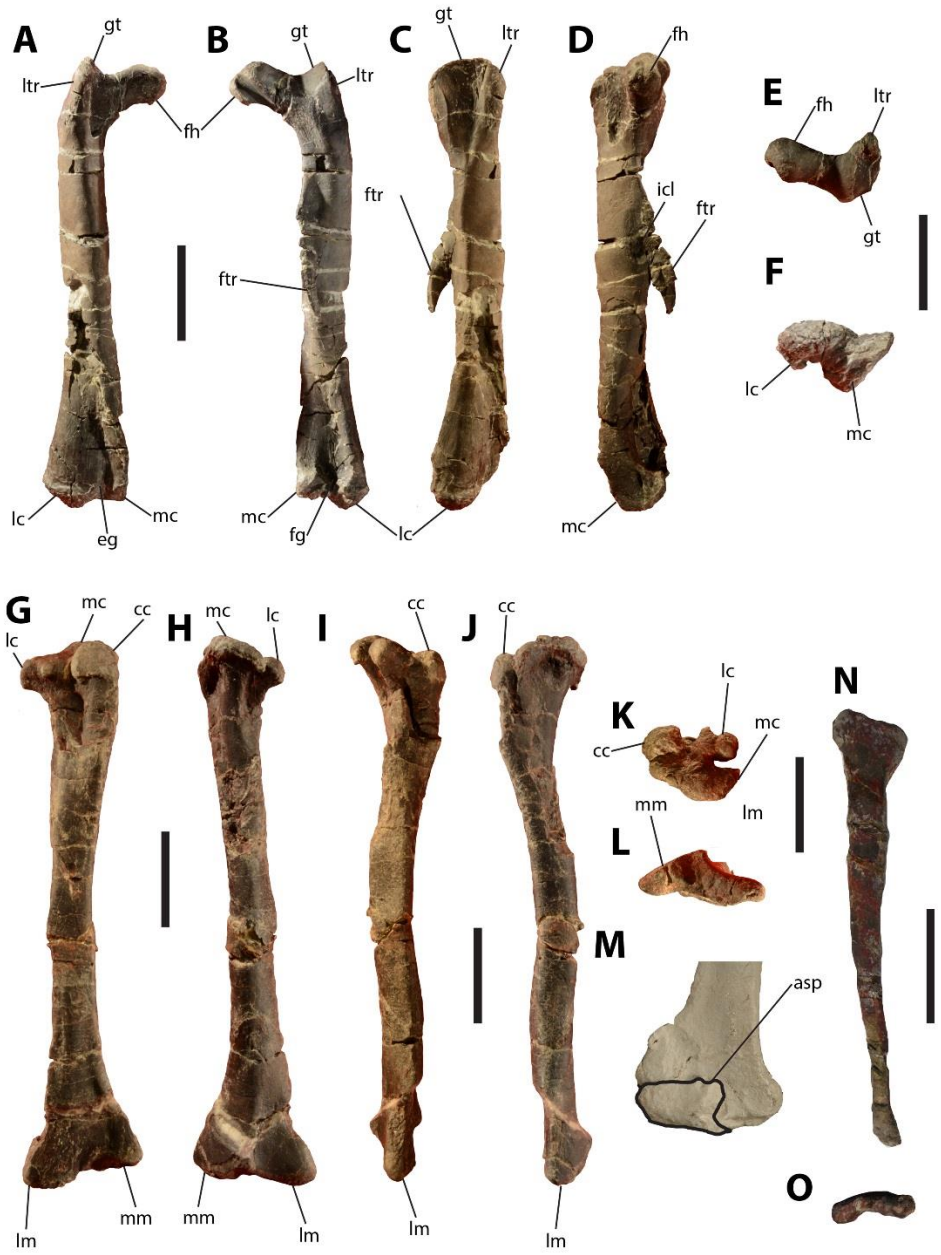

FIGURE 2.18. Hindlimb elements of *Oryctodromeus*. **A**, anterior; **B**, posterior; **C**, lateral; **D**, medial; **E**, proximal; **F**, distal views of right femur of MOR 1642. **G**, anterior; **H**, posterior; **I**, lateral; **J**, medial; **K**, proximal; **L**, distal views of right tibia of MOR 1636a. **M**, anterior view of tibia w/articulated astragalus from IMNH 44939. **N**, lateral; **O**, proximal views of Fibula from IMNH 44930. **Abbreviations**: **asp**, ascending process; **cc**; cnemial crest; **eg**, extensor groove; **fg**, flexor groove; **fh**, femoral head; **gt**, greater trochanter; **icl**, insertion pit for *M. caudifemoralis longus*; **lc**; lateral condyle; **lm**, lateral malleolus; **ltr**, lesser trochanter; **mc**, medial condyle; **mm**, medial malleolus. Scale bars equal 5 cm.

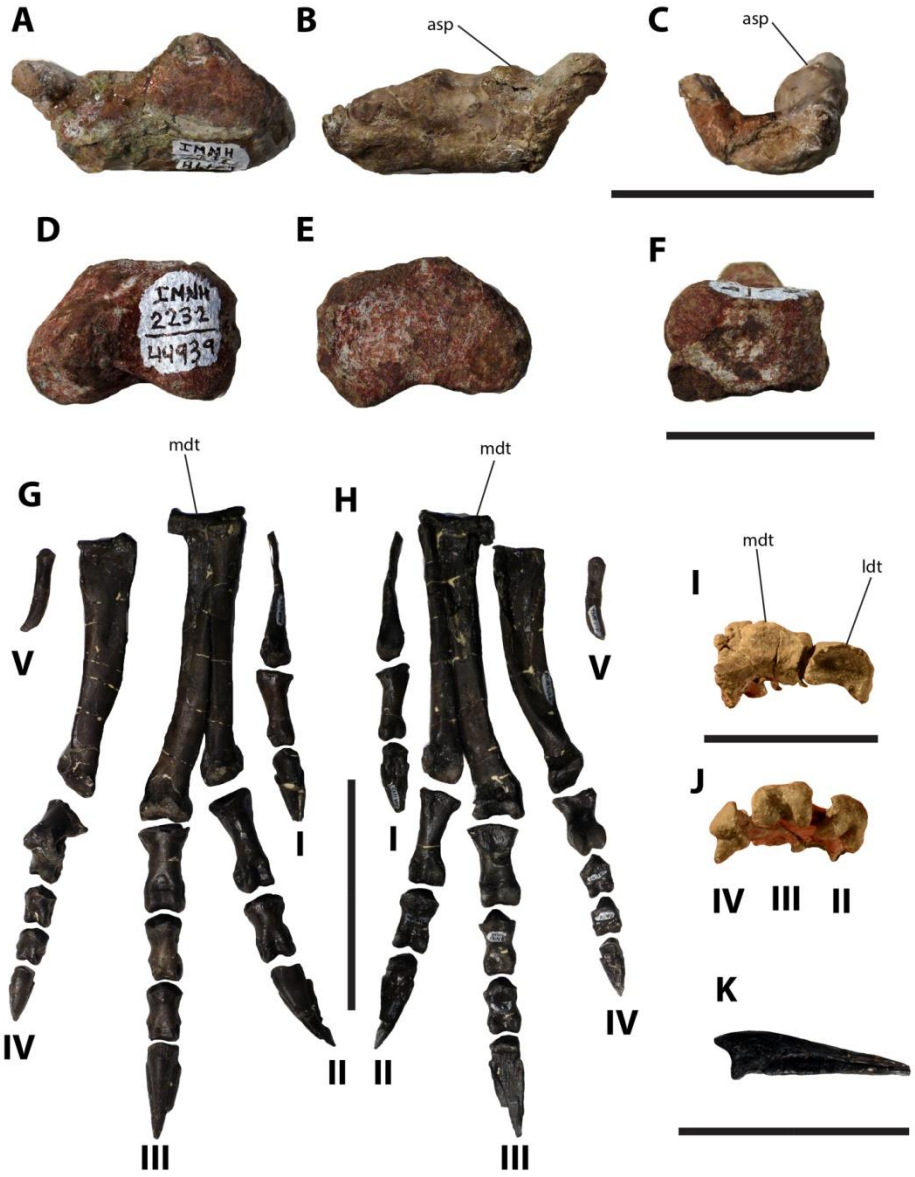

FIGURE 2.19. Tarsals and pes of *Oryctodromeus*. **A**, anterior; **B**, posterior; **C**, lateral views of left astragalus of IMNH 44930. **D**, proximal; **E**, distal; **F**, lateral views of right lateral distal tarsal of IMNH 44939. **G**, anterior; **H**, posterior views of right pes of MOR 1642, with lateral and medial tarsal. There are five phalanges in digit IV, though the two proximal-most phalanges are still articulated and make it appear there are four total phalanges. **I**, proximal view of lateral and medial tarsal of MOR 1642, articulated with metatarsals. **J**, distal view of articulated metatarsals of MOR 1642. **K**, lateral view of pes ungual from digit III. **Abbreviations**: **asp**, ascending process; **ldt**, lateral distal tarsal; **mdt**, medial distal tarsal. Scale bar (A-C) equals 5 cm. Scale bar (D-F) equals 2 cm. Scale bar (G-H) equals 10 cm. Scale bars (I-K) equal 5 cm.

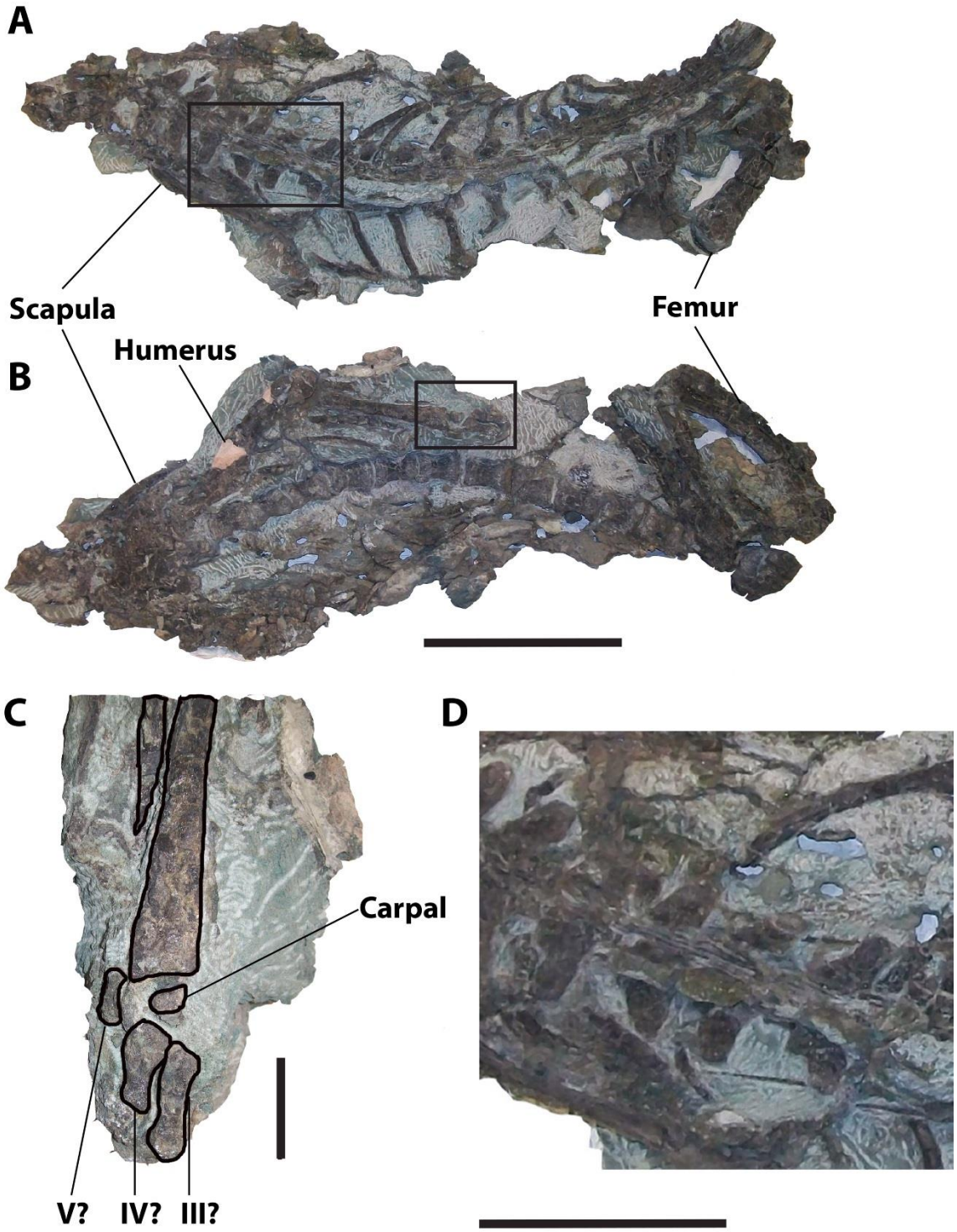

FIGURE 2.20. IMNH 44951, articulated specimen of *Oryctodromeus* with partial left manus. **A,** Dorsal; **B**, ventral views of specimen. **C**, inset of partial left manus with tentative identifications of metacarpals. **D**, inset from **A** showing tendons along dorsal column. Scale bar B equals 15 cm, scale bar D equals 5 cm.

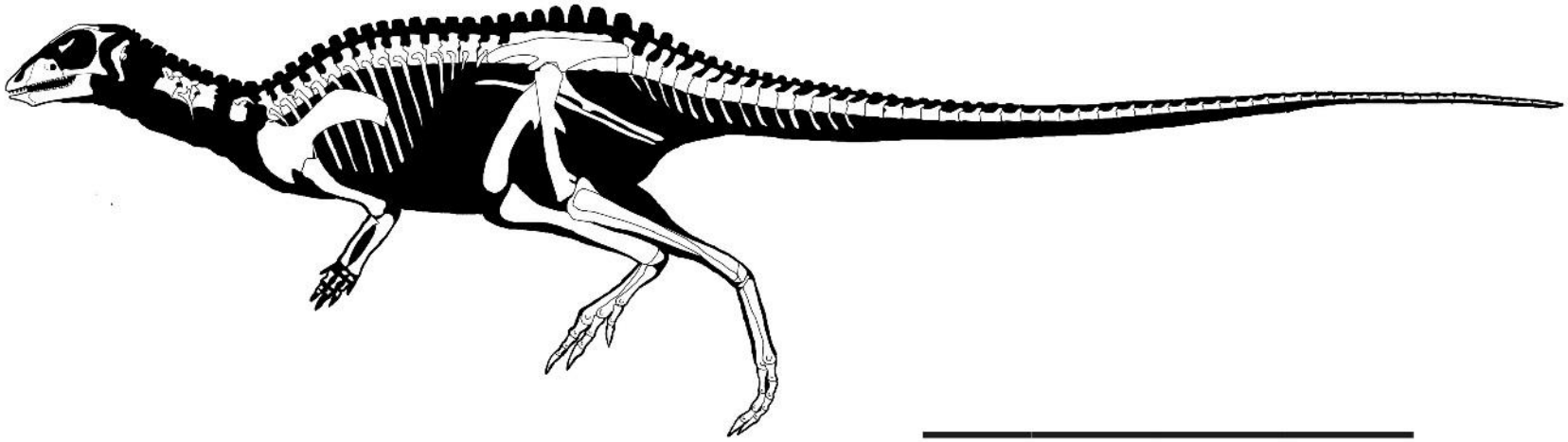

FIGURE 2.21. Skeletal restoration of *Oryctodromeus* in left lateral view. Restoration is based on elements from MOR 1636a and MOR 1642 and depicts all elements known for *Oryctodromeus*. Outline of dorsal spikes is artistic conjecture. Art by lead author. Scale bar equals 1 m.

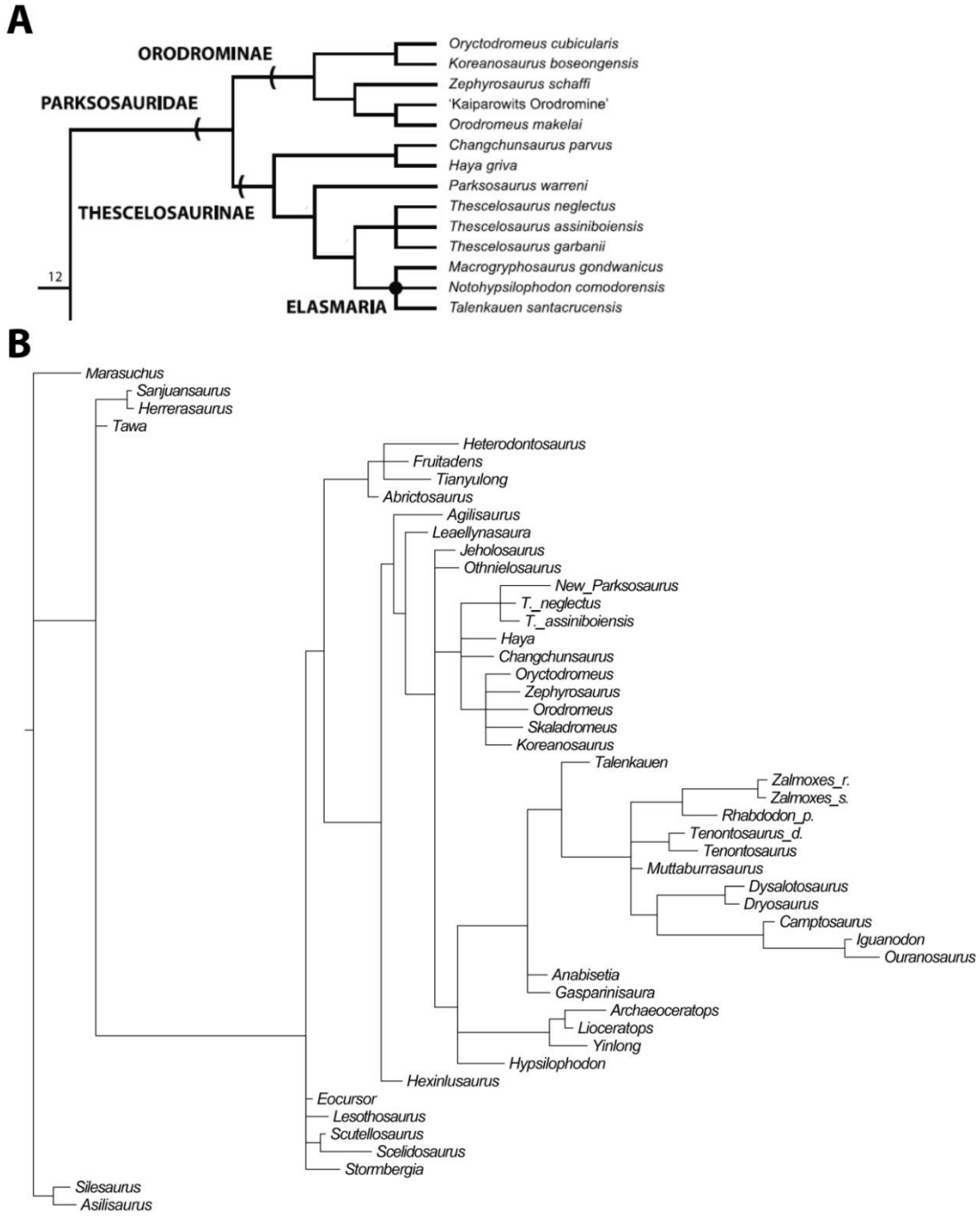

FIGURE 2.22. Phylogenetic relationships of *Oryctodromeus* and other neornithischians. **A**, inset of consensus tree from Boyd (2015, Fig. 2) showing recovered relationships of Orodrominae and related taxa. B, Bayesian consensus tree recovered in this analysis using forty-eight taxa and additional characters for *Oryctodromeus* using a revised matrix of Boyd (2015).

FIGURE 2.23. Artistic reconstruction of *Oryctodromeus* by Josh Cotton. Intended for cover of the *Journal of Vertebrate Paleontology* hosting the article.

LITERATURE CITED

Anderson, J. F., A. Hall-Martin, and D. A. Russell. 1985. Long-bone circumference and weight in mammals, birds, and dinosaurs. *Journal of Zoology, London (A)*: 207: 53-61.

Boyd C. A. 2014. The cranial anatomy of the neornithischian dinosaur *Thescelosaurus neglectus*. PeerJ 2:3669 DOI 10.7717/peerj.669.

Boyd C. A. 2015. The systematic relationships and biogeographic history of ornithischian dinosaurs. *PeerJ* 3:e1523 https://doi.org/10.7717/peerj.1523.

Brown, C. M., D. C. Evans, M. J. Ryan, and A. P. Russell. 2013. New data on the diversity and abundance of small-bodied ornithopods (Dinosauria, Ornithischia) from the Belly River Group (Campanian) of Alberta. Journal of Vertebrate Paleontology 33: 495-520.

Butler, R. J., P. Upchurch, and D. B. Norman. 2008. The phylogeny of the ornithischian dinosaurs. Journal of Systematic Palaeontology 6:1–40.

Calvo, J. O., J. D. Porfiri, and F. E. Novas. 2007. Discovery of a new ornithopod dinosaur from the Portezuelo Formation (Upper Cretaceous), Neuquén, Patagonia, Argentina. Arquivos do Museu Nacional 65: 471–483.

Cobban, W., C. Erdmann, R. Lemke, and E. Manghen. 1959. Revision of Colorado group on Sweetgrass arch, Montana: AAPG Bulletin 43:2786–2796.

Cobban, W., C. Erdmann, R. Lemke, and E. Manghen, E.1976. Type sections and members of the Blackleaf and Marias River Formations (Cretaceous) of the Sweetgrass arch, Montana. U.S. Geological Survey Professional Paper 974.

Cooper, M. R. 1985. A revision of the ornithischian dinosaur *Kangnasaurus coetzeei* Haughton, with a classification of the Ornithischia. Annals of the South African Museum 95:281–317.

Dorr, J.A. 1985, Newfound Early Cretaceous dinosaurs and other fossils in southeastern Idaho and westernmost Wyoming, Contributions from the Museum of Paleontology: University of Michigan 27: 73- 85.

Durkee, S. K., 1980, Depositional environment of the lower Cretaceous Smiths Formation within a portion of the Wyoming-Idaho thrust belt: Wyoming Geological Association 31st Annual Field Conference Guidebook: 101-116.

Dyman, T. S. and D. J. Nichols. 1988, Stratigraphy of the mid-Cretaceous Blackleaf and lower part of the Frontier Formations in parts of Madison and Beaverhead Counties, Montana: United States Geological Survey Bulletin 1773.

Dyman, T. S., W. J. Perry, and D. J. Nichols. 1988. Stratigraphy, petrology, and provenance of the Albian Blackleaf Formation and the Cenomanian to Turonian lower Part ofpa the Frontier Formation in part of Beaverhead and Madison Counties, Montana. Mountain Geologist 25: 113-127.

Dyman, T.S., Tysdal, R.G., Perry, W.J., Jr., Obradovich, J.D., Haley, J.C., and Nichols, D.J., 1997, Correlation of Upper Cretaceous strata from Lima Peaks area to Madison Range, southwestern Montana and southeastern Idaho. Cretaceous Research 18:751-766.

Fearon, J. L., and D. J. Varricchio. 2015. Morphometric analysis of the forelimb and pectoral girdle of the Cretaceous ornithopod dinosaur *Oryctodromeus cubicularis* and implications for digging. Journal of Vertebrate Paleontology. DOI: 10.1080/ 02724634.2014.936555.

Felsenstein, J. 1978. Cases in which parsimony or compatibility methods will be positively misleading. Systematic Zoology 24(4): 401-410.

Gates, T. A., Lund, E. K., Boyd, C. A., DeBlieux, D. D., Titus, A. L., Evans, D. C., Getty, M. A., Kirkland, J. I., and Eaton, J. G. 2013. Ornithopod dinosaurs from the Grand Staircase-Escalante National Monument Region, Utah, and their role in paleobiogeographic and macroevolutionary studies, in At the Top of the Grand Staircase: The Late Cretaceous in Southern Utah, Titus, A. L., and M. A. Loewen (eds), pp.463-481. Indiana University Press. Bloomington. Indiana.

Horner, J. R. and D. Weishampel.1988. A comparative embryological study of two ornithischian dinosaurs. Nature 332: 256-257

Kirkland, J.I. and S. K. Madsen, S.K. 2007. The Lower Cretaceous Cedar Mountain Formation, eastern Utah: the view up an always interesting learning curve: Fieldtrip Guidebook, Geological Society of America, Rocky Mountain Section.

Krumenacker, L. J. 2010, Chronostratigraphy and paleontology of the mid-Cretaceous Wayan Formation of eastern Idaho, with a description of the first *Oryctodromeus* specimens from Idaho. M.S. Thesis, Brigham Young University, Provo, Utah, 98 pp.

Krumenacker, L.J., Simon, D. J., Scofield, G., and Varricchio, D. J., 2016. Theropod dinosaurs from the Albian–Cenomanian Wayan Formation of eastern Idaho. Historical Biology 29: 170–186 http://dx.doi.org/10.1080/08912963.2015.1137913.

Maxwell W. D. and J. H. Ostrom. 1995. Taphonomy and paleobiological implications of *Tenontosaurus-Deinonychus* associations, Journal of Vertebrate Paleontology, 15: 707-712.

McDonald AT, J. Bird, J. I. Kirkland, and P. Dodson. 2012. Osteology of the Basal Hadrosauroid *Eolambia caroljonesa* (Dinosauria: Ornithopoda) from the Cedar Mountain Formation of Utah. PLoS ONE 7(10): e45712. doi:10.1371/journal.pone.0045712.

Min H., D. G. Lee, J. K. Kim, J. D. Lim, and P. Godefroit. 2011. A new basal ornithopod dinosaur from the Upper Cretaceous of South Korea. Neues Jahrbuch für Geologie und Palaeontologie, Abhandlungen 259: 1–24.

Novas, F. E., A. V. Cambiaso, A. Ambrioso, Alfredo. 2004. A new basal iguanodontian (Dinosauria, Ornithischia) from the Upper Cretaceous of Patagonia. Ameghiniana 41: 75–82.

Oriel, S.S., and L.J. Platt. 1980. Geologic map of the Preston 1o x 2o quadrangle, Idaho and Wyoming: U.S. Geological Survey Miscellaneous Investigations Series Map I-1127, scale 1:250,000.

Owen, R. 1842. Report on British fossil reptiles, Part II. Report of the British Association for the Advancement of Science (for 1841) 9: 60–204.

Rambaut, A., M. A. Suchard, D. Xie, and A. J. Drummond. 2014. Tracer v1.6, Available from http://beast.bio.ed.ac.uk/Tracer.

Ronquist, F., M. Teslenko, P. van der Mark, D. Ayres, A. Darling, S. Höhna, B. Larget, L. Liu, M. A. Suchard, and J. P. Huelsenbeck. 2012. MrBayes 3.2: Efficient Bayesian phylogenetic inference and model choice across a large model space. Systematic Biology 61: 539-542.

Rubey, W. W., 1973, New Cretaceous formations in the western Wyoming Thrust Belt: U.S. Geological Survey Bulletin 1372-1.

Scheetz, R.D., 1999, Osteology of *Orodromeus makelai* and the phylogeny of basal ornithopod dinosaurs. Ph.D. dissertation, Montana State University, Bozeman, Montana, 189 pp

Schmitt, J. G., and M. E. Moran. 1982, Stratigraphy of the Cretaceous Wayan Formation, Caribou Mountains, southeastern Idaho thrust belt: University of Wyoming Contributions to Geology 21: 55-71.

Seeley, H. G. 1887. On the classification of the fossil animals commonly named Dinosauria. Proceedings of the Royal Society of London 43:165–171.

Sternberg, C. M. 1937. Classification of *Thescelosaurus*: a description of a new species. Proceedings of the Geological Society of America 1936:375.

Sues, H. D. 1980. Anatomy and relationships of a new hypsilophodontid dinosaur from the Lower Cretaceous of North America. Palaeontographica Abteilung a Palaeozoologie-Stratigraphie 169: 51–72.

Varricchio, D. J., A. J. Martin, and Y. Katsura. 2007, First trace and body fossil evidence of a burrowing, denning dinosaur: Proceedings of the Royal Society B: Biological Sciences 274: 1361–1368.

Zanno, L. E., and P.J. Makovicky. 2013. Neovenatorid theropods are apex predators in the Late Cretaceous of North America: Nature Communications 4: 2827.

Zartman, R. E., T. S. Dyman, R. G. Tysdal, and R. C. Pearson. 1995. U-Pb ages of volcanogenic zircon from porcellanite beds in the Vaughn Member of the mid-Cretaceous Blackleaf Formation, southwestern Montana: United States Geological Survey Bulletin 2113B.

CHAPTER THREE

TAPHONOMY OF *ORYCTODROMEUS CUBICULARIS* FROM THE MID-CRETACEOUS (ALBIAN-CENOMANIAN) OF IDAHO, AND ADDITIONAL *ORYCTODROMEUS* BURROWS FROM IDAHO AND MONTANA

Contribution of Authors and Co-Authors

Manuscript in Chapter

Author: L.J. Krumenacker

Contributions: Conceived the study, performed the analyses, interpreted results, and wrote the manuscript.

Co-Author: David J. Varricchio

Contributions: Conceived the study, discussed results and implications, and edited earlier manuscripts.

Co-Author: John Wilson.

Contributions: Performed analyses, discussed implications, edited earlier manuscripts.

Co-Author: Ashley Ferguson.

Contributions: Edited the manuscript and assisted in specimen collection.

Manuscript Information Page

L.J. Krumenacker, David J. Varricchio, John Wilson, Ashley Ferguson

Palaeogeography, Palaeoclimatology, Palaeoecology

Status of Manuscript:
_X_ Prepared for submission to a peer-reviewed journal
__ Officially submitted to a peer-review journal
__ Accepted by a peer-reviewed journal
__ Published in a peer-reviewed journal

ABSTRACT

The mid-Cretaceous (Albian-Cenomanian) Wayan Formation of eastern Idaho and the Vaughn Member of the Blackleaf Formation of southwestern Montana both have vertebrate assemblages dominated by the small burrowing neornithischian dinosaur *Oryctodromeus cubicularis*. The dominance of this taxon in these sediments is marked, with other taxa represented by skeletal elements being rare in comparison. This relative abundance leads to questions on the processes responsible for the dominance of this fossorial taxon.

Oryctodromeus specimens occur in three distinct lithofacies, and can be divided into three distinct taphofacies dependent on degrees of articulation and association. Articulated specimens (taphofacies A) occur in bioturbated sandstones; articulated to associated specimens in pedogenic mudstones, siltstones, and fine-grained sandstones (taphofacies B); and isolated skeletal elements (taphofacies C) are found within the debris flow deposit of the Robison Bonebed (RBB). Two broad taphonomic modes are recognized: articulated to associated skeletons (mode B) which are represented by twelve specimens, and dozens of isolated elements (mode A) from the RBB.

A suite of taphonomic observations suggest that burial within unrecognized burrows can be inferred as a typical mode of preservation for partial to near complete skeletons of *Oryctodromeus*. The Wayan and Vaughn may represent an unusual occurrence of fossil assemblages and possibly Cretaceous paleocommunities dominated by a fossorial vertebrae taxon. The numerical dominance of *Oryctodromeus* in the multi-

taxic Robison Bonebed possibly reflects the original ecological abundance of this taxon. The occurrence of additional specimens consisting of skeletons of multiple individuals together, sometimes of varying ontogenetic stages, reinforces the suggestion of parental care.

Additional occurrences of *Oryctodromeus* burrows from the Wayan and Vaughn are reported, with the overall morphology and sizes being similar to the holotype burrow. While data for burrowing fossil taxa is available, it is mostly descriptive with lesser amounts of discussion of the apparent taphonomic processes involved. This study highlights the need for more actualistic studies associated with burrowing vertebrates and preservational processes.

1. Introduction

The latest Albian to Cenomanian Wayan Formation of eastern Idaho, and the coeval Vaughn Member of the Blackleaf Formation of western Montana both have vertebrate assemblages apparently dominated by the fossorial orodromine neornithischian *Oryctodromeus cubicularis* (Varricchio *et al*., 2007; Krumenacker, 2010; Krumenacker *et al*., 2016). Other vertebrate remains from the Wayan and Vaughn, excluding eggshell and rare eggs of the ootaxon *Macroelongatoolithus carlylei*, are exceedingly rare (Krumenacker *et al*., 2016) and consist almost entirely of isolated remains such as teeth, bones, and eggshell. The vast majority of non-*Oryctodromeus* taxa, excluding eggshell, are known from the Robison Bonebed (the RBB, IMNH 2251) and the H34D locality (IMNH 2167; Krumenacker *et al*., 2015; Krumenacker, 2016). Excluding a heavily taphonomically modified partial nodosaur skeleton from the H34D locality, fossils from these two localities consist of complete to incomplete bones, teeth, and eggshell of numerous taxa (Table 1). The RBB has produced many isolated and very rarely articulated elements referable to *Oryctodromeus*. Fossils from these locations also exhibit a wide taphonomic spectrum, with elements consisting of rolled bone pebbles, partial broken limb elements, partial to complete vertebrae, and bone and tooth shards. Non-*Oryctodromeus* skeletal elements from other localities are extremely rare, but again exhibit more substantial prediagenetic taphonomic modification. Taxa from the Vaughn are limited to *Oryctodromeus*, *Macroelongatoolithus* and other eggshell, and an isolated ankylosaur tooth (Varricchio *et al*., 2007; Simon, 2014).

Oryctodromeus is the first reported dinosaur with a burrowing habit. The holotype (a presumably mature individual) and paratype (two partial juveniles) specimens were found in a burrow infill within the Vaughn near Lima Peaks, Montana, USA (Varricchio *et al*., 2007; Fig. 1, Table 2). Since the description of the holotype and paratype specimens from the Lima Peaks area, numerous additional *Oryctodromeus* specimens (Table 2) have been recovered from the Wayan and the Vaughn (Krumenacker, 2010; Krumenacker *et al*., 2016). Two of these additional specimens have been associated with burrows and these burrows are reported here, one from the Wayan Formation and a second from the Vaughn Member in the Lima Peaks area.

The Wayan Formation and Vaughn Member are unique amongst reported dinosaurian fossil assemblages in being dominated by a single small burrowing neornithischian taxon (*Oryctodromeus*; Table 1; Dorr, 1985; Weishampel *et al*., 2002; Krumenacker, 2005; Krumenacker *et al*., 2014). Small dinosaurian (and other) vertebrate taxa are typically more incomplete and more rare in the fossil record in comparison to larger bodied taxa, making this pattern of *Oryctodromeus* occurrence in the Wayan and Vaughn unusual (eg. Behrensmeyer and Hook, 1992; Brown *et al*., 2013). The heavy dominance of *Oryctodromeus* in the Wayan and Vaughn assemblages suggests unusual taphonomic and/or ecological circumstances responsible for the preservation of relatively common, numerous partial to near complete, and well preserved specimens of these small bodied animals. Additionally, members of this clade are typically rare components of their respective assemblages (eg. Sues, 1980). Previous work has suggested that *Oryctodromeus* is the dominant and only well represented vertebrate in the Wayan and

Vaughn assemblages (Krumenacker, 2010; Krumenacker *et al*., 2016). These observations raise questions such as: Is *Oryctodromeus* really the dominant vertebrate taxon represented by skeletal material in the Wayan and Vaughn and to what extent? If so, why is *Oryctodromeus* the dominant taxon? Additionally, the initial description of *Oryctodromeus* included evidence for burrowing, parental care and social grouping; raising the question of if there is additional evidence supporting these habits. Here these questions will be addressed through detailing the taphonomic and geologic setting of *Oryctodromeus* occurrences, as well as comparisons of their taphonomy to the taphonomy of other burrowing taxa. In addition, two new burrows from the Wayan and Vaughn are described.

2. Methods and Materials

2.1 Regional Geology

The Wayan Formation and Vaughn Member of the Blackleaf Formation, deposited during the late Albian through the Cenomanian, occur in dominantly non-marine alluvial plain successions in eastern Idaho and southwestern and west-central Montana (Figs. 1-3; Dorr, 1985; Dyman and Nichols, 1988). Deposition occurred in small fluvial channels and associated floodplains in the proximal portions of the foreland basin associated with events of the Paris and Meade Thrusts (Schmitt and Moran, 1982; Wiltschko and Dorr, 1983; Dorr, 1985; Dyman and Nichols, 1988; Krumenacker, 2010). Sediments of the upper Vaughn are noticeably richer in volcanic ash and bentonite (Dyman, pers. comm.).

Both the Wayan and Vaughn are part of thick Cretaceous sequences in their respective areas (Figs 1-3). The Wayan, measuring 1,344 meters in thickness, forms a

substantial portion of the dominantly terrestrial Cretaceous packet in the Caribou Range, which measures over 3000 meters in total thickness (Schmitt and Moran, 1982; Krumenacker, 2010). Directly below the Wayan is the Smiths Formation, representing environments ranging from nearshore to fluvial. The Smiths is composed of a lower black shale member and an upper sandstone member (Rubey, 1973; Dorr, 1985). Overlying the Wayan is the Sage Junction Formation, a nearshore alluvial plain sandstone and mudstone dominated formation with abundant false-trunks of *Tempskya* (Rubey, 1973; Oriel and Platt, 1980; Dorr, 1985). The Cretaceous rocks of southwestern Montana, including the Vaughn, consist of up to 7000 meters of strata, with the Vaughn measuring at 270 meters thick near Lima Peaks, but having a highly variable regional thickness, with 878 meters near Drummond (Dyman and Nichols, 1988; Dyman *et al*., 1994). Underlying the Vaughn Member of the Blackleaf Formation is the Flood Member, composed of black shales sandwiched between or underlying sandstones (Dyman and Nichols, 1988). Underlying the Flood itself is the Aptian to Albian Kootenai Formation (Dyman *et al*., 1988). Overlying the Vaughn in southwestern Montana are the shales, sandstones, and conglomerates of the Cenomanian to Turonian Frontier Formation, deposited in marine to terrestrial environments (Dyman and Tysdal, 1990; Dyman *et al*., 1997; Dyman *et al*., 2008). High vegetative cover and the relatively fine-grained and easily eroded sediments limit outcrops of both the Wayan and Vaughn (Dorr, 1985; Krumenacker, 2010). *Oryctodromeus* producing areas in the Wayan Formation occur primarily within the Caribou Range of Bonneville and Caribou Counties, Idaho (Fig. 1; Krumenacker, 2010; Krumenacker *et al*., 2016). Within the Vaughn Member,

Oryctodromeus are known from the Lima Peaks area of Beaverhead County, Montana (Fig. 1; Varricchio *et al*., 2007). In combination, the nearly identical ages, bounding stratigraphic geologic units, and presence of *Oryctodromeus* in both the Wayan and Vaughn strongly suggest that these two geological units represent the same originally contiguous package prior to subsequent volcanism and tectonism.

2.2 Fieldwork

Sporadic fieldwork in the Wayan Formation was carried out by the University of Michigan, the Idaho Museum of Natural History, and personnel of Caribou-Targhee National Forest within the last two decades of the twentieth century (Dorr, 1985; Weishampel *et al*., 2002). Since 2002 prospecting and research has been carried out in the Wayan Formation by the authors. Limited stratigraphic work has been done in the Wayan with outcrop quality precluding detailed observations (Schmitt and Moran, 1982; Krumenacker, 2010). Fieldwork in the Vaughn has been ongoing since 2003, with exploratory work and collecting occurring in the Lima Peaks area of Beaverhead County, Montana (Varricchio *et al*., 2007; Ullmann *et al*., 2012). *Oryctodromeus* specimens from both geologic units have been collected using standard collection techniques. Measured sections and facies analysis of the Wayan are based on the measured sections of Krumenacker (2010) and personal notes of the lead author. Stratigraphic sections with *Oryctodromeus* locations are not available for the Vaughn. Facies analysis and description follow standard methods of definition and description. Specific locality data and collection information is available at the curating institutions, the Idaho Museum of

Natural History (IMNH), Pocatello, ID and the Museum of the Rockies (MOR), Bozeman, MT.

2.3 Photogrammetry

Photogrammetric modeling (Supplementary Information File One: (https://sketchfab.com/models/d58c01463d5f4149994a7a79a349fd6d) of the in-situ burrow structure from the Wayan was conducted in the field prior to jacketing and collection of a portion of the burrow in order to retain the complete morphological and contextual geological data which would otherwise be altered or lost upon excavation and preparation. In instances such as this one, photogrammetry is ideal as it retains color data, which characterizes the sedimentology of the burrow structure and surrounding rock, in association with three dimensional shapes. Prior to photographing, the burrow structure was consolidated with polyvinyl acetate (vinac), which to some degree enhanced the color of the structure; note that the burrow sediment was identical in color to the surrounding rock. One hundred seventy-eight high-resolution (18 megapixel) photos were taken with a Canon 60D DSLR and processed in Agisoft Photoscan Professional. A dense point cloud of 1,903,724 points (after cropping of extraneous points) was generated and used to construct a mesh of 5,005,591 vertices and 10,000,000 faces for maximum accuracy. The mesh was additionally decimated to 1,700,000 faces in order to produce a more widely accessible supplementary file of manageable size.

2.4 Specimen Preparation

Specimens were prepared using standard mechanical preparation techniques. Wayan Formation specimens were prepared at the BYU-Provo vertebrate paleontology

lab and in the Varricchio Paleontology Lab in Gaines Hall at Montana State University-Bozeman by the lead author. Vaughn Member specimens were skillfully prepared by Carrie Ancell in the Fossil Preparation Lab at the Museum of the Rockies, Bozeman, Montana. Due to the larger number of associated specimens and limited funds, some specimens described here (IMNH 45596 and IMNH 49842) are not fully prepared, with data being used from their current state of preparation.

2.5 Specimens

Specimens (Tables 1-2) foucsed upon in this study for elucidation of the burial settings of *Oryctodromeus* are only those that have been found *in-situ*. One individual is hypothesized to be represented by two separate specimens, IMNH 44951 and IMNH 45081. IMNH 45081, recovered in a sandstone nodule, is suspected to belong with IMNH 44951 which was recovered *in-situ*. Hereafter this apparent single individual is just referred to as IMNH 44951. Dozens of isolated and some associated specimens have been recovered as float (loose on the ground surface, Table 1), but are not used in detail here due the lack of geological context for the specimens. Some specimens discussed generally in this study consist of numerous isolated and a few articulated (vertebrae) remains from a multi-taxic bonebed (the RBB).

3. Results

3.1 Geology and Sedimentology

3.1.1 Measured Sections and Fossil Occurrence

Unfortunately, post-depositional tectonics and extensive vegetative cover have precluded putting *Oryctodromeus* specimens into a rigorous stratigraphic framework. The

available data shows that *Oryctodromeus* occurs at least in the lower and middle Wayan, sometimes in distinctly fossiliferous horizons (section 10.5 in Krumenacker, 2010). Its exact stratigraphic location in the Vaughn is also not well understood due to the isolated nature of the outcrop (Varricchio et al., 2007).

Measured sections and geological observations are discussed here to allow the definition of facies in the Wayan and Vaughn, with focus on those that have produced *Oryctodromeus* specimens. In addition to data from *Oryctodromeus*-producing localities in small outcrops that precluded stratigraphic measurement, three *Oryctodromeus*-producing measured sections from the Wayan Formation, described in Krumenacker (2010) are utilized here (Fig. 1). These sections are the Miners Delight Creek, McCoy Creek, and Tincup Canyon measured sections. Detailed locations of measured sections, due to their proximity to fossil locations, are not given. However specific data is available at IMNH. One additional section that has not produced *Oryctodromeus* is included as well, the Schmitt and Moran (1982) McCoy Creek section, hereafter referred to as the Schmitt and Moran section. Miners Delight, McCoy Creek, and the Schmitt and Moran section all occur in the Caribou Basin area of Bonneville County, Idaho; while the Tincup Creek section occurs in Caribou County, Idaho. The stratigraphic position of the Miners Delight Creek and McCoy Creek sections within the Wayan are uncertain, as the top and/or bottom of the Wayan is not exposed in these sections, and no marker beds have been recognized. While the sandstones that form ridges in these sections are laterally continuous and typically extend for many tens of meters, the lateral extent of the associated finer-grained sediments is uncertain, but the characteristics of the weathered

soils on the surface suggest a comparable degree of lateral continuity. The relationships of *Oryctodromeus* specimens in the Vaughn to measured sections are uncertain, so none are included here or in the facies association table (Table 2). Enough general geological observations and data (eg. Dyman and Nichols, 1988; Dyman et al., 1994) are available for the Vaughn for definition of some characteristic facies associated with *Oryctodromeus* (Table 1).

The Tincup Canyon measured section, not figured due to it being predominantly covered, contains one locality that has produced *Oryctodromeus* (Krumenacker, 2010). At 501 meters above the base of the section, a partial skeleton (IMNH 44946) has been recovered. The specimen was collected from a series of resistant nodules of red calcareous siltstone associated with calcareous nodules in an extremely weathered roadcut exposure. Green to gray reduction halos were present around some of the bones.

The McCoy Creek measured section (Fig. 3; Krumenacker, 2010) is the most fossiliferous measured section from the Wayan Formation, and consists of repetitive outcrops of trough-crossbedded sandstones forming ridges that are flanked by finer grained mudstones and siltstone. The section has produced two *Oryctodromeus* partial skeletons: IMNH 44920 (which is associated with a radiometric age of 99.1 + 1.5/- 1.3 Ma), and IMNH 45596 (Krumenacker, 2010). IMNH 44920 was recovered twenty meters above section base, from a calcareous gray siltstone that coarsens upward into a medium-grained sandstone with centimeter scale trough crossbeds in the uppermost portion. IMNH 45596 occurred within a small isolated outcrop of red calcareous siltstone

associated with calcareous nodules that coarsens upward into a gray coarse-grained sandstone. This specimen occurs 255 meters above the section base.

The Miners Delight section (Fig. 3) occurs in a series of better-developed outcrops and consists of 133 meters of section (Krumenacker, 2010). Five associated to partial skeletons (preparation is ongoing) are known from this series of outcrops, which consist of well-exposed alternating sandstone ridges flanked by more heavily weathered and finer-grained sediments. At the base of this section, IMNH 44951 has been recovered from a medium-grained calcareous sandstone. This sandstone is featureless in the vicinity of the fossil, but in laterally continuous sandstones adjacent to both sides of the locality centimeter-scale trough cross-bedding is evident before the outcrop becomes vegetated. Roughly thirty-five meters above section base IMNH 46169 was recovered. This specimen was recovered from a very heavily weathered outcrop of calcareous red siltstone with calcareous nodules. At roughly 125 meters above the base of the section IMNH 50846, 50847 and 50877 have been recovered. IMNH 50877 includes skeletal remains that have been recovered in association with the burrow that is described below. IMNH 50846 and 50877 come from the same horizon of heavily weathered calcareous red siltstones with calcareous nodules and are separated laterally by about six meters, while IMNH 50847 comes from an identical lithology about one meter lower in section.

The Schmitt and Moran section (Schmitt and Moran, 1982), begins at the base of the Wayan and continues upwards for 586 meters, with typical repetitive outcrops of mudstones, sandstones, and siltstones having been reported. Additional rare lithofacies such as volcanic ash are also reported. Radiometric and palynological ages have been

recovered from samples in this section as well (Schmitt and Moran, 1982; Krumenacker, 2010).

More *Oryctodromeus* specimens from the Wayan Formation are known from very small isolated and poorly exposed outcrops that have not been put in a stratigraphic framework. These are IMNH 44939, which occurred in an overturned outcrop of fine-grained red-gray sandstone with green reduction halos around the bones and with some cm scale calcareous nodules in association. This sandstone is capped by a very-resistant fine-grained red sandstone with prominent invertebrate traces on the base. IMNH 49842 occurs in a poorly exposed and small outcrop of medium-grained gray sandstone. Skeletal remains were recovered from a featureless calcareous sandstone nodule, weathered into segments, that occurred within poorly exposed steep beds of cm-scale trough crossbedded sandstones.

Due to the isolated nature of the outcrops that have produced the specimens described here for the Vaughn Member, they have not come from the context of measured sections. MOR 1636 was recovered in a burrow fill composed of sandstone that cross-cut three mudstone units. These mudstones consisted of, in ascending order, a nodular calcareous green-gray mudstone, a green-gray claystone, and another green-gray mudstone. These units were overlain by more claystone and sandstone (Varricchio *et al*., 2007). MOR 8660 and MOR 1642 were also recovered from gray-green mudstones, with MOR 8660 having come from a poorly preserved silty green mudstone fill that cross-cut the hosting green mudstone.

3.1.2 Lithofacies

Lithofacies for the Wayan Formation and Vaughn Member of the Blackleaf Formation are defined here. While the lack of extensive detailed stratigraphic work in these units prevents finer-scale observations of the relationships of these lithofacies and others not associated with fossil specimens, general observations can be made based on field observation and on research at specific fossil localities. Here these lithofacies are described in order of coarseness, with data on the lithologies, associations, and possible modes of formation being discussed (Table 2, 3). When *Oryctodromeus* specimens are known to be present in a lithofacies, they are indicated.

3.1.2.1 Lithofacies Gms: Matrix-Supported Conglomerates

Matrix-supported conglomerates are a rare but significant lithofacies limited to the Wayan (Schmitt and Moran, 1982; Krumenacker *et al*., 2016). Three localities are known of this lithofacies. These are the Minkin Bonebed, H34D, and the RBB. The Minkin Bonebed occurs in the lower Wayan, the RBB occurs in the middle of the Wayan, and H34D in the upper Wayan (Krumenacker, 2010; Krumenacker et al., 2016). Only the RBB has detailed geological data available. Based on the ex-situ boulders, an original thickness of one to two meters is likely for this discontinuous unit Sediment of the RBB consists of angular to semi-rounded intra-formationally sourced green mudstone pebbles and cobbles, caliche nodules, inter-formationally sourced red and black chert pebbles, as well as vertebrate remains (broken bones, teeth, eggshell) float in a matrix of coarse sand with chert grains.

At least forty-four isolated specimens, consisting of mostly isolated elements referred to *Oryctodromeus* have been recovered from this lithofacies at the RBB, with work and preparation ongoing on specimens recovered from here. In-situ observation of this fossiliferous lithofacies, known from only this one locality, is impossible due to construction activities that removed the entire lens of this sediment from the originating hillside prior to observation being possible. Based on recent observations this lithofacies may have graded into a finer-grained gray sandstone that fines upward into green siltstone and mudstone. The fact that this lithology is only exposed as ex-situ boulders does not allow detailed discernment of the lateral and stratigraphic relationships of this facies, but some generalities will be discussed.

3.1.2.2 Lithofacies Gcs: Clast-Supported Conglomerates

Clast-supported conglomerates are common in the basal Wayan Formation (Krumenacker, 2010) where they comprise the lower hundred meters. Such lithofacies are commonly deposited in fluvial channels proximal to the sediment source areas and in higher energy fluvial environment (Reading, 1996). In the Wayan these lithofacies consist of red and black chert pebbles, inter-formationally-sourced (Schmitt and Moran, 1982), in a brown to gray quartz and chert-rich sandstone matrix. These chert pebbles may approach cobble size (Schmitt and Moran, 1982; Krumenacker, 2010).

3.1.2.3 Lithofacies Sh: Horizontally Bedded Sandstones

Horizontally bedded sandstones are common within the Wayan Formation (Schmitt and Moran, 1982; Krumenacker, 2010) and may occur in repetitive beds over a meter thick. These sandstones are usually fine to medium-grained and silver-gray, dark

gray, or brown in color. These sandstones occur often in association with trough-cross bedded or massive featureless sandstones. Invertebrate traces, occasional bone shards, and compressions of woody material may be common.

3.1.2.4 Lithofacies Sm: Massive Sandstones

These lithofacies of massive featureless sandstones occur in the Wayan and may be from one to over ten meters in thickness. These beds are often in association with trough-crossbedded or laminar sandstones. These sediments consist of a fine to medium-grained gray to brown sandstones. They may contain cm scale calcareous nodules and chert pebbles. *Oryctodromeus* specimens are uncommon in these lithofacies, with those recovered being IMNH 44939 (representing three individuals), 44951, and 49842.

3.1.2.5 Lithofacies St: Trough-crossbedded Sandstones

Trough-crossbedded sandstones, commonly with cm to inch scale crossbeds, are also common in the Wayan and Vaughn. They may be over ten meters thick and laterally extensive for up to a kilometer (Weishampel *et al*., 2002). These beds form some of the most prominent outcrops in the Wayan and are less conspicuous and common in the Vaughn (Dorr, 1985; Schmitt and Moran, 1982; Krumenacker, 2010; Dyman et al., 1994). These sandstones may transition into the other sandstone lithofacies or form stacked crossbedded channels.

3.1.2.6 Lithofacies Fl: Laminated Fines

Laminated muds, laminated silts, and laminated very fine-grained sands comprise this lithofacies which may consist of beds a few centimeters thick to over a meter thick, occurring both in the Wayan and the Vaughn. These sediments may alternate or

interfinger with each other. They may be red, gray, brown, or green in color and may contain invertebrate traces and wavy laminations. Laminations may represent fluctuations in sediment grain size and energy regimes.

3.1.2.7 Lithofacies Sc: Carbonaceous Shales

Similar to the description above, carbonaceous shales are very rare, but have been reported in the Wayan Formation (Schmitt and Moran, 1982). This lithofacies consists of dark organic shales with plant debris. These deposits are commonly only a few cm thick and occur as isolated beds in sequences of the more abundant Fm lithofacies.

3.1.2.8 Lithofacies Fm: Massive Fines

These massive mudstones to siltstones, which are among the dominant lithofacies in the study area, have produced numerous *Oryctodromeus* specimens in both the Vaughn and the Wayan. These units may be tens in meters of thickness with color varying from gray, green, brown, red, and pink, with the latter two colors being dominant. These lithofacies commonly exhibit pedogenic features such as mottling, slickensides, insect burrows and unidentified invertebrate traces, root traces, and calcareous nodules smaller than a centimeter in diameter to those with a diameter of more than six centimeters (Dorr, 1985; Schmitt and Moran, 1982; Dyman et al., 1994; Krumenacker, 2010). The majority of *Oryctodromeus* specimens are recovered from these facies and they are: IMNH 44920, IMNH 44946, IMNH 45596, IMNH 46169, IMNH 50846, IMNH 50847, IMNH 50877, MOR 1636, MOR 1642 and MOR 8660 (Table 2).

3.1.2.9 Lithofacies Ls: Shaly Limestone

Shaly limestones are among the rarest lithofacies, but they have been reported in the Wayan Formation (Schmitt and Moran, 1982). In the Lima Peaks area in the Vaughn silty limestones have been observed (Dyman *et al*., 1994). Deposition of such lithofacies would have occurred in lower energy environments such as lakes or ponds where sediment would have settled and carbonate could have precipitated (Reading, 1996).

3.1.2.10 Lithofacies B: Ash

Gray to white volcanic ashes and bentonites, which weather out in the typical popcorn-texture are reported for the Wayan and Vaughn. Volcanic ash is a very rare component of the Wayan, but bentonite has been noted as a common component of the Vaughn in the Lima Peaks area (Schmitt and Moran, 1982; Dyman et al., 1994).

3.1.2.11 Lithofacies C: Caliche

Nodular caliche horizons occur in the Wayan and the Vaughn, with them being more common in the Wayan. Rocks from these horizons, commonly have a red to brown color when weathered but gray to red on a fresh surface. These beds form resistant ledges in outcrops and often litter outcrops with nodules and cobbles.

3.1.3 Lithofacies Associations

Lithofacies associations are packets of lithofacies that occur together that may be environmentally or genetically related (Boggs, 2001). Specific lithofacies associations occur in distinct and/or repeated successions in the Wayan and the Vaughn and have been observed in the discussed stratigraphic sections or during research at fossil localities. These associations are presented in Table Four and discusses in their stratigraphic or

paleontological context below. Successions discussed here and there context are then used to elucidate their depositional environments represented.

3.1.3.1: Mudstone to Trough-Crossbedded Sandstone Transition

This upward coarsening sequence has been noted in the lower thirty meters of the McCoy Creek Section (Figure 3, Table 3) in association with *Oryctodromeus* specimen IMNH 44920. Here a basal gray mudstone with a few cm scale calcareous nodules grades upward into a gray siltstone that continues to coarsen upwards into silver-gray medium to coarse-grained trough-crossbedded sandstones. It is typical in some outcrops to see a truncation with a sharp break between the sandstone and mudstone instead of a gradational transition.

3.1.3.2: Trough-crossbedded sandstone to massive sandstone

Trough-crossbedded sandstones that grade upward or laterally into featureless massive sandstones are common in the Wayan. Examples are visible within the fifty to seventy-meter interval of the McCoy Creek Section, where the transition occurs stratigraphically. Examples of this occurring laterally in association with *Oryctodromeus* remains occur in the lowermost portion of the Miners Delight Creek Section (IMNH 44951) and at IMNH vertebrate paleontology locality 2438 (specimen 49842). In the lateral transitions the featureless sandstone is only immediately (within one meter) adjacent to the skeletal concentrations, with trough-crossbedded sandstone occurring on both sides of the skeletal remains.

3.1.3.3: Trough-crossbedded sandstone to massive mudstone

This association has been noted within the Wayan and Vaughn, and occurs within all measured sections and is typically discernible in the better exposed outcrops. Discounting possible error due to poor outcrop quality, this appears to be the most common facies transition within the Wayan. This transition typically occurs with sharp contacts. Fine to coarse-grained gray or brown trough-crossbedded sandstones are overlain by fining upward sequences of mudstones and siltstones that are typically red, pink, purple, or gray that often contain calcareous nodules and other pedogenic features such as mottling, slickensides and invertebrate and *Oryctodromeus* burrows.

3.1.3.4: Chert Pebble Conglomerate to Trough-Crossbedded Sandstones

Transitions from clast-supported conglomerates to trough-crossbedded sandstones are common to the lower 100 meters of the Wayan Formation, forming the only recognized distinctive lithologies that can place one stratigraphically in this unit (Krumenacker, 2010). These beds may have sharp breaks between them or be more gradational. Outcrops at the Tincup Canyon and Schmitt and Moran sections provide the best examples of this facies association. Conglomerates contain red and black chert pebbles and cobbles that can rarely approach cobble size. These conglomerates transition upward into typical brown and gray sandstones.

3.1.3.5: Matrix-Supported Conglomerate to Massive Sand

One example of this association has been noted from IMNH vertebrate paleontology locality 2251, the Robison Bonebed. This locality occurs at an uncertain locality within the middle of the formation, possibly near 700 meters above section base

(Krumenacker *et al*., 2016). The fossiliferous lens of this lithofacies was entirely removed from its host hillside by construction activities and its exact stratigraphic context was lost. However, some general observations can be made. Remaining on the hillside below where the conglomerate occurred is a fine-grained gray-green massive sandstone with bone fragments. Observations made on conglomerate boulders at this locality indicate a basal layer of laminar sandstones below the conglomerate, with the laminar sandstones probably having transitioned into the massive sandstone.

3.2 Taphonomy of *Oryctodromeus*

Taphonomy is the study of the processes that affect a potential fossil from the time it is a living organism until the time it is a specimen in a museum collection. In studying the taphonomy of *Oryctodromeus* here the concern is the processes that are responsible for it being the apparently most common vertebrate taxon represented by skeletal remains from the Wayan and Vaughn assemblages. *Oryctodromeus* specimens occur in distinct patterns relative to the lithofacies they are preserved within. Completeness of specimens, the number and ontogenetic age of individuals that may be associated together, degrees and types of taphonomic modifications, and association with recognized burrows all correlate with the sedimentary context of the specimens. The apparent extreme abundance of *Oryctodromeus* also hints at possible taphonomic processes.

3.2.1 *Oryctodromeus* abundance

There are roughly 495 vertebrate specimens from the Wayan, from ninety-one localities, catalogued in the IMNH collections at the time of this writing. Of these

specimens, 114 are referred to *Oryctodromeus*, with these specimens coming from roughly thirty-two localities. Twelve of these specimens represent partial to near complete skeletons of *Oryctodromeus* (in various states of preparation), while the rest represent isolated to a few associated elements, recovered as loose elements on the ground surface (Tables 1-2).

Oryctodromeus itself represents forty-two percent of the identifiable Wayan assemblage, constituting fifty-three percent of surface finds, and thirty-six percent of specimens that have been recovered in-situ (with a heavy bias being exerted by the specimens recovered from matrix blocks of the RBB). Isolated elements from *Oryctodromeus* comprise roughly fifty percent of the skeletal elements identified within the multi-taxic assemblage of the Robison Bonebed (Krumenacker *et al*., 2016). Discounting eggshell and a nodosaur tooth, *Oryctodromeus* is the only vertebrate taxon identified from the Vaughn, with eight specimens having been catalogued in the MOR collections, which represent a minimum of eleven individuals of varying ontogenetic stages.

While the Wayan assemblage contains numerous taxa, the vast majority of these non-*Oryctodromeus* taxa are known from three localities, all of or associated with lithofacies Gms, IMNH 128 (the Minkin Bonebed), IMNH 2251 (RBB), and the H34D Quarry, IMNH 2167 (Krumenacker *et al*., 2016). Discounting localities that have produced exclusively *Oryctodromeus*, localities that have produced eggshell, primarily of the ootaxon *Macroelongatoolithus*, are the most abundant.

3.2.2 Taphofacies

Specimens can be divided into three taphofacies based on taphonomic modifications such as articulation, association of skeletal elements, completeness of skeletal elements, breakage, weathering, and abrasion. Recognition of these taphofacies facilitates recognition of the taphonomic processes operative in the Wayan and Vaughn that may answer questions regarding the relative abundance of *Oryctodromeus* in comparison to other vertebrate taxa in these assemblages. Due to their association with specimens of taphofacies B, new *Oryctodromeus* burrows are described with that taphofacies.

3.2.2.1 Taphofacies A: Fully to Nearly Articulated

Oryctodromeus of this taphofacies are known only in the Wayan. These specimens (Fig. 7; Table 2) are found much less frequently in comparison to taphofacies A, with only two (seventeen percent) having been found. Two specimens are known from this taphofacies. These are IMNH 44951 and IMNH 49842. This taphofacies occurs within lithofacies Sm.

Specimens exhibit no weathering, breakage, or abrasion. These individuals are dominantly articulated to fully articulated, with IMNH 44951 consisting of a completely articulated individual with even some manual phalanges in place (Table 2; Fig. 7). Missing elements for this individual consist mostly of the tail and most of the neck and skull, which appear to have weathered out prior to discovery. IMNH 49842 is only

partially prepared, but fully articulated hindlimbs in articulation with the pelvis, as well as an articulated axial column and forelimb elements are evident.

Both specimens in this taphofacies also exhibited ventral downward poses (Fig. 5) in their natural occurrence, with IMNH 44951 laying ventrally on its abdomen with limbs splayed outwards, and with IMNH 49842 having articulated legs crouched under the sacrum in a sitting or kneeling position.

Hematitic encrustation is missing on these specimens in contrast to those of taphofacies B. Calcite cracking and infilling is common as with all Wayan and Vaughn specimens. Some crushing has occurred on some elements as well.

3.2.2.2 Taphofacies B: Associated to Partially Articulated

Oryctodromeus specimens in taphofacies B (Tables 1-2) occur in the Wayan and in the Vaughn. The majority of partial to near complete skeletons of *Oryctodromeus* are of this taphofacies, representing ten (83%) of the total sample of twelve articulated to associated specimens (Table 2; Varricchio et al., 2007; Krumenacker, 2010). Additionally, all specimens recovered from recognized burrows are of this taphofacies. Including those described in this paper, three specimens (representing a minimum of five individuals) have been found in discernible burrows (MOR 1636a & b, MOR 8660, and IMNH 50877). These taphofacies correspond to lithofacies Fm.

Typically, specimens consist of strings of articulated vertebrae with or without ossified tendons; articulated pes (such as the three pes of varying size preserved in IMNH 44939), and associated limb and skull elements. More rarely, specimens may be entirely disarticulated as in MOR 1636 and b and IMNH 46169. Sorting of elements from

specimens has not occurred with elements of disparate Voorhies Groups such as phalanges, ribs, chevrons, vertebrae, limb and skull elements consistently occurring together.

Specimens of this taphofacies exhibit no pre-diagenetic breakage, weathering, or abrasion. Varying degrees of articulation and association occur (Table 2), and the number of individuals present varies from one individual to multiple individuals of varying ontogenetic stages (Table 2). In both the Wayan and the Vaughn specimens occur in dense concentrations of skeletal elements that are associated and/or articulated. These accumulations are typified by the holotype (MOR 1636a) and paratype (MOR 1636b) specimens, representing one presumably mature and at least two juvenile individuals. Breakage on specimens consists of sharp breaks on delicate and thin surfaces with no abrasion, suggesting that breakage is entirely a factor of recent weathering/preparation/collection. Thus, excluding modern weathering and erosion, elements were presumably complete prior to burial.

Pre-diagenetic bone surface flaking is non-existent on these specimens. Diagenetic modifications consist of hematite encrustation (complicating interpretations of bone surfaces), crushing, small scale faulting/offsets, and cracking. This diagenetic cracking, consisting of cracks and calcite infilling, occur perpendicular and parallel to the long axes of bones. However, there is no cracking with matrix infilling suggestive of pre-diagenetic weathering.

3.2.2.2.1 Taphofacies B: New *Oryctodromeus* burrows

During the excavation of an associated *Oryctodromeus* skeleton (IMNH 50877) from the Wayan Formation of Bonneville County Idaho in 2015, an unusual concretionary structure was noticed immediately behind the jacketed skeletal material (Fig. 3A-D; Supplementary File 1). Excavation of this structure revealed a sinuous and tubular structure that closely matched the morphology of the previously described burrow (Varricchio *et al*., 2007).

3.2.2.2.1.1 Wayan Burrow

This ichnofossil occurs in the Miners Delight Creek measured section of Krumenacker (2010), placing it near the top of this 133 meter thick partial section. This measured section itself occurs within an uncertain exact stratigraphic position within an outcrop of the Wayan Formation in the Caribou Range, Bonneville County, Idaho (Fig. 1, 3). The burrow (Fig. 4A-D, Supplementary File 1) occurs in a homogenous, heavily weathered and pedogenically altered red siltstone bed that occurs in multiple meters of similar red siltstones and mudstones sandwiched between sandstone beds. This same red siltstone horizon has produced other *Oryctodromeus* specimens within seven meters of this location (discussed below). This siltstone is highly calcareous with gray and green mottling and calcareous nodules up to 1 cm in diameter with decreasing abundance higher in section. This calcareous siltstone containing the burrow transitions upsection into a featureless red mudstone, about 1.5 meters thick, which is truncated by coarse-grained and cross-bedded fluvial sandstones that exhibit conglomeratic lenses of pebble-size caliche nodules and small unidentifiable bone fragments.

The burrow, though somewhat indistinctly preserved, consists of a single concreted unit in the lower portion and a more fractured structure higher in the weathered portions. The cohesive nature of the burrow contrasts with the uniformly fractured sediment around it. The periphery of the structure is somewhat ill-defined due to the lack of grain size differentiation between the structure and the surrounding matrix, and due to a multi-centimeter thick (2-3 cm) concretionary rind that flakes off of the areas of the outer portion of the trace. The presence of the concretionary rind, the indistinct periphery of the trace, and the lack of differences in sediment grain size has precluded the observation of any possible fine-scale features such as accessory smaller burrows, as those described for the holotype burrow (Varricchio *et al*., 2007), or scratch marks. The burrow loses definition as it ascends stratigraphically due to recent weathering and fracturing and appears to be truncated at the base of the red mudstone (Fig. 3). Unlike the holotype burrow from the Vaughn Member, this structure is not defined by a difference in sediment grain size. The sediment composing the burrow fill appears identical to that surrounding the structure, both being composed of red siltstone.

The description of the morphology here is done as if the sediments were in their original horizontal position. After documentation, the most terminal portion of the burrow was collected. This terminal portion had a natural break (Fig. 3A, C) facilitating collection and was more stable than the more highly fractured, weathered, and less distinct stratigraphically higher part of the structure that was left *in-situ* in the field. No bone has been observed in the portion of the burrow collected, but it is possible that some is inside. The structure is sinuous and semi-helical. Beginning at the upper truncated

contact with the red mudstone, the structure slopes downwards from the upper truncation at an estimated 5° for 82 cm. Though heavily weathered and damaged, the next portion of the burrow appears to turn to the right for an estimated 40 cm (this portion of the burrow was damaged from erosion and/or collection of skeletal elements prior to recognition of the structure) and continues down for another 29 cm and then turns horizontally, proceeding for another 62 cm. The final portion of the burrow consists of the original jacketed section that contained skeletal elements, adding another 58 cm in length. The total estimated length of this structure as preserved is 271 cm. The cross-section of the more distal portion of the burrow (near the skeletal concentration) measured 28 cm wide and 32 cm tall, though the sediment rind of the outer portions of the structure suggests slightly larger dimensions of a few additional centimeters. Though the original jacketed portion of the structure that contained the skeletal elements did not have a recognizable burrow structure, probably due to recent near surface weathering, this may have represented a distal expansion like that described for the Vaughn burrow (Varricchio *et al*., 2007).

Skeletal elements found in this burrow fill (catalogued as IMNH 50877) were collected before the trace was recognized (area of skeletal material is indicated in Fig. 4D). Elements recovered consisted of a left femur, a lateral distal tarsal, thirteen partial to near complete caudal vertebrae, two chevron fragments, a rib, and a few partial indeterminate bones. All of these elements appear to belong to one medium-sized individual similar in size to MOR 1636a. These bones were within the distal portion of the burrow removed in the field jacket, prior to burrow recognition. The elements were

scattered in various orientations in what would have been the original middle and upper portions of the stratigraphically deepest part of the burrow fill. The femur was semi-vertically oriented at roughly forty degrees, and near the top of what is interpreted as the top of the trace. Smaller bones, such as vertebrae, were aligned linearly along their long axis with the trend of the burrow and scattered from the top of the fill into the lower portions of the jacketed burrow fill. It is possible that additional skeletal elements are within the more proximal portion of the burrow fill that has been collected and left unprepared to preserve an example of the burrow, but none were noted during collection.

The morphology of this structure is similar to the previously described burrows of *Oryctodromeus* and possible other neornithischian burrows (Varricchio *et al*., 2007; Martin, 2009). The cross-sectional width and height of this trace is similar to that of the previously described burrow from the Vaughn (Varricchio *et al*., 2007) which had a diameter of roughly 30 cm. The sinuous form of the ichnofossil is also very similar in morphology to the burrows described by Varricchio *et al*. (2007) and Martin (2009). Unlike the holotype burrow, a terminal expansion was not recognized in this second example, possibly due to heavy weathering.

3.2.2.2.1.2 New Vaughn Burrow

A second burrow from the Vaughn has been found in the Lima Peaks area of Beaverhead County, Montana and was associated with MOR 8660 (Fig. 3E-F; Table 2). The structure occurred in a gray green claystone with the fill consisting of a silty green mudstone (Fig. 3E-F). This structure had a semi-circular outline and a diameter of roughly 30 cm on the long axis and roughly 20 cm on the shorter axis. The abrupt flat

edge of this burrow fill in cross section (Fig. 4E-F) suggests erosion and truncation of the burrow prior to eventual preservation. Preservation was poor and somewhat indistinct in the vertically oriented beds, and since most of the structure was missing little data is available. The remnants of this structure were noted after collection of a jacket containing skeletal elements from this location.

3.2.2.3 Taphofacies C: Isolated

Oryctodromeus specimens from this taphofacies are known solely from the RBB. Fossils are typically isolated but a few articulated strings of *Oryctodromeus* caudal and cervical-dorsal vertebrae are known. Taphonomic modification such as breakage and abrasion are dominant on these specimens with broken and partial isolated bones being by far the most common. A few isolated pristine elements are known, including a partial small *Oryctodromeus* dentary with fully erupted and complete tooth crowns. No associated individuals representing a significant portion of one individual, on par with those from the other two facies, are known from this facies/location. This taphofacies corresponds to lithofacies Gms.

4. Discussion

The discovery of the holotype and paratype specimens within a burrow, and the above descriptions of new burrows with associated specimens raise the question of how commonly *Oryctodromeus* specimens may be preserved within burrows, and how often these burrows may or may not be recognizable. These questions tie into the broader question of why *Oryctodromeus* appears to be the dominant vertebrate taxon in the Wayan and Vaughan assemblages. To answer these question, the depositional

environments in the Wayan and Vaughn need to be understood, and taphonomic modes need to be recognized. Once these are understood, further questions such as more specific possible burial settings in relationship to possible taphonomic biases, as well as possible additional evidence for sociality can be addressed.

4.1 Depositional Environments

While the somewhat superficial nature of the geological data presented here doesn't allow in-depth analysis, assessment of the lithofacies and lithofacies associations of the Wayan and Vaughn reinforce previous hypotheses regarding depositional environments within the Wayan and Vaughn depositional systems (Dorr, 1985; Schmitt and Moran, 1982; Krumenacker, 2010). Additionally, these data offer the potential for new insights into the taphonomic process operative in these systems.

The repetitive sequences of lenticular bodied cross-bedded sandstones, sometimes which have cut downwards into finer-grained pedogenic sediments, indicate the presence of moderate to lower energy river systems that were operative in the Wayan and Vaughn paleoenvironments. Cross-bedded sandstones in these lithofacies accumulated through lateral accretion. Conglomeratic sandstones (lithofacies Gcs), such as those with abundant chert pebbles and cobbles, indicate fluvial processes of higher energy levels and steeper gradient more proximal to the source areas than those of the finer-grained sands with no pebbles (Reading, 1996). Possibly these conglomeratic lithofacies represent braided river deposits closer to the Sevier Highlands, while the finer-grained channels represent the more distal meandering river systems of alluvial plain. The transition from these conglomeratic sands to finer-grained sandstones indicates a change in sediment

availability probably related to the distance to the source area and the stream gradient. The lithofacies from the Robison Bonebed (Gms), due to the poorly sorted cobble size clasts and the broken bones contained within, indicate a short-lived debris flow possibly associated with fluvial processes and energetic mass movement.

As noted by Schmitt and Moran (1982) and Dyman et al. (1994), mudstones and siltstones, here represented by lithofacies Fl, Flc, and Fm, dominate the Wayan and Vaughn. Muds and silts that compose these lithofacies accumulated through vertical accretion when sediment was supplied and settled through suspension during flood events. The pedogenic features common in these lithofacies were subsequently overprinted and indicate substantial subaerial exposure and hiatuses in deposition, in conjunction with variably fluctuating watertables as indicated by lithofacies C and features of lithofacies Fm. Calcareous nodules and caliche horizons would have formed through pedogenic processes and fluctuations in the water table leading to the precipitation of discrete zones of calcium carbonate, and indicate a semi-arid environment (Retallack, 2001). Synthesized these observations indicate that these alluvial plains were in a dominantly or regionally semi-arid environment subject to a monsoonal regime (Retallack, 2001). The less common sediments in this lithofacies that lack common calcareous nodules and that are more drab in color represent more poorly-drained humid areas with more stable water tables. Lithofacies Fl, Flc, and Lc also represent more humid areas with stable water tables such as lakes and ponds, due to their laminar nature, plant debris, and higher organic content. The facies association of mudstone coarsening upwards into trough-crossbedded sandstones suggests crevasse-

splay events were operative and occasionally may have buried individuals of *Oryctodromeus*. Ash falls and the subsequent bentonites (lithofacies B) indicate periodic volcanic input.

Associations of *Oryctodromeus* with various lithofacies indicate areas of preferential preservation and/or paleoecological preferences. The vast majority (ten of twelve) of the partial and associated skeletons, and all known *Oryctodromeus* burrows, come from lithofacies Fm, which represents the alluvial plains of the Wayan and Vaughn. These lithofacies dominantly represent well-drained floodplains. The only other lithofacies that is a source of partial and associated skeletons of *Oryctodromeus* are lithofacies Sm, these massive sands are distinctive in only being featureless in immediate proximity to the skeletal remains. The association of this taxon with these deposits indicate some sort of relationship to these river channels that will be explored subsequently. The last lithofacies that produces specimens is Gms. Here *Oryctodromeus* fossils occur as bones and teeth that exhibit highly variable degrees of taphonomic modification, reflecting the violent and intraformational nature of the deposit

4.2 Taphonomic Pathways and Histories

The origin of the *Oryctodromeus* accumulations in the late Albian to Cenomanian of the Wayan and Vaughn can be explained by relatively simple pathways post mortality, with two broad pathways being indicated. After death carcasses were subjected to varying levels of taphonomic processes such as skeletonization, disarticulation, weathering, breakage, and abrasion. Exposure to these processes was determined by exposure to destructive forces in relationship to how long the remains were subjected to

subaerial exposure on the ground surface, how much post-burial reworking and bioturbation may have been experienced, and to the environments the individuals were buried in.

The lack of breakage, abrasion, sorting, and the near complete to full articulation (Fig. 6 and 7) of specimens in Taphofacies A clearly show that these remains were not subjected to the more rigorous destructive processes that are commonplace in many environments prior to burial and fossilization. These observations also indicate either quick burial or emplacement within an environment that protected these remains from the damaging processes most typical of floodplain and fluvial depositional systems. The higher degrees of association and articulation all specimens of Taphofacies B indicate a greater time before burial, but still less destructive processes due to the lack of weathering and abrasion. The retention of delicate skull elements and manual phalanges, plus the three-dimensional compact nature of these specimens when recovered argue against fluvial sorting. Common bioturbation within these geological units also suggests that at least some disarticulation may be due to bioturbation of the remains after burial. The occurrence of Taphofacies A and B respectively, within lithofacies Sm and Fm indicate burial within alluvial plain environments and an association with fluvial channel sediments for the most complete specimens.

The isolated nature of specimens from Taphofacies C, as well as the fact that they exhibit substantial and varying degrees of taphonomic modification, indicate that preservational pathways were substantially different for these specimens. Taphonomic modifications here suggest that these elements were subjected to energetic and violent

forces during deposition of lithofacies Gms. Additionally, the fact that these deposits are intraformational in nature suggests that at least some of these *Oryctodromeus* remains may have been reworked from older deposits that may have included more complete remains typical of Taphofacies A and B. As discussed above, the nature of these deposits and the entombed specimens indicates violent and quick burial in an isolated sudden event such as a debris flow (Krumenacker *et al*., 2016).

4.2.1 *Oryctodromeus* Taphonomic Modes

Taphonomic modes are repetitive patters of fossil preservation in distinct sedimentary contexts in association with characteristic taphonomic features. *Oryctodromeus* can be divided into two distinct taphonomic modes based on the patterns of occurrence. Taphonomic Mode A consists of isolated elements and rare strings of articulated vertebrae, while Taphonomic Mode B consists of associated to articulated specimens.

4.2.1.1 Taphonomic Mode A: Isolated

This taphonomic mode consists of dominantly isolated *Oryctodromeus* sites with specimens that underwent the most significant taphonomic alteration prior to burial and preservation. This mode occurs in lithofacies Gms. These specimens occur at the RBB and number roughly forty-four specimens referable to *Oryctodromeus* (preparation is ongoing). Elements found typically consist of teeth; more robust limb elements such as femora, tibiae, and humeri; and vertebrae. The typically complete disarticulation and isolation of these elements (excluding the two specimens consisting of articulated strings of vertebrae), as well as the breakage of limb elements and vertebral processes,

demonstrate higher energy regimes, more significant transport, and likely more time to allow for complete skeletonization and scattering of the affected individuals. The occurrence of these specimens in a high energy intraformational debris flow indicates that the specimens were possibly reworked from other deposits of other facies.

4.2.1.2 Taphonomic Mode B: Associated to Articulated

This taphonomic mode includes all twelve of the articulated and associated specimens. Occurrences are in lithofacies Fm and Sm. All of these specimens share the commonalities of: 1) consisting of one or more individuals that are represented by more than one single short (six or less) string of vertebrae, 2) consisting of collections of appendicular and axial elements, and 3) a range from fully articulated to entirely disarticulated but preserved in a dense three-dimensional bone concentration. Individuals may occur solely or as closely associated individuals of similar (MOR 1642) or varying ontogenetic stages (IMNH 44939, IMNH 50846, MOR 1636). Fully articulated specimens are the least common, and consist of the two specimens from lithofacies Sm (Figures 5 and 7). Partially articulated specimens (Fig. 6), often with strings of articulated vertebrae (five specimens) and/or articulated pes (three specimens), are the most common degree of association and articulation. Full disarticulation is the least common, being represented by MOR 1636. All specimens not from the RBB (and therefore all articulated to associated specimens as well as specimens associated with recognized burrows) occur in this taphonomic mode. The near to full articulation of these specimen suggests rapid burial of the remains and/or little exposure to destructive processes prior to burial, as well as possibly a lack of transport of the remains. The presence of delicate features such as

the articulated partial manus of IMNH 44951 (with the remaining elements likely missing due to recent erosion) suggests the presence of soft tissues during burial, and that possibly this specimen was a very fresh carcass or even a living animal that was buried quickly in the burial event.

4.3 Paleoecological and Palaeobiological Implications

4.3.1 Burial Settings

Several general burial settings are possible for the *Oryctodromeus* specimens described here. Based on the paleoenvironmental and geological interpretations of the Wayan and Vaughn discussed above, burial of carcasses was possible on floodplains during overbank flooding events and associated crevasse splays, or in debris flows and associated events. Burial was also possible within the small fluvial channels in the Wayan and Vaughn in channel lags or channel fills, in lacustrine or ponded environments, or within burrows of the animals own construction (Schmitt and Moran, 1982; Dorr, 1985; Weishampel *et al*., 2002; Krumenacker, 2010; Krumenacker *et al*., 2016; Varricchio *et al*., 2007). Based on the lithofacies that *Oryctodromeus* specimens are preserved within, three burial settings are possible and are explored here. These are burial within alluvial plain surficial environments (represented by lithofacies Fm and possibly Sm), burial within fluvial channels (possibly represented by lithofacies Sm) and associated debris flows (represented by lithofacies Gms), and burial within floodplain burrows (which could be represented by lithofacies Fm and Sm).

4.3.1.1 Floodplain Burial

Burial of carcasses on floodplain surfaces through flood related processes is among the most common modes for preservation of terrestrial vertebrate fossils throughout Mesozoic and other terrestrial formations (eg. Behrensmeyer, 1991; Rogers, 1991; Suarez *et al*., 2007). Surficial floodplain burial includes burial by flood events, debris flows and loess deposition (eg. Dodson *et al*., 1980; Smith, 1993; Britt *et al*., 2009).

The taphonomic characters of vertebrate specimens buried within surficial floodplain environments runs the entire taphonomic spectrum varying from; complete articulated specimens, to associated but entirely disarticulated multiple individuals, to isolated and highly altered and unidentifiable bone fragments (eg. Dodson *et al*., 1980; Behrensmeyer and Hook, 1992; Paik *et al*., 2001; Eberth and Currie, 2005; Csiki *et al*., 2010). In specimens from these environments, degrees of weathering, abrasion, breakage, and predator/scavenger damage are again highly variable, with larger taxa generally being more common and better preserved (Behrensmeyer, 1988; eg. Bell and Campione, 2014; Paik *et al*., 2001; Rogers, 1990; Rogers *et al*., 2001). However, Behrensmeyer and Hook (1992) have noted that the preservation of smaller taxa may be preferentially favored in well-drained alluvial plain deposits.

The majority of *Oryctodromeus* specimens described here (83%; Table 2) were recovered from sediments deposited in moderate or lower energy alluvial plain environments represented by lithofacies Sm and Fm. The lack of aquatic invertebrates and organic or coaly debris, the lack of thin laminar sediments representative of ponded

environments, as well as the presence of pedogenic features such as calcareous nodules, invertebrate burrows, and mottling within the entombing sediments for these specimens indicate burial was generally within well-drained and not ponded or lacustrine environments. As previously mentioned, taphonomic observations indicate less exposure to destructive processes indicative of quick burial and/or preservation in areas not subjected to surficial taphonomic processes. Combined taphonomic and preservational observations suggest an autochthonous origin within the terrestrial alluvial plain environments.

4.3.1.2 Channel Burial

Preservation within fluvial channel deposits is also amongst the most common modes of preservation for vertebrate remains in the fossil record (Behrensmeyer, 1988; Behrensmeyer and Hook, 1992; Carpenter, 2013). Two general taphonomic modes for burial within fluvial channels have been previously defined: burial in channel lags and burial within channel fills (Behrensmeyer, 1988). Fossils from channel lags commonly consist of allochthonous, highly time averaged, isolated and varyingly damaged/modified elements from disparate taxa (Behrensmeyer, 1988). Fossils found in channel fill deposits also exhibit varying damage/modification, but there is more of a preponderance towards associated and articulated remains, as well as more commonly the presence of smaller taxa (Behrensmeyer, 1988; eg. Carpenter 2013).

Oryctodromeus remains associated with channel deposits, represented by lithofacies Sm and laterally adjacent lithofacies St, are rare and are only known from the Wayan. These specimens are IMNH 44951 and IMNH 49842. Both of these individuals

were found in poorly outcropping exposures of small scale trough-crossbedded sandstones that are typical of the Wayan. Crossbedding is prominent in both outcrops that the specimens originated from (Fig. 4); however, the sandstones immediately adjacent (within one meter) to both skeletal concentrations are featureless and lack any type of depositional structures. Nowhere else in these outcrops were structures lacking, except in immediate proximity to both specimens. The preservation of both of these specimens entirely within more fine-grained sediments within these channels, their state of articulation (Fig. 7), the lack of damage, and the lack of remains from other taxa argue against them being preserved with channel lags.

4.3.1.3 Burial Within Burrows

The taphonomy of fossorial vertebrates preserved within recognized burrows has received little description. In general, vertebrate skeletal elements associated with burrows are partial to complete skeletons that exhibit minimal predator/scavenger damage (excepting larded prey), breakage, weathering, and abrasion, and range from fully articulated to associated skeletons. Most descriptions are of Permian and Early Triassic taxa from the Karoo Basin of South Africa and Paleogene, (Damiana *et al*., 2003; Groenwald *et al*., 2001; Hunt *et al*., 1983; Smith, 1987; 1993; Stokes, 1982; Tobin, 2004). The preservation of the holotype and paratype of *Oryctodromeus* within a burrow, as well as the preservation of additional *Oryctodromeus* remains within burrows as described here, hints at the possibility of in-burrow preservation of skeletons of this taxon being a common and possibly often unrecognized occurrence.

4.3.1.4 Burial Assessment

Oryctodromeus specimens that have been recovered from recognized burrows (MOR 1636, MOR 8660, and IMNH 50877) have consisted of entirely disarticulated but closely associated skeletal remains, representing one or more individuals of differing ontogenetic stages, with no appreciable taphonomic modifications such as breakage, weathering and abrasion. Some associated specimens (IMNH 46169, IMNH 50846) that have not been found within recognized bourrows have exhibited the same preservational style of relatively pristine but fully disarticulated elements in bone-packed masses. Additional specimens where a burrow has not been recognized show a spectrum of partially articulated and associated elements to fully articulated skeletons. Additonally, *Oryctodromeus* specimens of taphofacies A and B closely match the taphonomic characters described for other burrowing fossil taxa (Damiana *et al*., 2003; Groenwald *et al*., 2001; Hunt *et al*., 1983; Smith, 1987; 1993; Stokes, 1982; Tobin, 2004). This gradation of taphonomic styles suggests the possibility of within-burrow preservation.

Specimens of taphofacies A (IMNH 44951 and IMNH 49842) are most intriguing. Due to its complete articulation, IMNH 44951 experienced extremely rapid burial, or at least was not subject to destructive forces typical for longer periods of subaerial exposure. Its preservation, as well as that of IMNH 49842, in sediments related to small fluvial channels suggests the possibility of carcasses buried within channels, or alternatively burial within burrows associated with this ephemeral or abandoned channel, and/or possible events of burrow collapse within these channel sediments (Fig. 4). The dorsal-up position of both specimens in their stratigraphic setting, with the legs of IMNH

49842 folded up under the specimen in a crouched position, and IMNH 44951 (Fig. 7) lying on its ventral surface when found also may favor a burial setting. While theoretically possible in a fluvial channel for specimens to have the dorsal surface facing up, the position of both these specimens in crouching positions, the lack of sedimentary features indicative of fluvial processes immediately around the bones, and bioturbation immediately adjacent to the specimens, the lack of other taxa or remains being preserved in the same channel deposits, and the burrowing lifestyle of *Oryctodromeus* all strongly suggest the most parsimonious explanation to be burial within collapsed or infilled burrows associated with these small channels. Additionally, due to their fully to near fully articulated state, these specimens both strongly resemble the results from trial ten (X) of Woodruff and Varricchio's (2011) experimental burrow modeling, where a water saturated rabbit skeleton buried in a simulated flood event resulted in an articulated skeleton within the model burrow.As demonstrated, specimens of taphofacies B experienced lesser degrees of pre-burial taphonomic modification (in comparison to those of taphofacies C) and were buried quickly or without experiencing greater degrees of modification.

Specimens of Taphofacies B (Table 2; Fig. 5) can be shown to have experienced more destructive forces and/or more residence time (in comparison to taphofacies A specimens) on the ground surface or within an open burrow prior to being entombed by sediments, with varying degrees of disarticulation occurring prior to, or during, burial. Arrangements of the skeletal elements of specimens of taphofacies B as found *in-situ* are similar to the burrow specimens (MOR 1642, MOR 8660, and IMNH 50877). The

arrangement of bones in discrete dense concentrations in specimens without recognized burrows is identical to those from burrows. Additionally, the bone concentrations of non-burrow specimens are similar to the results of *Oryctodromeus* burrow modeling by Woodruff and Varricchio (2011), with linear bone arrangements and dense bone concentrations resembling the results of most of their trials. The overall taphonomic state and geological setting of these specimens indicates either burial on the ground surface or in a subaqueous environment, with sufficient time to disarticulate to varying degrees; but not enough time for skeletons to weather, scatter out of a very concentrated area or lose small delicate elements to other destructive processes. Alternatively, the lack of damage to skeletal elements and the presence of most skeletal elements with these specimens could indicate sufficient time within an open burrow for the decay of most soft tissues, and disarticulation to occur prior to burial. It is possible disarticulation also occurred to some degree during a burrow filling event or burrow collapse.

Conditions less-conducive to the preservation of vertebrate remains within the Wayan and Vaughn are suggested by the rare and highly taphonomically modified specimens of non-*Oryctodromeus* taxa. Alternatively, the rarity of non-*Oryctodromeus* taxa may be due to ecological conditions or a combination of ecologic and taphonomic factors. The presence of various ootaxa in the Wayan and Vaughn, and the presence of extremely rare skeletal elements of other non-*Oryctodromeus* taxa from the Wayan and Vaughn do seem to suggest preservational biases were definitively operative. Evidence for this includes the fact that large oviraptorosaurs were known to have nested in these environments (Simon, 2014; Krumenacker *et al*., 2016) and that a diverse assemblage or

fauna(s) are indicated by the numerous taxa reported from the RBB (Krumenacker *et al*., 2016).

The complete absence of non-*Oryctodromeus* taxa found as *in-situ* skeletal (i.e. non-eggshell) remains in these floodplain deposits, also support the hypothesis of *Oryctodromeus* typically being preserved within unrecognized burrows. If *Oryctodromeus* remains were typically buried on the ground surface, this complete lack of any other associated and articulated partial or more complete skeletons of other taxa within floodplain sediments (the previously described nodosaur from H34D is from a crevasse splay or channel lag deposit) would be hard to explain. Behrensmeyer and Hook (1992) do note that smaller bodied taxa appear to have a higher preservation potential in mature paleosol sequences such as those of the Wayan and Vaughn. However, while smaller vertebrate taxa are typically among the most common in an ecosystem, it would be expected that within more than thirty-five years of prospecting in the Wayan and with the more cursory work in the Vaughn, that at least one occurrence of a few associated or a larger occurrence of articulated remains of a larger taxon or of another small taxon, such as the small theropods known from isolated teeth (Krumenacker *et al*., 2016) would have been found in the floodplain sediments by this point. It seems otherwise very anomalous that a few dozen *Oryctodromeus* partial to near complete skeletons have been found in the Wayan and Vaughn at this point.

Further, the vertebrate assemblage of the Wayan and Vaughn suggests processes favoring remains that were already buried by biological activities. The ootaxon *M. carlylei*, usually found in eggshell concentrations possibly representing nests or eggs

fragmenting as they are weathering out, are the next most abundant vertebrate fossil found in the Wayan (Simon, 2014; Krumenacker *et al*., 2016). The higher degree of porosity of Wayan and Vaughn *M. carlylei* eggs and eggshell is indicative of burial within sediment or vegetation mounds (Simon, 2014). While the totality of evidence discussed here does not firmly prove the burial of *Oryctodromeus* specimens of taphofacies A and B was typically within burrows, it is a reasonable explanation.

4.4. Sociality

The co-occurrence of the holotype and paratype specimens (MOR 1636), consisting of juvenile and adult elements preserved within the same bone mass, was interpreted as evidence of parental care (Varricchio *et al*., 2007). Three additional specimens (Table 2) consisting of the associated remains of presumably adult and juvenile individuals (IMNH 44939, IMNH 50846) as well as associations of multiple presumably mature individuals (MOR 1642), strongly reinforce the possibility of a communal habit. While the associations of multiple individuals, which constitute one-third of associated and articulated specimens, may be accidental and represent allochthonous assemblages, the same taphonomic features as described above for these same skeletons argue against major transportation and mixing of remains. The relatively common occurrence of multiple *Oryctodromeus* individuals together and in close proximity suggests a degree of social interaction and perhaps communal activities for this taxon.

In addition to multiple individuals having inhabited the same burrows, some evidence shows that *Oryctodromeus* burrows may have been in close proximity to each

other. In the Miners Delight Creek measured stratigraphic section (Krumenacker, 2010), two *Oryctodromeus* concentrations have been found in the same stratigraphic horizon (Fig. 3) and were separated by roughly seven meters of lateral distance. These occurrences, IMNH 50846 and IMNH 50877, both consist of an association of presumed mature and juvenile individuals,(this paper; Krumenacker, 2010). While a burrow is recognized for only IMNH 50877, the presence of varying ontogenetic stages with IMNH 50846 suggests possible preservation within a burrow.

4.5 Paleoecology

The original ecological abundance of *Oryctodromeus* may also be indicated by the relative abundance of specimens relative to other taxa. Generally in any ecosystem, small bodied animals are more abundant than larger bodied taxa (eg. Hechinger at al., 2011). While here it is hypothesized that the overwhelming abundance of *Oryctodromeus* in the Wayan and Vaughn assemblages are in-part due to preferential preservation of skeletal associations in burrows, the abundance of this taxon in these assemblages may also be reflective of a presumed ecological abundance in its original terrestrial paleoenvironments.

While a bias clearly exists heavily favoring the preservation of *Oryctodromeus* skeletons within the floodplain environments of the Wayan and Vaughn, isolated *Oryctodromeus* elements of taphonomic mode A comprise roughly fifty percent of the skeletal elements identified within the assemblage of the Robison Bonebed (Krumenacker *et al*., 2016). The Robison Bonebed is a coarse-grained and high energy deposit interpreted as a debris flow deposit possibly associated with a fluvial channel

(Krumenacker *et al*., 2016). Beyond the abundant *Oryctodromeus* elements preserved in this deposit, partial theropod bones and teeth, nodosaur remains, and large ornithopod remains occur in decreasing abundance. While the assemblage from the RBB is fragmentary and the identifications are tentative due to lack of preparation on most specimens, the numerical dominance of elements of *Oryctodromeus* in this allochthonous assemblage may represent ecological dominance of this taxon as would be expected for a smaller bodied animal, but bias is possible as well due to the reworked intraformational nature of this deposit.

The totality of evidence from the Wayan Formation and Vaughn Member of the Blackleaf Formation suggest a unique preservational bias was operative in these depositional systems, with the preservation of the fossorial ornithischian *Oryctodromeus* within its own burrows being favored more than the preservation of other, generally more typical, larger vertebrate taxa. While not conclusive, the combination of various lines of evidence supports this hypothesis. This evidence includes: 1) the relatively pristine pre-diagenetic taphonomic condition of associated to near complete skeletons of *Oryctodromeus*, 2) occurrence of *Oryctodromeus* specimens as dense skeletal masses identical to that of the holotype specimen as well as other fossil occurrences of burrowing taxa, 3) taphonomic conditions being identical for specimens known from burrows and those without recognized burrows, 4) recognition of two additional burrows with associated skeletal material, 5) abundance of *Oryctodromeus* partial to near complete skeletons in comparison to other taxa in floodplain and small channel deposits, 6) the near complete lack of skeletal remains of other taxa in floodplain and channel deposits,

and 7) the much greater degree of taphonomic modification to the very rare remains of other taxa found in the floodplain and channel deposits. Though the sample size is small, there are suggestions that degrees of articulation are related to proximity to fluvial channels (Woodruff and Varricchio, 2011).

5. Summary

Skeletal elements of *Oryctodromeus* heavily dominate the Wayan and Vaughn fossil vertebrate assemblages, with most other taxa known from isolated and fragmentary skeletal remains solely coming from a few multi-taxic localities related to high energy depositional events. Isolated elements of *Oryctodromeus* are known from one multi-taxic locality, the Robison Bonebed (RBB). At this locality *Oryctodromeus* accounts for half of the skeletal remains found. Associated to articulated skeletons of *Oryctodromeus* come from bioturbated sandstones and pedogenically overprinted alluvial plain deposits, with these specimens fitting into two taphofacies: Taphofacies A which consists of skeletons that are nearly to entirely articulated, and taphofacies B which has associated to partially articulated individuals. A third taphocies, C, encompasses mostly isolated and heavily taphonomically altered elements from the RBB. Three specimens from taphofacies B consist of multiple individuals of varying ontogenetic stages.

The taphonomic datas suggest the possibility that specimens of taphofacies A and B were preserved within unrecognized burrows, with those of taphofacies A having experienced quicker burial and/or burial in waterlogged burrows. Additional evidence for social groups, as well as parental care, is indicated with some of the *Oryctodromeus* specimens described. Whereas two-thirds of articulated to associated specimens consist

of apparently single individuals, occurrences of two or three individuals are common in the Wayan and Vaughn, with groupings of large presumably mature individuals (3.5m length) as well as associations of juvenile and mature individuals of similar sizes to the holotype and paratype.

Whereas the occurrence of assemblages dominated by the remains of fossorial taxa, or at least with commonly occurring fossorial taxa preserved within their burrows, is not highly unusual (eg. Smith 1993; Sundell, 1997), an example of a terrestrial Mesozoic assemblage dominated by the remains of fossorial dinosaurs, nearly to the exclusion of other taxa numerically and in most facies, is an unusual circumstance. The occurrence and relative abundance of *Oryctodromeus* in the very thick (1,344 meter) Wayan Formation, as well as the abundance of burrowing vertebrates in other anomalously thick (on the order of many hundreds to thousands of meters) sediments such as the Balfour Formation and Teekloof Formation, where burrowing vertebrate taxa also occur, may indicate a relationship between rates of sediment input and preservation of burrowing taxa (Turner, 1981; Smith, 1987; Abdala et al., 2006; Oghenekome, 2012). Studies of the taphonomy of modern burrowing vertebrates, as well as actualistic studies of the taphonomic processes associated with the preservation of vertebrate burrows and associated skeletal remains, are largely lacking. Further studies in these areas have potential to possibly recognize similar as yet-unrecognized fossorial assemblages and to facilitate greater understanding in this largely unexplored area of Mesozoic vertebrate paleontology.

Acknowledgements

Funds for this research were partially from and gratefully received from the Jurassic Foundation, as well as the Montana State University Graduate School in the form of a Competitive Research Grant. Barbara Beasley, Steve Robison, Ali Abusaidi, and Diane Wheeler facilitated permitting processes through the US Forest Service. Thanks to Jack Horner, John Scanella, and the Museum of the Rockies for access to specimens and records. Appreciation is expressed to Robert Simon for his donation of funds that contributed to the collection of the burrow specimen described herein. Steve Robison and Ted Dyman assisted with the collection of some of the specimens described here. Kelli Taddy and the students of the 2014 and 2016 MSU Paleontology Field Course assisted with fieldwork. David and Jodie Krumenacker helped with the collection of the Wayan Formation burrow described above. Elise Krumenacker helped excavate the Wayan burrow in between fleeing from aggressive bees.

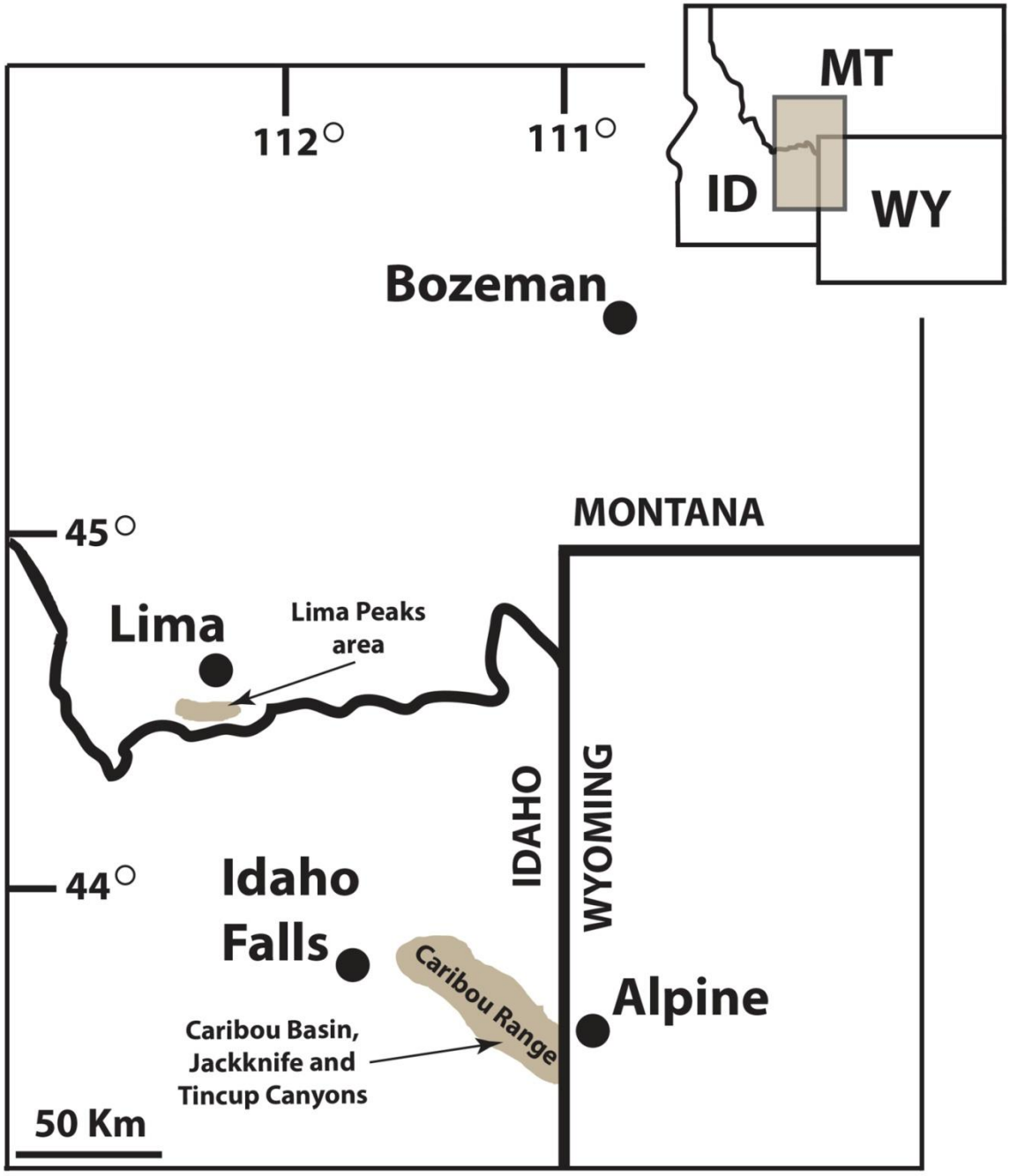

Fig 3.1. Outcrop areas of the Vaughn Member of the Blackleaf Formation (Montana) and the Wayan Formation (Idaho). *Oryctodromeus* specimens are known from all of the indicated areas.

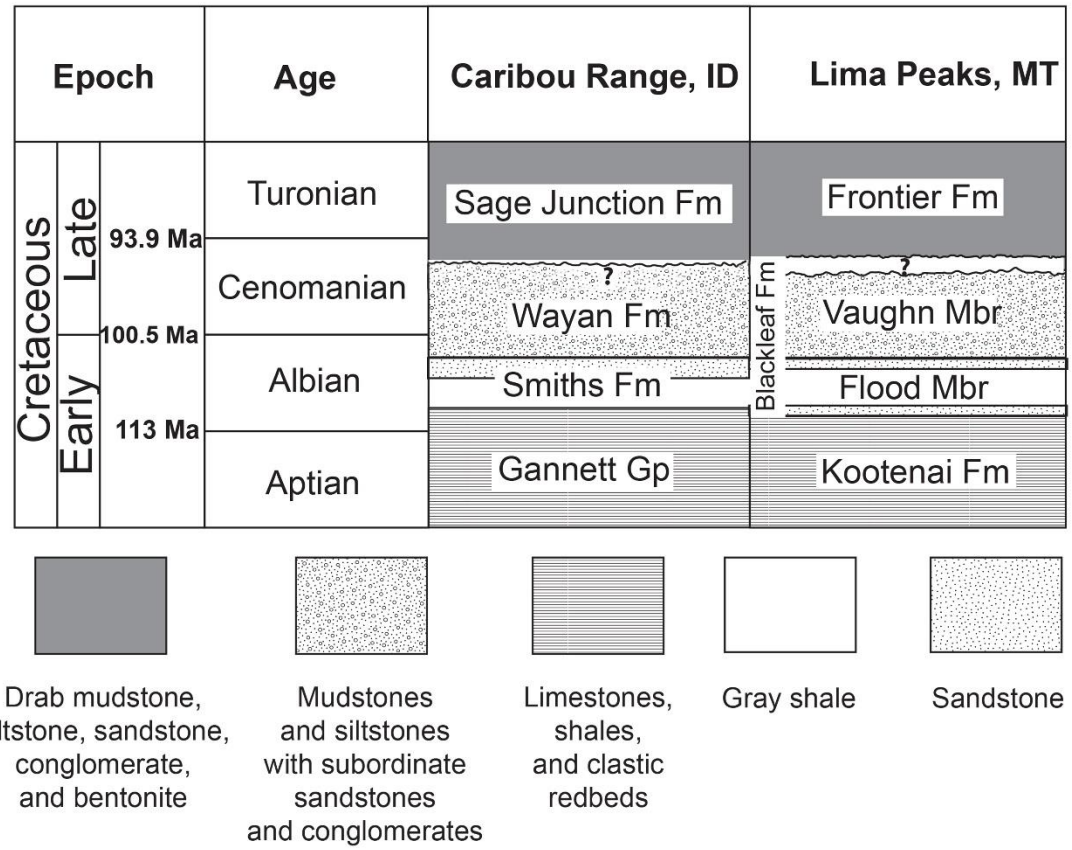

Fig 3.2. Chronostratigraphic setting of the Wayan Formation and Vaughn Member of the Blackleaf Formation. Data based on Dorr (1985) and Krumenacker (2010).

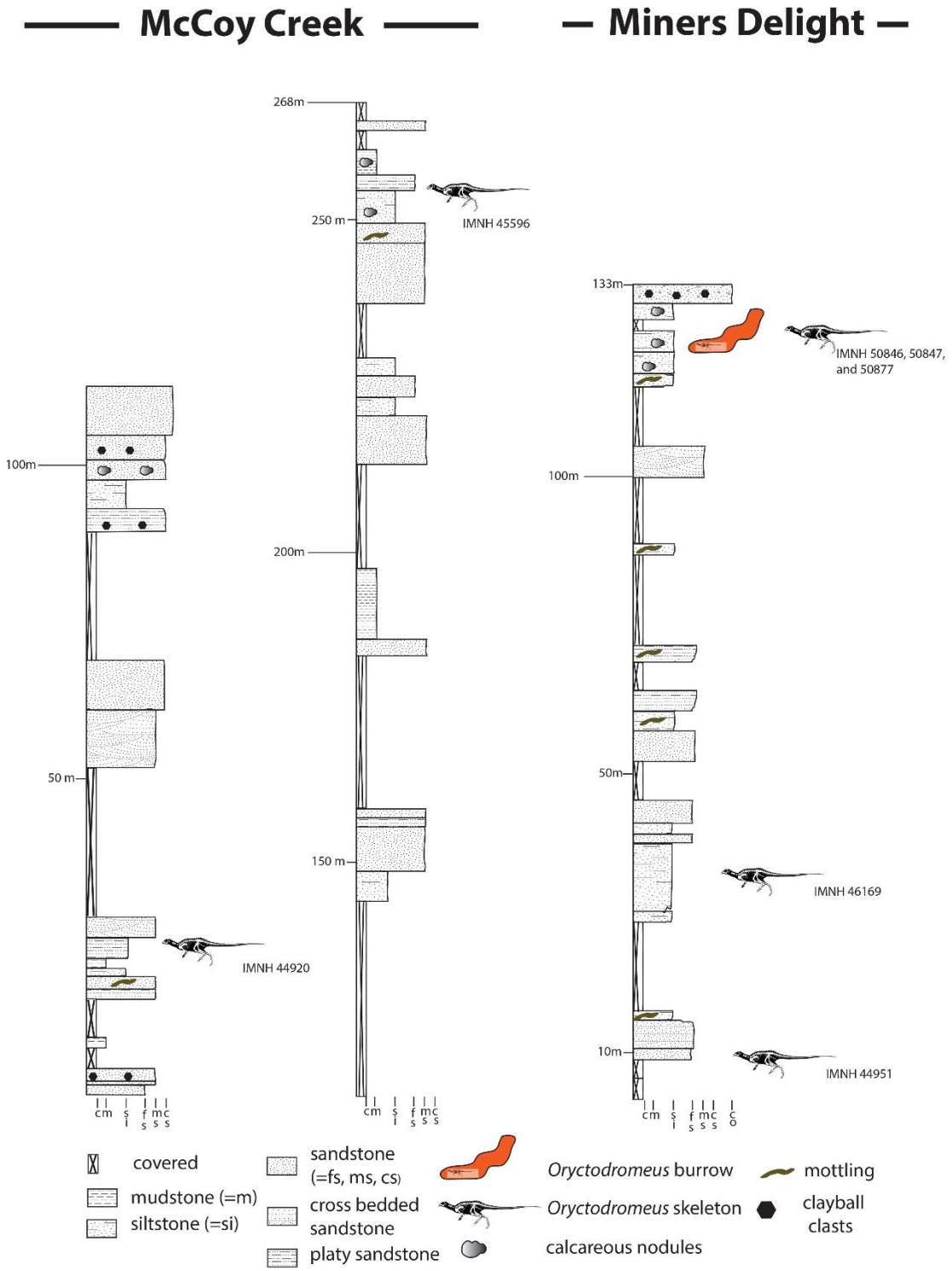

Fig. 3.3. McCoy Creek and Miners Delight Creek stratigraphic sections the Wayan Formation that have produced *Oryctodromeus* specimens. Tincup Canyon is not included due to excessive cover. Modified from Krumenacker (2010).

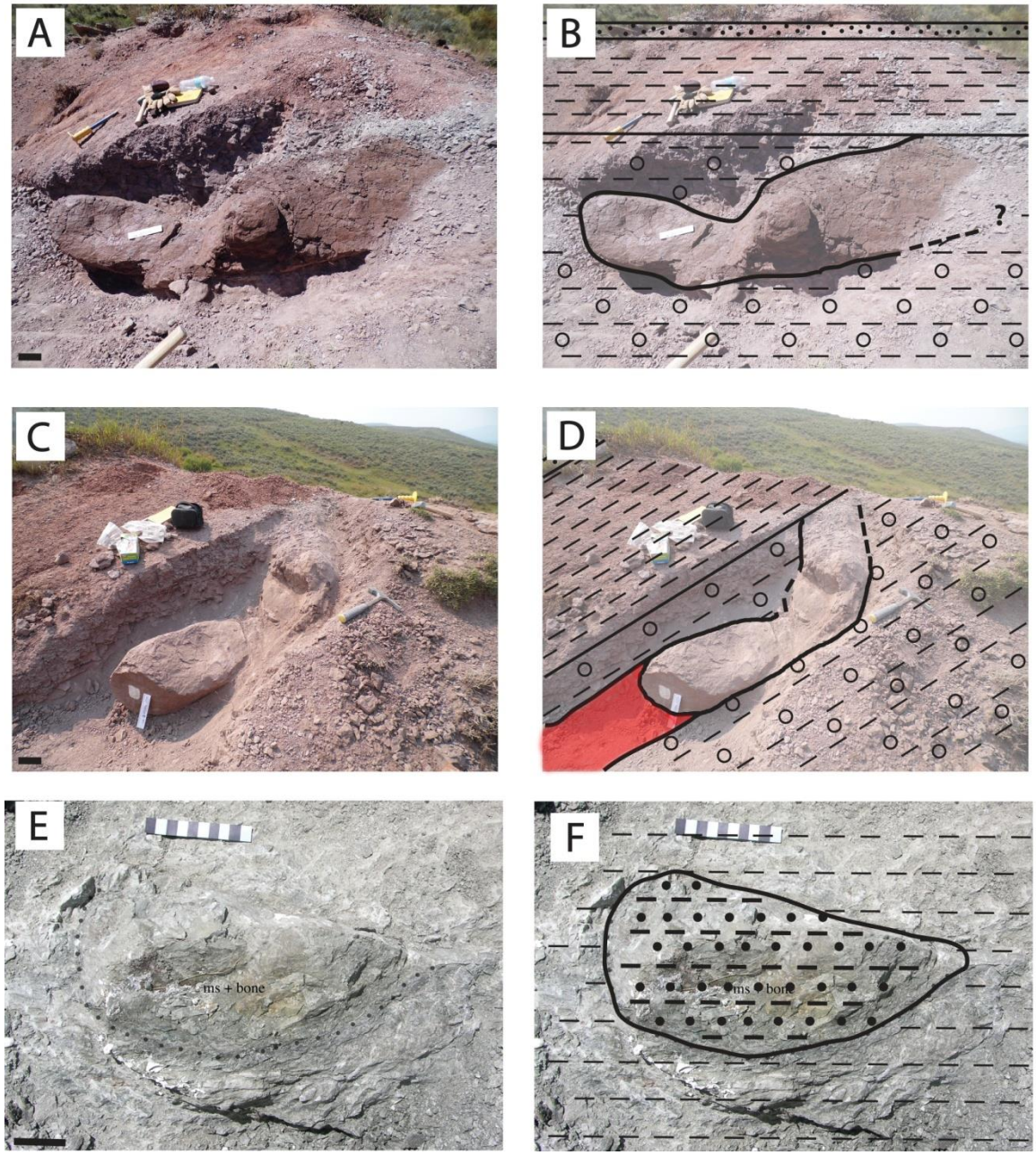

Fig. 3.4. *Oryctodromeus* burrows from the Wayan Formation (A-D) and Vaughn Member of the Blackleaf Formation (E-F); Wayan burrow in lateral (A-B) and ventrolateral (C-D) views, with interpretive sketch overlain photographs on the right (B, D). In ascending stratigraphic order the lithologies consist of calcareous nodule bearing red siltstone, red mudstone, and sandstone. The area that the partial skeleton of IMNH 50847 was collected from prior to recognition of the burrow is highlighted in red in D. Vaughn burrow associated with MOR 8660 (E-F) which consisted of a silty green mudstone in a gray mudstone. Scale bars in lower left of A and B equal 10 cm, scale bare in E equals 5 cm.

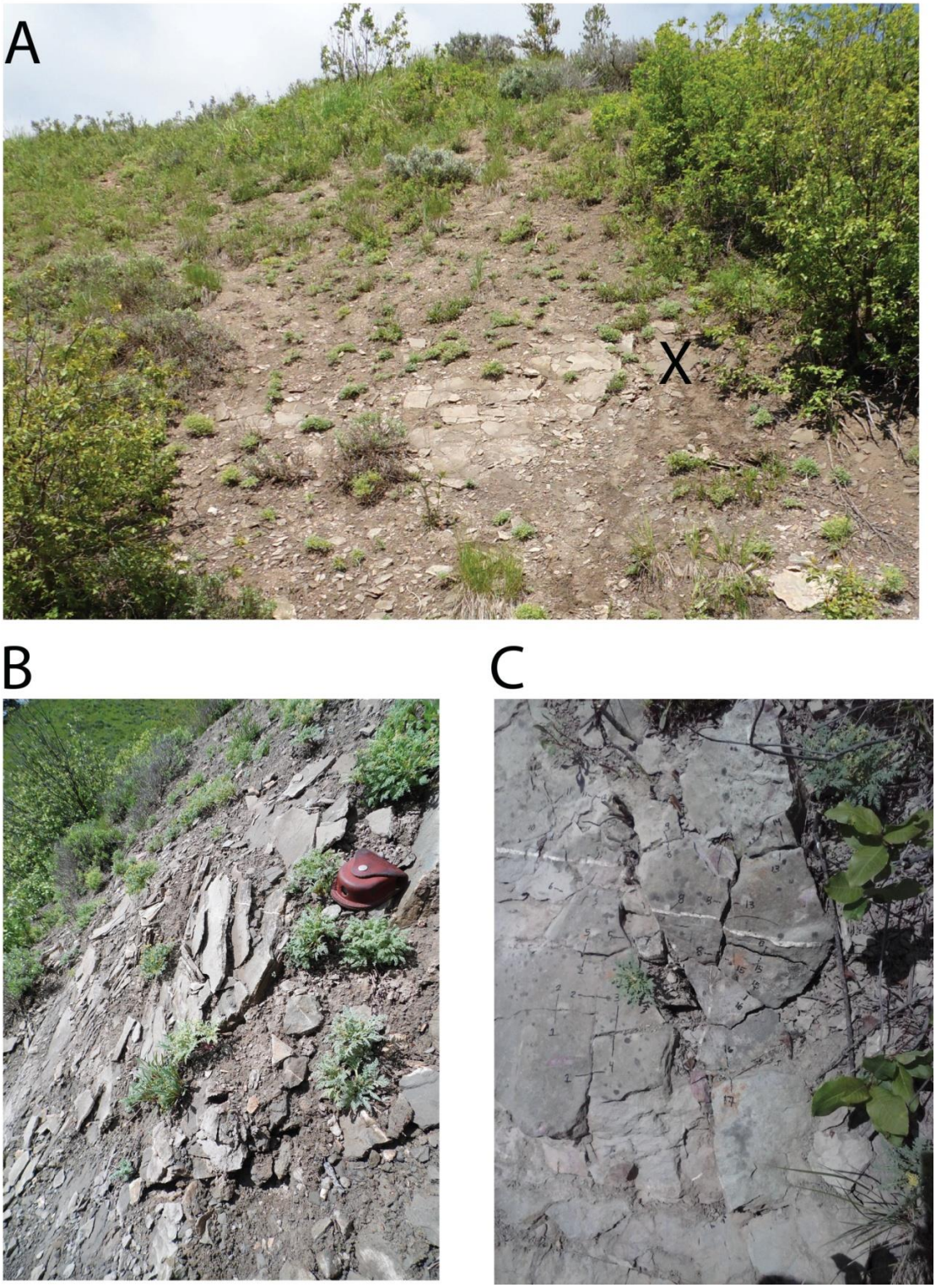

Fig. 3.5. Location of discovery of IMNH 49842. Outcrop with fossil locality marked with X (A). Crossbedded sandstones adjacent to specimen (B). Fossiliferous and featureless sandstone before collection of specimen (C).

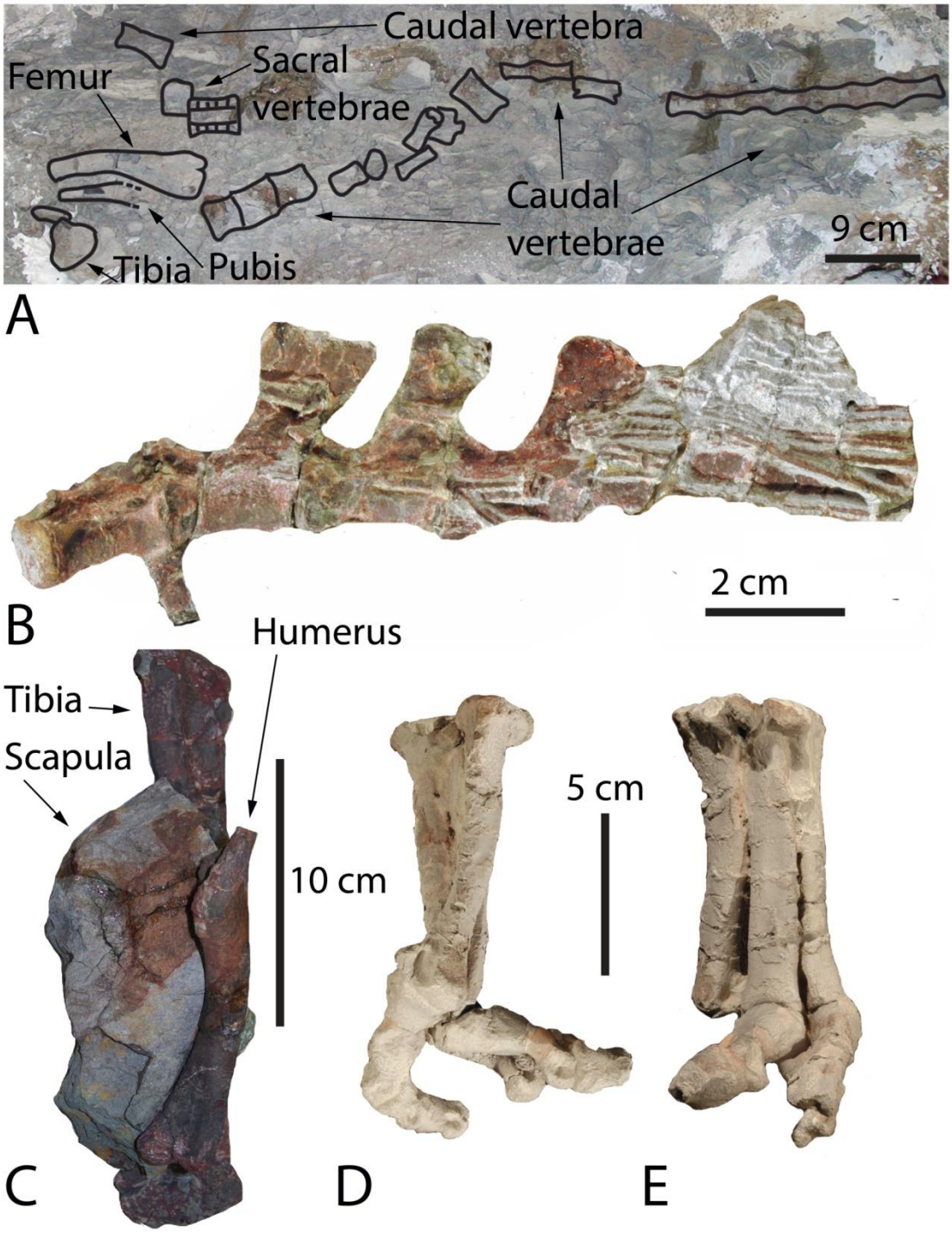

Fig. 3.6. Less articulated example specimens of taphofacies B**.** A) Elements of IMNH 44920 as situated in original field jacket. B) Articulated series of mid-caudal vertebrae from IMNH 44939. Aligned limb elements from IMNH 44939. D and E) Articulated partial pes from IMNH 44939 in lateral (D) and anterior (E) views.

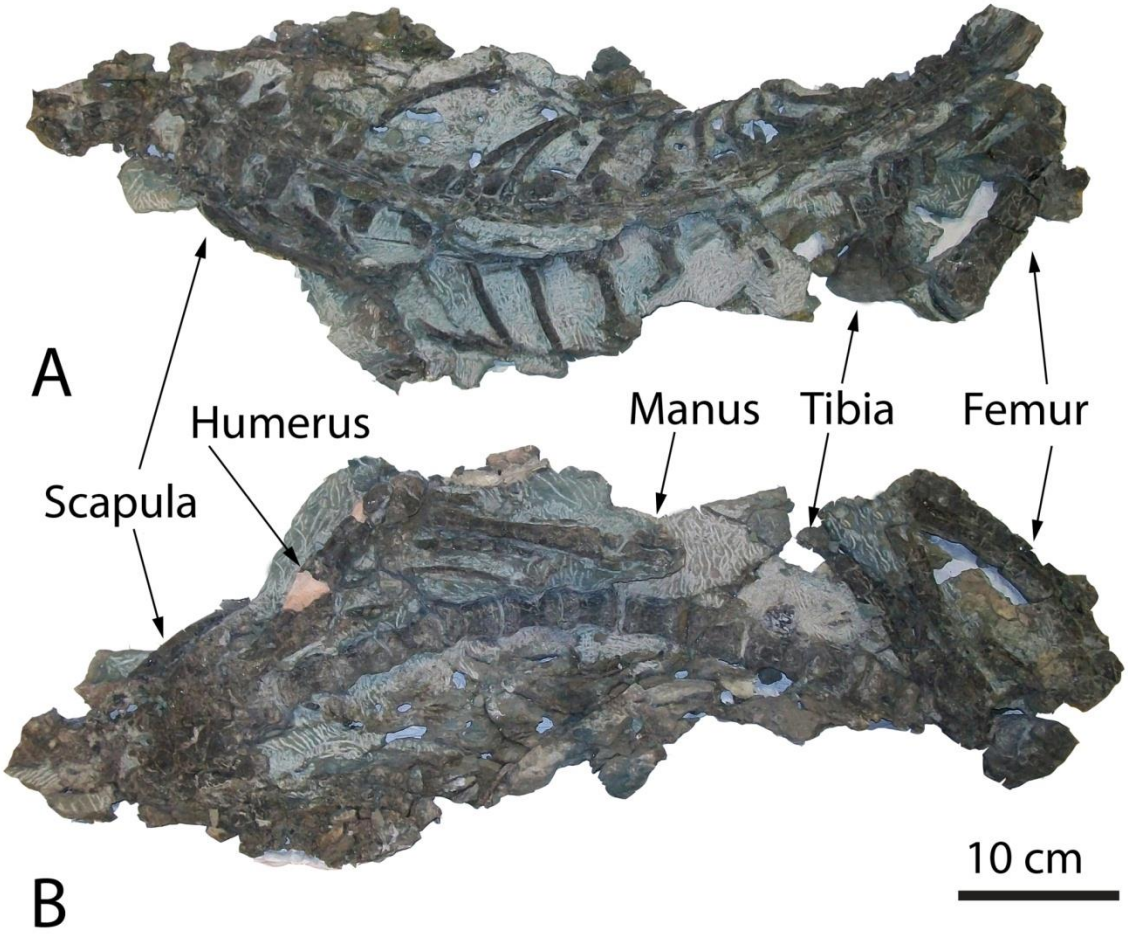

Figure 3.7. *Oryctodromeus* specimen, IMNH 44951, exhibiting full articulation. A) dorsal and B) ventral views, with limb elements indicated.

Table 3.1

Vertebrate taxa from the Vaughn Member of the Blackleaf Formation and Wayan Formation. Formation(s) taxa occur in (Formation), total number of specimens known (Total), number of surface finds (Surface Finds), *in-situ* finds (same), taphofacies of occurrence with number of specimen from each (Facies), percent of the total assemblage (Assemblage), percent of surface finds (Surface), and percent of *in-situ* specimens (*In-Situ*) indicated.

Taxon	Formation	Total	Surface Finds	*In-Situ* finds	Lithofacies	Assemblage	Surface	*In-Situ*
Deinosuchus -like crocodyliform	Wayan	1	0	1	C	<1%	n/a	1%
Small crocodyliform	Wayan	28	7	21	Gms	10%	8%	12%
Dromaeosaurids	Wayan	11	1	10	Gms	4%	1%	6%
Eutriconodont	Wayan	2	0	2	Gms	<1%	n/a	1%
Hadrosaurid	Wayan	2	0	2	Gms	<1%	n/a	1%
Iguanodontid	Wayan	5	1	4	n/a? (1), Gms (3)	2%	1%	2%
Cf. neovenatorid	Wayan	1	0	1	Gms	<1%	n/a	<1%
Large ornithopod indet.	Wayan	1	1	0	n/a	<1%	1%	n/a
Non-cimolodontan multituberculate	Wayan	1	0	1	n/a	<1%	n/a	<1%
Possible neoceratopsian	Wayan	2	0	2	Sm	<1%	n/a	1%
Nodosaur	Wayan	10	1	9	Gms	4%	1%	5%
Oryctodromeus	Vaughn, Wayan	114	49	65	Fm(16), Sm(5), Gms(44)	42%	53%	36%
Oviraptorosaur *(Macroelongatoolithus)*	Vaughn, Wayan	43	22	21	Fm(10), Gms(11)	16%	24%	12%
Small theropod indet.	Wayan	17	0	17	Fm(1), Gms(16)	6%	0%	9%
Large tyrannosauroid	Wayan	7	0	7	Gms	3%	0%	4%
Turtle unidet.	Wayan	24	11	13	Gms	9%	11%	7%

Table 3.2

Articulated and associated skeletons of *Oryctodromeus* used in this study. All IMNH specimens are from the Wayan and all MOR specimens are from the Vaughn. Specimen numbers, occurrence in a recognized burrow (Burrow) indicated by Y (yes) or N (no), minimum number of individuals (MNI), lithofacies of occurrence, taphofacies of occurrence, taphonomic Mode, ontogenetic stage (Ontogeny) with juvenile (J) and mature (M) ages indicated, elements that are articulated and associated (Articulation/Association), and elements present in each specimen (Elements) indicated. The Robison Bonebed (RBB) specimens, which consists of numerous unassociated specimens are included. Since forty-two of the fourt-four specimens from the RBB are isolated (two are articulated vertebral strings) the articulation/association column here is not counted as applicable. Abbreviations: F=Forelimb elements, H= Hindlimb elements, J=Juvenile, M=Mature, PG= Pelvic girdle elements, S= Skull elements, SG= Shoulder girdle elements, VC= Caudal vertebrae, VD= Dorsal vertebrae, VE= Cervical vertebrae, VS= Sacral vertebrae, and ?= Unknown as is an unprepared specimen.

Specimen	Burrow	MNI	Lithofacies	Taphofacies	Taph Mode	Ontogeny	Articulation/Association	Elements
IMNH 44920	N	1	Fm	B	B	M	AR (VC) AS (F, H, VD, VS)	F, H, VD, VS, VC
IMNH 44939	N	3	Fm	B	B	J, M	AR (VC) AS (F, H, VS)	F, H, VC, VS
IMNH 44946	N	1	Fm	B	B	M	AR (VC) AS (S, F, H, VE, VD, VS)	S, F, H, VE, VD, VS, VC
IMNH 44951*	N	1	Sm	A	B	M	AR (SG, F, PG, H, VC, VD, VS)	SG, F, PG, H, VC, VD, VS
IMNH 45081*	N	1	Sm	A	B	M	AR (H, VS)	H, VS
IMNH 45596	N	1	Fm	B	B	M	AR (H, VS) AS (VC)	H, VS, VC
IMNH 46169	N	1	Fm	B	B	M	AS (S, SG, F, H, VE, VD, VS, VC)	S, SG, F, H,VE, VD, VS, VC
IMNH 49842	N	1	Sm	A	B	M	AR (H) AS (VS, VC) ?	H, VS, VC, ?
IMNH 50846	N	2	Fm	B	B	J, M	AS (H, VE, VS, VC)	H, VE, VS, VC
IMNH 50877	Y	1?	Fm	B	B	J?, M	AS (F, H, VC)	F, H, VC
MOR 1636a,b	Y	3	Fm	B	B	J, M	?	S, SG, F, PG, H, VE, VD, VS, VC
MOR 1642	N	2	Fm	B	B	M	AR (VD, VS, VC) AS (S) ?	S, SG, F, PG, H, VE, VD, VS, VC
MOR 8660	Y	1	Fm	B	B	M	?	S, H, VS, VC
RBB	N	*44	Gms	C	A	J, M	n/a	F, H, S, SG, VC VD, VE, VS

Table 3.3

Lithofacies for the Wayan Formation and Vaughn Member. Based on field observations and Dorr (1985), Dyman *et al*. (1994), Krumenacker (2010), Krumenacker *et al*. (2016), and Schmitt and Moran (1982).

Facies Code	Sedimentary Facies	Hydrodynamic Conditions	Interpretation	Features	Burrow	Unit	Specimens
Gms	Matrix-supported conglomerate	High flow regime and rapid energetic deposition	Debris flow	Caliche nodules, green mudstone clasts, chert pebbles, bones, teeth eggshell	N	Wayan	Y
Gcs	Clast-supported conglomerate	High flow regime	Fluvial channel	Chert pebbles	N	Wayan	n/a
Sh	Horizontally bedded sand	Planar bed conditions	Fluvial channel	Chert pebbles	N	Vaughn Wayan	N
Sm	Massive sand	Bioturbation and rapid deposition	Fluvial channel or alluvial plain	Chert pebbles, calcareous nodules	Y?	Vaughn Wayan	Y
St	Trough crossbedded sandstone	Low flow regimes with unidirectional flow	Fluvial channel	Chert pebbles, caliche nodules, bone fragments, woody debris	N	Vaughn Wayan	N
Fl	Laminated mud, silt, sand	Suspension and weak traction current	Ponded or lacustrine environments	Plant debris	N	Vaughn Wayan	n/a
Flc	Shale, carbonaceous	Suspension settling	Poorly-drained lacustrine or ponded environments	Plant debris	N	Vaughn Wayan	N
Fm	Massive mud or silt	Suspension settling	Alluvial plain	Calcareous nodules, mottling, root traces, slickensides	Y	Vaughn Wayan	Y
Lc	Shaly limestone, carbonaceous	Carbonate precipiation and suspension settling	Poorly-drained lacustrine or ponded environments	n/a	N	Vaughn Wayan	N
B	Bentonite, gray volcanic ash	Volcanic ash fall	Volcanic ash fall	n/a	N	Vaughn Wayan	n/a
C	Caliche	Fluctuating watertable	Well-drained alluvial plain	Forms nodular horizons	N	Vaughn Wayan	n/a

Table 3.4
Facies associations for the Wayan Formation and Vaughn Member. Based on field observations and Dorr (1985), Dyman *et al*. (1994), Krumenacker (2010), Krumenacker *et al*. (2016), and Schmitt and Moran (1982).

Facies Association	Hydrodynamic Conditions	Stratigraphic occurrence
Upwards-coarsening transition from mudstone (Fm) to trough-crossbedded sandstone (St)	Suggests an increase in flow velocity, with low energy suspension settling transitioning to higher energy directional flow	Uncertain- McCoy Creek
Upwards transition from trough-crossbedded sandstone (St) to massive sandstone (Sm)	Transition from uniderectional energetic flow to: 1)rapid deposition, 2) liquefaction, 3) biotrubation.	Uncertain- McCoy Creek
Upwards transition from trough-crossbedded sandstone (St) to massive mudstone (Fm)	Suggests an decrease in flow velocity and directionality, with low energy suspension settling transitioning to lower energy suspension settling	Uncertain- McCoy Creek, Miners Delight Creek, Schmitt and Moran
Upwards transition from clast-supported conglomerate (Gcs) to torugh-crossbedded sandstone (St)	High energy deposition proximal to the source area transitioned to a lower energy sudden gravity flow, liquefaction, or to a unidirectional flow deposit disrupted by bioturbation	Basal Wayan Formation Schmitt and Moran,Basal Wayan Formation Tincup Canyon
Upwards transition from matrix-suported conglomerate (Gms) to massive sand (Sm)	High energy deposition transitioned to a lower energy sudden gravity flow, liquefaction, or to a unidirectional flow deposit disrupted by bioturbation	Middle Wayan- Robison Bonebed, Uncertain- McCoy Creek
Upwards transition from matrix-suported conglomerate (Gms) to trough-crossbedded sand (St)	High energy deposition proximal to the source area transitioned to a unidirectional flow	Lowest Wayan Schmitt and Moran, Lowest Wayan Tincup Canyon

References Cited

Behrensmeyer, A.K. 1988. Vertebrate preservation in fluvial channels. Palaeogeography Palaeoclimatology, Palaeoecology., Ecological and Evolutionary Implications of Taphonomic Processes 63: 183–199. doi:10.1016/0031-0182(88)90096-X.

Behrensmeyer, A.K. 1991. Terrestrial Vertebrate Accumulations; pp. 291-335 in Allison, P. and D. E. (eds.), Taphonomy: Releasing the Data Locked in the Fossil Record. Plenum, New York.

Behrensmeyer, A. K., and R. W. Hook. 1992. Paleoenvironmental contexts and taphonomic modes in the terrestrial fossil record; pp. 15-136 in Behrensmeyer, A. K., J. D. Damuth, W. A. DiMichele, R. Potts, H. D. Sues, and S. L. Wing (eds), Terrestrial Ecosystems Through Time. Chicago, University of Chicago Press.

Bell, P.R. and N. E. Campione. 2014. Taphonomy of the Danek Bonebed: a monodominant *Edmontosaurus* (Hadrosauridae) bonebed from the Horseshoe Canyon Formation, Alberta. Canadian Journal of Earth Sciences 51: 992–1006. doi:10.1139/cjes-2014-0062.

Britt, B.B., D. A. Eberth, R. D. Scheetz, B. W. Greenhalgh, and K. L. Stadtman. 2009. Taphonomy of debris-flow hosted dinosaur bonebeds at Dalton Wells, Utah (Lower Cretaceous, Cedar Mountain Formation, USA). Palaeogeography. Palaeoclimatology. Palaeoecology 280, 1–22. doi:10.1016/j.palaeo.2009.06.004.

Brown, C.M., D. C. Evans, N. E. Campione, L.J. O'Brien, and D. A. Eberth. 2013. Evidence for taphonomic size bias in the Dinosaur Park Formation (Campanian, Alberta), a model Mesozoic terrestrial alluvial-paralic system. Palaeogeography, Palaeoclimatology, Palaeoecology: 372, 108–122. doi:10.1016/j.palaeo.2012.06.027.

Carpenter, K. 2013. History, Sedimentology, and Taphonomy of the Carnegie Quarry, Dinosaur National Monument, Utah. Annals of the Carnegie Museum 81: 153–232. doi:10.2992/007.081.0301.

Csiki, Z., D. Grigorescu, V. Codrea, and F. Therrien. 2010. Taphonomic modes in the Maastrichtian continental deposits of the Haţeg Basin, Romania—Palaeoecological and palaeobiological inferences. Palaeogeography, Palaeoclimatology, Palaeoecology 293: 375–390.

Damiani, R., S. Modesto, A. Yates, and J. Neveling. 2003. Earliest evidence of cynodont burrowing. Proceedings of the Royal Society B: Biological Sciences 270: 1747–1751. doi:10.1098/rspb.2003.2427.

Dodson, P., A. K. Behrensmeyer, R. T. Bakker, and J. S. McIntosh. 1980. Taphonomy and Paleoecology of the Dinosaur Beds of the Jurassic Morrison Formation. Paleobiology 6: 208–232.

Dorr, J.A., 1985. Newfound Early Cretaceous dinosaurs and other fossils in southeastern Idaho and westernmost Wyoming. Contributions from the Museum of Paleontology, University of Michigan 27(3): 73-85.

Dyman, T.S., and D. J. Nichols. 1988. Stratigraphy of Mid-Cretaceous Blackleaf and lower part of the Frontier formations in parts of Beaverhead and Madison counties, Montana. U.S. Geological Survey Bulletin 1773.

Dyman, T.S., and R. G. Tysdal. 1990. Correlation of Lower and Upper Cretaceous Blackleaf Formation, Lima Peaks Area to Eastern Pioneer Mountains, Southwestern Montana. U. S. Geological Survey Miscellaneous Field Studies Map 2119.

Dyman, T.S., R. G. Tysdal, C. A. Wallace, and S. E. Lewis. 1994. Correlation chart of Lower and Upper Cretaceous Blackleaf Formation, eastern Pioneer Mountains, southwestern Montana, to Drummond in west-central Montana: U.S. Geological Survey Miscellaneous Series Map I-2478, with pamphlet.

Dyman, T.S., R. G. Tysdal, W. J. Perry, J. D. Obradovich, J. C. Haley, and D. J. Nichols. 1997. Correlation of Upper Cretaceous strata from Lima Peaks area to Madison Range, southwestern Montana and southeastern Idaho, USA. Cretaceous Research 18: 751–766. doi:10.1006/cres.1997.0079.

Eberth, D.A., and P.J. Currie. 2005. Vertebrate taphonomy and taphonomic modes; pp. 453-477 in Currie, P. J. and E. B. Koppelhus (eds.), Dinosaur Provincial Park: A Spectacular Ancient Ecosystem Revealed. Bloomington: Indiana University Press.

Fiorillo, A.R., 1988. Taphonomy of Hazard Homestead Quarry (Ogallala Group), Hitchcock County, Nebraska. Rocky Mountain Geology 26:57–97.

Groenewald, G.H., J. Welman, and J. A. Maceachern. 2001. Vertebrate burrow complexes from the Early Triassic *Cynognathus* Zone (Driekoppen Formation, Beaufort Group) of the Karoo Basin, South Africa. PALAIOS 16: 148–160. doi:10.1669/0883-1351(2001)016<0148:VBCFTE>2.0.CO;2.

Hechinger, R.F., K. D. Lafferty, A. P. Dobson, J. H. Brown, and A. M. Kuris. 2011. A Common Scaling Rule for Abundance, Energetics, and Production of Parasitic and Free-Living Species. Science 333: 445–448. doi:10.1126/science.1204337.

Hunt, R.M., X. Xiang-Xu, and J. Kaufman. 1983. Miocene Burrows of Extinct Bear Dogs: Indication of Early Denning Behavior of Large Mammalian Carnivores. Science 221: 364–366. doi:10.1126/science.221.4608.364.

Krumenacker, L.J., 2005. Preliminary report on new vertebrates from the upper Gannett Group (Aptian) and Wayan Formation (Albian) of east Idaho. Paludicola 5: 55–64.

Krumenacker, L. J. 2010, Chronostratigraphy and paleontology of the mid-Cretaceous Wayan Formation of eastern Idaho, with a description of the first *Oryctodromeus* specimens from Idaho. M.S. Thesis, Brigham Young University, Provo, Utah, 98 pp.

Krumenacker, L.J., D. J. Varricchio, G. P. Wilson, and S. Robison. 2014. The Robison Bonebed: A preliminary report on the most diverse vertebrate fossil site known from the mid-Cretaceous Wayan Formation of Idaho, in: 5. Presented at the Geological Society of America, p. 26.

Krumenacker, L.J., Simon, D. J., Scofield, G., and Varricchio, D. J., 2016. Theropod dinosaurs from the Albian–Cenomanian Wayan Formation of eastern Idaho. Historical Biology 29: 170–186 http://dx.doi.org/10.1080/08912963.2015.1137913.

Martin, A.J. 2009. Dinosaur burrows in the Otway Group (Albian) of Victoria, Australia, and their relation to Cretaceous polar environments. Cretaceous Research 30: 1223–1237.

Modesto, S.P., and J. Botha-Brink. 2010. A Burrow Cast with Lystrosaurus Skeletal Remains from the Lower Triassic of South Africa. PALAIOS 25: 274–281. doi:10.2110/palo.2009.p09-077r.

Oghenekome, M. E. 2012. Sedimentary environments and provenance of the Balfour Formation (Beaufort Group) in the area between Bedford and Adelaide, Eastern Cape Province, South Africa. M. S. thesis, University of Fort Hare, Alice, South Africa 150 pp.

Oriel, S.S., and L. B. Platt. 1980. Geologic map of the Preston 1 degree by 2 degrees Quadrangle, southeastern Idaho and western Wyoming. USGS Numbered Series No. 1127.

Paik, S., Kim, J. H., Park, K. H., Song, Y. S., Lee, Y. I., Hwang, J. I., and Huh, M., 2001. Palaeoenvironments and taphonomic preservation of dinosaur bone-bearing deposits in the Lower Cretaceous Hasandong Formation, Korea. Cretaceous Research 22: 627–642. doi:10.1006/cres.2001.0282.

Reading, H. G., 1996. Sedimentary Environments: Processes, Facies, and Stratigraphy: Blackwell Science, 688p.

Reichman, O.J., and S. C. Smith. 1990. Burrows and burrowing behavior by mammals; pp. 197-244 in Genoways, H. H. (ed.) Current Mammalogy, Plenum Press, NewYork.

Retallack, G.J. 1990. Soils of the Past – an Introduction to Palaeopedology. Unwin Hyman. Boston.

Rogers, R., A. B. Arcucci, F. Abdala, P. C. Sereno, C. A. Forster, and C. L. May. 2001. Paleoenvironment and Taphonomy of the Chanares Formation Tetrapod Assemblage (Middle Triassic), Northwestern Argentina: Spectacular Preservation in Volcanogenic Concretions. PALAIOS 16: 461-481.

Rogers, R.R., 1990. Taphonomy of Three Dinosaur Bone Beds in the Upper Cretaceous Two Medicine Formation of Northwestern Montana: Evidence for Drought-Related Mortality. PALAIOS: 394–413. doi:10.2307/3514834.

Rubey, W.W. 1973. New Cretaceous formations in the western Wyoming thrust belt. U. S. Geological Survey Bulletin 1372-I.

Schmitt, J.G., Moran, M.E., 1982. Stratigraphy of the Cretaceous Wayan Formation, Caribou Mountains, southeastern Idaho thrust belt. Rocky Mountain Geology 21: 55–71.

Shipman, P., 1981. Life History of a Fossil and Introduction To Taphonomy and Paleoecology. Harvard University Press. Cambridge, Massachusetts, and London.

Simon, D.J., 2014. Giant dinosaur (theropod) eggs of the Oogenus *Macroelongatoolithus* (Elongatoolithidae) from southeastern Idaho : taxonomic, paleobiogeographic, and reproductive implications. M. S. thesis, Montana State University, Bozeman, Montana, 121 pp.

Smith, R.M.H., 1993. Vertebrate Taphonomy of Late Permian Floodplain Deposits in the Southwestern Karoo Basin of South Africa. PALAIOS 8: 45–67. doi:10.2307/3515221.

Smith, R.M.H., 1987. Helical burrow casts of therapsid origin from the Beaufort Group (Permian) of South Africa. Palaeogeography, Palaeoclimatology, Palaeoecology 60: 155–169. doi:10.1016/0031-0182(87)90030-7.

Suarez, M.B., C. A. Suarez, J. I. Kirkland, L. A. González, D. E. Grandstaff, and D. O. Terry. 2007. Sedimentology, Stratigraphy, and Depositional Environment of the Crystal Geyser Dinosaur Quarry, East-Central Utah. PALAIOS 22: 513–527. doi:10.2110/palo.2006.p06-014r.

Sundell, K.S., 1997. Oreodonts: large burrowing mammals of the Oligocene. Journal of Vertebrate Paleontology 17(3): 80A.

Tobin, R.J., 2004. Taphonomy of ground squirrel remains in a Late Pleistocene ichnofabric, Nebraska, USA. Palaeogeography, Palaeoclimatology, Palaeoecology 214: 125–134.

Tysdal, R.G., T. S. Dyman, and D. J. Nichols. 1989. Lower Cretaceous Bentonitic Strata in- Southwestern Montana Assigned to Vaughn Member of Mowry Shale (East) and of Blackleaf Formation (West). Mountain Geologist 26: 53-61.

Turner, B. R. 1981. Revised stratigraphy of the Beaufort Group in the southern Karoo Basin. Palaeontologia Africana 24: 87-98.

Varricchio, D. J., A. J. Martin, and Y. Katsura. 2007, First trace and body fossil evidence of a burrowing, denning dinosaur: Proceedings of the Royal Society B: Biological Sciences 274: 1361–1368.

Varricchio, D. J., Moore, J., and F. Jackson. 2007. Preliminary vertebrate fauna of the mid Cretaceous Blackleaf Formation of Montana, in: Geological Society of America Abstracts with Programs for 59th Annual Meeting of the Rocky Mountain Section of the Geological Society of America p. 41.

Voorhies, M.R. 1969. Taphonomy and population dynamics of an early Pliocene vertebrate fauna, Knox County, Nebraska. Rocky Mountain Geologist 8: 1–69. doi:10.2113/gsrocky.8.special paper 1.1.

Weishampel, D.B., M. B. Meers, W. A. Akersten, and A. D. McCrady. 2002. New Early Cretaceous dinosaur remains, including possible ceratopsians, from the Wayan Formation of eastern Idaho. Idaho Museum of Natural History Occasional Paper 37: 5–17.

Wiltschko, D.V., Dorr, J.A., 1983. Timing of Deformation in Overthrust Belt and Foreland of Idaho, Wyoming, and Utah. AAPG Bulletin 67: 1304–1322.

Woodruff, D.C., and D. J. Varricchio. 2011. Experimental modeling of a possible *Oryctodromeus cubicularis* (dinosauria) burrow. PALAIOS 26: 140–151. doi:10.2110/palo.2010.p10-001r.

CHAPTER FOUR

ONTOGENETIC HISTOLOGY AND GROWTH OF THE NEORNITHISCHIAN DINOSAUR *ORYCTODROMEUS CUBICULARIS* FROM THE MIDDLE CRETACEOUS (ALBIAN-CENOMANIAN) OF MONTANA AND IDAHO

Contribution of Authors and Co-Authors

Manuscript in Chapter 4

Author: L.J. Krumenacker

Contributions: Conceived the study, performed the analyses, interpreted results, and wrote the manuscript.

Co-Author: David J. Varricchio

Contributions: Conceived the study, discussed results and implications, and edited earlier manuscripts.

Co-Author: John R. Horner.

Contributions: Discussed implications, edited manuscripts.

Co-Author: Kelli Taddy

Contributions: Discussed implications, performed analyses, edited manuscripts.

Manuscript Information Page

L.J. Krumenacker, David J. Varricchio, John R. Horner, and Kelli Taddy

Journal of Vertebrate Paleontology

Status of Manuscript:
__X_ Prepared for submission to a peer-reviewed journal
____ Officially submitted to a peer-review journal
____ Accepted by a peer-reviewed journal
____ Published in a peer-reviewed journal

ABSTRACT

Oryctodromeus, a small burrowing neornithischian dinosaur, is known from relatively abundant partial skeletons from the Wayan Formation of Idaho and the Vaughn Member of the Blackleaf Formation of Montana. Bone microstructure in the femora and tibiae from specimens of this taxon allow the definition of three growth stages of this taxon, juveniles, sexually mature sub-adults, and what are termed near-adults, that appear to have approached skeletal maturity. Juveniles are characterized by moderately vascularized fibrolamellar primary bone indicating rapid growth, with unfused neurocentral sutures from the anteriormost vertebrae to the proximal caudals and unfused scapulocoracoids. Sub-adults are characterized by fibrolamellar bone in the inner cortex that transitions to zonal and parallel fibered bone in the outer cortex, indicating the onset of sexual maturity. Sub-adults have fused neurocentral sutures in the caudals through middle caudals, with partially fused to fused sutures variably present more anteriorly. Scapulocoracoids at the sub-adult stage are variably fused. LAG's in sub-adults suggest a minimum age of three to four years. Near-adults are recognized by similar features to those of the sub-adults, but with avascular dense bone in the outermost cortex signifying a significant decrease in growth rates. In this growth stage neurocentral fusion is the most complete with fusion into the cervical vertebrae and scapulocoracoids being variably fused. The recognition of possible skeletally mature individuals is only tentative due to poor preservation of the largest elements. More moderate rates of vascularization in the cortex of *Oryctodromeus* indicate a reduced overall rate of growth in comparison to other

dinosaurian taxa, but similar growth rates to hypsilophodontid-grade taxa such as *Orodromeus* and *Tenontosaurus*. The pattern of neurocentral fusion allows additional age assessment. Fusion follows the pattern present in other small ornithischians, proceeding from posterior to anterior, with fusion of the scapulocoracoids being variable in near-adult individuals but complete in the largest individuals.

INTRODUCTION

Remains of the small burrowing neornithischian dinosaur *Oryctodromeus cubicularis* are moderately common in coeval middle Cretaceous (Latest Albian-Early Cenomanian) strata in southeastern Idaho and southwestern Montana (Varricchio *et al*., 2007; Krumenacker, 2010; Krumenacker *et al*., 2016). In fact the Wayan Formation of Idaho and the Vaughn Member of the Blackleaf Formation of Montana have vertebrate assemblages dominated by *Oryctodromeus*, with taphonomic evidence suggesting a bias towards preservation. This taxon is moderately well represented skeletally, with over a dozen partial to near complete skeletons known from the Wayan and Vaughn in total, with numerous isolated and some associated elements referred to this taxon as well.

Oryctodromeus has consistently placed within the Orodrominae, a clade of small neornithischians united through the presence of a sharp scapular spine and a fibula with a D-shaped cross section (Brown *et al*., 2013). According to Boyd (2015) *Oryctodromeus* and *Koreanosaurus* form a sister clade to *Zephyrosaurus*, *Orodromeus*, and an unnamed taxon from the Kaiparowits Formation. While only *Oryctodromeus* burrows have been discovered for taxa within this clade (Varricchio *et al*., 2007; Krumenacker *et al*., in prep), it is possible this clade was specialized for digging (Varricchio *et al*., 2007, Huh, 2011; Brown *et al*, 2013). Probable burrows for other small neornithischians outside of the Orodrominae have also been described from the Otway Group of Victoria, Australia (Martin, 2009).

Recovered *Oryctodromeus* specimens consist of varying ontogenetic stages, with the presence of two juveniles in association with a presumed adult having been interpreted as evidence of parental care (Varricchio *et al*., 2007). Associations of multiple specimens, with no remains of juvenile specimens, occur as well (such as in MOR 1642). Varricchio *et al*. (2007)

used specimen size and degree of neurocentral fusion in the holotype (MOR 1636a) and paratypes (MOR 1636b) to infer this parental care, but these ontogenetic assignments have not been tested through histological methods. One goal of this study is to test the ontogenetic state of these specimens and others found in association that appear to represent varying ontogenetic stages (IMNH 44939). In addition, we assess the histological features and growth of other available specimens that represent a gradation of sizes.

The bone histology and growth rates of numerous ornithischian dinosaurs of hypsilophodontid grade have been described (eg. Chinsamy, 1995; Scheetz, 1999; Horner at al., 2009; Cerda and Chinsamy, 2012; Werning, 2012). However investigations in the histology and growth rates of orodromines are limited to that of *Orodromeus* (Scheetz, 1999; Horner *et al*., 2009). Horner *et al*. (2009) found that *Orodromeus* grew at modest growth rates (indicated by lesser amounts of vascularization) in comparison to larger dinosaurs, with distinct lines of arrested growth (LAG's). In addition, it was found that *Orodromeus* experienced determinate growth, with adult ages of five to six years (Horner at al., 2009). The histology and growth of *Oryctodromeus* have not been previously described. Here we describe the long bone histology and growth of *Oryctodromeus* using femora and tibiae from seven individuals (Tables 1 and 2). The general bone histology as well as implications of the recovered data are then discussed relating to the growth rates and assessed ages of the individual specimens.

Fusion of neurocentral sutures on vertebrae, as well as in the skull and other areas of the skeleton has commonly been used as a means to relatively assess the maturity level of fossil archosaurs (eg. Brochu, 1996). In general, it has been assumed that a posterior to anterior sequence of vertebral suture closing may be prevalent in archosaurs, based on that condition being demonstrated in crocodylians (Brochu, 1996). However, the fusion of neural arches to vertebral centra in archosaurs, as well as fusion of other skeletal elements, is highly variable.

Recent research shows that using it for maturity-related assessments should be done with caution (Irmis, 2007; Bailleul *et al*., 2016). In some ornithopod and orodromine taxa such as *Camptosaurus*, *Dryosaurus*, *Orodromeus*, *Zephyrosaurus*, and *Thescelosaurus* neurocentral fusion has been shown to be open or partially fused in individuals of various sizes, with a lack of fusion in vertebral elements even in the largest *Thescelosaurus* specimens (Brown *et al*., 2011; Brown *et al*., 2013).

MATERIALS AND METHODS

All bones sampled belong to partial to near complete skeletons of *Oryctodromeus* from either the Wayan or Vaughn (Tables 1 and 2). These individuals include one juvenile individual and other individuals of varying sizes (Table 2). Juvenile remains having linear dimensions approximately two-thirds (Table 2) the size of presumed adults, are known from some locations (eg. MOR 1636b), and these juveniles are usually in direct association with presumed adult specimens (Varricchio *et al*., 2007).

Only femora and tibiae were sectioned, as they have been deemed the most useful elements for use in ontogenetic assessment (eg. Padian and Lamme, 2013). Specimens were chosen based on those that were deemed to have the most informative potential (least amounts of damage), and to span a range of sizes (Table 2). Thin sections (Table 1) were prepared via the standard methods of Padian and Lamm (2013). Prior to analysis each specimen was molded, photographed, and measured (Table 2; Appendix G) to ensure the original dimensions of each specimen were recorded. Sections of bones were broken out (Appendix G) and transverse sections of each element were cut at mid-shaft (just below the fourth trochanter for femora, Appendix G) with two slides prepared for each specimen, excepting MOR 1636b and MOR 1642. Due to substantial crushing of the specimen, MOR 1636b had four slides made in total. These

four slides were made from two separate areas to provide additional data in case some slides were uninformative. MOR 1642 had three slides made in an attempt to get a full cross section of cortex, because crushing and sediment infill had substantially deformed portions of the femoral shaft. For each specimen, one set of slides is curated at IMNH, with the remaining slides being curated in the Paleohistology Collection of MOR. Vascularity for IMNH 44920 measured manually through assessing the individual area of vascular canals in specimens in ImageJ and adding together the areas of individual vascular canals. Only this specimen was assessed due to issues of preservation. Images were taken under normal and polarized light, and optimized and constructed in Adobe Photoshop CS6 and Adobe Illustrator CS6.

Institutional Abbreviations: **IMNH**, Idaho Museum of Natural History, Pocatello, Idaho, USA; **MOR**, Museum of the Rockies, Bozeman, Montana, USA.

RESULTS AND HISTOLOGIC DESCRIPTION

We do not make all possible osteohistological observations in this description, but instead focus on those features that are relevant to maturity and growth. The term mature or adult when used in this discussion relates to skeletal maturity as indicated by the presence of an External Fundamental System (EFS). Discussion of sexual maturity, which has been shown to occur prior to skeletal maturity in a variety of dinosaurs (Erickson *et al*., 2007; Lee and Werning, 2008), is done informally here. Descriptions of individual specimens are organized by size class, element, and specimen number. Histological descriptions begin with features of the inner cortex and proceed outward, with descriptions of primary bone features being followed by description of secondary growth.

General Histological Features

Transverse sections through all of the sectioned specimens are similar in featuring a large medullary cavity that is surrounded by an outer cortex. Except for the smallest individual (MOR 1636b), the medullary cavities are oval-shaped and roughly one half to two-thirds the width of the entire diaphysis. Endosteal bone occurs somewhat sporadically in most specimens as a thin veneer in the deepest portions of the cortex. Excepting the sole juvenile specimen, which consists entirely of fibrolamellar bone, the main tissues in the compact bone are fibrolamellar tissue which occurs in the inner cortex and commonly grades into parallel fibered bone tissue in the outer portions of the cortex. Lines of arrested growth (LAG's) are evident in some specimens but rarely extend the full circumference of the cross section due to alterations such as microbial degradation, hematite mineralization, and remodeling of the bone tissue. In some of the more poorly preserved tibiae (IMNH 44939) concentric zones of bone tissue are generally present and recognizable but specific LAG's are not recognizeable. Hematite mineralization obscures details in some specimens, consisting of red diffuse areas that occur intermittently throughout the cortex (eg. Fig. 4C). What is interpreted as microbial degradation consists of amorphous darkened to indistinct areas associated with osteons and osteocyte lacunae that appear to have been enlarged and altered (eg. Fig. 2B), similar to examples of microbial degredation seen in *Maiasaura*, *Orodromeus*, and *Tenontosaurus* (eg. Horner *et al*., 2000; Horner *et al*., 2009). Primary osteons occur throughout the cortex but more typically in the outer cortex within the lamellar-zonal bone. In many specimens, a distinct column of secondary osteons will span outward through the entire cortex in the lateral

direction. More sporadic secondary osteons occur near the endosteal margin in the inner cortex of more mature individuals. Vascularization is dominantly longitudinal and occurs in a modest degree in most elements, with more vascularization generally occurring in the fibrolamellar bone.

MOR 1636B: 2016-05 T1-M Tibia

This tibia (Fig. 2; Appendix Fig. G4) is from the Vaughn of Beaverhead County, Montana. This is the smaller (lesser in length) of two tibiae (representing two individuals) from a collection of elements representing a minimum of two reported juveniles found within the burrow fill of the holotype specimen of *Oryctodromeus* (Varricchio *et al*., 2007). The greatest diameter of the cross section is about 1.7cm (Fig. 2A). Complete understanding of the histological features of this specimen is difficult, because of mineralization, extensive crushing and fracturing of the bone, with large section of the cortex having been displaced into the medullary cavity. Due to this and hematite mineralization and microbial degradation only localized observations of the histological features are possible. Excepting the middle and distal caudals, all vertebral elements (dorsals, sacrals, and caudals) have unfused neurocentral sutures, with the centra and neural arches being separated.

Crushing has distorted what appears to have been a larger (in comparison to more mature individuals) medullary cavity (Fig. 2A). The entire cortex consists of fibrolamellar tissue. LAG's are absent in this specimen. Lacunae and lamella (Fig. 2B-C), which are visible in patches of unrecrystallized areas, are well-developed in association with primary osteons, which are well-developed throughout the cortex. In the outer quarter of the cortex and along the periosteal border primary osteons occur in a zonal arrangement. Vascular canals in the inner cortex, as best as can be observed, are mostly

longitudinal arranged, but transition to more reticular pattern near to the periosteal surface (Fig. 2B-C). A moderate degree of vascularity is indicated by the number of vascular canals throughout most of the tissue.

IMNH 44920: PHT 2016-06C FE1-I Femur

This femur (Fig. 3; Appendix Fig. G1) belongs to a partial skeleton of a single individual of the second size class from the Wayan Formation of Bonneville County, Idaho. Preservation of this femur is excellent with no crushing on the midshaft where the section was removed, but some crushing on the more distal end. There are some cracks and calcite infilling of the bone and some portions of the outer cortex have separated from the main body of the bone, with calcite infilling (Fig. 3A). The transverse section in the area of the mid-shaft, where the section was removed measures 20.4 mm in maximum diameter. Associated elements exhibit a lack of fusion in the anterior caudal vertebrae and those more anterior, with one scapulocoracoid being unfused and the other partially fused.

A well-developed medullary cavity (Fig. 3A) occupies the center of the element and is slightly more than half the total diameter of this section, measuring 11.3 mm in the wider dimension. At large scale the inner periphery of the cortex is smooth and not scalloped as in the tibiae discussed below (IMNH 44939, MOR 1636a), at higher magnifications the endosteum is slightly scalloped. Endosteal bone, roughly less than one-twentieth of a millimeter in thickness, lines most of the endosteal border.

Cortical bone is moderately vascularized within the inner cortex, with more vascularization in the medial and anterior-facing areas in comparison to other areas of the cortex. The inner cortex consists of fibrolamellar bone with randomly arranged primary osteons, in the outer cortex primary osteons are more transversly elongated and are arranged more orderly in a

circumferential pattern (Fig. 3B-F). In the outer half of the cortex, which consists of lamellar-zonal bone, two to three LAG's (the third, which lies between the other two, is less distinct and tentative) are visible (Fig. 7A-B). There is no evidence of an External Fundamental System (EFS) in this specimen, with the outer periphery of the cortex maintaining vascularity and developing primary osteons (Fig. 3C and E). Distinct areas of secondary reconstruction are locally prominent, with secondary osteons in the anterior and medial portions of the inner cortex and in a distinct column that transects the entire cortex on the middle lateral side of the femur (Fig. 3A-B, C, and E-F).

IMNH 44939 (smaller tibia): 2016-06C T2-I

Specimen IMNH 44939, from the Wayan Formation of Caribou County, Idaho, consists of an aggregation of three individuals represented by forelimb, hindlimb, and elements of the posterior (sacral and caudal) column. Three individuals of varying size are represented by this specimen (based on tibiae and pes). Two tibiae from this specimen (Fig. 4) are examined in this study. They are referred to via their length (smaller and larger tibia). The smaller tibia discussed here (Fig. 4A-C; Appendix Fig. G5) is more robust than the larger specimen discussed below. All caudal vertebrae catalogued with this specimen (middle and proximal caudals) do not overlap and appear to represent one individual. Each of these caudals have fused neurocentral sutures, but sacral vertebrae (which do not overlap and are associated with the caudals in matrix) are unfused. No other vertebrae are preserved. In Table 2, where fusion data is presented, this data is presented identically for both specimens of IMNH 44939, since determing which vertebrae correspond to which tibiae is impossible.

The smaller tibia exhibits excellent external preservation with no crushing or distortion. A hematitic rind remains present on portions of the element in portions where it was difficult to remove during preparation. Preservation of histological features in this element is poorer in comparison to most other specimens discussed here due to the hematite mineralization and recystallization. Histologic structures such as lacunae and lamella are often difficult to observe due to the alteration of the fine structure of the bone, which appears as a grainy to crystalline surface with red to dark brown patches obscuring detail (Fig. 3B-C, and E-F). The transverse section in the area of the mid-shaft, where the section was removed measures 22.1 mm in maximum.

The large medullary cavity occupies half of the width of the element in the thin section. The endosteal periphery of the medullary cavity has distinct scalloped edges representing bone resorption. There is a thin veneer of circumferentially deposited endosteal bone, measuring roughly one-twentieth a millimeter in thickness.

The cortical vascularity of this element is moderate with mostly longitudinal canals scattered throughout the cortex. Although the microstructure is poorly preserved, the inner third of the cortex appears more vascular than most portions if the outer two-thirds (excluding a vascular column). The inner half of the cortex appears to consists of fibrolamellar bone with random vascularity and poorly-preserved primary osteons. The outer cortex transitions to parallel fibered bone. No LAG's have been observed, probably due to the alteration as well, but distinct zonal areas are visible within the cortex. Based on observations of other specimens the vascularity in the outer cortex is interpreted as poorly-preserved osteons., with no signs of an EFS. A distinct area of vascularity with

some prominent erosion rooms projects towards the mid-lateral surface of the tibial shaft in cross section (Fig. 4A-B).

IMNH 44939 (larger tibia): 2016-06C T4-I

The larger of the two tibiae (Fig. 4D-F; Appendix Fig. G7) from this specimen is also very well preserved externally with some hematitic encrustation. This bone is longer but more gracile than the other tibiae. The greatest diameter of this specimen is about 18 mm. The transverse section in the area of the mid-shaft, where the section was removed measures 19.7 mm in maximum diameter. Histological preservation of this element is poor as well due to the mineralization and recrystallization like the other tibia from IMNH 44939.

As in the other tibia, the medullary cavity occupies half of the width of the entire element. And the endosteal periphery of the medullary cavity also has distinct scalloped edges (Fig. 4D) and extensive endosteal bone of similar thickness to the other tibia from IMNH 44939. A distinct area in the anterolateral area of the endosteal region (Fig. 6D-E) contains an unusual area of vascularized bone with erosion rooms that is flanked internally and externally by endosteal bone.

Vascularity is slightly more profuse in the inner cortex, possibly representing poorly-preserved secondary reconstruction. Though the microstructure is poorly preserved due to recrystallization the inner half of the cortex appears to consist of fibrolamellar bone. Some primary osteons are visible in the patchy areas in the inner cortex, being easier to discern than in the previous specimen. No LAG's were recognizeable, but distinct zonal areas (Fig. 4D) are visible within the cortex. Parallel fibered bone makes up the outer half of the cortex. As in most other elements described here, a distinct area of vascularity, probably representing poorly

preserved secondary osteons projects towards the anterolateral area of the tibial shaft in cross section (Fig. 4A).

IMNH 50877: FE2-I Femur

This specimen consists of a femur (Fig. 5A-B; Appendix Fig. G2) from an associated but very fragmentary partial skeleton in a burrow fill from the Wayan Formation of Caribou County, Idaho. This bone retains its three-dimensional structure but has been distorted to a degree, with the femoral head being offset ventrally and some crushing being present. The entire specimen has a hematitic rind. Preservation of this element is also poor, due to hematite mineralization, crushing, and distortion (Appendix Fig.G2). Due to portions of the cortex missing in the mid-diaphysis, this section was taken more distally then in other femora (Appendix Fig. G2). The greatest diameter of the specimen thin section is 24.8 mm. The few vertebrae that were preserved with this specimen, mid and anterior caudals, all have fused neurocentral sutures. No scapulocoracoids have been found with this specimen.

The medullary cavity occupies two-thirds of the width of the entire element, possibly due to the section being from a more distal area of the element. Endosteal bone occurs in the endosteal border and in trabeculae bone ringing the medullary cavity. Dense-fibered and avascular to moderately vascular cancellous bone and numerous erosion rooms form the majority of the inner cortex. Internal structures such as lacunae and lamella are difficult to observe due to the alteration of the fine structure of the bone, but distinct primary osteons are visible in some patchy areas of better preservation within the central cortex (Fig. 5B). No LAG's were discernible in this thin section, probably due to the hematitic alteration. Another distinct area of vascularity projects towards the mid-lateral surface of the femur shaft in cross section (Fig. 5A). Vascularity is moderate with mostly longitudinal canals scattered throughout the cortex with no signs of an EFS.

MOR 1636A: 2016-05 T3-M Tibia

This tibia (Fig. 5C-F; Appendix Fig. E6) is from the holotype specimen of *Oryctodromeus*. This specimen was used because no femur was found with the holotype. This element is grouped within the middle size class (Class 2). The three-dimensional form of the bone is preserved with only slight crushing in a few areas of the diaphysis. Internal preservation is also much better than the other tibiae examined here. The maximum diameter of the thin section specimen is 22.5 mm. Fusion of the vertebral column consists of partially fused cervical centra with vertebrae being more posterior having fully fused neurocentral sutures. The left scapulocarocaoid is fused in this individual while the right is not. Internal preservation of this element is much better than the other tibiae, and despite the darker colored inner cortex this specimen allows better discernment of its internal features.

Similar to the other tibiae, the medullary cavity occupies nearly two-thirds of the width of the entire element in this thin section. The endosteal border of the medullary cavity is marked by a thin layer of endosteal lamellar bone up to one-tenth of a millimeter in thickness. The medullary cavity is much less scalloped than in the two Wayan examples (IMNH 44939).

Vascularity of this element is moderate, comparable with other specimens. As in other specimens, the inner cortex consists of fibrolamellar bone. Additionally, five LAG's, as well as possible sixth in the outermost periosteum were recognized in the outer half of the cortex. Secondary osteons do occur within the inner portions of the cortex. The outer cortex consists of parallel fibered bone with some primary osteons. In contrast to all the other elements examined here, excepting MOR 1636b, a distinct column of vascularity that projects through the entire cortex is not visible in this thin section. However, a distinct area of secondary remodeling occurs in the inner half of the anterolateral portion of the cortex (Fig. 5D). Sharpeys fibers also occur in the outer cortex.

MOR 1642: 2016-05 FE3-M Femur

This femur (Fig. 6; Appendix Fig. G3) is from a Vaughn specimen from Beaverhead County, Montana, and represents the largest size class (class three). This specimen represents a minimum of two nearly identical sized individuals, based on limb and skull elements. This bone is moderately well preserved, with mineral recrystallization, appearing as a grainy indistinct surface, birefringent under polarized light, making discernment of histological features difficult. There is also crushing and sediment infill in the diaphysis just below the fourth trochanter. Due to this alteration two sets of slides were made from this specimen in order to try and obtain a complete sample of cortex. The greatest diameter of the specimen in this thin section, including the section of fourth trochanter, is 40.3 mm. Fusion in this individual (and/or the similar sized individual preserved with it under the same specimen number) is the most extensive, with complete fusion of the neurocentral sutures in all vertebrae and in all the scapulocoracoids.

The medullary cavity again dominates the center of the bone, occupying slightly more than half of the diameter of the element in thin section excluding the fourth trochanter. Distinct dark areas around the inner cortex make discernment of details there difficult and the presence of endosteal bone is unceratin. Prominent areas or cancellous secondary bone with erosion rooms dominate most areas around the medullary cavity. Excepting the high degree of vascularization in the fourth trochanter (Fig. 6E), vascularization in this specimen, which is apparently longitudinal, is difficult to assess due to the patchy mineral recrystallization. Osteonal development is harder to recognize in this specimen due to the recrystallization, with some primary osteons being visible sporadically in the inner cortex, which consists of fibrolamellar bone. Radiating columns of vascularity (Fig. 5A-B) occur in the posterolateral and anterolateral areas of the cortex, with prominent erosion rooms and poorly preserved secondary osteons. These radiating plumes extend through the entire cortex laterally, anteriorly, and posteriorly aligned with the fourth trochanter.

As in most other specimens, the outer cortex consists of lamellar-zonal bone. Four LAG's were noted in the cortex (Fig. 7E-G), with two occurring more centrally in the inner cortex and two more peripherally. The periosteal area consists of a prominent dark line (Fig. 6A-B and D; Fig. 7E-G) where the bone structure is not discernible.

DISCUSSION

The histological observations made above allow discernment of the growth patterns of *Oryctodromeus*. Recognition of the growth patterns and rates represented within the bones, as well as the development of skeletal fusion, allow the recognition of gradational growth stages within this taxon.

Growth Stages

The histologic observations made here suggest that three growth stages are represented by this studied sample. Each group appears to represent discrete ontogenetic stages of development. These stages can be here defined as juvenile, sub-adult, and near-adult stages.

The juvenile stage is represented by only one studied specimen, MOR 1636b. The length of this specimen, is roughly two-thirds the linear dimension of the tibia from a presumed adult it was found with (MOR 1636a, see below). At this stage deposition of primary bone occurred as moderately vascularized fibrolamellar bone tissue (Fig. 2). Fibrolamellar bone is generally viewed as the result of faster rates of bone deposition (Reid, 1996; Chinsamy-Turan, 2005). The rate of growth appears to have been more moderate due to the moderate levels of vascularization of the cortex. The level of vascularization of the periosteum indicates an animal still growing at an increased level

compared to the more mature individuals. The lack of any LAG's in this specimen is probably due to the young age. The lack of secondary osteons and bone tissue type indicate that was a young and fast growing individual. At this stage neurocentral fusion was only present in the middle and the more posterior caudals of these young individuals, based on the vertebrae preserved with MOR 1636b.

Specimens referred to a sub-adult stage comprise almost half (three of the seven) specimens studied. Specimens referred to this stage are IMNH 44920, the smaller tibia/individual of IMNH 44939, and IMNH 50877 (Tables 1-2). While detailed microstructural features within IMNH 44939 (smaller tibia) and IMNH 50877 are not as well preserved as the other specimens, as a whole this stage can be summarized through the following features: a thin layer of endosteal bone is intermittently present in the innermost cortex, a distinct pattern within the cortex of the bone where the inner half of the bone consists of a fibrolamellar tissue that transitions to parallel fibered/lamellar-zonal bone tissue. At this stage, secondary bone with associated secondary osteons, erosion rooms, and bone remodeling are common in portions of the inner cortex; with secondary osteons also forming the radially projecting columns of secondary osteons that extend towards some of the apical areas of the periosteum. Vascularity is still relatively constant in the outer cortex, with no sign of an EFS, though a slowing down in growth is indicated by the transition to the parallel fibered zonal bone (Ricqles 1980; Reid, 1994; Varricchio 1993). The scalloped areas of the cortex, especially prominent in IMNH 44939 indicate areas of significant bone remodeling and cortical drift. The cancellous bone of IMNH 50877 is anomalous compared to the other femora and tibiae studied here,

with a possible explanation being that this section was sampled from more distal on the femur then on other specimens. The radiating plumes of bone remodeling, due to their location on lateral surfaces of the bone, may be related to areas of active stress. Specimens of this age show that neurocentral fusion was well underway and proceeding in a posterior to anterior direction, with at minimum the mid and more distal caudal vertebrae having fused sutures. Fusion of the pectoral girdle was variable at this stage, as indicated by IMNH 44920.

A final stage termed near-mature is used here for the largest individuals, with this stage being represented by three specimens, MOR 1636a, the longer tibia from IMNH 44939 and MOR 1642 (Fig. 6). Due to the poor preservation of the cortex, MOR 1642 is only tentatively referred to this stage based on its size (the largest of the femora) and on it having the most extensive skeletal fusion. The presence of vague avascular and dense bone in the periosteum of the largest tibia from IMNH 44939 and in the tibia from MOR 1636a suggests the presence or proximity to development of an EFS (Fig. 4D) and a more reduced rate of skeletal growth in comparison to younger individuals (Ricqles, 1980; Chinsamy-Turan, 2005). A markedly cancellous and remodeled inner cortex (Fig. 6C-D) in MOR 1642 suggests a greater level of maturity in this specimen, but also indicates that this specimen itself had not stopped growing. The greater size of this specimen in comparison to all others sampled suggests a greater level of maturity, but the lack of an EFS and inability to recognize a greater number of LAG's in this specimen in comparison to others suggests this might be due to individual or sexual variation. Skeletal fusion at this age was most developed, with closed sutures in all observed vertebrae (cervicals

through distal caudals) and complete fusion of the scapulocoracoids in the largest individuals (MOR 1642). For MOR 1642, which has the most robust and longest femora of any *Oryctodromeus* specimens, a minimum mass of twenty-eight kilograms is suggested through the equation of Anderson *et al*. (1985). This is slightly more than a weight of twenty kilograms estimated from a femur of a large presumably adult *Orodromeus* (MOR 473).

Age

Lines of arrested growth (LAG's) have been demonstrated to represent some sort of environmental influences that are related to periodic annual cycles (Castanet, 2004; Padian and Horner, 2004; Chinsamy-Turan, 2005). Some of what are interpreted as LAG's here are not entirely circumferential (probably due to diagenetic processes) indicating some need for caution.

The lack of LAG's in the juvenile specimen MOR 1636b (Fig. 2) indicate that this individual may have been less than a year old, or alternatively that diagenetic and taphonomic processes have made them impossible to recognize (Fig. 2). Future better preserved juvenile specimens may allow an increased assessment for this age class. Regarding sub-adult individuals, while LAG's are not discernible in either individual from IMNH 44939 (Fig. 4) or IMNH 50877 (Fig. 5), the individuals represented by IMNH 44920 (Figs. 3 and 7A-B) and MOR 1636a (Figs. 5 and 7C-D) do offer some data. IMNH 44920 preserves two to three LAG's in the outer cortex. This suggests a minimum age of three to four years for IMNH 44920. MOR 1636a, also has five to six LAG's, which suggests an age of six to seven years.

MOR 1642 (Fig. 6, and 7 E-G), is the largest individual in our sample, however its poorly preserved nature makes a confident age assessment difficult. Two LAG's are visible in portions of the inner cortex (Fig. 7F), and what are tentatively identified as two LAG's are visible in areas of the outer cortex (Fig. 7G). This data suggests that this individual had an age greater than fours years.

Fusion

The pattern of neurocentral fusion and fusion of the scapulocoracoid in individual *Oryctodromeus* appears to correlate favorably with the three age stages defined above. Juvenile individuals lack fusion of the neurocentral sutures and scapulocoracoids, those of the intermediate size class have mostly fused vertebrae with those of the anterior dorsal column and cervicals being partially fused to unfused. In this intermediate age class fusion in the scapulocoracoids is variable, even in single individuals. The largest individual, MOR 1642, has the most extensive fusion, with full fusion in all preserved vertebrae and in all scapulocoracoids. Based on these data *Oryctodromeus* appears to have neurocentral fusion that progresses in the posterior to anterior pattern seen in crocodylians and some ornithopods and neornithischians (Brochu, 1996; Irmis, 2007). Additionally, fusion of the scapulocoracoid appears to be ontogenetically based.

Comparisons

The inferred growth strategy of *Oryctodromeus* proposed here correlates well with other neornithischians and the orodromine *Orodromeus*. Other orodromines such as *Zephyrosaurus*, *Koreanosaurus*, *Albertadromeus*, and the unnamed Kaiparowits orodromine have not been subjected to histological analysis. *Orodromeus* was shown to have a more moderate growth rate in comparison to larger dinosaurian taxa, with adult ages of four to six years being estimated based on LAG's (Horner *et al*., 2009). This is

similar to our age estimates for the similarly sized *Oryctodromeus* here. Additionally, the lower vascularity of the long bones discussed here and the fibrolamellar inner cortex and zonal parallel fibered outer cortex are similar to those of *Orodromeus* of similar growth stages (Scheetz, 199; Horner *et al*., 2009).

Other hypsilophodontid ornithopods, here considered a paraphyletic grade of neornithischians, also compare well with *Oryctodromeus* in various histologic aspects. Fibrolamellar bone in the inner cortex that transitions to parallel fibered bone in the outer cortex, which has been taken as an indicator of sexual maturity prior to skeletal maturity, has also been noted in the small neornithischian *Gasparinasaura* as well as hypsilophodontids from the late Early Cretaceous of Australia (Woodward *et al*., 2011; Cerda and Chinsamy, 2012). In contrast, in femora of sub-adult iguanodontian *Dryosaurus* (no skeletally mature individuals have been recognized) there is circumferential vascularity though the outer cortex which grades into laminar tissues (Horner *et al*., 2009).

While the skeletal histology of *Oryctodromeus* is most similar to *Orodromeus* and other small hypsilophodontid grade ornithopods, similar growth patterns have been noted in other small dinosaurs. For instance, *Troodon*, from the Campanian Two Medicine Formation of Montana has been shown to have similar growth patterns (Varricchio, 1993). This is in contrast to the small cerapodan *Psittacosaurus*, which has been shown to have had an increased rate of growth during later growth stages (Erickson and Tumanova, 2000). In contrast to other large ornithopods, *Tenontosaurus* has been shown to have had a slower growth trajectory, similar to that of *Oryctodromeus* (Werning, 2012).

Social Implications

Oryctodromeus is the first described fossorial dinosaur, with evidence for parental care and social groupings having been reported (Varricchio *et al*., 2007; Krumenacker *et al*., in prep). The holotype specimen, MOR 1636a, here recognized as a near-adult individual, was found within a burrow fill with the remains of a minimum of two juvenile individuals (MOR 1636b, utilized in this study). If, as has been hypothesized, this larger near-adult individual is the parent of the younger juveniles associated with it, this implies sexual maturity may have occurred close to skeletal maturity; or at least that this animal was reproductively active near skeletal maturity. A larger sample size is needed to further test this idea.

Also, the association of two individuals, represented by MOR 1642, both of which are of of similar size based on femoral lengths, suggest that groupings of *Oryctodromeus* also occurred without younger juvenile individuals in association. IMNH 44939, which consists of one sub-adult, one near-adult, and a juvenile individual, lends support to the idea that social groupings of this taxon consisted of more than just one single sexually mature sub-adult with juveniles.

CONCLUSIONS

Based on the histological sections and the skeletal fusion of the specimens discussed here, skeletal growth in the orodromine *Oryctodromeus* can be divided into three stages reflecting an overall decrease in growth rates. These stages are defined as juvenile, sub-adult, and near-adult. The juvenile stage can be defined through moderately vascularized fibrolamellar bone lacking the zonal parallel fibered outer cortex and LAG's of older individuals. Sub-adults are characterized by moderate secondary bone growth and reworking in the inner cortex, where secondary osteons and erosion rooms occur. A combination of characters such as development of secondary reworking of the inner cortex, development of the columns of secondary bone, and the transition from fibrolamellar tissues in the inner cortex to parallel fibered tissue in the outer

cortex characterize this stage. This sub-adult stage is interpreted as representing sexual maturity. LAG's present at this stage suggest a minimum age of three to four years for these individuals. The possibly near skeletally mature specimens (larger tibia of IMNH 44939, tibia from MOR 1636a, and the femur from MOR 1642) have similar histologic features to those of the sub-adults, with the addition of more dense and avascular bone in the outer cortex (IMNH 44939), more secondary bone, and somewhat less vascular bone.

The combined histologic evidence suggests that *Oryctodromeus* grew similar to its close relative *Orodromeus*. With a rapid growth rate as a juvenile and younger sub-adult. Periodic growth is indicated by LAG's, and this occurred closer to sexual maturity, when growth rates slowed down, as indicated by the zonal parallel fibred bone tissue. Assuming that the LAG's in these specimens were deposited annually, sexual maturity occurred at a rough age of four years. The similarity of this growth strategy with *Orodromeus* suggests that this may be a basal characteristic of the orodromine clade, but additional sampling of other orodromine taxa is required to test this. Additionally, greater histological sampling of parksosaurid ornithischians would greatly enhance our knowledge of the growth patterns and rates of these small and underutilized neornithischians.

ACKNOWLEDGEMENTS

First and foremost, thanks to Ellen-Therese Lamm for her lab instruction and help to the lead author as he learned paleohistological techniques. Appreciation is expressed to Bob Harmon for his assistance with molding and casting of the specimens used in this study. Thanks to the entire MSU PaleoHistology Class of 2017 for assisting with this project and expediting the process. Funding that supported this research was gratefully received from the Jurassic Foundation as well as a generous personal donation from

Robert Simon. Steve Robison, Ted Dyman, Ashley Ferguson, and the indomitable Elise Krumenacker assisted with collection of some of the specimens. Thanks to Carrie Ancell for her skilled preparation of MOR 1636 and MOR 1642.

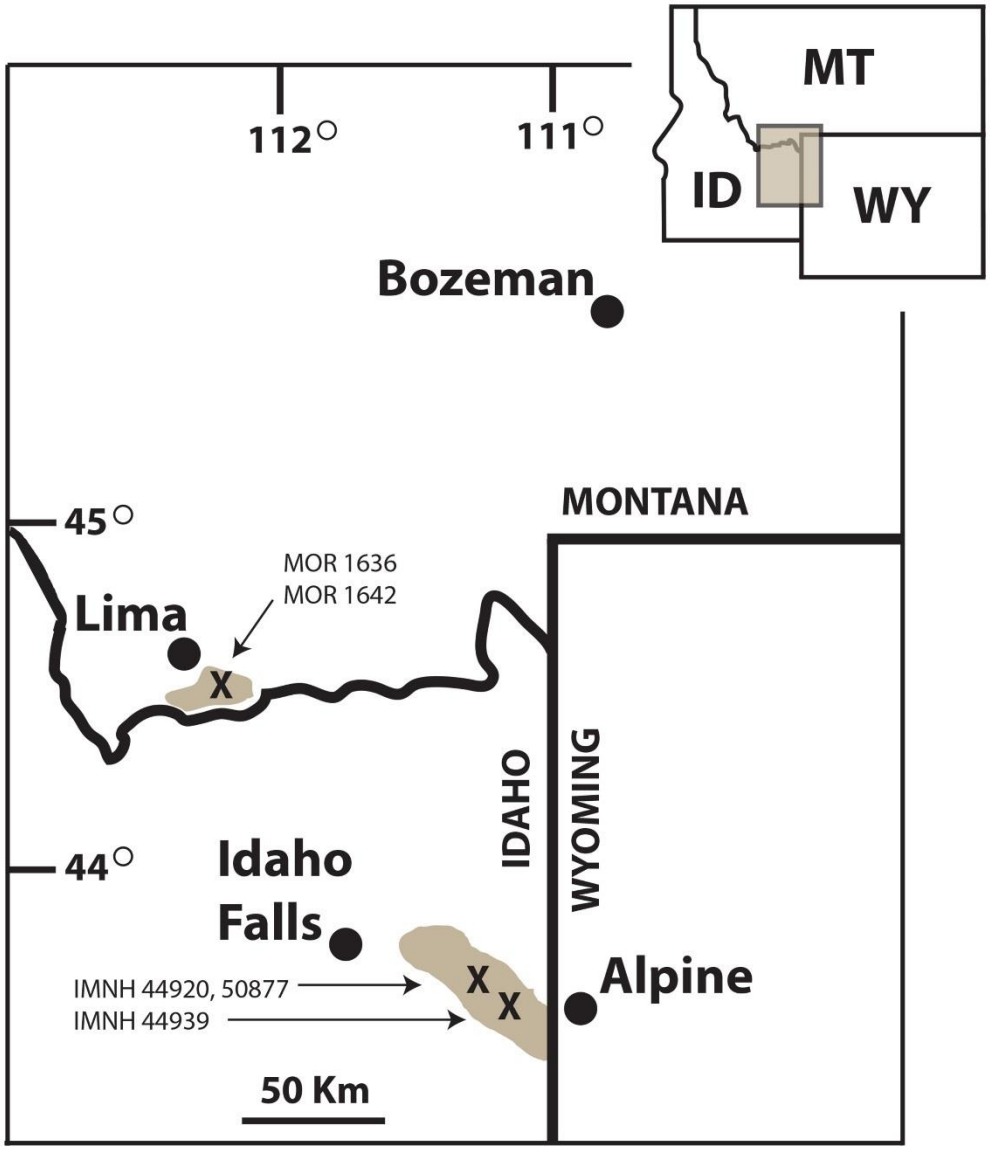

Fig 4.1. Field locations of *Oryctodromeus* specimens used in this study. MOR specimens were recovered from the Vaughn Member in Beaverhead County, Montana. IMNH 44920 and 50877 are from Bonneville County Idaho and IMNH 44939 is from Caribou County Idaho.

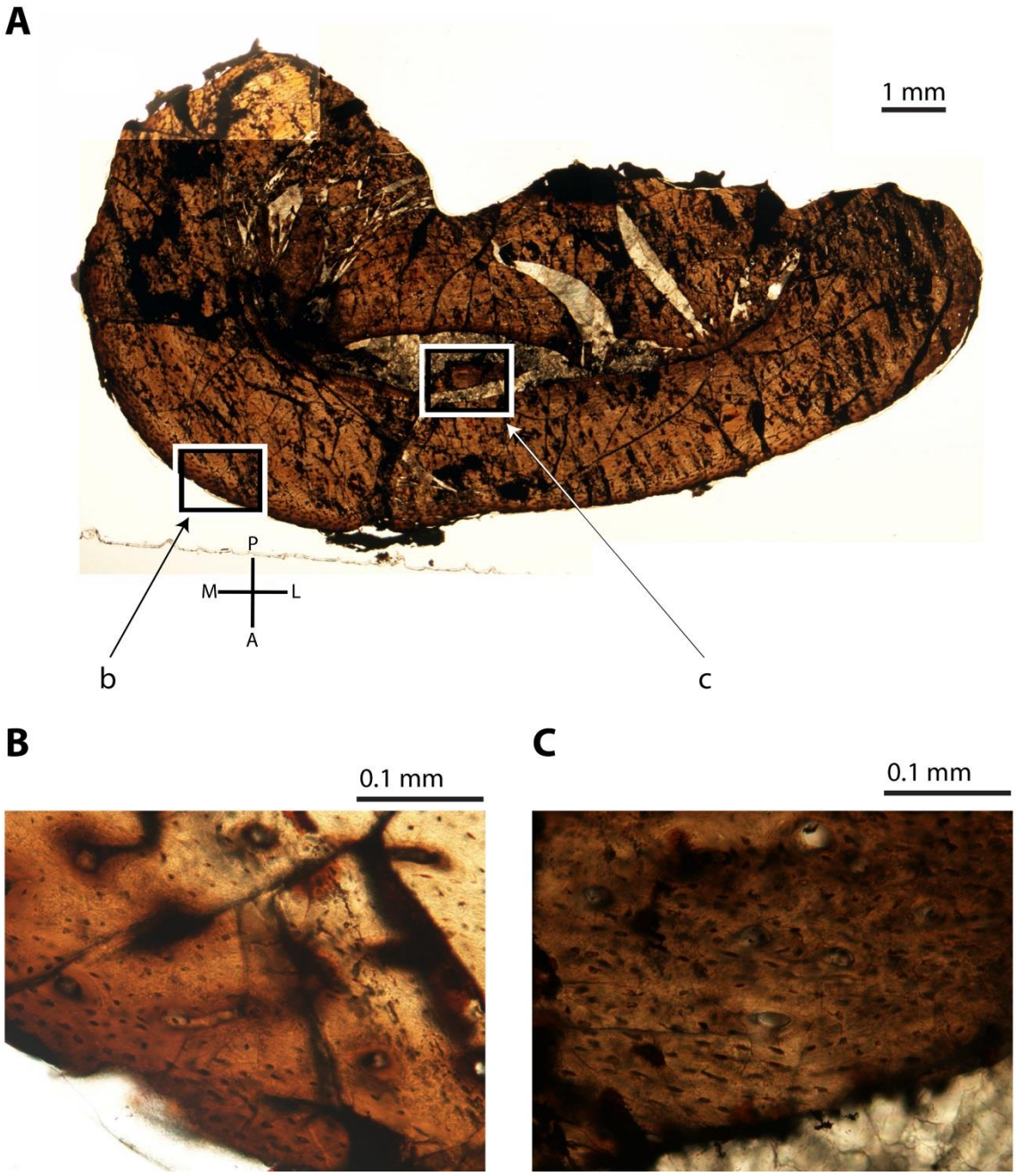

FIGURE 4.2. Histological sections of juvenile *Oryctodromeus* tibia MOR 1636b (slide PHT 2016-05 MOR 1636b T1-M-1) seen under normal light. **A**, composite image of entire element showing orientation of specimen and locations of images B and C; **B**, outermost periosteum with primary osteons and lacunae evident; C, inner cortex, possibly endosteum, with primary osteons and lacunae. **Abbreviations**: **A**, anterior, **L**, lateral; **M**, medial; **P**, posterior.

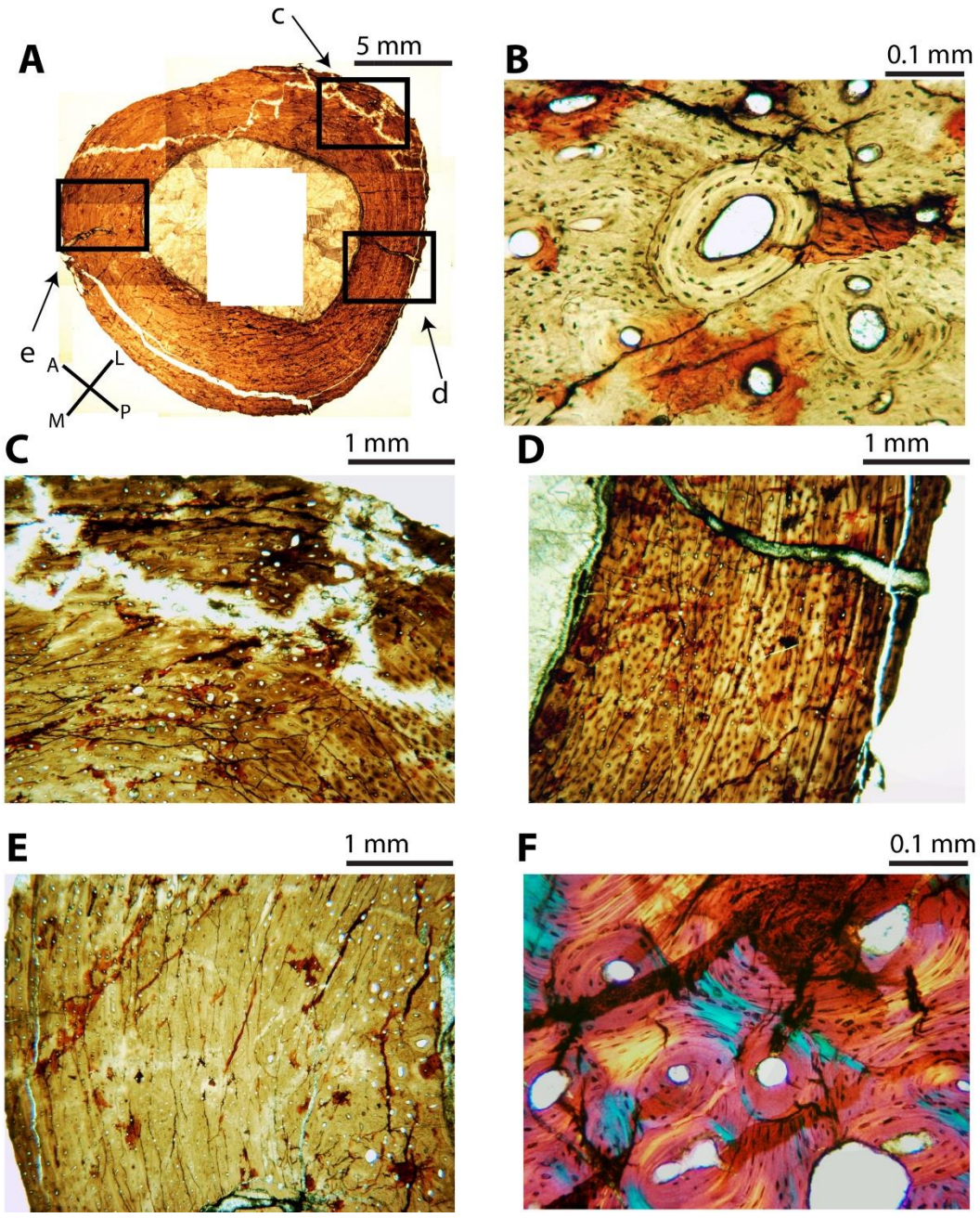

FIGURE 4.3. Histological sections of sub-adult *Oryctodromeus* femur IMNH 44920 (slide PHT 2016-06C IMNH 44920 FE1-I-1) seen under normal and polarized light. **A**, composite image of entire element showing specimen orientation and locations of images C, D and E; **B**, secondary osteon and primary osteons in cortex; **C**, radially oriented secondary osteons in remodeled bone extending through the cortex; **D**, Cortex with inner fibrolamellar bone transitioning to outer parallel-fibered bone; **E**, cortex with secondary osteons in secondary bone near the medullary cavity; **F**, secondary osteons and erosion rooms in polarized light. **Abbreviations**: **A**, anterior, **L**, lateral; **M**, medial; **P**, posterior.

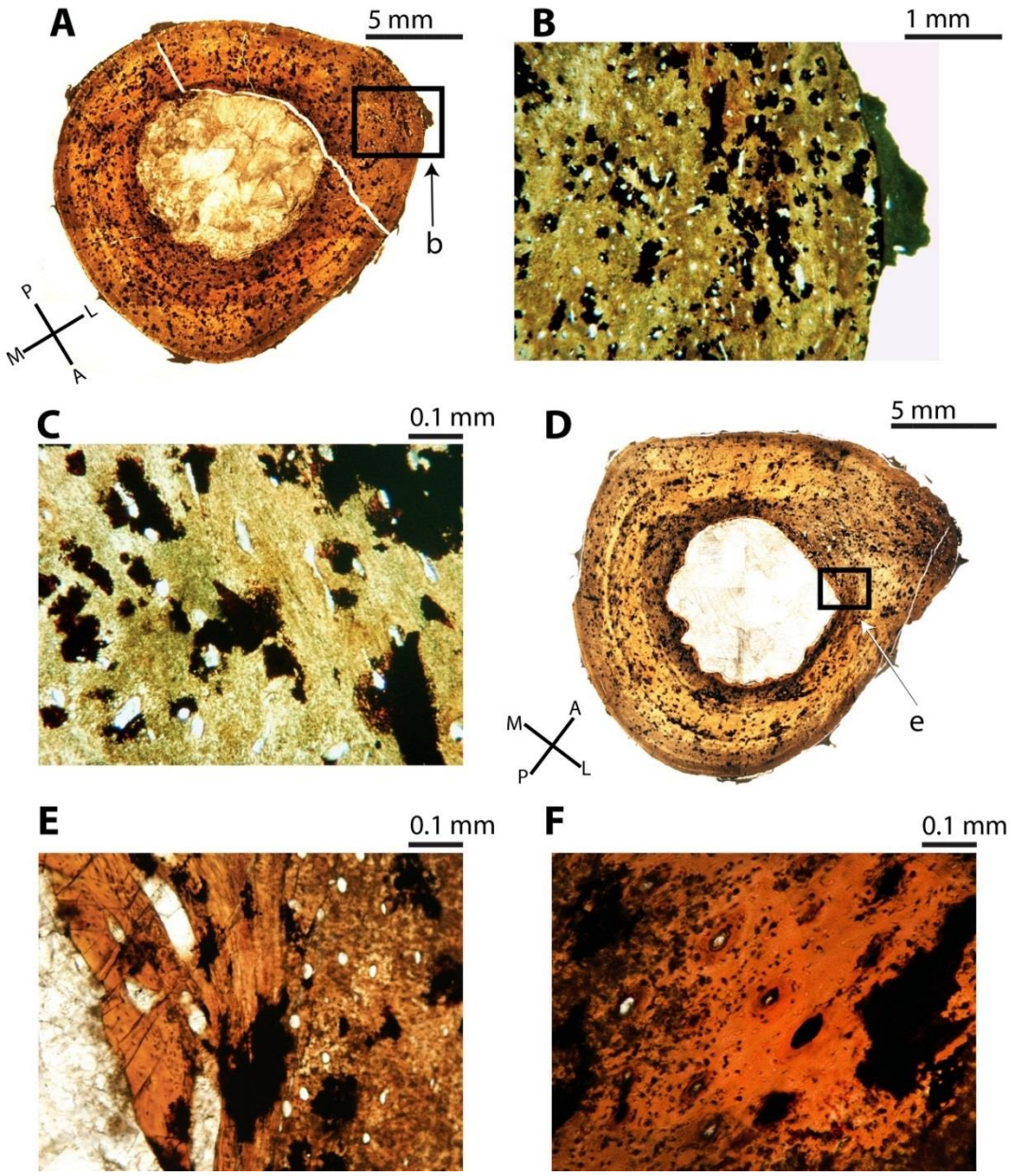

FIGURE 4.4. Histological sections of sub-adult *Oryctodromeus* tibiae, representing two individuals, from IMNH 44939 (slides PHT 2016-06C IMNH 4439 T2-I-1 for A-C and PHT 2016-06C IMNH 44939 T4-I-1 for D-F) seen under normal light. **A**, composite image of smaller tibia from IMNH 44939 showing specimen orientation and location of image b; **B-C**, cortex with hematite mineralization and poorly preserved osteons; **D**, composite image of larger tibia from IMNH 44939 showing specimen orientation and location of image e; **E**, Inner cortex with erosion rooms and secondary bone and transition to primary bone; **F**, primary osteons in cortex. **Abbreviations**: **A**, anterior, **L**, lateral; **M**, medial; **P**, posterior.

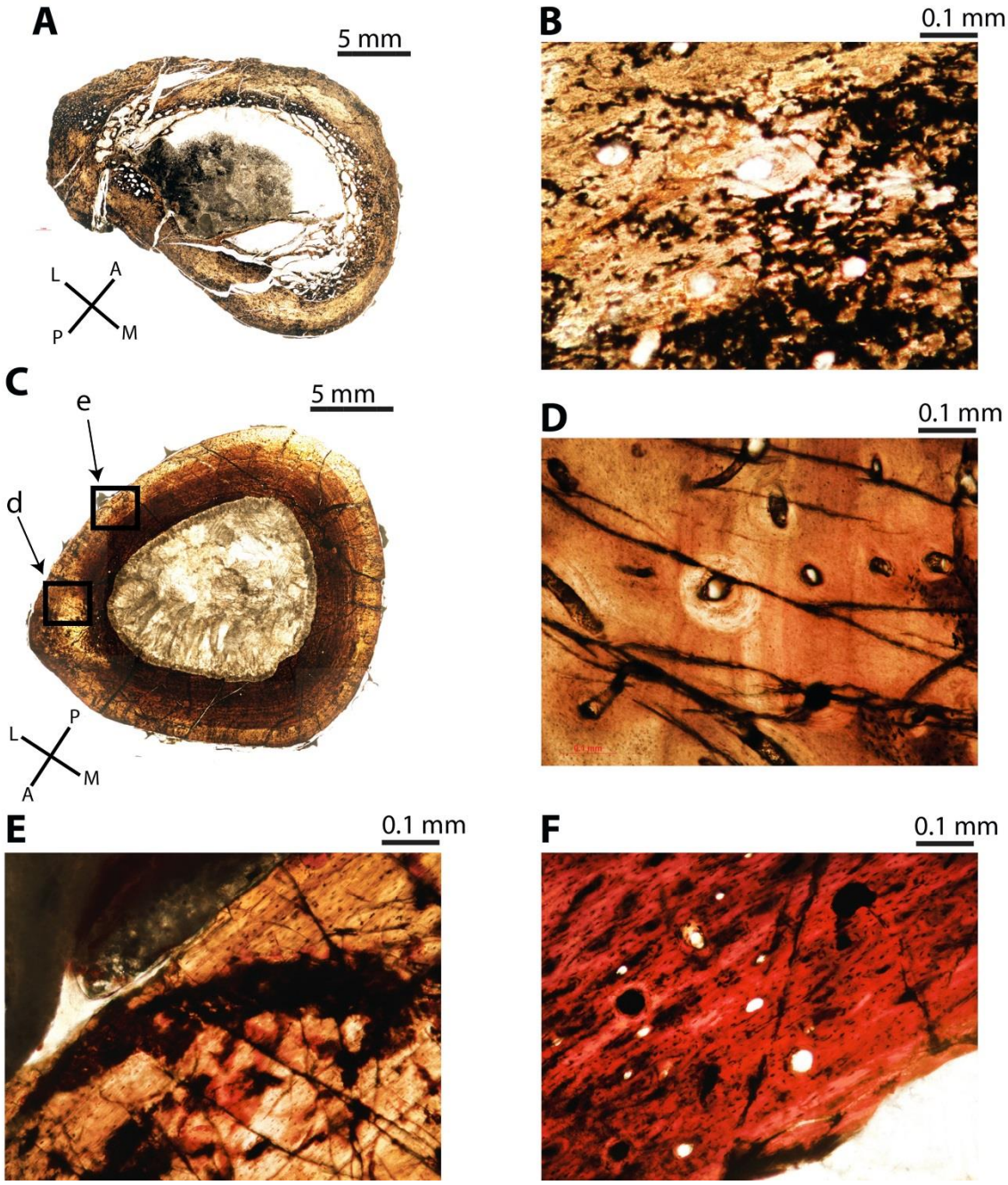

FIGURE 4.5. Histological sections of sub-adult *Oryctodromeus* femur (IMNH 50877, slide PHT 2016-06C IMNH 50877 FE2-I-1, A-B) and tibia (MOR 1636a T3-M, C-F) seen under normal light. **A**, composite image of femur from IMNH 50877 showing specimen orientation; **B,** cortex with hematite mineralization and poorly preserved primary osteons; **C**, composite image of MOR 1636b showing specimen orientation; **D**, primary osteon in fibrolamellar bone; **E-F**, Lamellar-zonal bone in outer (E) and fibrolamellar bone in inner (F) cortex. **Abbreviations**: **A**, anterior, **L**, lateral; **M**, medial; **P**, posterior.

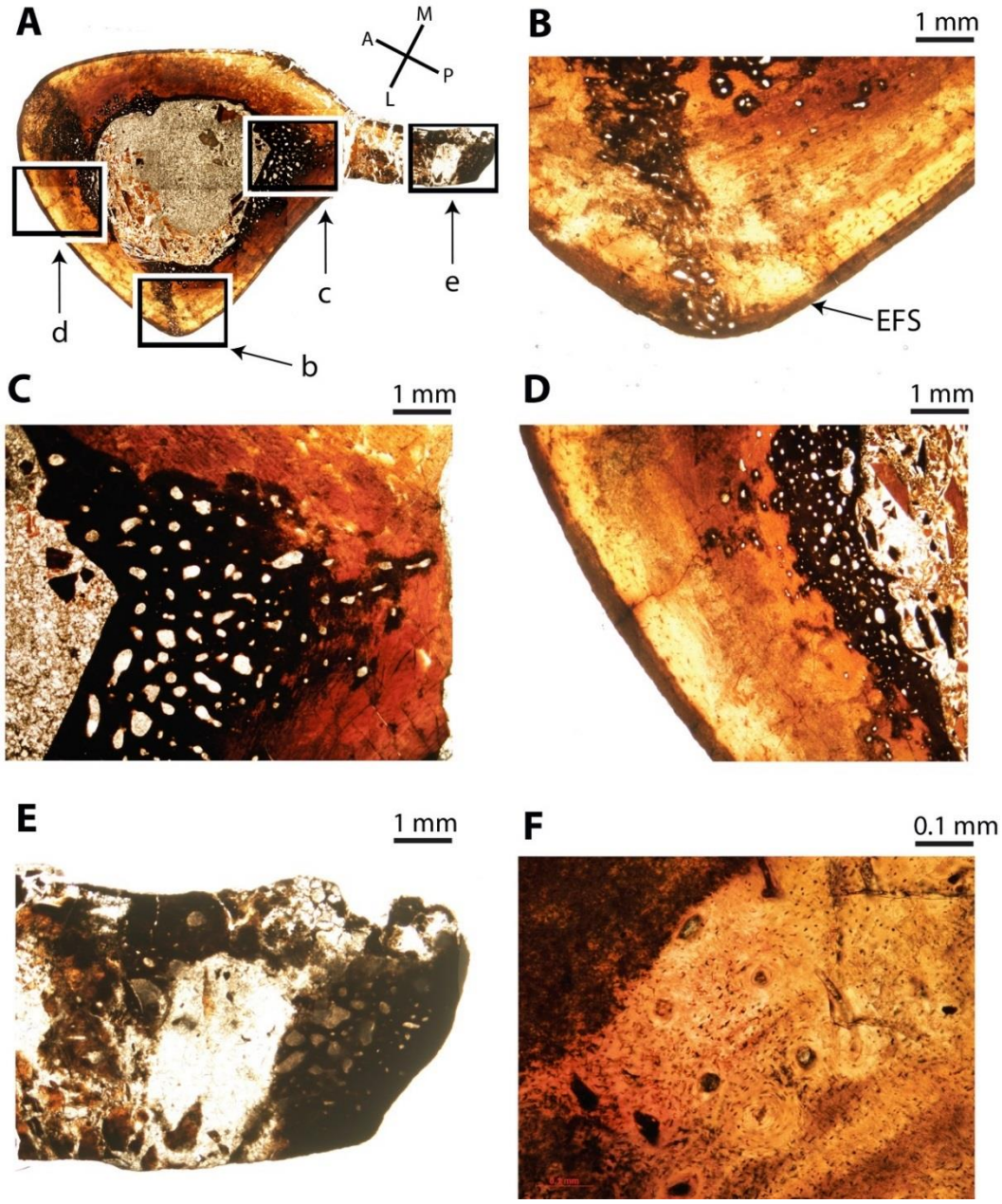

FIGURE 4.6. Histological sections of *Oryctodromeus* femur (MOR 1642 slide PHT 2016-05 MOR 1642 FE3-M-3) seen under normal light. **A**, composite image of femur from MOR 1642 showing specimen orientation and locations of images b, c, d, and e; **B,** cortex showing radially projecting vascularity and external fundamental system (EFS); **C**, inner cortex showing erosion rooms and vascularity; **D**, cortex showing erosion rooms, vascularity and EFS; **E**, cancellous bone within fourth trochanter; **F**, fibrolamellar bone and primary osteons within cortex. **Abbreviations**: **A**, anterior, **L**, lateral; **M**, medial; **P**, posterior.

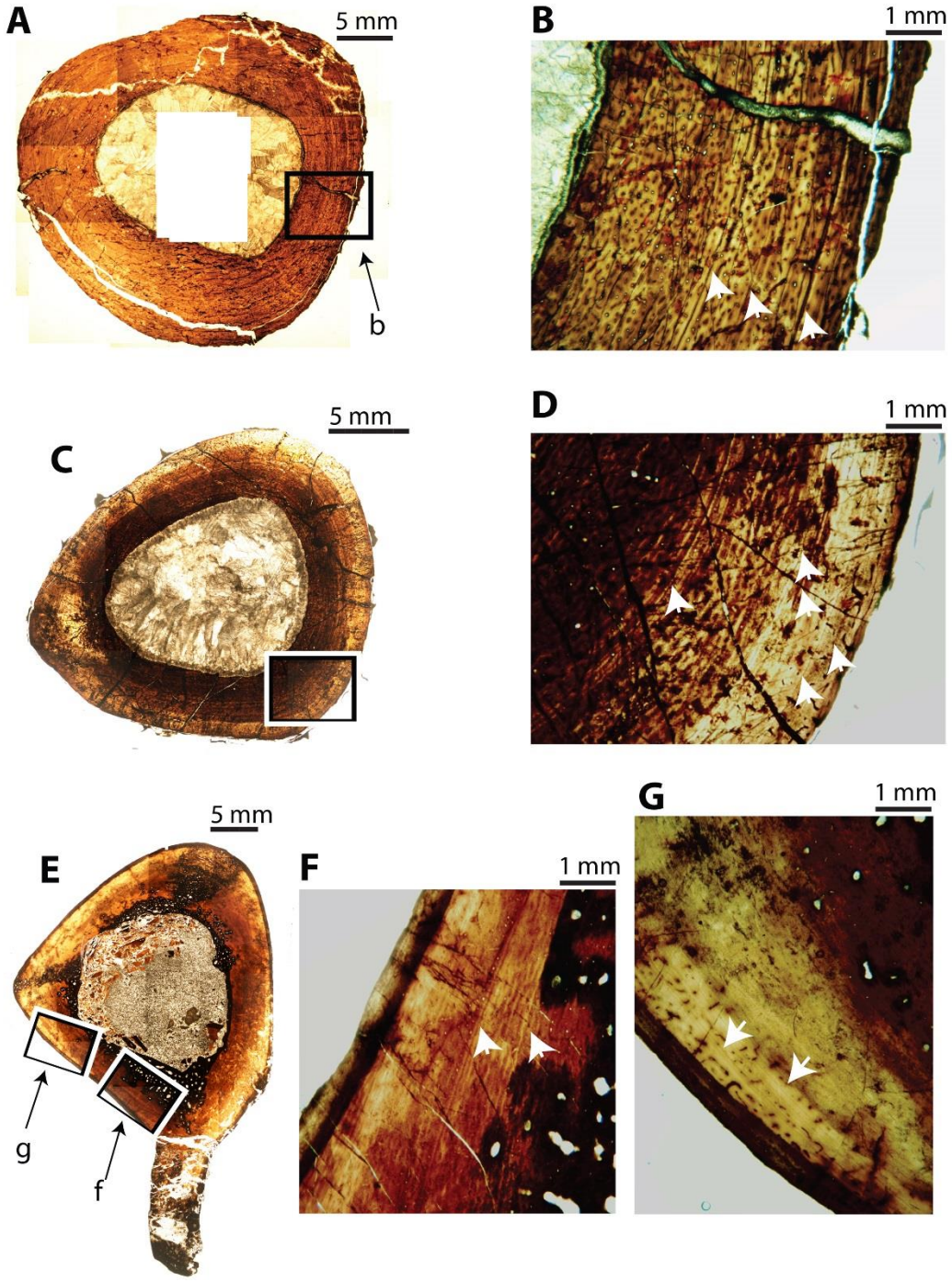

FIGURE 4.7. Histological sections of *Oryctodromeus* specimens showing LAG's (denoted by white arrows). **A**, composite image of femur from IMNH 44920; **B,** cortex of IMNH 44920 showing three LAG's; **C**, composite image of MOR 1636a; **D**,cortex of MOR 1636a showing three LAG's; **E**, composite image of MOR 1642; **F**, cortex of MOR 1642 showing 2 LAG's in the inner cortex; **G**. cortex of MOR 1642 showing 3 LAG's in the outer cortex.

TABLE 4.1 Specimens and slides of *Oryctodromeus* utilized in this study. Specimen number (some specimens consist of multiple associated individuals), element type, geological formation, and slides made from each specimen are indicated. Slides are curated at IMNH (Pocatello) and MOR (Bozeman).

Specimen	Element	Formation	Slides
IMNH 44920	L. femur	Wayan	PHT 2016-06C IMNH 44920 FE1-I-1
			PHT 2016-06C IMNH 44920 FE1-I-2
IMNH 44939	L. tibia (small)	Wayan	PHT 2016-06C IMNH 44939 T2-I-1
			PHT 2016-06C IMNH 44939 T2-I-2
IMNH 44939	R. tibia (large)	Wayan	PHT 2016-06C IMNH 44939 T4-I-1
			PHT 2016-06C IMNH 44939 T4-I-2
IMNH 50877	L. femur	Wayan	PHT 2016-06C IMNH 50877 FE2-I-1
			PHT 2016-06C IMNH 50877 FE2-I-2
MOR 1636b	R. tibia	Vaughn	PHT 2016-05 MOR 1636b T1-M-1
			PHT 2016-05 MOR 1636b T1-M-2
			PHT 2016-05 MOR 1636b T1-M-3
			PHT 2016-05 MOR 1636b T1-M-4
MOR 1636a	R. tibia	Vaughn	PHT 2016-05 MOR 1636a T3-M-1
			PHT 2016-05 MOR 1636a T3-M-2
MOR 1642	R. femur	Vaughn	PHT 2016-05 MOR 1642 FE3-M-1
			PHT 2016-05 MOR 1642 FE3-M-2
			PHT 2016-05 MOR 1642 FE3-M-3

Specimen	Element Sampled	Femur Length	Tibia Length	FC	FAD	FPD	FS	FAC	FMC	FDC	FSC	EB	LZ	2O	EFS	LAG's	Age (yr)	Maturity
MOR 1636b	Tibia	13.0 cm	14.9 cm *15.5 cm	0	0	0	0	0	1	1	0	0	0	0	0	n/a	<1?	J
IMNH 44920	Femur	19.1 cm	(≤22.7 cm)	n/o	n/o	0	0	0	1	1	P	1	1	1	0	2 to 3	>2	SA
IMNH 44939	Tibia (Small)	(≥19.3 cm)	23.0 cm	n/o	n/o	n/o	0	1	1	n/o	0	1	1	1	0	n/o	n/o	SA
IMNH 50877	Femur	20.2 cm	(≤24.0 cm)	n/o	n/o	n/o	n/o	1	1	1	n/o	1	1	1	0	n/o	n/o	SA
MOR 1636a	Tibia	(≥21.0 cm)	25.0 cm	1	1	1	1	1	1	n/o	P	1	1	1	?	5 to 6	>5	NA
IMNH 44939	Tibia (Large)	(≥23.5 cm)	28.0 cm	n/o	n/o	n/o	n/o	1	1	n/o	0	1	1	1	0	n/o	n/o	NA
MOR 1642	Femur	23.0 cm	*28.9 cm *28.7 cm *23.9 cm	1	1	1	1	1	1	1	1	n/o	1	1	?	4	>4	NA?

TABLE 4.2 Specimens of *Oryctodromeus* utilized in this study with element type, element length, select histological features present, assessment of fusion present in preserved elements, number of LAG's, estimated annual age, and assigned maturity levels indicated. A 0 indicates an absence of a feature and a 1 indicates a presence of a feature. An asterisk indicates a specimen that was not histologically sampled, but is listed for comparison. Greater than and equal or less then and equal symbols and measurements within parentheses indicate estimated length of missing femora or tibiae for individual specimens (based on 1.19 tibial-femoral ratio from Varricchio *et al*., 2007). **Abbreviations**: **CE**, cervical vertebra of uncertain position; **EB**, endosteal bone; **EFS**, external fundamental system; **FAC**, fusion of anterior caudal vertebrae; **FAD**, fusion of anterior dorsal vertebrae; **FC**, fusion of cervical vertebrae; **FDC**, fusion of distal caudal vertebrae; **FMC**, fusion of middle caudal vertebrae; **FPD**, fusion of posterior dorsals; **FS**, fusion of the sacral vertebrae neurocentral sutures; **FSC**, fusion of the scapulocoracoid; **IC**, inner cortex; **J**, juvenile; **L**, left; **LAG's**, lines of arrested growth; **LZ**, lamellar-zonal bone; **MC**, middle caudal vertebrae; **n/o**; not observable; **NA**, near-adult; **OC**, outer cortex; **P**, partial; **PC**, posterior caudal vertebrae; **PD**, posterior dorsal vertebrae; **R**, right; **S**, sacral vertebrae; **SA**, sub-adult; **SC**, scapulocoracoid; **2O**, secondary osteons.

LITERATURE CITED

Anderson, J. F., A. Hall-Martin, and D. A. Russell. 1985. Long-bone circumference and weight in mammals, birds, and dinosaurs. *Journal of Zoology, London (A)*: 207: 53-61.

Bailleul, A. M., J. B. Scannella, J. R. Horner, and D. C. Evans. 2016. Fusion Patterns in the Skulls of Modern Archosaurs Reveal That Sutures Are Ambiguous Maturity Indicators for the Dinosauria. *PLoS ONE* 11(2): e0147687. doi:10.1371/journal.pone.0147687

Boyd, C. A. 2015. The systematic relationships and biogeographic history of ornithischian dinosaurs. *PeerJ* 3:e1523.

Brochu, C. A. 1996. Closure of neurocentral sutures during crocodilian ontogeny: implications for maturity assessment in fossil archosaurs. *Journal of Vertebrate Paleontology*: 16 :49-62.

Brown, C. M., C. A. Boyd, and A. P. Russell. 2011. A new basal ornithopod dinosaur (Frenchman Formation, Saskatchewan, Canada), and implications for late Maastrichtian ornithischian diversity in North America. *Zoological Journal of the Linnaean Society* 163:1157–1198.

Brown, C.M., D. C. Evans, N. E. Campione, L.J. O'Brien, and D. A. Eberth. 2013. Evidence for taphonomic size bias in the Dinosaur Park Formation (Campanian, Alberta), a model Mesozoic terrestrial alluvial-paralic system. Palaeogeography, Palaeoclimatology, Palaeoecology: 372, 108–122. doi:10.1016/j.palaeo.2012.06.027.

Castanet, J., S. Croci, F. Aujard, M. Perrett, J. Cubo, and E, de Margerie. 2004. Lines of arrested growth in bone and age estimation in a small primate: *Microcebus murinus*. *Journal of Zoology, London* 263: 31-39.

Cerda, I. A., and A. Chinsamy. 2012. Biological implications of the bone microstructure of the Late Cretaceous Ornithopod Dinosaur *Gasparinisaura cincosaltensis*. *Journal of Vertebrate Paleontology* 32:355-368. DOI: 10.1080/02724634.2012.646804.

Chinsamy, A. 1995. Ontogenetic changes in the bone histology of the Late Jurassic ornithopod *Dryosaurus lettowvorbecki*. Journal of Vertebrate Paleontology 15:96–104.

Chinsamy-Turan, A. 2005. The Microstructure of Dinosaur Bone: Deciphering Biology with Fine-Scale Techniques. Johns Hopkins University Press, Baltimore and London, 195 pp.

Erickson, G. M., and T. A. Tumanova. 2000. Growth curve of *Psittacosaurus mongoliensis* Osborn (Ceratopsia: Psittacosauridae) inferred from long bone histology. Zoological Journal of the Linnean Society 130:551–566.

Erickson, G. M., K. Curry-Rogers, D. J. Varricchio, M. A. Norell, and X. Xu. 2007. Growth patterns in brooding dinosaurs reveals the timing of sexual maturity in non-avian dinosaurs and genesis of the avian condition. *Biology Letters* 3:558–561.

Horner, J. R., de Ricqle`s, A. & Padian, K. 2000 Long bone histology of the hadrosaurid dinosaur Maiasaura peeblesorum: growth dynamics and physiology based on an ontogenetic series of skeletal elements. Journal of Vertebrate Paleontology 20: 115–129.

Horner, J. R., Ricqles A. R., K. Padian, R. D. Scheetz. 2009 Comparative Long Bone Histology and Growth of the 'Hypsilophodontid' Dinosaurs *Orodromeus makelai*, *Dryosaurus altus*, and *Tenontosaurus tillettii* (Ornithischia: Euornithopoda). Journal of Vertebrate Paleontology 29: 734–747.

Huh, M., D. G. Lee, J. K. Kim, J. D. Lim, and P. Godefroit. 2011. A new basal ornithopod dinosaur from the Upper Cretaceous of South Korea. Neues Jahrbuch fur Geologie und Palaontologie Abhandlungen 259: 1-24.

Irmis, R. B. 2007. Axial skeleton ontogeny in the Parasuchia (Archosauria: Pseudosuchia) and its implications for ontogenetic determination in archosaurs. *Journal of Vertebrate Paleontology* 27: 350-361.

Krumenacker, L. J. 2010, Chronostratigraphy and paleontology of the mid-Cretaceous Wayan Formation of eastern Idaho, with a description of the first *Oryctodromeus* specimens from Idaho. M.S. Thesis, Brigham Young University, Provo, Utah, 98 pp.

Krumenacker, L.J., Simon, D. J., Scofield, G., and Varricchio, D. J., 2016. Theropod dinosaurs from the Albian–Cenomanian Wayan Formation of eastern Idaho. Historical Biology 29: 170–186 http://dx.doi.org/10.1080/08912963.2015.1137913.

Lee, A. H., and S. Werning. 2008. Sexual maturity in growing dinosaurs does not fit reptilian growth models. *Proceedings of the National Academy of Sciences of the United States of America* 105:582–587.

Martin, A.J. 2009. Dinosaur burrows in the Otway Group (Albian) of Victoria, Australia, and their relation to Cretaceous polar environments. Cretaceous Research 30: 1223–1237.

Padian, K., J. R. Horner, and A. de Ricqles. 2004. Growth in small dinosaurs and pterosaurs: the evolution of archosaurian growth strategies. *Journal of Vertebrate Paleontology* 24:555–571.

Padian, K., and E. T. Lamm, editors. Bone Histology of Fossil Tetrapods: Advancing Methods, Analysis, and Interpretation. 1st ed., University of California Press, 2013.

Reid, R. E. H. 1984a. The histology of dinosaurian bone, and its possible bearing on dinosaurian physiology. Symposium of the Zoological Society of London 52: 629–663.

Reid, R. E.H. 1996. Bone histology of the Cleveland-Lloyd dinosaurs and of dinosaurs in general. Part I: introduction to bone tissues. Brigham Young University Geology Studies 41:25–72.

Ricqles A. 1980. Tissue structure of the dinosaur bone: functional significance and possible relation to dinosaur physiology; pp. 103–139 in R. D. K. Thomas and E. C. Olson (eds.), A Cold Look at the Warm-Blooded Dinosaurs. AAAS Selected Symposium 28. Westview Press, Boulder, Colorado.

Scheetz, R.D., 1999, Osteology of *Orodromeus makelai* and the phylogeny of basal ornithopod dinosaurs. PhD. Thesis in Biology, Montana State University, Bozeman, 189 pp.

Varricchio, D. J. 1993. Bone microstructure of the Upper Cretaceous theropod dinosaur *Troodon formosus*. *Journal of Vertebrate Paleontology* 13:99–104.

Varricchio, D. J., A. J. Martin, and Y. Katsura. 2007, First trace and body fossil evidence of a burrowing, denning dinosaur: Proceedings of the Royal Society B: Biological Sciences 274: 1361–1368.

Werning, S. (2012). The Ontogenetic Osteohistology of *Tenontosaurus tilletti*. *PLoS ONE* 7 (3) DOI: 10.1371/journal.pone.0033539.

Woodward, H. N., T. H. Rich, A. Chinsamy, and P. Vickers-Rich. 2011. Growth dynamics of Australia's Polar dinosaurs. *PLoS ONE* 6:e23339. doi: 10.1371/journal.pone.002339

CHAPTER FIVE

CONCLUSIONS

This dissertation provides a detailed description of multiple aspects of the paleobiology, taphonomy, and relationships of the small burrowing dinosaur *Oryctodromeus cubicularis*. While most orodromines are rare components of their faunal assemblages and are relatively poorly understood, *Oryctodromeus* is reasonably well-represented and is the most common taxon represented by skeletal elements in the vertebrate assemblages of the Wayan Formation and the Vaughn Member of the Blackleaf Formation. This relative abundance of this taxon provides an opportunity for it to be one of the better understood members of the orodromine clade.

Numerous adaptions in the skeleton of this taxon are related to the digging habit of this animal, including the fused premaxillae, enlarged and fused scapulocoracoids, an enlarged sacrum, and the elongate and angular femoral heads (Varrichhio et el., 2007, this paper). The recognition of an extremely long tail facilitates additional questions about the morphology of the burrows and movement within. Additional analysis supports the placement of *Oryctodromeus* within the orodromine clade but provides no additional resolution.

The abundance of *Oryctodromeus* within the Wayan and Vaughn assemblages supports the possibility of biases favoring the preservation of this taxon in comparison to skeletal elements of other taxa. Taphonomic analysis suggests the possibility that this taxon may have been preferentially preserved within its own burrows, that may often go unrecognized. Additional specimens that consist of two or three individuals of various

ontogenetic stages, sometimes preserved in additional burrows described here, support the initial hypothesis of parental care in this taxon.

Paleohistological sampling demonstrates that *Oryctodromeus* had a growth strategy similar to that of its close relative *Orodromeus*. Three growth stages, representing juveniles, sub-adults, and nearly-grown adults are recognized in the specimens sampled. Growth was slower than that seen in larger dinosaurs, however the growth rate of this animal correlates well with smaller dinosaurs such as *Orodromeus*. Patterns of neurocentral fusion follow the patterns seen in other small dinosaurs, proceeding posteriorly to anteriorly, and provide additional means to at least tentatively assess the maturity levels of other specimens.

Oryctodromeus is a unique dinosaur due to its demonstrated habits of fossorial behavior and parental care, and due to its relative commonality in the geological units in which it is found. The occurrence of this taxon within the lesser sampled biotas of the early Late Cretaceous demonstrate significant potential for discoveries in the Wayan and Vaughn that will continue to add important information to this poorly understood interval in terrestrial ecosystems.

Literature Cited

Varricchio, D. J., A. J. Martin, and Y. Katsura. 2007, First trace and body fossil evidence of a burrowing, denning dinosaur: Proceedings of the Royal Society B: Biological Sciences 274: 1361–1368.

CUMULATIVE LITERATURE CITED

Anderson, J. F., A. Hall-Martin, and D. A. Russell. 1985. Long-bone circumference and weight in mammals, birds, and dinosaurs. *Journal of Zoology, London (A)*: 207: 53-61.

Bailleul, A. M., J. B. Scannella, J. R. Horner, and D. C. Evans. 2016. Fusion Patterns in the Skulls of Modern Archosaurs Reveal That Sutures Are Ambiguous Maturity Indicators for the Dinosauria. *PLoS ONE* 11(2): e0147687. doi:10.1371/journal.pone.0147687

Behrensmeyer, A.K. 1988. Vertebrate preservation in fluvial channels. Palaeogeography Palaeoclimatology, Palaeoecology., Ecological and Evolutionary Implications of Taphonomic Processes 63: 183–199. doi:10.1016/0031-0182(88)90096-X.

Behrensmeyer, A.K. 1991. Terrestrial Vertebrate Accumulations; pp. 291-335 in Allison, P. and D. E. (eds.), Taphonomy: Releasing the Data Locked in the Fossil Record. Plenum, New York.

Behrensmeyer, A. K., and R. W. Hook. 1992. Paleoenvironmental contexts and taphonomic modes in the terrestrial fossil record; pp. 15-136 in Behrensmeyer, A. K., J. D. Damuth, W. A. DiMichele, R. Potts, H. D. Sues, and S. L. Wing (eds), Terrestrial Ecosystems Through Time. Chicago, University of Chicago Press.

Bell, P.R. and N. E. Campione. 2014. Taphonomy of the Danek Bonebed: a monodominant *Edmontosaurus* (Hadrosauridae) bonebed from the Horseshoe Canyon Formation, Alberta. Canadian Journal of Earth Sciences 51: 992–1006. doi:10.1139/cjes-2014-0062.

Boyd C. A. 2014. The cranial anatomy of the neornithischian dinosaur *Thescelosaurus neglectus*. PeerJ 2:3669 DOI 10.7717/peerj.669.

Boyd, C. A. 2015. The systematic relationships and biogeographic history of ornithischian dinosaurs. *PeerJ* 3:e1523.

Britt, B.B., D. A. Eberth, R. D. Scheetz, B. W. Greenhalgh, and K. L. Stadtman. 2009. Taphonomy of debris-flow hosted dinosaur bonebeds at Dalton Wells, Utah (Lower Cretaceous, Cedar Mountain Formation, USA). Palaeogeography. Palaeoclimatology. Palaeoecology 280, 1–22. doi:10.1016/j.palaeo.2009.06.004.

Brochu, C. A. 1996. Closure of neurocentral sutures during crocodilian ontogeny: implications for maturity assessment in fossil archosaurs. *Journal of Vertebrate Paleontology*: 16 :49-62.

Brown, C. M., C. A. Boyd, and A. P. Russell. 2011. A new basal ornithopod dinosaur (Frenchman Formation, Saskatchewan, Canada), and implications for late Maastrichtian ornithischian diversity in North America. *Zoological Journal of the Linnaean Society* 163:1157–1198.

Brown, C.M., D. C. Evans, N. E. Campione, L.J. O'Brien, and D. A. Eberth. 2013. Evidence for taphonomic size bias in the Dinosaur Park Formation (Campanian, Alberta), a model Mesozoic terrestrial alluvial-paralic system. Palaeogeography, Palaeoclimatology, Palaeoecology: 372, 108–122. doi:10.1016/j.palaeo.2012.06.027.

Brown, C. M., D. C. Evans, M. J. Ryan, and A. P. Russell. 2013. New data on the diversity and abundance of small-bodied ornithopods (Dinosauria, Ornithischia) from the Belly River Group (Campanian) of Alberta. Journal of Vertebrate Paleontology 33(3): 495-520.

Butler, R. J., P. Upchurch, and D. B. Norman. 2008. The phylogeny of the ornithischian dinosaurs. Journal of Systematic Palaeontology 6:1–40.

Calvo, J. O., J. D. Porfiri, and F. E. Novas. 2007. Discovery of a new ornithopod dinosaur from the Portezuelo Formation (Upper Cretaceous), Neuquén, Patagonia, Argentina. Arquivos do Museu Nacional 65: 471–483.

Carpenter, K. 2013. History, Sedimentology, and Taphonomy of the Carnegie Quarry, Dinosaur National Monument, Utah. Annals of the Carnegie Museum 81: 153–232. doi:10.2992/007.081.0301.

Castanet, J., S. Croci, F. Aujard, M. Perrett, J. Cubo, and E, de Margerie. 2004. Lines of arrested growth in bone and age estimation in a small primate: *Microcebus murinus*. *Journal of Zoology, London* 263: 31-39.

Cerda, I. A., and A. Chinsamy. 2012. Biological implications of the bone microstructure of the Late Cretaceous Ornithopod Dinosaur *Gasparinisaura cincosaltensis*. *Journal of Vertebrate Paleontology* 32:355-368. DOI: 10.1080/02724634.2012.646804.

Chinsamy, A. 1995. Ontogenetic changes in the bone histology of the Late Jurassic ornithopod *Dryosaurus lettowvorbecki*. Journal of Vertebrate Paleontology 15:96–104.

Chinsamy-Turan, A. 2005. The Microstructure of Dinosaur Bone: Deciphering Biology with Fine-Scale Techniques. Johns Hopkins University Press, Baltimore and London, 195 pp.

Cobban, W., C. Erdmann, R. Lemke, and E. Manghen. 1959. Revision of Colorado group on Sweetgrass arch, Montana: AAPG Bulletin 43:2786–2796.

Cobban, W., C. Erdmann, R. Lemke, and E. Manghen, E.1976. Type sections and members of the Blackleaf and Marias River Formations (Cretaceous) of the Sweetgrass arch, Montana. U.S. Geological Survey Professional Paper 974.

Cooper, M. R. 1985. A revision of the ornithischian dinosaur *Kangnasaurus coetzeei* Haughton, with a classification of the Ornithischia. Annals of the South African Museum 95:281–317.

Csiki, Z., D. Grigorescu, V. Codrea, and F. Therrien. 2010. Taphonomic modes in the Maastrichtian continental deposits of the Haţeg Basin, Romania Palaeoecological and palaeobiological inferences. Palaeogeography, Palaeoclimatology, Palaeoecology 293: 375–390.

Damiani, R., S. Modesto, A. Yates, and J. Neveling. 2003. Earliest evidence of cynodont burrowing. Proceedings of the Royal Society B: Biological Sciences 270: 1747–1751. doi:10.1098/rspb.2003.2427.

Dodson, P., A. K. Behrensmeyer, R. T. Bakker, and J. S. McIntosh. 1980. Taphonomy and Paleoecology of the Dinosaur Beds of the Jurassic Morrison Formation. Paleobiology 6: 208–232.

Dorr, J.A., 1985. Newfound Early Cretaceous dinosaurs and other fossils in southeastern Idaho and westernmost Wyoming. Contributions from the Museum of Paleontology, University of Michigan 27(3): 73-85.

Durkee, S. K., 1980, Depositional environment of the lower Cretaceous Smiths Formation within a portion of the Wyoming-Idaho thrust belt: Wyoming Geological Association 31st Annual Field Conference Guidebook, p. 101-116.

Dyman, T.S., and D. J. Nichols. 1988. Stratigraphy of Mid-Cretaceous Blackleaf and lower part of the Frontier formations in parts of Beaverhead and Madison counties, Montana. U.S. Geological Survey Bulletin 1773.

Dyman, T.S., and R. G. Tysdal. 1990. Correlation of Lower and Upper Cretaceous Blackleaf Formation, Lima Peaks Area to Eastern Pioneer Mountains, Southwestern Montana. U. S. Geological Survey Miscellaneous Field Studies Map 2119.

Dyman, T.S., R. G. Tysdal, W. J. Perry, J. D. Obradovich, J. C. Haley, and D. J. Nichols. 1997. Correlation of Upper Cretaceous strata from Lima Peaks area to Madison Range, southwestern Montana and southeastern Idaho, USA. Cretaceous Research 18: 751–766. doi:10.1006/cres.1997.0079.

Eberth, D.A., and P.J. Currie. 2005. Vertebrate taphonomy and taphonomic modes; pp. 453-477 in Currie, P. J. and E. B. Koppelhus (eds.), Dinosaur Provincial Park: A Spectacular Ancient Ecosystem Revealed. Bloomington: Indiana University Press.

Erickson, G. M., and T. A. Tumanova. 2000. Growth curve of *Psittacosaurus mongoliensis* Osborn (Ceratopsia: Psittacosauridae) inferred from long bone histology. Zoological Journal of the Linnean Society 130:551–566.

Erickson, G. M., K. Curry-Rogers, D. J. Varricchio, M. A. Norell, and X. Xu. 2007. Growth patterns in brooding dinosaurs reveals the timing of sexual maturity in non-avian dinosaurs and genesis of the avian condition. *Biology Letters* 3:558–561.

Fearon, J. L., and D. J. Varricchio. 2015. Morphometric analysis of the forelimb and pectoral girdle of the Cretaceous ornithopod dinosaur *Oryctodromeus cubicularis* and implications for digging. Journal of Vertebrate Paleontology. DOI: 10.1080/02724634.2014.936555.

Felsenstein, J. 1978. Cases in which parsimony or compatibility methods will be positively misleading. Systematic Zoology 24(4): 401-410.

Fiorillo, A.R., 1988. Taphonomy of Hazard Homestead Quarry (Ogallala Group), Hitchcock County, Nebraska. Rocky Mountain Geology 26:57–97.

Gates, T. A., E. K. Lund, C. A. Boyd, D. D. DeBlieux, A. L. Titus, D. C. Evans, M. A. Getty, J. I. Kirkland, and J. G. Eaton, J. G. 2013. Ornithopod dinosaurs from the Grand Staircase-Escalante National Monument Region, Utah, and their role in paleobiogeographic and macroevolutionary studies, in At the Top of the Grand Staircase: The Late Cretaceous in Southern Utah, Titus, A. L., and Loewen, M. A. (eds). 463-481. Indiana University Press.

Groenewald, G.H., J. Welman, and J. A. Maceachern. 2001. Vertebrate burrow complexes from the Early Triassic *Cynognathus* Zone (Driekoppen Formation, Beaufort Group) of the Karoo Basin, South Africa. PALAIOS 16: 148–160. doi:10.1669/0883-1351(2001)016<0148:VBCFTE>2.0.CO;2.

Hechinger, R.F., K. D. Lafferty, A. P. Dobson, J. H. Brown, and A. M. Kuris. 2011. A Common Scaling Rule for Abundance, Energetics, and Production of Parasitic and Free-Living Species. Science 333: 445–448. doi:10.1126/science.1204337.

Horner, J., and D. Weishampel. 1988, A comparative embryological study of two ornithischian dinosaurs. Nature 332: 256-257.

Horner, J. R., de Ricqle`s, A. & Padian, K. 2000 Long bone histology of the hadrosaurid dinosaur Maiasaura peeblesorum: growth dynamics and physiology based on an ontogenetic series of skeletal elements. Journal of Vertebrate Paleontology 20: 115–129.

Horner, J. R., Ricqles A. R., K. Padian, R. D. Scheetz. 2009 Comparative Long Bone Histology and Growth of the 'Hypsilophodontid' Dinosaurs *Orodromeus makelai*, *Dryosaurus altus*, and *Tenontosaurus tillettii* (Ornithischia: Euornithopoda). Journal of Vertebrate Paleontology 29: 734–747.

Huh, M., D. G. Lee, J. K. Kim, J. D. Lim, and P. Godefroit. 2011. A new basal ornithopod dinosaur from the Upper Cretaceous of South Korea. Neues Jahrbuch fur Geologie und Palaontologie Abhandlungen 259: 1-24.

Hunt, R.M., X. Xiang-Xu, and J. Kaufman. 1983. Miocene Burrows of Extinct Bear Dogs: Indication of Early Denning Behavior of Large Mammalian Carnivores. Science 221: 364–366. doi:10.1126/science.221.4608.364.

Irmis, R. B. 2007. Axial skeleton ontogeny in the Parasuchia (Archosauria: Pseudosuchia) and its implications for ontogenetic determination in archosaurs. *Journal of Vertebrate Paleontology* 27: 350-361.

Kirkland, J.I. and S. K. Madsen. 2007, The Lower Cretaceous Cedar Mountain Formation, eastern Utah: the view up an always interesting learning curve: Fieldtrip Guidebook, Geological Society of America, Rocky Mountain Section, 1-108 p.

Krumenacker, L.J., 2005. Preliminary report on new vertebrates from the upper Gannett Group (Aptian) and Wayan Formation (Albian) of east Idaho. Paludicola 5: 55–64.

Krumenacker, L. J. 2010, Chronostratigraphy and paleontology of the mid-Cretaceous Wayan Formation of eastern Idaho, with a description of the first *Oryctodromeus* specimens from Idaho. M.S. Thesis, Brigham Young University, Provo, Utah, 98 pp.

Krumenacker, L.J., D. J. Varricchio, G. P. Wilson, and S. Robison. 2014. The Robison Bonebed: A preliminary report on the most diverse vertebrate fossil site known from the mid-Cretaceous Wayan Formation of Idaho, in: 5. Presented at the Geological Society of America, p. 26.

Krumenacker, L.J., Simon, D. J., Scofield, G., and Varricchio, D. J., 2016. Theropod dinosaurs from the Albian–Cenomanian Wayan Formation of eastern Idaho. Historical Biology 29: 170–186 http://dx.doi.org/10.1080/08912963.2015.1137913.

Lee, A. H., and S. Werning. 2008. Sexual maturity in growing dinosaurs does not fit reptilian growth models. *Proceedings of the National Academy of Sciences of the United States of America* 105:582–587.

Martin, A.J. 2009. Dinosaur burrows in the Otway Group (Albian) of Victoria, Australia, and their relation to Cretaceous polar environments. Cretaceous Research 30: 1223–1237.

Maxwell W. D. and J. H. Ostrom. 1995. Taphonomy and paleobiological implications of *Tenontosaurus-Deinonychus* associations, Journal of Vertebrate Paleontology, 15: 707-712.

McDonald AT, J. Bird, J. I. Kirkland, and P. Dodson. 2012. Osteology of the Basal Hadrosauroid *Eolambia caroljonesa* (Dinosauria: Ornithopoda) from the Cedar Mountain Formation of Utah. PLoS ONE 7(10): e45712. doi:10.1371/journal.pone.0045712.

Min H., D. G. Lee, J. K. Kim, J. D. Lim, and P. Godefroit. 2011. A new basal ornithopod dinosaur from the Upper Cretaceous of South Korea. Neues Jahrbuch für Geologie und Palaeontologie, Abhandlungen 259: 1–24.

Modesto, S.P., and J. Botha-Brink. 2010. A Burrow Cast with Lystrosaurus Skeletal Remains from the Lower Triassic of South Africa. PALAIOS 25: 274–281. doi:10.2110/palo.2009.p09-077r.

Novas, F. E., A. V. Cambiaso, A. Ambrioso, Alfredo. 2004. A new basal iguanodontian (Dinosauria, Ornithischia) from the Upper Cretaceous of Patagonia. Ameghiniana 41: 75–82.

Oghenekome, M. E. 2012. Sedimentary environments and provenance of the Balfour Formation (Beaufort Group) in the area between Bedford and Adelaide, Eastern Cape Province, South Africa. M. S. thesis, University of Fort Hare, Alice, South Africa 150 pp.

Oriel, S.S., and L. B. Platt. 1980. Geologic map of the Preston 1 degree by 2 degrees Quadrangle, southeastern Idaho and western Wyoming. USGS Numbered Series No. 1127.

Owen, R. 1842. Report on British fossil reptiles, Part II. Report of the British Association for the Advancement of Science (for 1841) 9: 60–204.

Padian, K., J. R. Horner, and A. de Ricqles. 2004. Growth in small dinosaurs and pterosaurs: the evolution of archosaurian growth strategies. *Journal of Vertebrate Paleontology* 24:555–571.

Padian, K., and E. T. Lamm, editors. Bone Histology of Fossil Tetrapods: Advancing Methods, Analysis, and Interpretation. 1st ed., University of California Press, 2013.

Paik, S., Kim, J. H., Park, K. H., Song, Y. S., Lee, Y. I., Hwang, J. I., and Huh, M., 2001. Palaeoenvironments and taphonomic preservation of dinosaur bone-bearing deposits in the Lower Cretaceous Hasandong Formation, Korea. Cretaceous Research 22: 627–642. doi:10.1006/cres.2001.0282.

Rambaut, A., M. A. Suchard, D. Xie, and A. J. Drummond. 2014. Tracer v1.6, Available from http://beast.bio.ed.ac.uk/Tracer.

Reading, H. G., 1996. Sedimentary Environments: Processes, Facies, and Stratigraphy: Blackwell Science, 688p.

Reichman, O.J., and S. C. Smith. 1990. Burrows and burrowing behavior by mammals; pp. 197-244 in Genoways, H. H. (ed.) Current Mammalogy, Plenum Press, New York.

Reid, R. E. H. 1984a. The histology of dinosaurian bone, and its possible bearing on dinosaurian physiology. Symposium of the Zoological Society of London 52: 629–663.

Reid, R. E.H. 1996. Bone histology of the Cleveland-Lloyd dinosaurs and of dinosaurs in general. Part I: introduction to bone tissues. Brigham Young University Geology Studies 41:25–72.

Ricqles A. 1980. Tissue structure of the dinosaur bone: functional significance and possible relation to dinosaur physiology; pp. 103–139 in R. D. K. Thomas and E. C. Olson (eds.), A Cold Look at the Warm-Blooded Dinosaurs. AAAS Selected Symposium 28. Westview Press, Boulder, Colorado.

Rogers, R., A. B. Arcucci, F. Abdala, P. C. Sereno, C. A. Forster, and C. L. May. 2001. Paleoenvironment and Taphonomy of the Chanares Formation Tetrapod Assemblage (Middle Triassic), Northwestern Argentina: Spectacular Preservation in Volcanogenic Concretions. PALAIOS 16: 461-481.

Rogers, R.R., 1990. Taphonomy of Three Dinosaur Bone Beds in the Upper Cretaceous Two Medicine Formation of Northwestern Montana: Evidence for Drought-Related Mortality. PALAIOS: 394–413. doi:10.2307/3514834.

Ronquist, F., M. Teslenko, P. van der Mark, D. Ayres, A. Darling, S. Höhna, B. Larget, L. Liu, M. A. Suchard, and J. P. Huelsenbeck. 2012. MrBayes 3.2: Efficient Bayesian phylogenetic inference and model choice across a large model space. Systematic Biology 61: 539-542.

Rubey, W.W. 1973. New Cretaceous formations in the western Wyoming thrust belt. U. S. Geological Survey Bulletin 1372-I.

Scheetz, R.D., 1999, Osteology of *Orodromeus makelai* and the phylogeny of basal ornithopod dinosaurs. PhD. Thesis in Biology, Montana State University, Bozeman, 189 pp.

Schmitt, J.G., Moran, M.E., 1982. Stratigraphy of the Cretaceous Wayan Formation, Caribou Mountains, southeastern Idaho thrust belt. Rocky Mountain Geology 21: 55–71.

Seeley, H. G. 1887. On the classification of the fossil animals commonly named Dinosauria. Proceedings of the Royal Society of London 43:165–171.

Shipman, P., 1981. Life History of a Fossil and Introduction To Taphonomy and Paleoecology. Harvard University Press. Cambridge, Massachusetts, and London.

Simon, D.J., 2014. Giant dinosaur (theropod) eggs of the Oogenus *Macroelongatoolithus* (Elongatoolithidae) from southeastern Idaho : taxonomic, paleobiogeographic, and reproductive implications. M. S. thesis, Montana State University, Bozeman, Montana, 121 pp.

Smith, R.M.H., 1993. Vertebrate Taphonomy of Late Permian Floodplain Deposits in the Southwestern Karoo Basin of South Africa. PALAIOS 8: 45–67. doi:10.2307/3515221.

Smith, R.M.H., 1987. Helical burrow casts of therapsid origin from the Beaufort Group (Permian) of South Africa. Palaeogeography, Palaeoclimatology, Palaeoecology 60: 155–169. doi:10.1016/0031-0182(87)90030-7.

Sternberg, C. M. 1937. Classification of *Thescelosaurus*: a description of a new species. Proceedings of the Geological Society of America 1936:375.

Suarez, M.B., C. A. Suarez, J. I. Kirkland, L. A. González, D. E. Grandstaff, and D. O. Terry. 2007. Sedimentology, Stratigraphy, and Depositional Environment of the Crystal Geyser Dinosaur Quarry, East-Central Utah. PALAIOS 22: 513–527. doi:10.2110/palo.2006.p06-014r.

Sues, H. D. 1980. Anatomy and relationships of a new hypsilophodontid dinosaur from the Lower Cretaceous of North America. Palaeontographica Abteilung a Palaeozoologie-Stratigraphie 169(1–3): 51–72.

Sundell, K.S., 1997. Oreodonts: large burrowing mammals of the Oligocene. Journal of Vertebrate Paleontology 17(3): 80A.

Tobin, R.J., 2004. Taphonomy of ground squirrel remains in a Late Pleistocene ichnofabric, Nebraska, USA. Palaeogeography, Palaeoclimatology, Palaeoecology 214: 125–134.

Tysdal, R.G., T. S. Dyman, and D. J. Nichols. 1989. Lower Cretaceous Bentonitic Strata in- Southwestern Montana Assigned to Vaughn Member of Mowry Shale (East) and of Blackleaf Formation (West). Mountain Geologist 26: 53-61.

Turner, B. R. 1981. Revised stratigraphy of the Beaufort Group in the southern Karoo Basin. Palaeontologia Africana 24: 87-98.

Varricchio, D. J. 1993. Bone microstructure of the Upper Cretaceous theropod dinosaur *Troodon formosus*. *Journal of Vertebrate Paleontology* 13:99–104.

Varricchio, D. J., A. J. Martin, and Y. Katsura. 2007, First trace and body fossil evidence of a burrowing, denning dinosaur: Proceedings of the Royal Society B: Biological Sciences 274: 1361–1368.

Varricchio, D. J., Moore, J., and F. Jackson. 2007. Preliminary vertebrate fauna of the mid Cretaceous Blackleaf Formation of Montana, in: Geological Society of America Abstracts with Programs for 59th Annual Meeting of the Rocky Mountain Section of the Geological Society of America p. 41.

Voorhies, M.R. 1969. Taphonomy and population dynamics of an early Pliocene vertebrate fauna, Knox County, Nebraska. Rocky Mountain Geologist 8: 1–69. doi:10.2113/gsrocky.8.special paper 1.1.

Weishampel, D.B., M. B. Meers, W. A. Akersten, and A. D. McCrady. 2002. New Early Cretaceous dinosaur remains, including possible ceratopsians, from the Wayan Formation of eastern Idaho. Idaho Museum of Natural History Occasional Paper 37: 5–17.

Werning, S. (2012). The Ontogenetic Osteohistology of *Tenontosaurus tilletti*. *PLoS ONE* 7 (3) DOI: 10.1371/journal.pone.0033539.

Wiltschko, D.V., Dorr, J.A., 1983. Timing of Deformation in Overthrust Belt and Foreland of Idaho, Wyoming, and Utah. AAPG Bulletin 67: 1304–1322.

Woodruff, D.C., and D. J. Varricchio. 2011. Experimental modeling of a possible *Oryctodromeus cubicularis* (dinosauria) burrow. PALAIOS 26: 140–151. doi:10.2110/palo.2010.p10-001r.

Woodward, H. N., T. H. Rich, A. Chinsamy, and P. Vickers-Rich. 2011. Growth dynamics of Australia's Polar dinosaurs. *PLoS ONE* 6:e23339. doi: 10.1371/journal.pone.002339

Zanno, L. E., and P.J. Makovicky. 2013. Neovenatorid theropods are apex predators in the Late Cretaceous of North America: Nature Communications 4: 2827.

Zartman, R. E., T. S. Dyman, R. G. Tysdal, and R. C. Pearson. 1995. U-Pb ages of volcanogenic zircon from porcellanite beds in the Vaughn Member of the mid-Cretaceous Blackleaf Formation, southwestern Montana: United States Geological Survey Bulletin 2113B.

APPENDICES

APPENDIX A

CHARACTERS USED IN PHYLOGENETIC ANALYIS, BASED ON PRELIMINARY CHARACTERS OF BOYD (2015), WITH NEW DATA FOR *ORYCTODROMEUS* ADDED

1. Preorbital skull length / total skull length less than or equal to 50% (0), greater than 50% (1).

2. Fusion of the premaxillae absent (0), present (1).

3. Predentary bone absent (0), present (1).

4. Rostral bone absent (0), present (1).

5. Oral margin of the premaxilla smooth (0), denticulate (1).

6. Lateral surface of the oral margin of the premaxillae flat (0), modestly flared, broadly everted (2).

7. Position of the ventral margin of the premaxilla level with the maxillary tooth row (0), ventrally deflected (1).

8. Anterior-most premaxillary tooth position at the anterior margin (0), inset at least the width of one tooth crown (1).

9. Premaxilla-maxilla diastema absent (0), present (1).

10. Premaxilla-maxilla diastema flat (0), arched with caniform anterior dentary tooth (1).

11. Anterior premaxillary foramen absent (0), present (1).

12. Premaxillary border of external naries present (0), absent (1).

13. Anterodorsal surface of the premaxilla smooth (0), highly rugose (1).

14. Premaxillary posterolateral process excludes maxilla from nasal margin absent (0), present (1).

15. Posterolateral concavity within the posterior end of the premaxilla, near lateral margin, for receipt of the anterolateral boss of the maxilla absent (0), present (1).

16. Overlap of the dorsal process of the premaxilla onto the rostral process of the nasals absent (0), present (1).

17. Contact between premaxilla and lacrimal absent (0), present (1).

18. Premaxillary sulcus on the anterior process of the maxilla absent (1 process) (0), present (2 processes) (1).

19. Special foramina medial to dentary an maxillary tooth rows absent (0), present (1).

20. Buccal emargination on the maxilla absent (0), present (1).

21. Development of buccal emargination of maxilla Gradual and shallow beveling of the ventrolateral surface of the maxilla (0), prominent ridge on lateral surface of the maxilla (1).

22. Notch in maxilla for the lacrimal absent (0), present (1).

23. Fossa situated low along the premaxilla/maxilla boundary absent (0), present (1).

24. Supraorbital absent (0), one present (1), two or more present (2).

25. Supraorbital free (0), projects into orbit from contact with lacrimal/prefrontal (1), incorporated into the orbital margin (2).

26. Length of supraorbital 100-71% maximum anteroposterior length of the orbit (0), 70% or less maximum anteroposterior length of the orbit (1).

27. Ratio of greatest posterior expanse of the jugal divided by height of skull greater than 25% (0), less than 25% (1).

28. Anterior process of the jugal straight (0), curved (1).

29. 'Maxilla-jugal contact jugal dorsal to the maxilla (0), jugal inserts into the maxilla (1).

30. Contact between jugal and lacrimal jugal just touches lacrimal (0), jugal meets lacrimal with more contact (1), jugal-lacrimal butt joint (2).

31. Jugal contribution to the antorbital fenestra present (0), absent (1).

32. Jugal-postorbital articulation contact faces anteriorly (0), contact faces partially laterally (1), postorbital inserts into a socket in the jugal (2).

33. Depth of the jugal versus transverse breadth deeper than broad (0), broader than deep (1).

34. Jugal contribution to the infratemporal fenestra forms caudoventral margin (0), only the ventral margin (1).

35. Shape of the anteroventral corner of the infratemporal fenestra formed by the jugal oblique (0), to right acute (1).

36. 'Jugal-quadratojugal contact butt or high angle scarf joint (0), jugal overlaps quadratojugal laterally along the posterodorsal portion and medially along the posteroventral portion (1).

37. 'Jugal-quadrate contact no contact (0), contact present (1).

38. Location of jugal or quadratojugal contact with quadrate near or slightly above distal end (0), well above distal end (1).

39. Jugal horn absent (0), ornamented surface, but no boss (1), low boss (2), tall, posteriorly projecting boss (3).

40. Maxillary process on medial side of jugal medially projected and modestly arched (0), straight and grooved (1), anteromedially projected and arched (2).

41. Shape of ectopterygoid facet on medial surface of the jugal abbreviated (0), deep groove (1), rounded scar (2).

42. Quadratojugal foramen absent (0), present (1).

43. Contact between the dorsal process of the quadratojugal and descending process of the squamosal present (0), absent (1).

44. Shape of the quadratojugal anteroposteriorly long, dorsoventrally short (0), anteroposteriorly short, dorsoventrally tall (1).

45. 'Quadrate-quadratojugal articulation contact greater than 50% length of quadrate (0), less than 50% total length of quadrate (1).

46. Proximal head of the quadrate recurved (0), straight (1).

47. Ventral portion of the quadrate shaft vertical or anteroventrally angled (0), posteroventrally angled (1).

48. Quadrate orientation posteriorly leaning (0), vertical (1), anteriorly leaning (2).

49. Quadrate jugal wing moderate (0), shortened (1).

50. Ventral extent of jugal wing of quadrate at or near distal end (0), above distal end (1).

51. Pit in lateral side of quadrate at the base of the jugal wing present (0), absent (1).

52. Quadrate notch (tiny foramen between jugal wing of quadrate and quadratojugal, absent (0), present (1).

53. Orientation of the distal condyles of the quadrate dorsomedially sloped or horizontal (0), dorsolaterally sloped (1).

54. Dorsal extent of the pterygoid wing of the quadrate arises at the dorsal head of the quadrate (0), arises below the dorsal head of the quadrate (1).

55. Size of pterygoid wing of quadrate large, anteromedially extending fan of bone (0), small (1).

56. Groove on the base of the posterior side of the pterygoid wing of the quadrate absent (0), present (1).

57. Length of ventral process of squamosal relative to total quadrate length less than 30% (0), greater than 30% (1).

58. Paroccipital process shape oriented horizontally and slightly widened distally (0), distal end pendant (1).

59. Parietosquamosal shelf absent (0), present (1).

60. Orbital edge of postorbital smooth, continuous arc (0); anteriorly directed inflation into orbit (1).

61. Orbital margin of postorbital clean margin (0), striated and rugose (1).

62. Robustness of postorbital 'non-robust' (0), robust (1).

63. Placement of the synovial socket for the head of the laterosphenoid in frontal and postorbital (0), postorbital only (1), frontal only (2), no synovial Joint (3).

64. Percentage of frontal that participates in the orbital margin greater than 25% of the frontal length (0), less than 25% of the frontal length (1).

65. Position of frontals relative to orbit over all of orbit (0), positioned over posterior half of orbit (1)

66. Shape of frontals arched over orbit (0), dorsally flattened (1).

67. Combined width of frontals versus length wider than long (0), longer than wide (1).

68. Size of frontals relative to nasals frontals > 120% nasal length (0), frontals between 120% and 60% nasal length (1), frontals less than 60% length of nasal (2).

69. Length of the oral margin of the predentary Less than the length of the oral margin of the premaxilla (0), equal to or greater than the oral margin of the premaxilla (1).

70. Shape of anterior tip of predentary pointed (0), rounded (1).

71. Oral margin of the predentary smooth (0), denticulate (1).

72. Ventral process of the predentary present (0), very reduced or absent (1).

73. Number of ventral processes of predentary one (0), two (1).

74. Dentary symphysis shape V-shaped (0), spout-shaped (1).

75. Position of anterior-most tip of dentary within dorsal 1/3 of dentary height (0), near mid-height (1), within lower 1/3 of dentary height (2), anterior tip of dentary curves ventrally below ventral margin of the dentary (3), anterodorsally curved, higher than the base of the dentary tooth row (4).

76. Dorsal and ventral margins of the dentary converge (0), rostrally parallel (1).

77. Medial surface of the dentary straight (0), medially arched (1).

78. Ratio of dentary depth just anterior to the rising coronoid process to length of dentary 15-20% (0), 21-35% (1).

79. Dentary tooth row shape in lateral view straight (0), sinuous (1).

80. Coronoid Process absent or weakly developed (0), present (1).

81. Dentary contribution to the coronoid process absent (0), present (1).

82. Position of posterior end of tooth row relative to the coronoid process Tooth row ends anterior to coronoid process (0), posterior end of tooth row shrouded by coronoid process (1).

83. Shape of coronoid process inconspicuous subtriangular subrectangular (0), dorsally elongated with lobe-shaped distal expansion (1).

84. 'Post-coronoid length of mandible 36% or greater total length of mandible (0), 25-35% total length of mandible (1), less than 25% total length of mandible (2).

85. Shape of the dorsal margin of the surangular convex or diagonal (0), concave (1).

86. Surangular foramen absent (0), present (1).

87. Ridge or process on lateral surface of surangular, anterior to the jaw suture absent (0), a strong, anteroposteriorly extending ridge present (1), a dorsally directed, finger-like process present (2).

88. Size of the distal condyles of the quadrate subequal (0), medial condyle larger (1), lateral condyle larger (2).

89. Maximum length of external nares versus maximum anteroposterior diameter of the orbit less than 15% basal skull length (0), greater than 15% basal skull length (1).

90. Position of external nares close to the buccal margin and below the level of the orbit (0), positioned higher than maxilla (1).

91. Antorbital fenestra present (0), absent (1).

92. Antorbital fossa rounds smoothly onto maxilla along some part of its margin (0), sharply defined or extended as a secondary lateral wall enclosing the fossa (1).

93. Maxillary fenestra absent (0), present (1).

94. Antorbital fossa shape triangular (0), ovate or circular (1).

95. Size of external opening of the antorbital fossa present, greater than 10% basal skull length (0), present, less than 10% basal skull length (1), absent (2).

96. Shape of the lower margin of the orbit circular (0), subrectangular (1).

97. Extent of the ventral edge of the infratemporal fenestra extends to or below the ventral margin of the orbit (0), positioned well above the ventral margin of the orbit (1).

98. External mandibular fenestra present (0), absent (1).

99. Angle between the base and long axis of the braincase greater than 35 degrees (0), less than 35 degrees (1).

100. Median ridge on floor of the braincase absent (0), present (1).

101. Composition of the occipital condyle basioccipital and exoccipital contribute (0), exoccipital excluded (1).

102. Nuchal crest on the supraoccipital absent (0), present (1).

103. Contribution of supraoccipital to the edge of the foramen magnum contributes to greater than 5% of the margin of the foramen magnum (0), contributes less than 5% of the margin of the foramen magnum (1), excluded from margin of foramen magnum (2).

104. Location of posttemporal foramen at the boundary between the parietal and the paroccipital process (0), within the opisthotic (1), within the squamosal (2).

105. Posttemporal foramen morphology consists of an enclosed foramen (0), dorsally open groove (1).

106. Ventral keep on basioccipital absent (0), present (1).

107. Floor of basioccipital flat (0), arched (1).

108. Position of the basioccipital tubera lower than basisphenoid (0), level with basisphenoid (1).

109. Contribution of occipital condyle to the foramen magnum over 30% of the occipital condyle (0), 30-20% of the occipital condyle (1), less than 20% of the occipital condyle (2).

110. Length of basisphenoid (from base of the parasphenoid process to the posterior edge of the basisphenoid) versus length of basioccipital basisphenoid shorter (0), subequal basisphenoid (1), longer (2).

111. Position of foramen for cranial nerve V notches anteroventral (0), edge of prootic (1), enclosed within the prootic (2).

112. Premaxillary teeth present (0), absent (1).

113. Number of premaxillary teeth per side 6 (0), 5-4 (1), 3-1 (2).

114. Enlarged anterior caniniform tooth in the dentary absent (0), present (1).

115. Relationship between denticles and ridges on mandibular crowns ridges absent (0), only simple denticles present (1), at least some denticles confluent with ridges that extend to base of crown (2).

116. Position of the apex of the maxillary teeth centrally placed (0), posterior of center (1).

117. Premaxillary tooth shape recurved, transversely flattened, constricted at the base (0), straight, subcylindrical, unconstricted at the base. (1).

118. Spacing of maxillary teeth space between the roots and crowns of adjacent teeth (0), lack of space between crowns of adjacent teeth up through the occlusional margin (1),

lack of space between roots of adjacent teeth (2), no space between crowns within one tooth position (3).

119. Placement of the apical ridge on the dentary teeth anterior to centrally placed (0), placed posterior of center (1).

120. Shape of maxillary tooth roots in anterior or posterior view straight (0), curved (1).

121. Transition from crown to root in maxillary teeth distinct neck below crown (0), crown tapers to root (1).

122. Maxillary occlusional surface teeth independently occlude (0), teeth share a continuous occlusional surface (1).

123. Shape of lingual surface of maxillary teeth concave (0), convex flat (1).

124. Distribution of enamel on maxillary and dentary teeth equally enameled (0), enamel primarily on one side (1).

125. Distribution of ridges on mandibular teethridges on both sides of the crown (0), ridges limited to one side (1).

126. Shape of maxillary tooth crowns low and spade-like, rectangular, or triangular (0), high diamond-shaped maxillary crowns (1), laterally flattened, posteriorly recurved crowns (2), conical (3).

127. Number of maxillary teeth per side 12 or less (0), 13-19 (1), 20 or more (2).

128. Relationship between ridges and denticles on maxillary teeth Smooth face with simple denticles (0), ridges confluent with denticles and extend to base of crown (1).

129. Presence of a primary ridge on the maxillary teeth absent (0), present (1).

130. No cingulum on maxillary teeth cingulum present (0), cingulum absent (1).

131. No cingulum on dentary teeth cingulum absent (0), cingulum present (1).

132. Placement of maxillary teeth placed near the lateral margin (0), inset medially (1).

133. Maxillary crown shape height less than 50% (0), length '50-90% (1), subequal '110-150% (2), greater than 150% (3).

134. Dentary crown shape less than 50% higher than mesiodistally wide (0), greater than 50% higher than mesiodistally wide (1).

135. Denticles restricted to apical third of maxillary and dentary tooth crowns absent (0), present (1).

136. Shape of dentary tooth roots in anterior or posterior view straight (0), curved (1).

137. Shape of dentary crowns rectangular, triangular, or leaf-shaped (0), lozenge-shaped (1), laterally flattened, posteriorly recurved (2), conical (3).

138. Number of dentary tooth positions 13 or fewer (0), 14-17 (1), 18 or more (2).

139. Number of ridges on dentary crowns fewer than ten (0), ten or more (1).

140. Primary ridge on dentary teeth no ridge more prominent than the others (0), prominent ridge present (1).

141. Anterior two dentary teeth lack denticles, first tooth strongly reduced absent (0), present (1).

142. Number of cervical vertebrae less than 10 (0), 10 or more (1).

143. Shape of cervical vertebrae plateocoelous or amphicoelous (0), opisthocoelous (1).

144. Ventral surface of the cervical vertebrae rounded (0), presence of a broad, flattened keel (1), presence of a sharp ventral keel (2).

145. Length of the anterior cervical centra less than 1.5 times longer than tall (0), equal or greater than 1.5 times longer than tall (1).

146. Epipophyses on anterior cervical three present (0), absent (1).

147. Position of neural spine on dorsal centrum Neural spines arise anteriorly or centered over centrum (0), posteriorly positioned on centrum (1).

148. Number of dorsal vertebrae 14 or less (0), 15 (1), 16 (2), 17 or more (3).

149. Number of sacral vertebrae 3 or fewer (0), 4-5 (1), 6 (2), 7 or more (3).

150. Height of sacral spines less than twice the height of the centra (0), 2-2.5 times the height of the centra (1), greater than 2.5 times the height of the centra (2).

151. Direction of sacral neural spines lean posteriorly (0), lean anteriorly (1).

152. Height of neural spine on proximal caudal vertebrae less than 1.5 times taller than height of centrum (0), greater than 1.5 times taller than height of centrum (1).

153. Position of caudal neural spines spine entirely over centrum (0), spine extends beyond own centrum (1).

154. Position of caudal ribs caudal ribs entirely on centrum (0), caudal ribs from neurocentral suture (1), caudal ribs from neural arch (2).

155. Placement of longest rib on caudal vertebrae first caudal vertebra bears the longest rib (0), longest rib posterior to first (1).

156. Axial epiphyses (at least vestigially) present (0), absent (1).

157. Transition from tuberculum and capitulum of dorsal ribs from vertical to near horizontal occurs between dorsal vertebrae 2-4 (0), occurs between dorsal vertebrae 5-6 (1), occurs between dorsal vertebrae 6-8 (2).

158. Presence of partial ossification of the sternal segments of the cranial dorsal ribs absent (0), present (1).

159. Presence of a sharp scapular spine on the anterodorsal corner of the scapula spine low or broad (0), spine sharp and pronounced (1).

160. Thickness of scapular neck minimum width of neck less than 20% maximum length (0), minimum width of neck greater than 20% maximum length (1).

161. Ratio of coracoid width to length width less than 60% the length (0), 61-100% (1), width greater than the length of the coracoid (2).

162. Position of coracoid foramen: Foramen enclosed within the coracoid (0), open along coracoid-scapula articular contact surface (1).

163. Ratio of length of sternal process of the coracoid to the base of the coracoid notch versus the width of its base at the same point: less than 70% (0), greater than 70% (1).

164. Ovoid fossa positioned anteroventral to the glenoid fossa on the coracoid absent (0), present (1).

165. Shape of sternals: crescent shaped (0), hatchet Shaped (1), expanded along anterior and posterior ends and constricted in the middle (2).

166. Length of humerus compared to length of scapula: humerus longer than or subequal to scapula (0), scapula longer than humerus (1).

167. Ratio of forelimb length to hind limb length (head of the humerus to tip of the manus versus head of the femur to tip of the pes: forelimb longer than 40% the length of the hind limb (0), forelimb equal to or less than 40% the length of the hind limb (1).

168. Shape of the humerus: straight (0), at least a modest caudal flexure at the level of the deltopectoral crest (1).

169. Shape of the deltapectoral crest in lateral view: rounded (0), angular and inconspicuous (1).

170. Height of olecranon process: low (0), moderate to high (1).

171. 'Cross-sectional shape of the ulna at midshaft triangular or oval (0), cylindrical (1).

172. Shape of the shaft of the ulna straight (0), bowed (1).

173. Ratio of minimal radial width to length of radius less than 10% (0), greater than 10% (1).

174. Fusion of the carpus: unfused (0), fused (1).

175. Metacarpal I length relative to metacarpal II greater than 50% (0), less than 50% (1).

176. Orientation of manual digit I compared to digit III less than 25 degrees (0), 25 to 60 degrees (1), greater than 60 degrees (2).

177. Shape of ungual of manual digit I clawlike (0), subconical (1), absent (2).

178. 'First phalanx of manual digits II-IV', less than twice the size of second phalanx (0), greater than twice the size of second phalanx (1).

179. Shape of unguals on manual digits II and III claw-shaped (longer than wide) (0), hoof-shaped (wider than long) (1).

180. Number of phalanges on manual digit III 4 (0), 3 (1).

181. Number of phalanges on manual digit IV 3 (0), 2 (1), 1 (2).

182. Number of phalanges on digit V two (0), one (1), zero (2).

183. Ilium acetabulum shape: high to normal acetabulum (0), short to long acetabulum (1).

184. Ventral acetabular flange present (0), absent (1).

185. 'Development of supra-acetabular rim on the ilium weak or absent (0), strong (1).

186. Shape of the dorsal margin of the ilium in lateral view straight to slightly convex (0), sinuous (1).

187. Orientation of the external surface of the preacetabular process laterally facing and roughly in the same plane of the iliac body (0), twisted about the long axis (1).

188. Length of preacetabular process: anterior tip posterior to distal end of the pubic peduncle (0), anterior tip anterior to distal end of the pubic peduncle (1).

189. Ratio of length of the postacetabular process versus the total ilium length 40-21%' (0), less than 20% (1), greater than 40% (2).

190. Presence of a vertical brevis shelf on the ilium present (0), absent or horizontal (1).

191. Articulation of the ischiac peduncle of the ilium with a sacral rib absent (0), present (1).

192. Lateral swelling of the ischiadic peduncle of the ilium absent (0), present (1).

193. Size of the pubic peduncle of the ilium more robust than the ischial peduncle, expands in lateral view (0), smaller than the ischial peduncle, tapers distally (1).

194. Pubis articulates with sacrals: pubis not secondarily supported (0), pubis supported only by sacral rib (1), pubis supported directly by sacral centrum (2).

195. Orientation of pubis: anteroventrally facing (0), vertically oriented (1), posteroventrally rotated (2).

196. Anterior process of the pubis present and straight (0), present and dorsally curved (1), absent (2).

197. Angle between prepubic process and pubic shaft greater than 150 degrees (0), less than 100 degrees (1).

198. Shape of prepubic process short, peg-shaped (0), mediolaterally flattened (1), rod-shaped (2), dorsoventrally flattened (3).

199. Ratio of the length of prepubic process (from obturator notch) versus length of ilium' less than 20% (0), greater than 20% (1).

200. Proximal articulation surfaces of the ischium iliac and pubic peduncles continuous, but separated by a fossa (0), iliac and pubic peduncles separated by a concave surface (1).

201. Size of iliac peduncle of ischium compared to the pubic peduncle: pubic peduncle larger (0), subequal or iliac peduncle larger (1).

202. Shape of dorsal margin of ischial shaft at mid-length in lateral view: straight (0), caudodorsally convex (1), caudodorsally concave (2).

203. Presence of a groove on the dorsal edge of the ischium absent (0), present (1).

204. Presence of a tab-shaped obturator process: absent (0), present (1).

205. Position of the obturator process on the ischium proximal 40% (0), distal 60% (1).

206. Shape of ischial shaft flat and blade-like (0), ovoid to subcylindrical (1).

207. Extent of ischial symphysis along at least 50% of the ischial shaft (0), only present distally (1).

208. Presence of an enlarged "foot" on the distal end of the ischial shaft absent (0), present (1).

209. Ratio of minimum diameter of the femur to total femur length less than 15% (0), greater than 15% (1).

210. Shape of femoral shaft in anterior view straight (0), distinctly bowed (1).

211. Angle between the neck of the femoral head and the femoral shaft less than or equal to 100 degrees (0), greater than 100 degrees (1).

212. 'Presence of a neck-like constriction under the head of the femur absent (0), present (1).

213. 'Presence of a "trench" between the greater trochanter and the head of the femur: absent (0), present femoral head and greater trochanter distinct (1).

214. Shape of the lateral surface of the greater trochanter of femur convex (0), flattened (1).

215. Presence of an intertrochanteric notch between the lesser and greater trochanters on the femur: present (0),absent (1).

216. Dorsal extent of the lesser trochanter of femur lower than or equal to the height of the greater trochanter (0), higher than the height of the greater trochanter (1).

217. Location of the lesser trochanter anterior and medial to greater trochanter (0), anterior and somewhat lateral to greater trochanter (1).

218. Presence and shape of lesser trochanter prominent crest (0), wide, similar in width to the greater trochanter, and separated from it by a wide cleft (1), narrow, closely appressed to the expanded greater trochanter (2).

219. Height of lesser trochanter relative to the head of the femur significantly lower (0), approximately the same height (1).

220. Shape of the fourth trochanter of the femur 'Mound-like' (0), sharp ridge, pendant subtriangular (1), vestigial (rugosity or scar) (2).

221. Location of insertion scar of *M. caudifemoralis longus* on femur extends from fourth trochanter onto medial surface of femoral shaft (0), widely separated from fourth trochanter, restricted to medial surface of femoral shaft (1).

222. Position of the fourth trochanter entirely on the proximal half of the femur (0), midshaft or more distally placed (1)

223. Anterior intercondylar groove on the distal femur absent (0), present (1).

224. Shape of anterior intercondylar groove broad, shallow ""V""-shaped, edges of groove meet at greater than 90 degrees to one another (0), tight, deep ""V""-shaped, edges of groove meet at less than 90 degrees (1), deep, narrow, ""U""-shaped with partial enclosure by slight expansion of medial condyle (2), "U""-shaped groove partially enclosed by expansions of both medial and lateral condyles, canal fully enclosed by fusion of lateral and medial condyles (3).

225. Posterior intercondylar groove on the femur fully open (0), medial condyle inflated and at least partially covering (1).

226. Length of posterior intercondylar groove less than 1/4 length of femur (0), greater than 1/4 length of femur (1).

227. Ratio of femur to tibia length: femur shorter than or equal to tibial length (0), femur longer (1).

228. 'Cross-sectional shape of tibia' triangular (0), rounded (1).

229. Size of the lateral proximal condyles on the tibia: equal in size (0), fibular condyle smaller (1), only one condyle present (2), fibular condyle larger (3).

230. Lateral extension of the tibial posterior flange does not reach fibula (0), extends posterior to medial margin of fibula (1), extends posterior to entire distal end of fibula and calcaneum (2), absent (3).

231. Cnemial crest of tibia present and straight (0), present and arcs anterolaterally (1).

232. Shape of cnemial crest of tibia rounded (0), sharply defined (1).

233. Ratio of the size of lateral distal condyle on the femur versus that of the medial distal condyle subequal (0), 80-60% (1), 59-50% (2), 49-40% (3), 39-30% (4), 29-20% (5).

234. 'Cross-sectional shape of the fibular shaft' elliptical or rounded (0), D-shaped throughout its length (1).

235. Size and shape of astragalus ascending process short (0), triangular and tooth-like (1), spike-like (2), relatively large (3).

236. Height of posterior side of astragalus low (0), high (1).

237. Height of anterior side of astragalus high (0), moderate (1), low (2).

238. Astragalus articular surface for fibula more than 30% of proximal surface (0), less than 30% of proximal surface (1).

239. Angle between the tibial and fibula articular facets on the calcaneum greater than 120 degrees (0), less than 120 degrees (1).

240. Number of distal tarsals 3 or more (0), 2 or less (1).

241. Shape of medial distal tarsal in dorsal view blocky (0), thin and rectangular (1), round (2).

242. Placement of the medial distal tarsal articulation does not cover any part of metatarsal II (0), over at least part of metatarsal II (1).

243. Lateral distal tarsal shape square (0), kidney shaped (1).

244. Presence of metatarsal I : present (0), absent (1).

245. Presence of metatarsal V: present (0), absent (1).

246. Metatarsal V size compared to metatarsal III less than 25% (0), 25%-50% (1), greater than 50% (2).

247. Diameter of the midshafts of metatarsals I and V subequal to or greater than metatarsals II-IV (0), less than metatarsals II-IV (1).

248. Number of functional digits in the pes four (0), three (1).

249. Presence of phalanges in pedal digit I present (0), absent (1).

250. 'Shape of unguals on pedal digits II-IV: claw-shaped (longer than wide) (0), hoof-shaped (Aproximately as wide as long) (1).

251. Presence of ossified hypaxial tendons down the tail: absent (0), present (1).

252. Presence of epaxial ossified tendons: absent(0), present (1).

253. Arrangement of epaxial tendons longitudinally arranged into a single layer (0), double-layered lattice (1).

254. Presence of postcranial osteoderms absent (0), present (1).

255. Presence of dermal sculpturing of the skull and/or mandible, absent (0), present (1).

APPENDIX B

CHARACTERS MATRIX USED IN PHYLOGENETIC ANALYIS, BASED ON PRELIMINARY CHARACTERS OF BOYD (2015), WITH NEW DATA FOR *ORYCTODROMEUS* ADDED. A POLYMORPHIC STATE INDICATED BY A (0, 1)

Taxon	10	20	30
Marasuchus	?????????? ?????????? ??????????		
Silesaurus	?00000000- 00?1?1?000 -?00--??0?		
Asilisaurus	??0??????? ????????0? ??????????		
Sanjuansaurus	?????????? ????????00 -00?????0?		
Herrerasaurus	100000000- 00010?0000 -000--0002		
Tawa	10000000?? 000???0000 -000--0002		
Pisanosaurus	?????????? ????????01 1?????????		
Heterodontosaurus	0?10001111 0001?01001 1001010001		
Fruitadens	?????0?111 ????0??011 1?????????		
Echinodon	??1??0???? ???????001 1?????????		
Lycorhinus	????????11 ???????001 1?0???????		
Tianyulong	0?10001111 ?001010??1 ???????0?2		
Abrictosaurus	??10?01111 00?1????01 100101????		
Eocursor	?????????? ?????????1 ??????????		
Lesothosaurus	0?10??0110 1?110??011 01010?0001		
Scutellosaurus	??1000??10 ?0??????11 0??????0??		
Scelidosaurus	??1???0?0? ?0?1????11 10????????		
Emausaurus	??1???0?0? 0??1????11 10????????		
Stormbergia	?????????? ?????????? ??????????		
Agilisaurus	001001010- ?0?1?100?1 1002001110		
Hexinlusaurus	0?1??????? ??????0??1 1??1011001		
Yandusaurus	??1??????? ?????????1 1?????????		
Leaellynasaura	?????????? ?????????1 1??????0??		
Jeholosaurus	0?10000110 1011?11011 1011001002		
Yueosaurus	?????????? ?????????? ??????????		
Othnielosaurus	?????????? ?????????? ???????0??		
New *Parksosaurus*	????????10 ???1??0?11 10?????00?		
T. neglectus	1110010110 1011110011 1012001002		
T. assiniboiensis	?????????? ?????????? ????0?????		
T. garbanii	?????????? ?????????? ??????????		
Talenkauen	??1001?110 ?0???100?1 1?0???????		
Notohypsilophodon	?????????? ?????????? ??????????		
Macrogryphosaurus	?????????? ?????????? ??????????		
Haya	0010000110 1001110?11 101200100?		
Changchunsaurus	0110010110 10111?0011 1?1?0??00?		
Oryctodromeus	?11001?1?? 10111??01? ???????0??		
Zephyrosaurus	?110?0?110 101?11?011 111101?10?		
Orodromeus	0010011110 ?0011?0011 1?11011002		
Kaiparowits Taxon	??1??????? ?????????? ??????????		
Koreanosaurus	?????????? ?????????? ??????????		

Taxon	10	20	30
Archaeoceratops	0011000110	0101000?11	1001010002
Lioceratops	0?11000110	01010?1?11	100???0002
Yinlong	0011?00110	01?1001?11	1001011002
Stenopelix	??????????	??????????	??????????
Micropachycephalosaurus	??????????	??????????	??????????
Wannanosaurus	??????????	??????????	???21??0??
Hypsilophodon	0010001110	1011010011	1011010011
Atlascoposaurus	??????????	?????????1	1?????????
Qantassaurus	??????????	??????????	??????????
Anabisetia	??????????	????????11	1?0???????
Gasparinisaura	0?1???????	?????????1	10?100?011
Zalmoxes r.	1010001--0	1011?0?011	10????0002
Zalmoxes s.	??1???????	??????????	??????0002
Tenontosaurus d.	1?1001?110	?0?1??11?1	1?010?????
Tenontosaurus	1???0?????	?????1?0??	??0???0011
Rhabdodon p.	??????????	????0??0??	??????????
Muttaburrasaurus	??????????	?0?1??0??1	10?10?001?
Elrhazosaurus	??????????	??????????	??????????
Dysalotosaurus	0010010---	00?1001111	1001010011
Dryosaurus	0010010---	00?1001111	1001000001
Callovosaurus	??????????	??????????	??????????
Valdosaurus	??????????	??????????	??????????
Camptosaurus	1?101?????	????00?1??	??????0011
Iguanodon 1	1?101?????	????0??1??	???????012
Ouranosaurus	1?10??????	????0??1??	???????012

Taxon	40	50	60
Marasuchus	?????????? ?????????? ??????????		
Silesaurus	??0?1??00? ?????101?? ??100??00?		
Asilisaurus	??0??????? ??????02?? ??????????		
Sanjuansaurus	?????????? ?????????? ??????????		
Herrerasaurus	0?0101000? ?0100102?? 0??1000001		
Tawa	000000000? ?00000???? ???00?1000		
Pisanosaurus	?????????? ?????????? ??????????		
Heterodontosaurus	000000003? ?000000000 ?0?00?0100		
Fruitadens	?????????? ?????????? ??????????		
Echinodon	?????????? ?????????? ??????????		
Lycorhinus	?????????? ?????????? ??????????		
Tianyulong	0?0???000? ?????????? ??????????		
Abrictosaurus	0?0??????? ?????????? ??????????		
Eocursor	?????????? ?????????? ????????0?		
Lesothosaurus	0?0?000??? ?000?0000? ?0000?0000		
Scutellosaurus	?0110??00? ??1??00?00 1?000?0000		
Scelidosaurus	0?1??????? ?0???????? ???????00?		
Emausaurus	0?1??????? ?0???????? ????????0?		
Stormbergia	?????????? ?????????? ??????????		
Agilisaurus	11?010000? ?0100100?? 10??0?0000		
Hexinlusaurus	100?0?0?0? ?01??000?? ??????0101		
Yandusaurus	?????????? ?????000?? ???00?????		
Leaellynasaura	10001?000? ?????000?0 ???00?????		
Jeholosaurus	110010001? ?110000000 1010010101		
Yueosaurus	?????????? ?????????? ??????????		
Othnielosaurus	????1????? ?????????? ?????????0		
New *Parksosaurus*	?101100?0? ?1?0??00?? ?1??01????		
T. neglectus	110001000? 0A10000000 1111010101		
T. assiniboiensis	?????????? ?????????? ????????01		
T. garbanii	?????????? ?????????? ??????????		
Talenkauen	?????????? ?????????? ??????????		
Notohypsilophodon	?????????? ?????????? ??????????		
Macrogryphosaurus	?????????? ?????????? ??????????		
Haya	1?0010000? ?1100000?? ?1??0?0101		
Changchunsaurus	??001?002? ?0101??0?? 1???000?00		
Oryctodromeus	??0?1???10 0????00000 101001?101		
Zephyrosaurus	110?1?0030 0???000000 0010011101		
Orodromeus	10011?0030 0A10?00000 ?011011101		
Kaiparowits Taxon	?2??1???3? ?????????? ???????1??		
Koreanosaurus	?????????? ?????????? ??????????		
Archaeoceratops	010100001? ?0111000?0 10010?0?10		
Lioceratops	?10100002? ?011000000 00000?0110		

Taxon	40	50	60
Yinlong	010100001? ?010111?0 00?00?0?10		
Stenopelix	?????????? ?????????? ??????????		
Micropachycephalosaurus	???????0?? ??????00?? ??0???????		
Wannanosaurus	?10?0???1? 0????????? ??????0?10		
Hypsilophodon	100110000? ?110000000 10000?0000		
Atlascoposaurus	?????????? ?????????? ??????????		
Qantassaurus	?????????? ?????????? ??????????		
Anabisetia	?????????? ?????????? ??????????		
Gasparinisaura	1?0010010? ?010000011 10????0000		
Zalmoxes r.	1?0?01?10? ?011000111 10010?0100		
Zalmoxes s.	1?00010?0? ?????0??11 ??011?0?00		
Tenontosaurus d.	100001000? ?010000?1?1 ?0??1?010?		
Tenontosaurus	10??1100?? ?1???0??0? ?00?1001??		
Rhabdodon p.	?????????? ?????0???? ?000?0????		
Muttaburrasaurus	100000110? ?0?0??01?? ?1??0???0?		
Elrhazosaurus	?????????? ?????????? ??????????		
Dysalotosaurus	0100001101 000010011? 0101010100		
Dryosaurus	0100001101 000010010? 0101000100		
Callovosaurus	?????????? ?????????? ??????????		
Valdosaurus	?????????? ?????????? ??????????		
Camptosaurus	11??101??0 10???0??0? ?1011011?0		
Iguanodon 1	1???100??2 10???1??1? ?1011001?0		
Ouranosaurus	0???1?0??2 10???1??1? ?1001?0??0		

Taxon	70	80	90
Marasuchus	?????????? ?????????? ??????????		
Silesaurus	???00111-- ---?40??00 000?0??100		
Asilisaurus	?????????? ????4????? ??????????		
Sanjuansaurus	?????????? ?????????? ??????????		
Herrerasaurus	00000??2-- ---010?000 0000010?01		
Tawa	00??????-- ---010?000 00000???10		
Pisanosaurus	?????????? ???????001 1?10000???		
Heterodontosaurus	00?000110? 0100?00101 1010000000		
Fruitadens	?????????? ???0?0??0? ?0????????		
Echinodon	?????????? ?1?000?101 10????????		
Lycorhinus	?????????? ?????????? ??????????		
Tianyulong	????????1? 0???01?101 10110??200		
Abrictosaurus	?????????1 01-0?0??01 101?0?????		
Eocursor	?????????? ???0???000 101000????		
Lesothosaurus	00000010?? ?0010?0000 1??00010??		
Scutellosaurus	00?00?1??? ????000000 10????11?0		
Scelidosaurus	?????????? ???1????10 1?????11??		
Emausaurus	?????????? ?0?1????10 1?????11??		
Stormbergia	?????????? ?????????? ??????????		
Agilisaurus	000000011?? ?001?0?101 1011000100		
Hexinlusaurus	?0?0001??? ???1201001 1?????????		
Yandusaurus	?????????? ?????????? ??????????		
Leaellynasaura	???00?1??? ?????????? ??????????		
Jeholosaurus	0000001110 0001201001 1111010000		
Yueosaurus	?????????? ?????????? ??????????		
Othnielosaurus	00??00???? ??0?1?10?1 1?????????		
New *Parksosaurus*	?0???????? ??????0?01 101?0?????		
T. neglectus	10?1011100 0011201101 1111012?00		
T. assiniboiensis	0001011??? ?????????? ??????????		
T. garbanii	?????????? ?????????? ??????????		
Talenkauen	????????10 0011?0?1?1 1?????????		
Notohypsilophodon	?????????? ?????????? ??????????		
Macrogryphosaurus	?????????? ?????????? ??????????		
Haya	10?0011000 0011111101 1?1?00??00		
Changchunsaurus	00??????10 001111?101 1110012000		
Oryctodromeus	?00??0???0 00?1??1??1 1????1????		
Zephyrosaurus	100001???? ?????0???1 1???0??1??		
Orodromeus	101000???? ???1211101 10100102?0		
Kaiparowits Taxon	??000????? ???1?????1 1?????????		
Koreanosaurus	?????????? ?????????? ??????????		
Archaeoceratops	10?0010111 00110?1101 1110000200		
Lioceratops	10?0000110 0011011101 10100?0?00		

Taxon	70	80	90
Yinlong	?0?0000110 0011001101 101001??00		
Stenopelix	?????????? ?????????? ??????????		
Micropachycephalosaurus	?????????? ?????????? ????????2??		
Wannanosaurus	?0?10????? ?????0??01 101?000???		
Hypsilophodon	0000001111 0001201101 1011010000		
Atlascoposaurus	?????????? ?????1???1 1?????????		
Qantassaurus	?????????? ???1201101 10????????		
Anabisetia	?????????? ?????1???1 1?????????		
Gasparinisaura	00?0?0???? ???120?101 1?100100??		
Zalmoxes r.	1100110211 001101?101 1111012201		
Zalmoxes s.	?10?111??1 ???1010101 111?01?2??		
Tenontosaurus d.	?10?01??11 1?0121?101 111?01??01		
Tenontosaurus	??1001?1?0 1????101?? ?1?0?12?11		
Rhabdodon p.	?????????? ?????111?1 11??110???		
Muttaburrasaurus	???1?10??? ?????????1 1????1????		
Elrhazosaurus	?????????? ?????????? ??????????		
Dysalotosaurus	???000?111 1011101101 1110110?11		
Dryosaurus	??1000?111 1011211101 1110100?11		
Callovosaurus	?????????? ?????????? ??????????		
Valdosaurus	?????????? ?????????? ??????????		
Camptosaurus	011101?2?0 1?1??111?? ?1?111??11		
Iguanodon 1	?11111?2?0 1?1??110?? ?1?211???1		
Ouranosaurus	011111?2?? ??0???10?? ???111????		

Taxon	100	110	120
Marasuchus	0????????? ?????????? 0?????????		
Silesaurus	0???0?0000 ??0??000?2 001001?0-0		
Asilisaurus	?????????? ?????????? ????0???-?		
Sanjuansaurus	??0??????? ?????????? ?????-?0-?		
Herrerasaurus	00010000?? 0?0010???? ?0100-10-?		
Tawa	0?0100000? ??0??????? ?0200-10-?		
Pisanosaurus	?????????? ?????????? ???????1??		
Heterodontosaurus	010000000? 00?100?0?2 002110120?		
Fruitadens	?????????? ?????????? ?0210?01??		
Echinodon	?????????? ?????????? ?020??11-?		
Lycorhinus	??00?????? ?????????? ???1?-?1??		
Tianyulong	???000?0?? ?????????? ?0211?11??		
Abrictosaurus	00?????0?? ?????????? ?0200-11??		
Eocursor	???????0?? ?1???????? ???0??????		
Lesothosaurus	00???000?? 01?1000?01 00000-0110		
Scutellosaurus	??????0??? 0????????? ?00000010?		
Scelidosaurus	?0???????? ?????????? ??????0???		
Emausaurus	?0???????? ?????????? ??????0???		
Stormbergia	?????????? ?????????? ??????????		
Agilisaurus	01000001?? 000??1???? ?01000010?		
Hexinlusaurus	0?00?00??? ?????????? ????0-?1-?		
Yandusaurus	??00?????? ?????????? ?????-?1-?		
Leaellynasaura	?????????? ?????????? ???????1??		
Jeholosaurus	01000001?? 0?0101?1?0 00001-010?		
Yueosaurus	?????????? ?????????? ??????????		
Othnielosaurus	?????????1 0????00?1? ????1-??00		
New *Parksosaurus*	01011001?0 0?????1??? 0???1??10?		
T. neglectus	0101000110 0?10111100 10001-0100		
T. assiniboiensis	?????????1 0010111100 0?????????		
T. garbanii	?????????? ?????????? ??????????		
Talenkauen	?????????? ?????????? ?0?01??1??		
Notohypsilophodon	?????????? ?????????? ??????????		
Macrogryphosaurus	?????????? ?????????? ??????????		
Haya	0?110001?? 000101???? ?0101-010?		
Changchunsaurus	0?0??001?? 0????1???1 ?0100-010?		
Oryctodromeus	?????00??0 010??11?1? ?0100???00		
Zephyrosaurus	?0???00?11 00?1011112 001???0100		
Orodromeus	0100000110 0101011111 ?010??0100		
Kaiparowits Taxon	??????0??? ????0????? ???00??100		
Koreanosaurus	?????????? ?????????? ??????????		
Archaeoceratops	000?00010? ??0??1???? ?0201?01??		
Lioceratops	0????0010? 0?0101???? 10201?01??		

Taxon	100	110	120
Yinlong	01011000?? 0??101???2 1020?001??		
Stenopelix	?????????? ?????????? ??????????		
Micropachycephalosaurus	?????????? ?????????? ??????????		
Wannanosaurus	??????01?? ?????????? ????0???1?		
Hypsilophodon	011000111? 0001011001 00001-0200		
Atlascoposaurus	?????????? ?????????? ???????201		
Qantassaurus	?????????? ?????????? ????????0?		
Anabisetia	?????????? 0????0???? ????1-?1-?		
Gasparinisaura	0101?001?? 010100??2? 0??0???1??		
Zalmoxes r.	??01?101?? 000200??1? 01-011-201		
Zalmoxes s.	?????10??? 0?0200???? ???01-??0?		
Tenontosaurus d.	010111010? 01???1???? 00201???01		
Tenontosaurus	???1?11?0? 012??10020 ?1?01???01		
Rhabdodon p.	?????????0 ?????100?? ????????0?		
Muttaburrasaurus	1?0????1?? 0?0??1???? ????1??10?		
Elrhazosaurus	?????????? ?????????? ??????????		
Dysalotosaurus	0101100100 00?1111022 11-0??-21?		
Dryosaurus	0101100100 00?1110020 11-011-211		
Callovosaurus	?????????? ?????????? ??????????		
Valdosaurus	?????????? ?????????? ??????????		
Camptosaurus	???1?00?01 10???00120 01?0????11		
Iguanodon 1	?????0???1 112??00022 0??0????11		
Ouranosaurus	?????????1 112??00002 ???0????1?		

Taxon	130	140	150
Marasuchus	?????????? ?????????? ????1?0?0?		
Silesaurus	001?-3?0-1 0030003?-- -002100210		
Asilisaurus	????-3???? 0??0003?-- -???100?00		
Sanjuansaurus	10?0?2?001 ?04?0????? -00??0?000		
Herrerasaurus	10?0-21001 00410?21-- -00?10000?		
Tawa	10?0-20001 00410?2?-- -???10??0?		
Pisanosaurus	0??????10? ?100???1?0 0?????0???		
Heterodontosaurus	11?1100111 01?11000?1 10?100002?		
Fruitadens	0??0-0?000 11?0??0?00 ??0??????2?		
Echinodon	0??0?0?000 11200?0??0 ??????????		
Lycorhinus	00???0?000 ?13?1????? ??????????		
Tianyulong	0????0?000 11????0??0 ??????????		
Abrictosaurus	0??1?00000 113?1?01?0 1???????1?		
Eocursor	???0?????? 1??0000?00 ????????1?		
Lesothosaurus	00000010?0 10??000?0? 0????0????		
Scutellosaurus	0000-0?000 1020000200 00011?011?		
Scelidosaurus	???0?????? ????0????? 0????0????		
Emausaurus	???0?????? ????0????? 0?????????		
Stormbergia	?????????? ?????????? ??0??0????		
Agilisaurus	00?0???100 11300?0200 001??1?11?		
Hexinlusaurus	00?000?100 11300?0200 ?00101011?		
Yandusaurus	00?0001100 ?13?0????0 ??0???????		
Leaellynasaura	?11??0?100 ?13?0????? ??????????		
Jeholosaurus	1????01100 11200?0100 00010?1120		
Yueosaurus	?????????? ?????????? ?0010?????		
Othnielosaurus	00?000?100 1?200001?0 ?0010??120		
New *Parksosaurus*	0???00?10? 11?0?10?00 ??0?1?0???		
T. neglectus	0010002100 1120002?1 000111?3?		
T. assiniboiensis	?????????? ?1???????? ??0???????		
T. garbanii	?????????? ?????????? ??????????		
Talenkauen	?????0?11? ?1???????1 ?00?10?2??		
Notohypsilophodon	?????????? ?????????? ??01?????0		
Macrogryphosaurus	?????????? ?????????? ?10?10102?		
Haya	?020?01100 11?00?01?1 000?0???2?		
Changchunsaurus	01?0?0?100 11200?0?01 ?0010??1??		
Oryctodromeus	00??????0? 11?00?0?01 ??021?1131		
Zephyrosaurus	0010001100 ?12?00???? ??020?0???		
Orodromeus	000000???0 112?000??? ?002010130		
Kaiparowits Taxon	000??0?0?0 11?0000?01 ??021?????		
Koreanosaurus	?????????? ?????????? ??021?0??0		
Archaeoceratops	11?1?0??10 1141??0??1 0???0???2?		
Lioceratops	1??110?100 11?00?01?1 0?????????		

Taxon	130	140	150
Yinlong	00???010?0 ?12?0????? ??????????		
Stenopelix	?????????? ?????????? ????????2?		
Micropachycephalosaurus	?????????? ????0????? ??????????		
Wannanosaurus	?????????? 0??00?00?0 ??0?0?????		
Hypsilophodon	1111100100 1100010101 0001010120		
Atlascoposaurus	111?00?111 ?1?0010?11 ??????????		
Qantassaurus	????0????? 0?40010001 0?????????		
Anabisetia	1??1?0??11 ?1??0????0 ??????????		
Gasparinisaura	11?1?00111 ?10?0?000? 0??1????21		
Zalmoxes r.	111111?100 0110011011 ??010?0?32		
Zalmoxes s.	11111????? 0110011011 0?0?0?0?32		
Tenontosaurus d.	11111?0001 ?11?011001 011?0?1121		
Tenontosaurus	11111??001 ?11?011001 011?0?1121		
Rhabdodon p.	11111??101 ?11?01??11 ??0???1??1		
Muttaburrasaurus	11???0?11? ?1??0????1 ?011??1?2?		
Elrhazosaurus	?????????? ?????????? ??????????		
Dysalotosaurus	???11?1111 011?011001 0011??112?		
Dryosaurus	111111?111 011?011101 0?111?1?21		
Callovosaurus	?????????? ?????????? ??????????		
Valdosaurus	?????????? ?????????? ??121?????		
Camptosaurus	11111??011 ?11??1?100 ??0???1??2		
Iguanodon 1	11111??011 ?11??1?200 ??1???1??2		
Ouranosaurus	????1????? ?1???1???? ??????1???		

Taxon	160	170	180
Marasuchus	????1????0	?????0????	??????????
Silesaurus	01??????00	00???0?020	?00???????
Asilisaurus	?00?????00	00????0???	??????????
Sanjuansaurus	????????00	001??????2	??????????
Herrerasaurus	??0?????00	?0????0??2	?0000?0000
Tawa	????????00	?0?????01?	???00?0?01
Pisanosaurus	??????????	??????????	??????????
Heterodontosaurus	?000010000	1????00012	0000000000
Fruitadens	??????????	??????????	??????????
Echinodon	??????????	??????????	??????????
Lycorhinus	??????????	??????????	??????????
Tianyulong	??????????	???????102	??????????
Abrictosaurus	??????????	?????0000?	???????0??
Eocursor	????????00	?????0?00?	???????0??
Lesothosaurus	??0??1????	10????1??0	00?00?0???
Scutellosaurus	?0??????0?	1000??0000	??00???00?
Scelidosaurus	?????0?0??	??????0???	??????????
Emausaurus	??????????	??????????	??????????
Stormbergia	?00??1??00	1000??1??1	??1???????
Agilisaurus	?0?1?1?000	1000?01100	?0000??000
Hexinlusaurus	?002????00	10???0?100	0?000?0000
Yandusaurus	????????01	000??0?1??	??????????
Leaellynasaura	??????????	??????????	??????????
Jeholosaurus	0001????00	??0??01000	0000??????
Yueosaurus	??0?????00	?????0?002	??????????
Othnielosaurus	??11???100	100??0?100	?0?00?00??
New *Parksosaurus*	?001???100	?00000???1	?00???????
T. neglectus	0111??0100	?0??200100	00000?0000
T. assiniboiensis	??1????2??	??????????	??????????
T. garbanii	??????????	??????????	??????????
Talenkauen	??????????	?????0??2?	??????????
Notohypsilophodon	0???????0?	?0?????120	??????????
Macrogryphosaurus	0??????1??	????????2?	??????????
Haya	?0111??000	101000?001	????0?????
Changchunsaurus	???????000	?0?00??10?	??????????
Oryctodromeus	01121?2?10	1001?00101	000???????
Zephyrosaurus	??11??0?1?	100???????	0?????????
Orodromeus	00010?0?10	1000???111	1000???000
Kaiparowits Taxon	????????1?	?0?1???111	???0000000
Koreanosaurus	???????011	101000?101	0?????????
Archaeoceratops	0011??????	??????????	??????????
Lioceratops	??????????	??????????	??????????

Taxon	160	170	180
Yinlong	?????????? ?????????? ??????????		
Stenopelix	?????????0 ?????????? ??????????		
Micropachycephalosaurus	0????????? ?????????? ??????????		
Wannanosaurus	?????????? ???????10? ??????????		
Hypsilophodon	0011110100 1100000101 0100000000		
Atlascoposaurus	?????????? ?????????? ??????????		
Qantassaurus	?????????? ?????????? ??????????		
Anabisetia	????????00 100??0?02? ??0???????		
Gasparinisaura	0?1101??0? 100?????10 ?00???????		
Zalmoxes r.	0101????00 ?0?????110 ?1????????		
Zalmoxes s.	?1??????00 0010???110 ?1????????		
Tenontosaurus d.	011????000 100001?110 0100???10?		
Tenontosaurus	01110?1000 100001?110 0100000101		
Rhabdodon p.	0111????0? 000????101 01????????		
Muttaburrasaurus	????????00 ?0?????0?1 0100??????		
Elrhazosaurus	?????????? ?????????? ??????????		
Dysalotosaurus	0112??00? 010?0???11 010????10?		
Dryosaurus	01120?100? 01?????011 000?0??10?		
Callovosaurus	?????????? ?????????? ??????????		
Valdosaurus	?????????? ?????????? ??????????		
Camptosaurus	11111?000? 110????011 01111??101		
Iguanodon 1	11111?200? 210?????12 10111??111		
Ouranosaurus	??????2?0? 21???????2 10?1??????		

Taxon	190	200	210
Marasuchus	??0001002- ?00?02---0 12?0-0?00?		
Silesaurus	??0000002? 000002---0 1000-01001		
Asilisaurus	??00000??? ????02---0 ???0-0110?		
Sanjuansaurus	???11????? ????02---??????????		
Herrerasaurus	220110002? 000002---1 00?0-10000		
Tawa	1?0010?02? ??0?02---1 1????1??00		
Pisanosaurus	???0?????? ?0????????1 1?????0???		
Heterodontosaurus	0001100101 ?00?200001 0000-01100		
Fruitadens	?????????? ?????????? ????????0?		
Echinodon	?????????? ?????????? ??????????		
Lycorhinus	?????????? ?????????? ??????????		
Tianyulong	?????????? ????2????? ?010?0?0??		
Abrictosaurus	???1100101 ?00??????? ???0??????		
Eocursor	??01100101 ?00?200001 0010-00?00		
Lesothosaurus	?100000100 000?200001 0010?00000		
Scutellosaurus	0??0100100 ?00?200??1 1?10?00000		
Scelidosaurus	??001??110 ?00?????0? ??00??1???		
Emausaurus	?????????? ?????????? ??????????		
Stormbergia	??00100100 100?20000? ?011001000		
Agilisaurus	??10100100 101?21?211 0011000000		
Hexinlusaurus	??01000101 101?200211 00010??000		
Yandusaurus	?????????? ?????????? ??????????		
Leaellynasaura	?????????? ????2003?1 000100?000		
Jeholosaurus	??01000101 1110200?11 00?1?00001		
Yueosaurus	?????????? ?????????? ?0??????00		
Othnielosaurus	0001000101 1110200211 01?100?000		
New *Parksosaurus*	????001?01 11??2????1 1201101001		
T. neglectus	0001010101 1111200211 0001101001		
T. assiniboiensis	??010?11?1 111?21021? ????????01		
T. garbanii	?????????? ?????????? ??????????		
Talenkauen	??0?01010? ?1??20?1?? ?????1??0?		
Notohypsilophodon	?????????? ?????????? ??????????		
Macrogryphosaurus	??010101?1 111120011? ??0??111??		
Haya	??01000121 ?11220021? ?00100??00		
Changchunsaurus	???1?????? ?????????? ??????????		
Oryctodromeus	??1100012? 1112200211 1?01001000		
Zephyrosaurus	?????001?? ???2?????? ?101?1????		
Orodromeus	0?01000121 11122002?1 000100?000		
Kaiparowits Taxon	1????????? ???2?????? ????????00		
Koreanosaurus	???1?????1 11???????1 1???????00		
Archaeoceratops	??01001101 111?20030? ???0??????		
Lioceratops	?????????? ?????????? ??????????		

Taxon	190	200	210
Yinlong	??01011101 ??1?20030? ????????0?		
Stenopelix	??01000101 ?01?20?3?1 ?110-010??		
Micropachycephalosaurus	???1??01?? ??1??????? ???????000		
Wannanosaurus	???1???1?? ?????????? ????????00		
Hypsilophodon	??01000101 1111201211 0001101000		
Atlascoposaurus	?????????? ?????????? ??????????		
Qantassaurus	?????????? ?????????? ??????????		
Anabisetia	??01010101 ??1?200111 10010??100		
Gasparinisaura	??01010101 1110200211 1?01?01?00		
Zalmoxes r.	??1110110? ?1????????1 1100-11011		
Zalmoxes s.	??1110110? 111?200211 1100-11111		
Tenontosaurus d.	??11010101 ?11?21?111 1101001110		
Tenontosaurus	??11010101 1110201111 1001000010		
Rhabdodon p.	??1??0???? 1??2?????? 10?0?1?111		
Muttaburrasaurus	0?1101?1?1 ?11?2??111 ????????1?		
Elrhazosaurus	?????????? ?????????? ????????00		
Dysalotosaurus	??11010101 1111211111 010101?101		
Dryosaurus	??11010101 1110211111 0A0101?101		
Callovosaurus	?????????? ?????????? ????????00		
Valdosaurus	?????????1 ????2?12?? ?001?11?00		
Camptosaurus	??1?000??? 1??0??1??? 1A?1?1?110		
Iguanodon 1	??1?010??? 1??1?????? 11?1?1?110		
Ouranosaurus	??1??????? ?????????? 1????1?1??		

Taxon	220	230	240
Marasuchus	?000000001	?00-000?23	0-0?0020-0
Silesaurus	?00-000001	?00-011?21	000?0020-?
Asilisaurus	??0?000000	?0??01??21	00??0020-?
Sanjuansaurus	010??????1	?00-001?20	?0??0021-?
Herrerasaurus	0100000001	?00-001120	100?0021-1
Tawa	010??00001	?0???0??21	10??0021-?
Pisanosaurus	??????????	?????????1	10???001??
Heterodontosaurus	0000101212	?00-000??2	100??????0
Fruitadens	??0?101212	?00-00???2	10???0010?
Echinodon	??????????	??????????	??????????
Lycorhinus	??????????	??????????	??????????
Tianyulong	??????????	??1000????	??????????
Abrictosaurus	????0?1112	?00-??0??2	??????????
Eocursor	000?000102	000-000112	1000??????
Lesothosaurus	?000000102	00????0??2	??0?3?0101
Scutellosaurus	0000000102	000-000??2	100?0?????
Scelidosaurus	??0?0?010?	?0????1??2	??????????
Emausaurus	??????????	??????????	??????????
Stormbergia	000000010?	?00-000032	10???001??
Agilisaurus	?100001102	?00-0001?2	??000?????
Hexinlusaurus	1000000102	?00-000122	10100001?1
Yandusaurus	??????????	??0-00????	??1???????
Leaellynasaura	0?0?101202	?0??000??2	10??00010?
Jeholosaurus	0110001212	?00-000132	10?0000111
Yueosaurus	?11??01212	00???????2	??????????
Othnielosaurus	1110001212	?00-00?0?2	101?210111
New *Parksosaurus*	0111101212	01???001?2	10100001??
T. neglectus	0111001212	?110001022	1020000111
T. assiniboiensis	011100121?	0110001022	10?00001?1
T. garbanii	??????????	??100??02?	10?00001?1
Talenkauen	??????12?2	?1????1???	??????????
Notohypsilophodon	?11?00121?	??0-00???2	10??0?????
Macrogryphosaurus	??????????	??????????	??????????
Haya	0111001212	?00-000???	?????0?1?1
Changchunsaurus	011?00121?	????????3?	10????????
Oryctodromeus	1111001212	0010000032	101100010?
Zephyrosaurus	11?10012??	????00?0?2	??11002101
Orodromeus	0111?01212	?01000000?	1011200101
Kaiparowits Taxon	0111?01212	??0-00??2?	1001????01
Koreanosaurus	1111001212	?00-00013?	1011??????
Archaeoceratops	1110?0121?	?????????2	????001101
Lioceratops	??????????	??????????	??????????

Taxon	220	230	240
Yinlong	?????01212 ?0???????? ??????????		
Stenopelix	??1?????1? ?????????2 ??????????		
Micropachycephalosaurus	1110?0121? 00??0???3? 10????????		
Wannanosaurus	??????1??? ?00???00?? ??????????		
Hypsilophodon	111000121? 00??000032 1020100111		
Atlascoposaurus	?????????? ?????????? ??????????		
Qantassaurus	?????????? ?????????? ??????????		
Anabisetia	?110111212 ?010000??? ??????????		
Gasparinisaura	?111111212 ?00-000022 1010002111		
Zalmoxes r.	0111001212 0110101l?2 101?00210?		
Zalmoxes s.	0111001212 0111101l?2 10??0???0?		
Tenontosaurus d.	0110001212 ?111101122 1030??????		
Tenontosaurus	0110001212 0111101022 1030002111		
Rhabdodon p.	?110001??? 00??1?10?? ?01?012???		
Muttaburrasaurus	0110001212 0110101??2 1?1?0101?1		
Elrhazosaurus	011000121? 101200???? ??0???????		
Dysalotosaurus	0110011212 1011101??2 103?31?11?		
Dryosaurus	0110011212 1010101002 103?310111		
Callovosaurus	0110001112 101110???? ??????????		
Valdosaurus	0110001212 1012100022 1130???101		
Camptosaurus	01?0001??? 01111?11?? ?0?0012???		
Iguanodon 1	?1?0101??? 01131?11?? ?15?012???		
Ouranosaurus	?0?0?01??? 0??????1?? ?140012???		

Taxon	250	255
Marasuchus	???002000?	00-0?
Silesaurus	???0011??0	00-00
Asilisaurus	??????1???	00-0?
Sanjuansaurus	??????????	00-??
Herrerasaurus	0??0021000	00-00
Tawa	???00?1000	00-00
Pisanosaurus	?????????0	???00
Heterodontosaurus	0000??1000	01-00
Fruitadens	??????????	?????
Echinodon	??????????	????0
Lycorhinus	??????????	?????
Tianyulong	???0??1000	11000
Abrictosaurus	???0001?00	???00
Eocursor	??????????	???00
Lesothosaurus	10?????0??	?1?00
Scutellosaurus	???0???00?	?1?10
Scelidosaurus	??????????	?1?11
Emausaurus	??????????	???10
Stormbergia	????0????0	?1?0?
Agilisaurus	???0001000	01100
Hexinlusaurus	1110011000	00-00
Yandusaurus	?????????0	?????
Leaellynasaura	???0001000	?????
Jeholosaurus	11100??000	?1100
Yueosaurus	???0????00	?????
Othnielosaurus	1110001000	???00
New *Parksosaurus*	1??0001000	11000
T. neglectus	1100001000	11000
T. assiniboiensis	1?00001000	11?00
T. garbanii	1100001000	?????
Talenkauen	???0??1???	?1???
Notohypsilophodon	?????????0	?????
Macrogryphosaurus	??????????	?????
Haya	1???001000	01100
Changchunsaurus	???0??1000	?1?00
Oryctodromeus	???0001000	11100
Zephyrosaurus	1100??1000	???00
Orodromeus	1100001000	0??00
Kaiparowits Taxon	1110001000	???0?
Koreanosaurus	??????????	???0?
Archaeoceratops	11?0??1000	???00
Lioceratops	??????????	?????

Taxon	250 255
Yinlong	???0???000 ?????
Stenopelix	???000?000 01000
Micropachycephalosaurus	?????????? ?????
Wannanosaurus	?????????? ?????
Hypsilophodon	1110011000 11000
Atlascoposaurus	?????????? ?????
Qantassaurus	?????????? ?????
Anabisetia	???000100? 1????
Gasparinisaura	21101-1110 ?1000
Zalmoxes r.	????1????? ???00
Zalmoxes s.	?????????? ?1000
Tenontosaurus d.	11?0011000 11000
Tenontosaurus	1100A01000 11000
Rhabdodon p.	201?1-?1?? ???00
Muttaburrasaurus	???01-1??0 ???00
Elrhazosaurus	?????????? ?????
Dysalotosaurus	?0?00?1110 11000
Dryosaurus	111?001110 11000
Callovosaurus	?????????? ?????
Valdosaurus	1?011--1-? ?????
Camptosaurus	?0??1??100 ??1??
Iguanodon 1	201?1??111 ??1??
Ouranosaurus	2??????1?? ?????

APPENDIX C

TRACER PLOT OF BAYESIAN ANALYSES

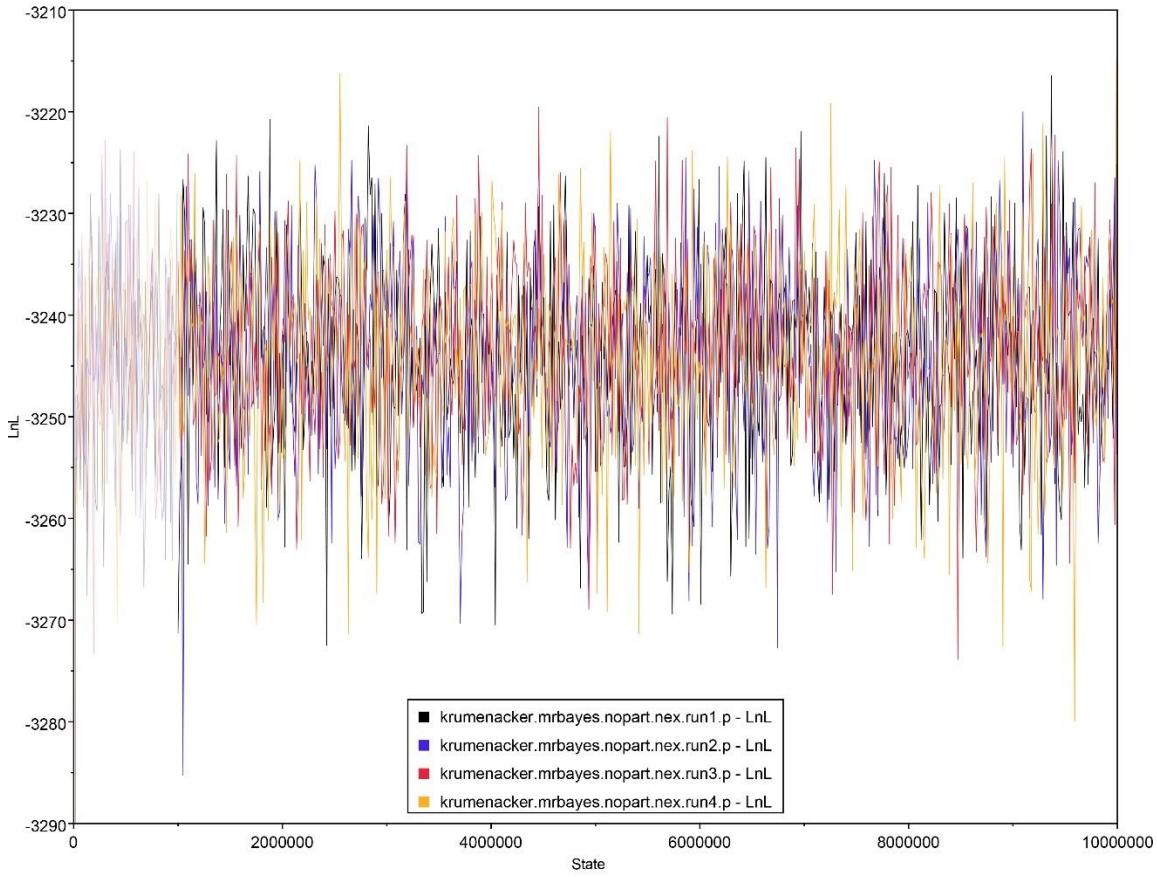
-3210
-3220
-3230
-3240
-3250
-3260
-3270
-3280
-3290
LnL
0
2000000
4000000
6000000
8000000
10000000
State
krumenacker.mrbayes.nopart.nex.run1.p - LnL
krumenacker.mrbayes.nopart.nex.run2.p - LnL
krumenacker.mrbayes.nopart.nex.run3.p - LnL
krumenacker.mrbayes.nopart.nex.run4.p - LnL

APPENDIX D

FIRST PHYLOGENETIC TREE

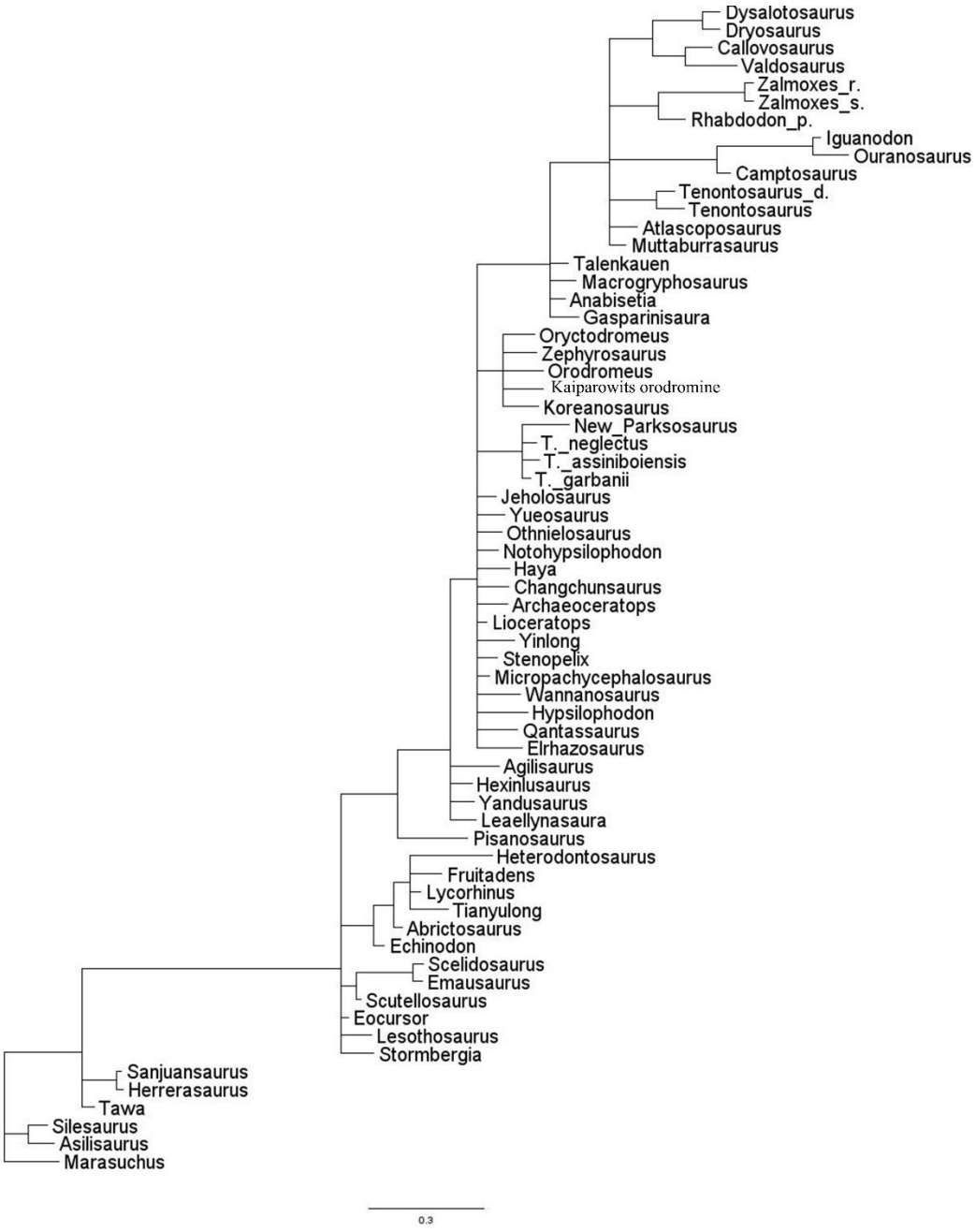
Dysalotosaurus
Dryosaurus
Callovosaurus
Valdosaurus
Zalmoxes_r.
Zalmoxes_s.
Rhabdodon_p.
Iguanodon
Ouranosaurus
Camptosaurus
Tenontosaurus_d.
Tenontosaurus
Atlascoposaurus
Muttaburrasaurus
Talenkauen
Macrogryphosaurus
Anabisetia
Gasparinisaura
Oryctodromeus
Zephyrosaurus
Orodromeus
Kaiparowits orodromine
Koreanosaurus
New_Parksosaurus
T._neglectus
T._assiniboiensis
T._garbanii
Jeholosaurus
Yueosaurus
Othnielosaurus
Notohypsilophodon
Haya
Changchunsaurus
Archaeoceratops
Lioceratops
Yinlong
Stenopelix
Micropachycephalosaurus
Wannanosaurus
Hypsilophodon
Qantassaurus
Elrhazosaurus
Agilisaurus
Hexinlusaurus
Yandusaurus
Leaellynasaura
Pisanosaurus
Heterodontosaurus
Fruitadens
Lycorhinus
Tianyulong
Abrictosaurus
Echinodon
Scelidosaurus
Emausaurus
Scutellosaurus
Eocursor
Lesothosaurus
Stormbergia
Sanjuansaurus
Herrerasaurus
Tawa
Silesaurus
Asilisaurus
Marasuchus
0.3

APPENDIX E

SECOND PHYLOGENETIC TREE

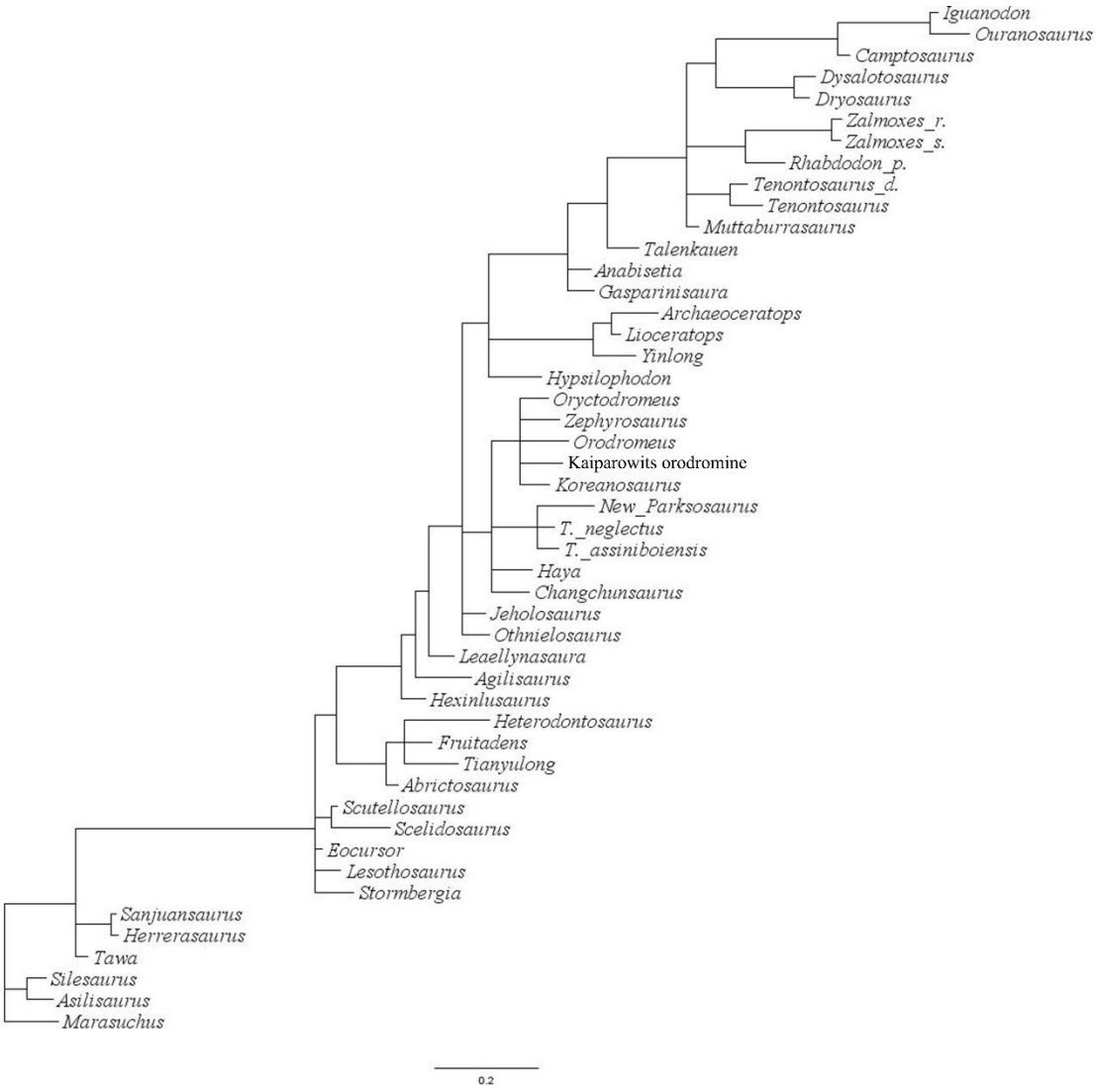
Iguanodon
Ouranosaurus
Camptosaurus
Dysalotosaurus
Dryosaurus
Zalmoxes_r.
Zalmoxes_s.
Rhabdodon_p.
Tenontosaurus_d.
Tenontosaurus
Muttaburrasaurus
Talenkauen
Anabisetia
Gasparinisaura
Archaeoceratops
Lioceratops
Yinlong
Hypsilophodon
Oryctodromeus
Zephyrosaurus
Orodromeus
Kaiparowits orodromine
Koreanosaurus
New_Parksosaurus
T._neglectus
T._assiniboiensis
Haya
Changchunsaurus
Jeholosaurus
Othnielosaurus
Leaellynasaura
Agilisaurus
Hexinlusaurus
Heterodontosaurus
Fruitadens
Tianyulong
Abrictosaurus
Scutellosaurus
Scelidosaurus
Eocursor
Lesothosaurus
Stormbergia
Sanjuansaurus
Herrerasaurus
Tawa
Silesaurus
Asilisaurus
Marasuchus
0.2

APPENDIX F

THIRD PHYLOGENETIC TREE

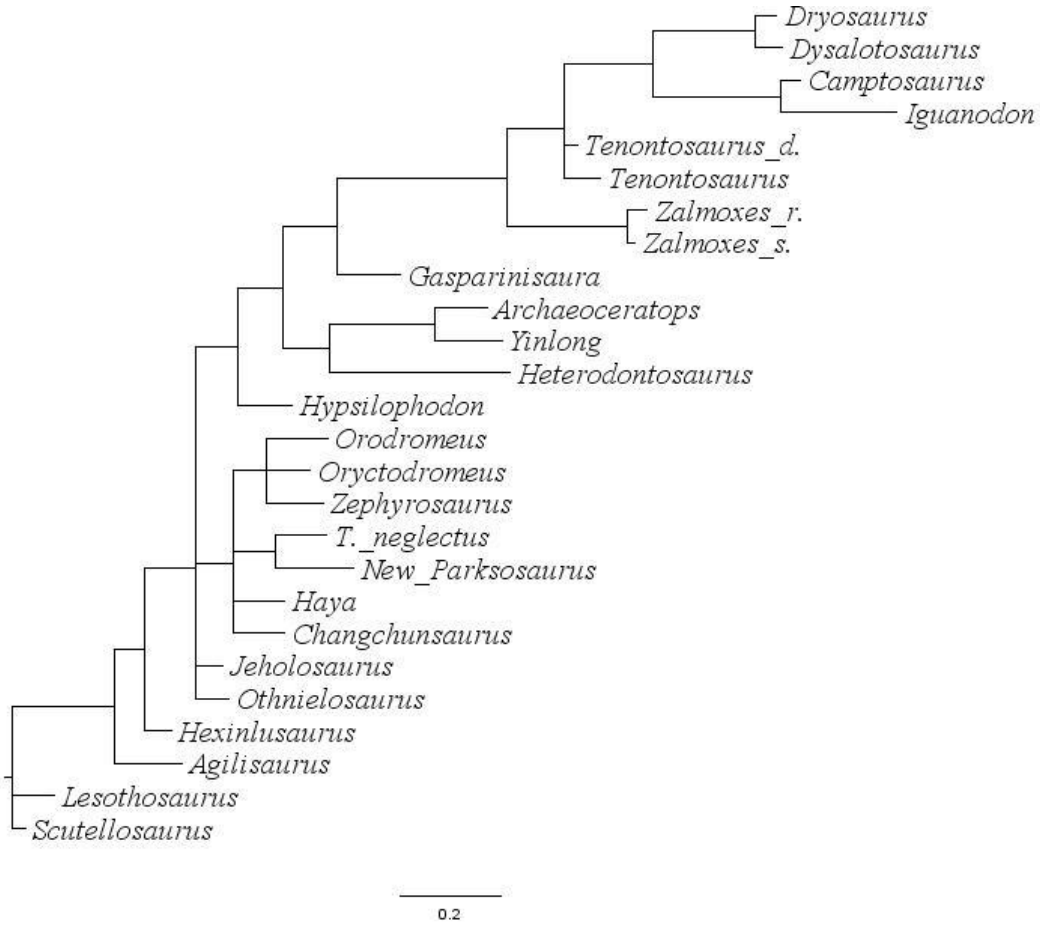
Dryosaurus
Dysalotosaurus
Camptosaurus
Iguanodon
Tenontosaurus_d.
Tenontosaurus
Zalmoxes_r.
Zalmoxes_s.
Gasparinisaura
Archaeoceratops
Yinlong
Heterodontosaurus
Hypsilophodon
Orodromeus
Oryctodromeus
Zephyrosaurus
T._neglectus
New_Parksosaurus
Haya
Changchunsaurus
Jeholosaurus
Othnielosaurus
Hexinlusaurus
Agilisaurus
Lesothosaurus
Scutellosaurus
0.2

APPENDIX G

ILLUSTRATIONS OF ELEMENTS USED FOR HISTOLOGICAL ANALYSIS

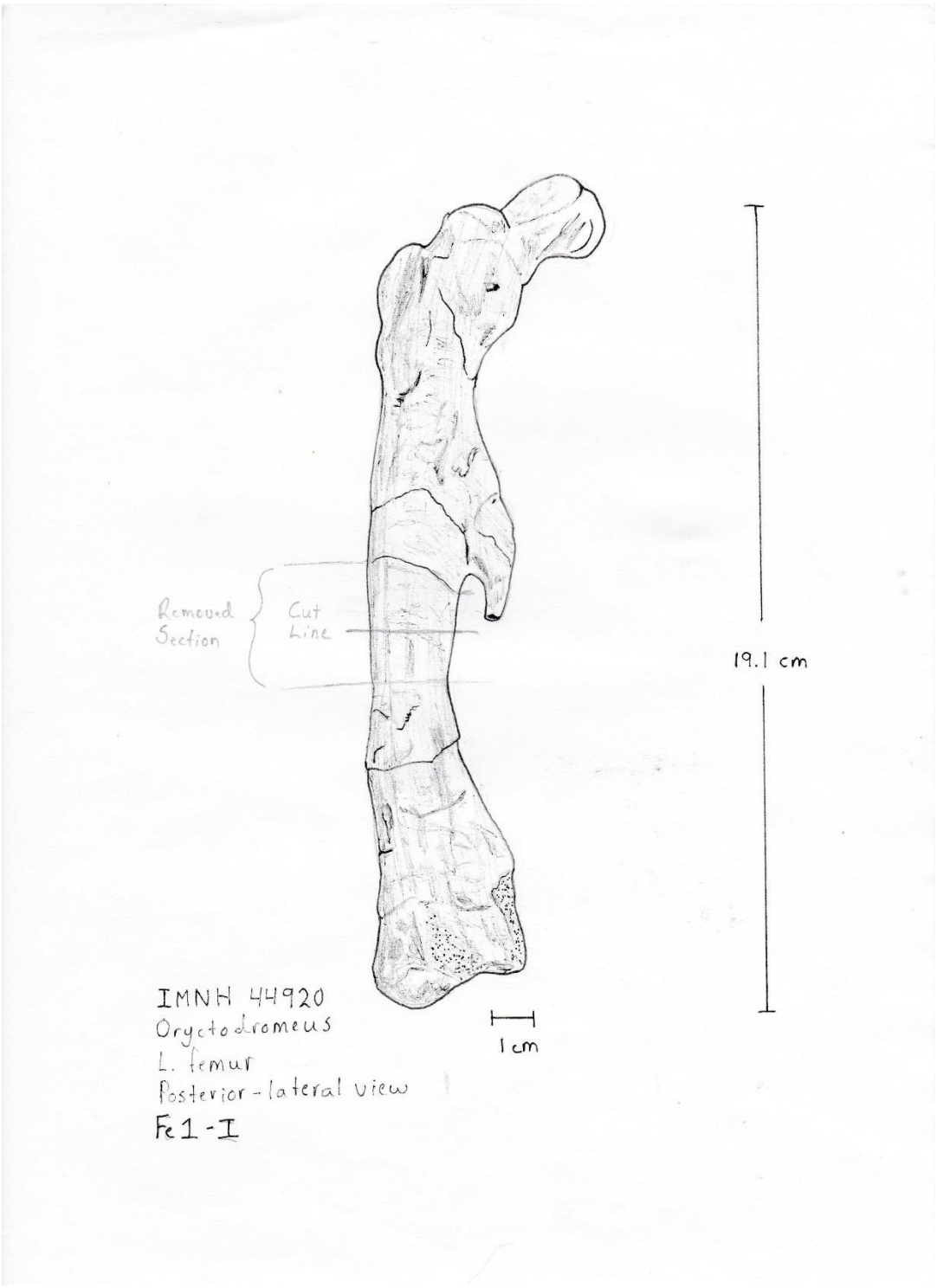

Appendix G1 Figure. Femur Fe1-I (IMNH 44920) used for histological analysis. Removed section and cut line indicated. Scale is 1 cm.

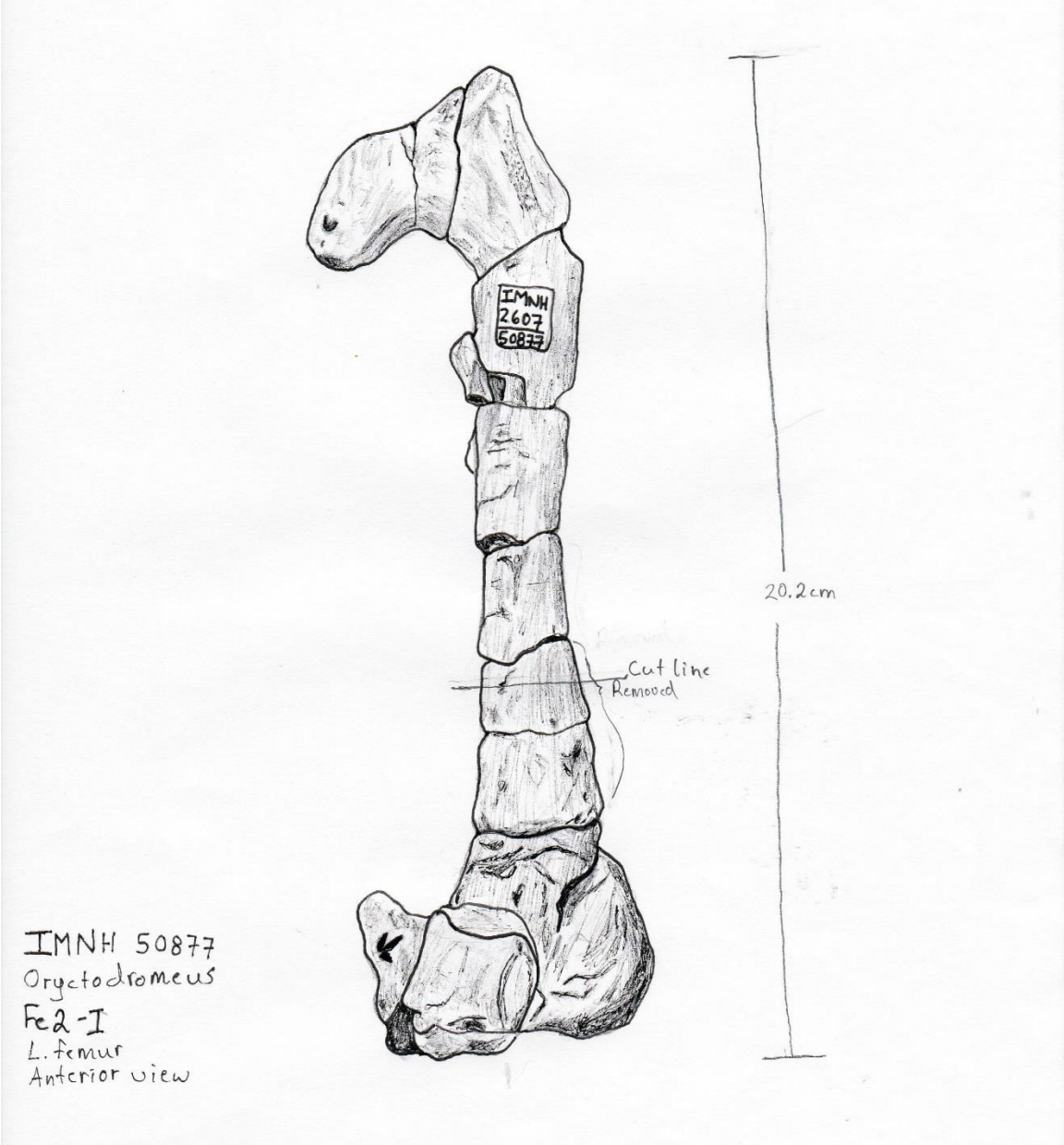

Appendix G2 Figure. Femur Fe2-I (IMNH 50877) used for histological analysis. Removed section and cut line indicated. Scale is 1 cm.

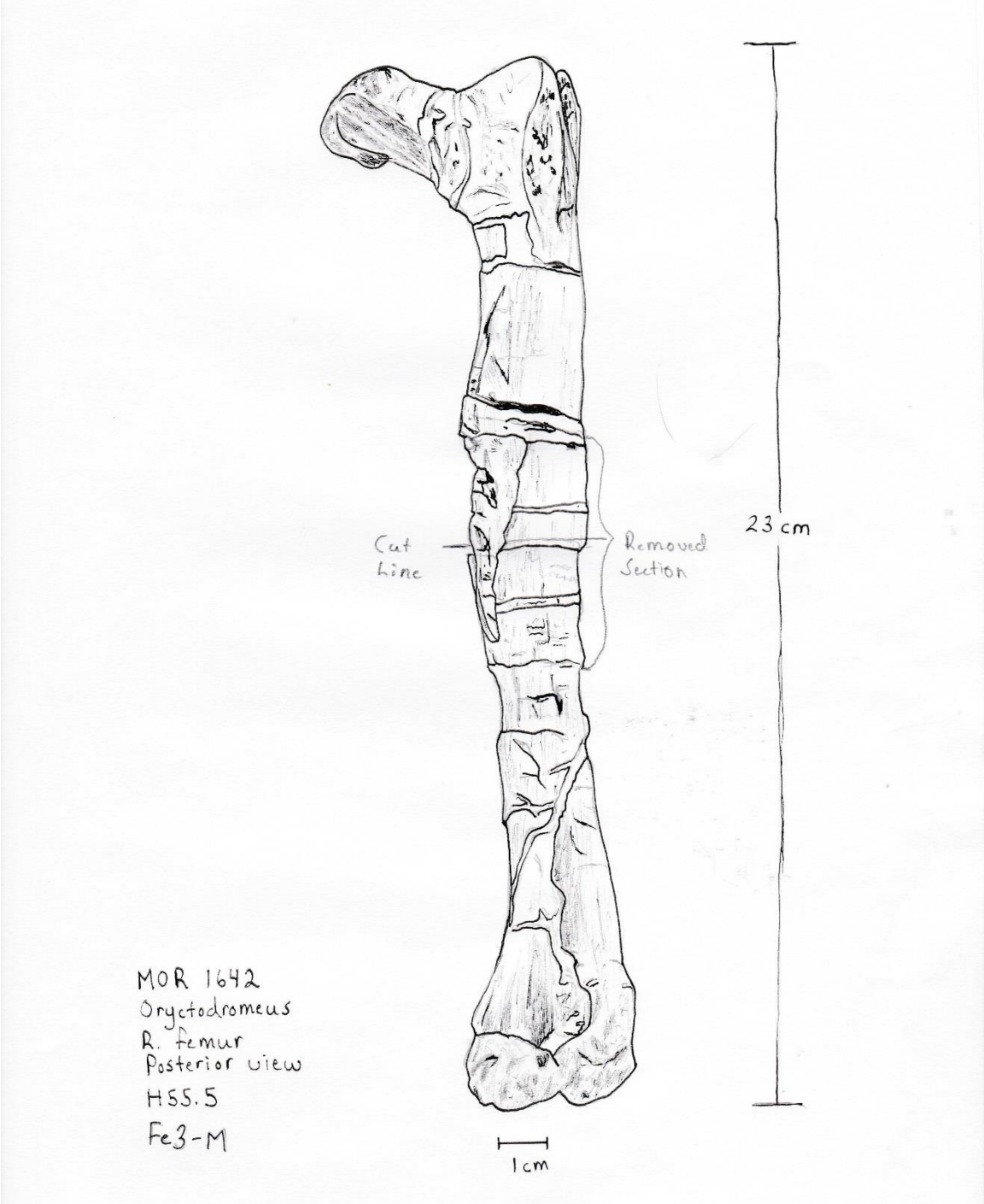

Appendix G3 Figure. Femur Fe3-M (MOR 1642) used for histological analysis. Removed section and cut line indicated. Scale is 1 cm.

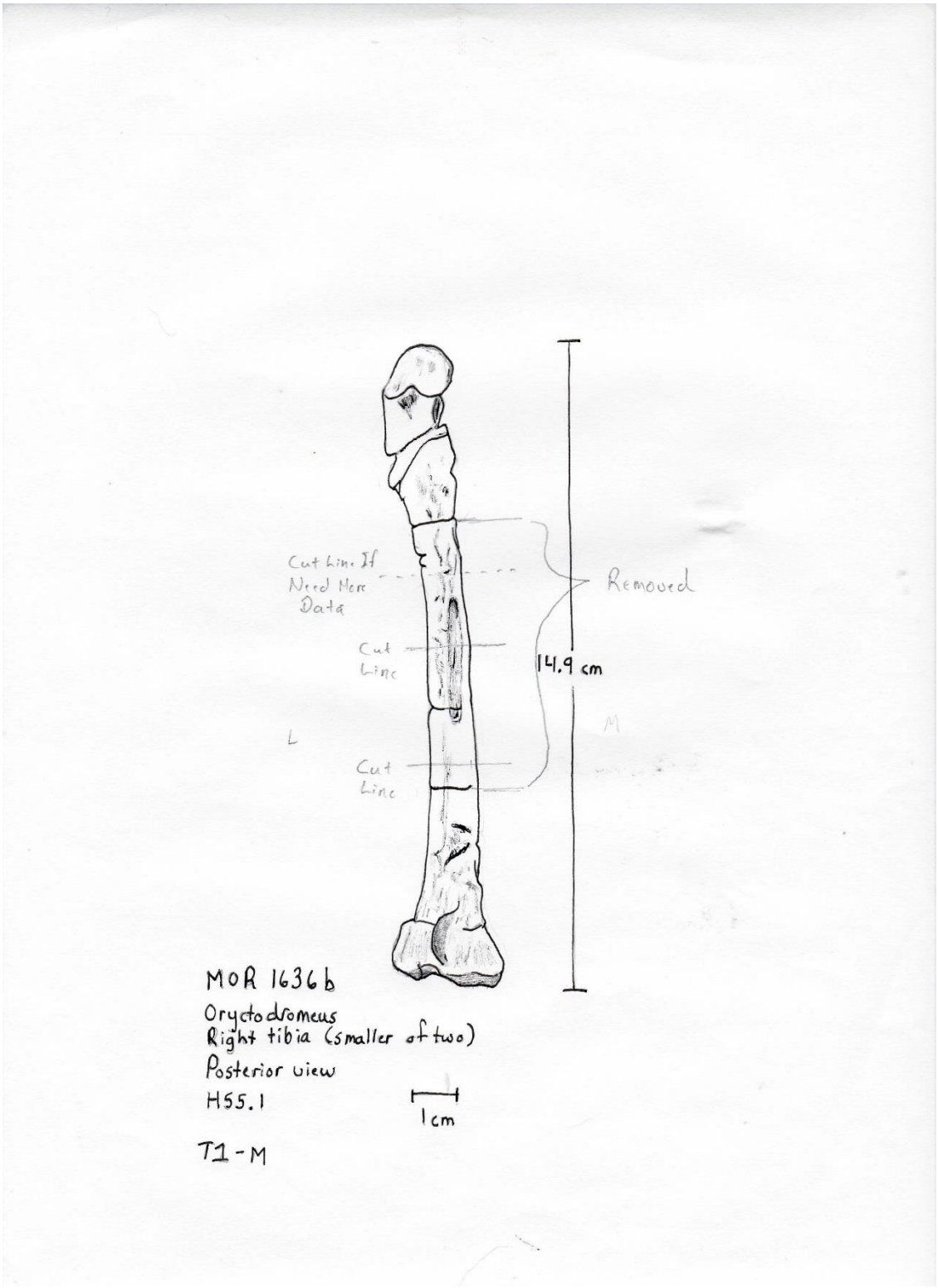

Appendix G4 Figure. Tibia T1-M (MOR 1636b) used for histological analysis. Removed section and cut lines indicated. Scale is 1 cm.

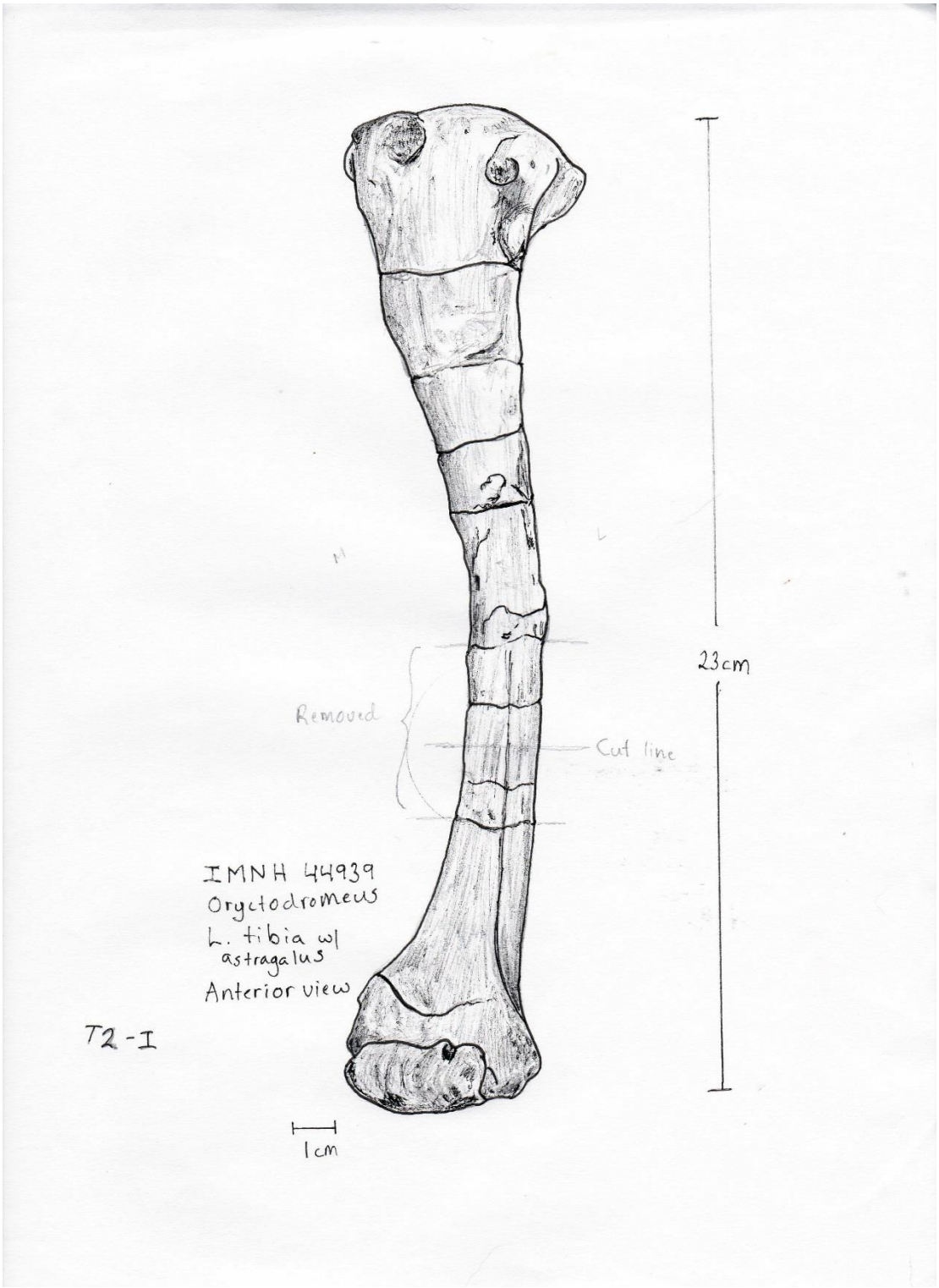

Appendix G5 Figure. Tibia T2-I (IMNH 44939) used for histological analysis. Removed section and cut line indicated. Scale is 1 cm.

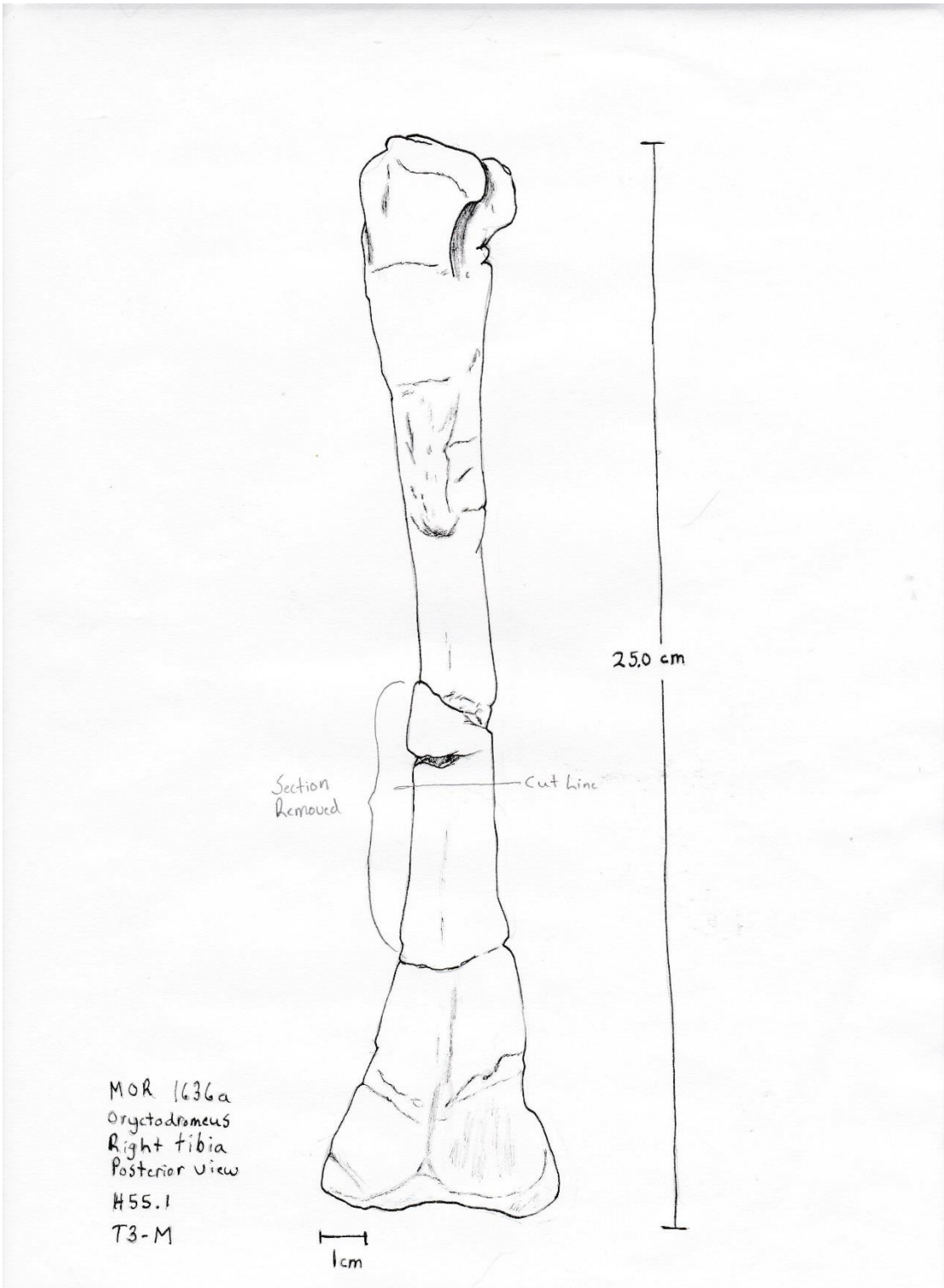

Appendix G6 Figure. Tibia T3-M (MOR 1636a) used for histological analysis. Removed section and cut line indicated. Scale is 1 cm.

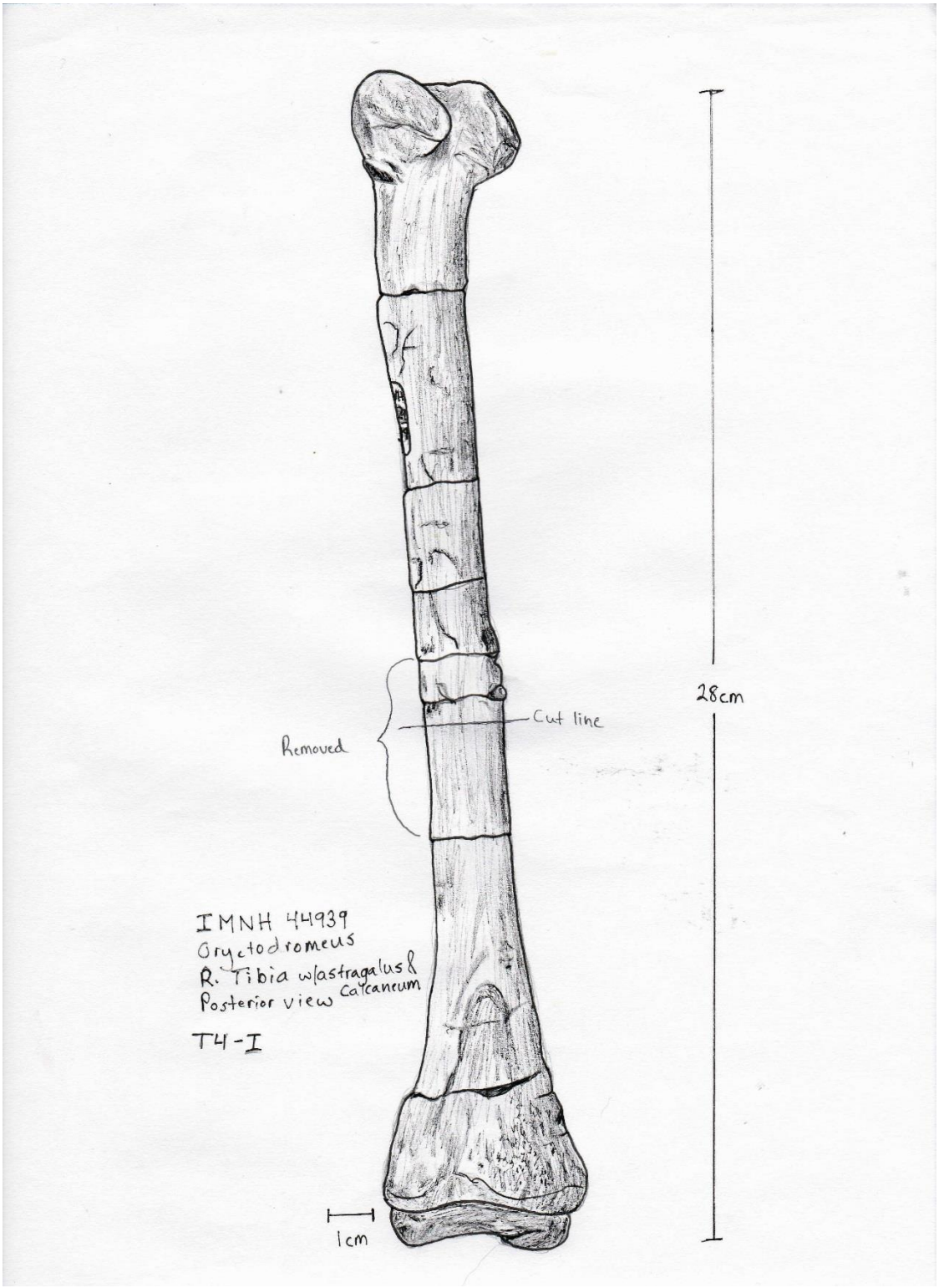

Appendix G7 Figure. Tibia T4-I (IMNH 44939) used for histological analysis. Removed section and cut line indicated. Scale is 1 cm.